Annual variation of bare arable soil areas on a global scale

In Polish:

Roczna zmienność areału gleb ornych nie pokrytych roślinnością w skali globalnej

Jakub Ceglarek

Faculty of Geography and Geology

Department of Soil Science and Remote Sensing of Soils

Supervised by:

prof. zw. dr hab. Inż. Jerzy Cierniewski

PhD Thesis

Adam Mickiewicz University

Poznań 2019

Składam najserdeczniejsze podziękowania
prof. zw. dr hab. Inż. Jerzemu Cierniewskiemu
za opiekę promotorską, wsparcie i przewodnictwo
w trakcie realizacji niniejszej pracy.

This thesis is a part of a project (2014/13/B/ST10/02111, financed by the Polish National Science Center) aimed at quantifying the annual variation in solar shortwave radiation reflected from bare soil on a global scale.

Contents

Contents

Abstract

Arable land around the world has a 12% share of the global land area. This thesis was created as a part of a project aimed at estimation of shortwave radiation reflected from those surfaces according to various scenarios based on the farming methods. This thesis was created as a part of a project aimed at estimation of shortwave radiation reflected from those surfaces according to various scenarios based on the farming methods. Its key element was the estimation of the bare soil area, defined for its spectral properties, as the area of arable land not covered by vegetation on more than 15% on its surface. In conventional agriculture, during the period immediately following the planting of crops, the soil stays bare until the newly planted crops reach defined above share of surface cover. This work focuses on estimating the periods of bare soil that occur after the planting of 13 major crops at the global scale; those selected crops are wheat, maize, barley, sorghum, soybeans, millet, cotton, rapeseed, groundnuts, potato, cassava, rye, and sugar beet. The supplementary objective of the study was to determine which soil groupings, and in what proportions, were bare during those periods. Arable land, divided into extensive agricultural regions located on six continents, was analyzed.

The estimation of bare soil acreage was performed based on publicly available spatial datasets including the distribution of arable land in the world, crop calendars containing planting dates and the geographic distribution of crops. The arable land in the world was first divided into agricultural regions inspired by the division proposed by United States Department of Agriculture. For each region, average daily temperatures were used to predict plant growth stages. For each crop within a region, the planting date was used as the beginning of the bare soil period, which ended when it reached a stage where at least 15% of the surface was covered by vegetation. The aggregated periods concerning every crop within any given region resulted in an annual variation of bare soil area. The acreages of soil grouping used in agriculture for any region were then extracted based on the location of arable land and the region’s boundaries.

Abstract

The global annual variation of bare soil area shows that the maximum level occurs around the 140th day of the year (DOY) (middle of May), influenced primarily by the planting of crops occurring in the northern hemisphere. Up to 1.5 million km^{2}of soil surface stays bare at that time. Centered on that maximum is a period of bare soil lasting for almost four months, between the 92nd DOY and the 200th DOY (early April and end of July), when two lesser maxima were observed, of around 900,000 and 700,000 km^2, respectively. The equivalent of that period, resulting from planting in the southern hemisphere, starts around the 330th DOY (middle of November) and lasts for about a month, reaching almost 400,000 km^2. The other distinguishable episode of bare soil in the southern hemisphere was noted between the 15th and the 25th DOY (second half of January) when its area reached 100,000 km^2.

Asia is the super region with by far the largest area of arable land and consequently, it sports the highest acreage of bare soil. During the aforementioned maximum in the northern hemisphere occurring around the 140th DOY, the Asian super region contributes around 700,000 km^2 of bare soil, which is almost half of the bare soil area for the whole northern hemisphere at that time, with *Lithosols*, *Cambisols*, and *Gleysols* being the major soil groupings that stay bare. In Europe, two distinct periods of bare soil were found; during the first, starting around the 40th DOY (middle of February) and lasting until the 150th DOY (end of May), the steady increase of the bare soil area lasts until the 140th DOY (middle of May) when it reaches almost 500,000 km^2, after which a rapid decline was observed. The second, manifesting two and a half months later, lasts between around the 230th and the 290th DOY (middle of August to middle of October), and exceeds 100,000 km^2. *Chernozems*, *Cambisols*, and *Luvisols* are dominant soil groupings on arable land in Europe. Similar trends, related to the European bare soil areas, were found in the North American super region, where a period of maximum bare soil area occurs in late spring, and a second period, characterized by a much smaller area, follows the main one three months later. The maxima coincide with the aforementioned ones in Asia and Europe, reaching 300,000 km^2 of bare soil around the 140th DOY. Similar to Europe, the second period sports a much smaller bare soil area, short of 30,000 km^2. The dominant soil groupings in agricultural use in North America are *Kastanozems*, *Luvisols*, and *Chernozems*. Africa is a super region whose area is divided between both northern and southern hemispheres, which shows in the annual variation of its bare soil area. Three distinct periods were found there, the major one around the middle of a

year lasted for about two and a half months, between the 167th and the 230th DOY (middle of June to middle of August) with the bare soil area being up to almost 400,000 km^2. The other peak occurs about a month and a half earlier, between the 95th and the 115th DOY (roughly the month of April) and is characterized by a bare soil area exceeding 120,000 km^2. The last notable episode of bare soil in Africa manifests itself between the 317th DOY and the 10th day of the following year (middle of November to the middle of January), with the area of soil uncovered by vegetation reaching almost 100,000 km^2. *Luvisols* together with *Arenosols*, followed by *Vertisols*, are the most extensively farmed soil groupings in Africa. The majority of arable land in the southern hemisphere is found in the South American super region, which is reflected in the annual variation of bare soil area, which is similar to that of the whole southern hemisphere. The maximum lasts for around two weeks, between the 330th and the 345th DOY (end of November to the middle of December), when almost 500,000 km^2 of arable soil is bare. A secondary peak was observed between the 15th and the 30th DOY (second half of January), sporting around 100,000 km^2 of bare soil area. *Ferrasols* is the most commonly farmed soil grouping in the region, followed by *Phaozems* and *Luvisols*. In Oceania, the maximum area of bare soil slightly exceeds 25,000 km^2 for about two weeks in the first half of June, followed by a rapid decline. A secondary period is characterized by a longer duration but the smaller area, lasting between the 313th and the 14th DOY (middle of November to middle of January) with about 5,000 km^2 of arable land which is not covered by vegetation at that time. *Luvisols* are the dominant soil grouping under cultivation in Oceania, followed by *Planosols*, *Solonetz*, and *Vertisols*.

The obtained variations of bare soil areas together with the corresponding share of soil groupings for all regions were used in other work in order to estimate the amount of shortwave radiation reflected from those surfaces according to various scenarios based on the farming methods.

Streszczenie (in Polish)

Grunty orne stanowią około 12% powierzchni lądów na całym świecie. Niniejsza praca powstała w ramach projektu dążącego do oszacowania ilości promieniowania krótkofalowego odbijanego od tych powierzchni. Kluczowym jej elementem było oszacowanie areału odkrytej gleby, definiowanej ze względu na jej właściwości spektralne, jako powierzchni gruntów ornych niepokrytych roślinnością w stopniu większym niż 15%. W przypadku rolnictwa konwencjonalnego, w okresie bezpośrednio po sianiu lub sadzeniu roślin gleba pozostaje odkryta, dopóki nowo zasiane lub zasadzone rośliny nie osiągną fazy wzrostu powodującej pokrycie powierzchni w wyżej zdefiniowanym stopniu. Praca ta koncentruje się na oszacowaniu okresów kiedy gleba pozostaje odkryta, które występują po sianiu lub sadzeniu 13 głównych upraw w skali globalnej; te wybrane uprawy to pszenica, kukurydza, jęczmień, sorgo, soja, proso, bawełna, rzepak, orzeszki ziemne, ziemniaki, maniok, żyto i burak cukrowy. Celem badania było ustalenie, które główne grupy glebowe (major soil groupings wg definicji FAO–UNESCO) oraz w jakich areałach pozostają odkryte. Przeanalizowane zostały grunty orne podzielone na regiony rolnicze położone na sześciu kontynentach.

Oszacowanie areału odkrytej gleby przeprowadzono przy użyciu publicznie dostępnych zbiorów danych przestrzennych, w tym rozmieszczenia gruntów ornych na świecie, geograficznego rozmieszczenia upraw oraz kalendarzy upraw zawierających daty sadzenia. Używane zbiory danych zostały w pierwszej kolejności podzielone na regiony rolnicze zainspirowane podziałem zaproponowanym przez Departament Rolnictwa Stanów Zjednoczonych. Dla każdego z tych regionów zastosowano średnie dzienne temperatury w celu oszacowania etapów wzrostu roślin. Dla każdej uprawy w regionie data sadzenia została wykorzystana jako początek okresu występowania odkrytej gleby, który kończy się, gdy osiągnie etap, w którym gleba zostaje pokryte roślinnością. Zagregowane okresy dotyczące każdej uprawy w danym regionie posłużyły do ustalenia rocznej zmienności powierzchni odkrytej gleby. Areały głównych grup glebowych wykorzystywanych w rolnictwie dla każdego z regionów zostały następnie obliczone na podstawie lokalizacji gruntów ornych i granic regionu.

Analizując wszystkie grunty orne na świecie, maksymalny poziom odkrycia występuje około 140 dnia roku (day of year - DOY);(połowa maja), i jest spowodowany przede wszystkim

przez sianie oraz sadzenie roślin uprawnych na półkuli północnej. W tym czasie do 1,5 mln km^2 powierzchni gruntów ornych nie jest pokryta przez rośliny. Wyżej opisane maksimum występuje podczas okres odsłoniętej gleby trwającego przez prawie cztery miesiące, między 92 DOY a 200 DOY (początek kwietnia a koniec lipca), kiedy zaobserwowano dwa pomniejsze maksima, odpowiednio około 900 000 i 700 000 km^2. Odpowiednik tego okresu, wynikający z siania oraz sadzenia na półkuli południowej, zaczyna się około 330 DOY (połowa listopada) i trwa około miesiąca, osiągając prawie 400 000 km^2. Inny wyraźnie widoczny okres odkrytej gleby na półkuli południowej odnotowano między 15 a 25 DOY (druga połowa stycznia), kiedy jego powierzchnia osiągnęła 100 000 km^2.

Azja to kontynent o zdecydowanie największym areale odkrytej gleby wynikający ze zdecydowanie największej powierzchni gruntów ornych. Podczas wspomnianego maksimum na półkuli północnej, występującego około 140 DOY, azjatycki region odpowiada za około 700 000 km^2 odkrytej gleby, a więc prawie połowę powierzchni odkrytej gleby dla całej półkuli północnej w tym czasie, z *Lithosols*, *Cambisols* i *Gleysols* jako głównymi grupami gleb, które pozostają odkryte. W Europie znaleziono dwa odrębne okresy odkrytej gleby; podczas pierwszego, rozpoczynającego się około 40 DOY (połowa lutego) i trwającego do 150 DOY (koniec maja), stały wzrost powierzchni odkrytej gleby trwa do 140 DOY (połowa maja), kiedy osiąga ona prawie 500 000 km^2, po czym następuje gwałtowny spadek tego areału. Drugi, zaczynający się dwa i pół miesiąca później, trwa od około 230 do 290 DOY (od połowy sierpnia do połowy października) i przekracza 100 000 km^2. *Chernozems*, *Cambisols* i *Luvisols* są dominującymi grupami glebowymi na gruntach ornych w Europie. Podobne tendencje jak w przypadku odsłoniętych gleb na kontynencie europejski zanotowano w Ameryce Północnej, w przypadku której okres największej powierzchni odkrytej gleby występuje późną wiosną, a drugi okres, obejmującym znacznie mniejszy areał, następuje trzy miesiące później. Maksymalne wartości występują w podobnym okresie jak w wyżej wymienionych Azji i Europie, osiągając 300 000 km^2 odkrytej gleby około 140 DOY. Podobnie jak w Europie, drugi okres charakteryzuje się znacznie mniejszą powierzchnię odkrytej gleby, poniżej 30 000 km^2. Dominującymi grupami glebowymi uprawianymi w Ameryki Północnej są *Kastanozems*, *Luvisols* i *Chernozems*. Afryka jest kontynentem zajmującym półkulą północną, jak i południową, co jest odzwierciedlone w rocznym przebiegu areału odkrytej gleby. Wyróżniono tam trzy osobne okresy, największy z nich występuje w połowie roku i trwa około dwóch i pół miesiąca, między 167 a 230 DOY (od połowy czerwca do połowy sierpnia), podczas którego

powierzchnia odkrytej gleby osiąga prawie 400 000 km^2. Drugi szczyt występuje około półtora miesiąca wcześniej, między 95 a 115 DOY (w kwietniu) i charakteryzuje się areałem odkrytej gleby przekraczającym 120 000 km^2. Ostatni znaczący okresy odkrytej gleby w Afryce ustalono między 317 DOY a 10 dniem następnego roku (od połowy listopada do połowy stycznia), przy czym odkryty areał gleby sięga prawie 100 000 km^2. *Luvisols* wraz z *Arenosols* oraz *Vertisols*, są najbardziej ekstensywnie uprawianymi grupami glebowymi w Afryce. Roczna zmienność powierzchni odsłoniętej gleby na kontynencie Ameryki Południowej ma podobny przebieg jak w przypadku całej półkuli południowej. Maksimum areału odsłoniętej gleby trwa przez około dwa tygodnie, między 330 a 345 DOY (koniec listopada do połowy grudnia), kiedy prawie 500 000 km^2 gruntów ornych pozostaje odkrytych. Drugi szczyt zaobserwowano między 15 a 30 DOY (druga połowa stycznia), w którego trakcie około 100 000 km^2 gruntów ornych jest odsłoniętych. *Ferrasols* są najczęściej uprawianą grupą glebową na kontynencie, a następnie *Phaozems* i *Luvisols*. W Oceanii maksymalny areał odkrytej gleby nieznacznie przekracza 25 000 km^2 przez okres około dwóch tygodni w pierwszej połowie czerwca, po czym następuje jego gwałtowny spadek. Drugi okres charakteryzuje się dłuższym czasem trwania, ale mniejszym areałem, utrzymującym się od 313 do 14 DOY (od połowy listopada do połowy stycznia) z około 5000 km^2 gruntów ornych, które nie są w tym czasie pokryte roślinnością. *Luvisols* są dominującą grupą glebową pod uprawą w Oceanii, a następnie *Planosols*, *Solonetz* i *Vertisols*.

1. Introduction

1.1. Arable land

1.1.1. Arable land around the world

Arable land can be defined in a couple of ways; according to the Oxford English Dictionary (2013), the word arable comes from the Latin word *arabilis*, meaning "able to be plowed" and describes land capable of being used for growing crops. However, the definition used by the Food and Agriculture Organization of the United Nations (FAO), as well as the World Bank (2018) is quite different; according to them, arable land is land under active cultivation of agricultural crops. In that sense, the former definition refers to potential, and the latter to the actual use of land. For this thesis, arable land is defined as per the FAO. Arable land is made up of two components: vegetation in various development phases and bare soil. Globally, just short of 40% of land (about 50 million km^2) is used for some kind of agriculture; arable land makes up about 29% of all agricultural land (FAO, 2018), with the rest made up of pastures (68%) and permanent crops (3%). Therefore, about 12% of total land area in the world was arable in 2015, a figure that is steadily growing every year (World Bank 2018), not without consequences for the natural environment (Foley *et al.*, 2005). The geographic distribution of arable land corresponds to fertile soils and suitable climates (Ramankutty, 2000), with the major agricultural regions of the world being: the Corn Belt in the United States, the Ganges floodplain, the wheat-corn belt in Europe, the Pampas in Argentina as well as wheat belts in Australia (Monfreda, Ramankutty and Foley, 2008). In contrast, croplands are generally absent in very dry or cold climates, like deserts, highly elevated zones, and in higher latitudes.

1.1.2. Historical changes in arable land

Changes in global arable land over the last three centuries (XVIII to XX) were analyzed by Ramankutty and Foley (1999). It was a period of rapid expansion of agriculture, first in Europe and soon after in North America and Russia. Since around the year 1850, exponential

growth of arable land was observed in Africa, South and Central Americas, Southeast Asia and Australia. During those three centuries, China observed steady growth of its cropland area. Even though the total area of croplands increased substantially in the 20th century, the cropland base (average area of cropland per person) has diminished from around 0.75 ha per person to 0.35 ha per person (Ramankutty *et al.*, 2002). More recently, Beddow et al. (2010) have looked at the changes in the cropped area for the years from 1960 to 2000, and the overarching theme is a reduction of cropped area in temperate regions, with a simultaneous increase in tropical regions. That trend is expected to continue as the growing global population, expected to reach about 10 billion people by 2050 (United Nations, Department of Economic and Social Affairs, 2017; Thatcher *et al.*, 2018), will lead to an increasing demand for food (Regmi, Takeshima and Unnevehr, 2009; Foley *et al.*, 2011; Tilman *et al.*, 2011; Alexandratos and Bruinsma, 2012; Valin *et al.*, 2014). Dietary changes induced by the growing average wealth, especially the increasing demand for meat and dairy products, will require even more farmed land (Trostle, 2008; Godfray *et al.*, 2010; Senker, 2011; Toulmin, 2012), as will an expanding interest in biofuels (The Royal Society, 2008; Cassidy *et al.*, 2013; Littlejohns *et al.*, 2018). However, changes in the area of arable land are not uniform around the world. The overall trend is that arable land is increasing in tropical regions while diminishing in temperate ones (Ramankutty *et al.*, 2002). Currently, the greatest potential for an increase in arable area exists in Tropical Africa and Northern South America (Buringh and Dudal, 1987), mostly at the expense, unfortunately, of tropical rain forests (Carvalho *et al.*, 2001; Skole *et al.*, 2006). Regarding the longer perspective, however, at the end of the 21st century the changing climate is predicted to hinder the potential for agriculture in those tropical regions while improving the conditions for agriculture at higher latitudes (Ramankutty *et al.*, 2002).

1.1.3. Arable land's impact on climate

Various authors have analyzed the historical anthropological land cover changes and related climate response (Brovkin *et al.*, 1999, 2006; Diffenbaugh and Sloan, 2002; Matthews *et al.*, 2003, 2004; Gibbard *et al.*, 2005; Davin and Noblet-Ducoudre, 2010). During the last centuries, the dominant land cover change was the transformation of forests into croplands (Ramankutty and A. Foley, 1999; Ellis *et al.*, 2010; Meiyappan and Jain, 2012), with 15% to 30% of forests already converted to cropland or pasture, predominantly in temperate regions of Eurasia and North America (Goldewijk, 2001). Land cover change is considered to be one of

the major culprits of environmental change (Defries, Foley and Asner, 2004; Foley *et al.*, 2005; Turner, Lambin and Reenberg, 2007). The past and ongoing transformation of forests into croplands has a direct effect on surface physical properties, chiefly on its albedo (α) (defined as the ratio between reflected and incoming radiation within the shortwave 0.3–3.0 μm portion of the solar spectrum (Coulson and Reynolds, 1971; Oke, 1987)), and on its roughness and evapotranspiration (Bala *et al.*, 2007; Davin, de Noblet-Ducoudré and Friedlingstein, 2007; Bonan, 2008; Davin and Noblet-Ducoudre, 2010). Compared to forests, cropland is characterized by higher average annual α but lower evapotranspiration and surface roughness. The increased α has a cooling effect, which is especially pronounced in temperate and boreal regions due to the difference between α values of forest and croplands being amplified by the presence of snow in winter (Betts, 2000). On the other hand, warming due to reduced evapotranspiration is strongest in tropical regions, especially during the dry season (von Randow *et al.*, 2004; Davin and Noblet-Ducoudre, 2010). Taking those cooling and warming processes together, the net effect of the replacement of forests by croplands seems to be cooling, especially in higher latitudes (Bala *et al.*, 2007). However, when arable land is bare, the α can be lower than that of forests.

1.2. Soil

1.2.1. Bare soil's albedo

As was mentioned earlier, arable land is comprised of two components, vegetation cover and bare soil, that feature in various proportions throughout the year. During periods when arable land lies bare without vegetation, its α depends mostly on the color of the soil, as well as its roughness and moisture content. If plants cover less than 15% of a surface, the α values are similar to the α of the soil lying beneath them. When vegetation covers between 15% and 40% of a surface, the α is determined by both soil and crop, and when vegetation cover increases to more than 40%, the surface inherits the spectral properties of the crop (Baumgardner *et al.*, 1986). When the surface α is controlled by a soil component, the major factor influencing it is the soil color determined by the presence and quantity of SOM and other soil pigments, like carbonates ($CaCO_3$) and iron oxides (Fe_2O_3) (Mikhajlova and Orlov, 1986). Raising the content of SOM and Fe_2O_3 tends to lower the soil α, while increasing the

content of $CaCO_3$ leads to lighter soil and lower α values. Besides soil color, which tends to remain stable over time, the surface α is also controlled by more dynamic soil properties, surface roughness, and moisture. Soil moisture is defined as the water contained in the unsaturated soil zone (Hillel, 1998). Increasing the soil moisture tends to make soil darker and therefore to lower its α. However, if the groundwater table lies deep beneath the soil surface, then the surface quickly reaches air-dried moisture state and the α rises again. A surface reaches the lowest α when moisture content increases to the field capacity, with a further rise in moisture having no additional significant effect on the surface α level (Liu, Wang and Fu, 2008). Going the other way, the surface reaches its highest α level when the moisture decreases from field capacity to hygroscopic capacity, where further drying of the surface stops having a significant effect on the α level.

The roughness of soil surfaces is another factor influencing the surface α that is considered dynamic over time. The roughness of soil surface is related to its irregularities caused by factors like soil texture, aggregate size and shape, infiltration, rock fragments, land management and vegetation cover (Thomsen *et al.*, 2015). In actively farmed arable land it is predominantly a product of soil treatments and tools that were used on a given surface. Reducing the size of soil aggregates and smoothing out irregularities tend to increase the overall α level of a surface. Soil surfaces that have large, irregular aggregates, separated by deep spaces between them tend to absorb a higher amount of incoming radiation compared to surfaces sporting smaller, smoother aggregates (Mikhajlova and Orlov, 1986). The impact of surface roughness on the soil α is dynamic and changes together with illumination conditions, namely by the proportion of diffuse and direct incident radiation, the severity of cloud cover and solar zenith angle (θs). The rate of change of α together with changing θs was reported by Monteith and Szeicz (1961), Kondratyev (1969), Pinty, Verstraete et al. (1989), Oguntunde, Ajayi, and Giesen (2006), Cierniewski et al. (2015a) and Cierniewski, Ceglarek et al. (2018a). If most of the incoming radiation is direct (clear sky conditions), then the α level rises together with increasing θs, reaching its maximum just after sunrise and before sunset. Consequently, during the local solar noon, when θs is the lowest during the day, the minimal values of α are observed. That rate of the α–value rise depends on the roughness of a surface, where smooth surfaces observe a rapid increase of α together with rising θs, whereas for very rough surfaces the α level remains mostly unchanged during the day. Higher proportions

of diffused solar radiation (especially when cloud cover is high) tend to diminish the effect of changing θs on the surface α. The surface roughness affects therefore both the initial level of the surface α as well as the rate of its change with the changing of θs.

Taking into account the three soil surface properties (color, roughness, and moisture content) described in the previous subsection, the range of α (during local noon) tends to be 0.05–0.15 for rough, wet and dark-colored soils, and 0.35–0.4 for smooth, dry and light-colored ones (Oke, 1987; Dobos, 2006).

1.2.2. Classification of soils

Soil classification is an attempt to group soils that share similar properties (biological, chemical and physical) into units that can be mapped. A number of soil classification systems has been developed over the years, and the emphasis on classification criterion has gradually shifted from the genetic approach to using soil properties as a base for differentiating between soil units. Many countries have developed national soil classification systems, most notably the United States (Soil Survey Staff, 1975), Russia (Lev *et al.*, 2001), France (Baize *et al.*, 1995), Australia (Isbell, 2016), Brazil (EMBRAPA, 2006) and Poland (Polskie Towarzystwo Gleboznawcze, 2011). Over time, a consensus about the classification of major soil units that should be distinguished has been developed, taking several stages into account. Early soil classifications focused on soil-forming factors and environment, dividing classified soils into zonal (determined mainly by climate and vegetation) and azonal (determined mostly by parent material and time) categories. Subsequent systems focused on the processes (e.g., leaching, salinization, ferrallitization or accumulation) occurring in the soil, characterized roughly by soil properties. Starting with the 7th Approximation of the USDA (United States Department of Agriculture) Soil Taxonomy, the modern approach to soil classification was conceived, where soil properties had to be precisely defined and quantified in order to define diagnostic soil horizons. Postmodern soil classification can be distinguished, making use of statistics and fuzziness, and include numerical classification systems. The objective of the latter system is to minimize within-class variance while between-class variance is maximized, based on some objective criteria. It can, therefore, be summarized by stating that the development of soil classification systems evolved, from being preconception driven and arbitrary, into objective information of soil units (FAO, 2019).

1.2.3. Contemporary soil classification systems

Among the current, most widely and globally used soil classification systems are: the USDA Soil Classification System, also called Soil Taxonomy; the FAO–UNESCO Soil Classification System; and the World Reference Base; and they are briefly summarized below.

1.2.3.1. USDA Soil Classification System

The USDA Soil Classification System has its roots in the late fifties when it was conceived by the Soil Conservation Service of the United States Department of Agriculture. The system was subject to several approximations, starting with the 7th Approximation, which after considerable revisions was published in 1975 as "Soil Taxonomy: A Basic System of Soil Classification for Making and Interpreting Soil Surveys" (Soil Survey Staff, 1975). The system sports multiple categories of classification, in hierarchical order. From the most general, highest categories to lower, more detailed categories those are: order, suborder, great group, subgroup, family, and series, and they are briefly described below.

Orders are the highest category in the Soil Taxonomy. Currently, there are 12 distinct soil orders (Soil Survey Staff, 1998), up from 10 when the system was introduced. The soils are classified into orders based on the existence or lack thereof of major diagnostic horizons or features displaying the forming process. The processes themselves are not distinguished at that level; the distinction is based on markers left by processes that are dominant factors in the formation of soil. Classification at this level is useful in understanding the global patterns of soil distribution.

Suborders are one hierarchical level below orders and currently include 64 variants, with various soil orders being divided into a varying number of suborders. The basis of this division changes between different soil orders; however, they are focused on soil moisture regimes and diagnostic horizons. The suborder level also tries to distinguish important properties that influence soil genesis.

Great Groups sit at one level below suborders, numbering more than 300 individual great groups. Whereas order and suborder levels are quite generic and do not allow for detailed consideration of more than a few of the most important horizons, at the great group

level all the horizons present are taken into account. Temperature and moisture regimes are considered as properties of a soil, as well as a cause of said properties.

Subgroups include more than 2,400 distinct variations. In contrast to orders, suborders and great groups that focus on features or properties dominant in a given soil unit, subgroups emphasize the description of secondary soil properties. The processes described at that level include either processes that are dominant in other orders, suborders or great groups, or those properties that are a criteria for any soil unit above subgroup level.

Families are a somewhat unusual level, created with the intent to both group and subdivide the soils belonging to higher categories. The main principles behind family level were the usefulness for growing plants and the management of soil. Examples of such families include particle-size, mineralogy, cation exchange activity, and soil temperature among others. A given soil unit can belong to various families, depending on which properties were used for classification.

Series make up the lowest, most homogenous category level, with over 19,000 individual series identified in the United States alone. The differentiae used at this level are generally the same as in the previous ones; however, the range of values for selected properties is narrower than those used in families and other higher levels. Similar to the families level, this division has mostly pragmatic meaning, focused on interpretative applications of a system.

1.2.3.2. The FAO–UNESCO Soil Classification System

The system of soil classification proposed by FAO–UNESCO was an attempt at making a truly international and universal system. The system was developed in 1974 in order to create a soil map of the world (FAO–UNESCO 1974). This system was not supposed to replace any national systems, but to provide a common framework for the transfer of experience, making a first overview of the world's soil and to promote common soil nomenclature. For those reasons, the system is relatively simple and the soil units are broad. When it was first conceived, the FAO–UNESCO system had two levels; the first level comprised 26 Major Soil Groupings and the second level consisted of 106 Soil Units. FAO has been revising the system since it was published; the revision of 1988 increased the number of units to 28 and 153 in the

1st and 2nd level, respectively (FAO 1988). Soil Subunits, the third hierarchical level was introduced to the system in the 1990 revision; however, at that level the subunits were not defined, but guidelines about naming and identification were provided instead. The introduction of this system has led to the creation of a global map of soil, at a scale of 1:5 000 000 that, although very general, was a useful resource to map the diversity of soils around the world.

1.2.3.3. The World Reference Base

Building on top of and replacing the existing FAO–UNESCO Soil Classification System as an international standard, the World Reference Base (WRB) was first presented in 1998 as an attempt to correlate local and national systems (FAO–UNESCO 1988). Besides being based on the FAO–UNESCO system, the WRB was also heavily influenced by Soil Taxonomy, and the French and Russian national soil classification systems. The WRB started as a tool for correlating soil resource information at a world scale; it subsequently became a de facto global soil classification system. Since its inception, the WRB has seen a couple of revisions, the second edition appearing in 2006 and the third and current edition in 2014. The WRB is a two-level hierarchical classification system, the first level sports 32 Reference Soil Groups (RSG) and the second is constructed by combining RSG with qualifiers that allow for more precise characterization of soil.

1.2.4. Remote sensing of soils

Remote sensing (RS) is the art of getting information about an object without interacting with it directly. In soil science, the sources of remotely sensed information are sensors carried by satellites, airplanes and recently unmanned aerial vehicles or drones (Melesse *et al.*, 2007). The principles of RS are the detection and discrimination of objects by measuring radiant energy reflected or emitted by the surface (Aggarwal, 2006). The radiation reflected or emitted from soil depends on the range of its chemical and physical properties, so it is possible to discriminate between different soil surfaces and properties based on that radiation (Mulder *et al.*, 2011; Dewitte *et al.*, 2012). Among the soil properties that are estimated using RS are soil quality (Obade and Lal, 2013), soil moisture (Lakshmi, 2013; Das and Paul, 2015), soil fertility (Du *et al.*, 2009; Tinti *et al.*, 2015), soil salinity (Metternicht and

Zinck, 2003; Asfaw, Suryabhagavan and Argaw, 2016) or occurrences of bare soil (Dematte *et al.*, 2009; Li and Chen, 2014; Cierniewski, Królewicz and Kaźmierowski, 2017; Cierniewski, Ceglarek and Kaźmierowski, 2018b). There are five types of resolution in RS: spatial (how fine details can be distinguished in photos), temporal (observation frequency; how often photos are taken in the same area), spectral (ability to define fine wavelength intervals), radiometric (also called contrast; the sensors' ability to distinguish between objects with similar reflectance), and angular (the capacity to observe the same area from different angles); and each sensor has to balance them due to technical limitations. The main trade-off is between spatial and spectral resolution; a high spatial resolution is associated with low spectral resolution. The use of RS in gathering information about soil on a global scale is limited due to most methods being developed and calibrated for regional scales (Wulf *et al.*, 2015). The accuracy deterioration of RS methods at the global scale is attributed to sensor noise (Phillips *et al.*, 2009), and topographic and atmospheric distortions (Richter and Schläpfer, 2002).

A common way of obtaining useful information from remotely sensed images is through spectral indices (Xue and Su, 2017) that try to capture vegetation properties as a single value. Coming back to the fact that different surface features vary in their spectral response, proper manipulation of spectral channels can highlight desired features (Jiang *et al.*, 2008; Kuzucu and Balcik, 2017). Among the most widely used satellite data are those obtained from the family of Landsat satellites, from which various indices are derived (Vermote *et al.*, 2016). Among these are Normalized Difference Vegetation Index (NDVI), Enhanced Vegetation Index (EVI), Soil Adjusted Vegetation Index (SAVI) or Normalized Difference Moisture Index (NDMI). NDVI is probably the most well known and widespread of the spectral indices; it combines response from red and near-infrared bands to estimate the amount of vegetation for a given pixel (Rouse, Haas and Deering, 1973). EVI is functionally similar to NDVI as it is also used for studying vegetation; however, in addition to the two bands used in NDVI, blue band is also used. Whereas NDVI is chlorophyll sensitive, EVI cares about the structural properties of canopy and leaf areas, making the two indices complementary. A version of EVI that omits blue band has been proposed (Jiang *et al.*, 2008) in order to extend the usability of the index to the images of the first satellites that lacked blue band. SAVI is a modified version of NDVI that introduces an adjustment factor to the formula, shown to minimalize the influence of soil brightness on the index variation (Huete, 1988). NDMI was developed in order

to monitor changes of water content in vegetation, making use of near-infrared and shortwave infrared spectral bands (Gao, 1996). The increasing availability of sensors with very high spectral resolution prompted the development of hyperspectral indices (Thenkabail and Lyon, 2011). Taking advantage of narrower spectral bands allows for the distinguishing of plant species and various stress factors inhibiting their growth (Roberts, Roth and Perroy, 2011).

1.3. Types of agriculture

In this section, conventional-till, reduced-till and no-till agricultural practices related to soil preparation are listed and explained briefly. The factor differentiating these tillage regimes is the share of the surface covered by crop residue after tillage. Tillage refers to the mechanical preparation of soil and includes practices such as plowing, harrowing, cultivating or rototilling. Reduction of tillage practices and an increase in residue cover tends to diminish soil erosion.

1.3.1. Conventional and intensive agriculture

In conventional agriculture, less than 15% of plant residue cover remains after planting. Conventional tillage generally involves plowing and harrowing, leading to a rough surface. This tillage type generally leads to numerous tillage trips, resulting in substantial fuel consumption and carbon emissions. The techniques employed in this tillage method are based on mechanical soil manipulation, starting with plowing and subsequent harrowing. These operations result in the loosening and aeration of the top layers of the soil, mixing nutrients, plant residues, and organic matter, as well as the removal of weeds. The intensive till is an extreme version of conventional agriculture, characterized by numerous field operations, as well as usage of tools such as the disk or chisel plow, the rolling basket or soil cutter. In conventional tilling methods, bare soil occurs mostly around the dates of planting and harvesting. The soil stays bare before the planting as it is being prepared for the sowing of crops; after planting it stays bare for as long as the crops take to develop; the soil is also bare after the harvest. The soil is at increased risk of wind- and water-based soil erosion during those periods.

1.3.2. Reduced tillage

Reduced tillage is an intermediate step between conventional and conservation tillage. In this system, between 15% and 30% of residue remains on the surface (CTIC 2004). A reduction in tillage can be achieved by the reduction in the number of tilling trips and the implementation of multifunction farming tools. Tillage operations are reduced to only those deemed necessary under given conditions (Gajri, Majumdar and Sharma, 2009). Land preparation and seeding are combined into one operation, and plowing is often eliminated. The soil erosion caused by wind or rain is reduced due to the crop residue left on the surface.

1.3.3. Conservation agriculture

Conservation agriculture (CA), however, is becoming ever more popular, and under such a regime, occurrences of bare soil are minimalized (Derpsch *et al.*, 2010; Friedrich, Derpsch and Kassam, 2012). In order to achieve CA benefits, more than 30% of the soil surface must remain covered by crop residue after any tillage and planting operations (CTIC 1993). The focus is put on avoiding the mechanical disturbance of soil, keeping soil cover and using varied cropping systems (Kassam, Derpsch and Friedrich, 2014). In conservation systems the soil erosion due to water and wind is diminished, the accumulation of SOM in the soil is increased and soil biological activity is enhanced (Busari *et al.*, 2015). Weed control is usually achieved by the use of herbicides. The following tillage methods are classified under CA: no tillage, reduced tillage, mulch tillage, and ridge tillage.

1.3.3.1 No tillage

In the most radical form of CA, the no-tillage system the soil is left undisturbed from harvest to planting, barring nutrient injections. The need for tillage is avoided by directly depositing a seed in the soil, made possible by using special seeding equipment such as seed drills and seed openers that create soil openings only of sufficient width and depth to allow proper seed coverage (Midwest Plan Service, 2000). No-till agriculture often uses crop rotation as an additional form of weed control. Due to permanent residue on the soil, carbon sequestration is improved compared to conventional agriculture and SOC accumulation in the soil is increased (Stagnari, Ramazzotti and Pisante, 2009; Corsi *et al.*, 2012).

1.3.3.2. Mulch tillage

The mulch till is another variant of CA in which the soil surface is disturbed by tillage and crop residue is mixed with the soil, leaving some amount of residue on the surface (SCSA 1987). It is usually achieved by replacing chisel plows, sweep cultivators or disk cultivators by moldboard or disk plows in tillage (Lal, 2016). The effect is that the residue is buried only shallowly, maintaining good aeration in the soil.

1.3.3.3. Ridge tillage

In ridge tillage, crops are planted on ridges formed by shallow cultivation equipment during the preceding and current planting seasons. The soil is left undisturbed between harvest and planting, barring eventual nutrient injections (Gajri, Majumdar and Sharma, 2009). The crop residue remains in the rows between the ridges. Ridge tillage is especially favorable on level fields, in soils that have poor drainage and are therefore often too wet (Shi *et al.*, 2012).

1.4. Crops

1.4.1. Major farming crops

Among many plant species existing in nature, humans mostly cultivate less than 70 of them, a staggeringly low number in comparison to natural ecosystems, with estimates of over 100 species of trees alone found within one hectare of tropical rain forests (Fowler and Mooney, 1990; Perry, 1994). Among those crops, there are 12 cereal crops, 23 vegetable crops, and some 35 nuts and fruits. Taken together, cultivated areas of just wheat, maize, rice, and barley constitute over half of the total cultivated areas in the world (Leff, Ramankutty and Foley, 2004).

1.4.2. Geographic distribution of major farming crops

The first attempts at mapping the global geographic distribution of major crops were made by the United States Department of Agriculture/Joint Agricultural Weather Facility (USDA/JAWF) in 1981, with revisions in 1987 and 1994. The authors divided the world into major agricultural areas and provided data about growth cycle, area, and yield of selected

crops, aggregating data coming from censuses. In the late 1990s, a new approach arose; the census data began to be fused with maps of agricultural land cover obtained from satellite imagery (Ramankutty and Foley, 1998; Frolking *et al.*, 1999; Hurtt *et al.*, 2001). The geographic distribution of major crops was prepared by Leff, Ramankutty, and Foley in 2004. Using such an approach presents data for 18 crops. The authors use census data from various countries and the FAO and combine it with the global land use dataset (Ramankutty and Foley, 1998). This approach has led to a gridded map, where each cell shows the area under cultivation for each of the selected crops. Heistermann (2006) created a dataset showing distributions of 17 crops. Like Leff before him, he fused census data at various administrative levels with a land cover map, but instead of showing fractions of the farmed area under crop, cells in his dataset show just the dominant crop in each cell. In 2008, Monfreda, Ramankutty, and Foley used a similar approach of fusing census data with an updated global cropland map (Ramankutty *et al.*, 2008) producing gridded maps for 175 crops (M3), also including their average yields in addition to the farming area. Based on the M3 dataset, combined with crop calendars supplemented by the FAO, Portmann et al. (2008) developed a dataset showing the monthly farming area of 26 irrigated crops. To record the monthly irrigated and rainfed crop areas around the year 2000 (MIRCA2000), the global dataset was subsequently developed by Portmann, Siebert et al. (2010). In this version, the authors focused on distinguishing between rainfed and irrigated farming areas, again presenting data in monthly periods. The Global Agro-Ecological Zones (GAEZ) dataset was created by the FAO (Fischer *et al.*, 2012), combining the existing M3 dataset with socio-economic data such as population density and location of markets. This dataset provides information on area, yield, and production for 23 crops, separating rainfed and irrigated ones. The most recent attempt at mapping geographic crop distribution in the year 2000 is the spatial production allocation model (SPAM), proposed by You et al. (2014). The SPAM extends the methodology used in M3 and MIRCA by incorporating informed prior spatial distribution of crop areas into the entropy-based model, creating a dataset of 20 major crops, disaggregated into four classes (high-input irrigated, high-input rainfed, low-input rainfed and subsistence). Wood-Sichra, Joglekar, and You (2016) published an updated crop distribution database in 2005 based on SPAM. Beyond updating the year, the main differences compared to the previous SPAM dataset are an increased number of analyzed crops from 20 to 42 and improvements to the entropy equations. All of the gridded

models mentioned above have a cell size of 5 arc min, which equals to around 9.2 km at the equator.

1.4.3. Plant development and growing degree days

Phenology is the study of the life cycle of plants and animals, and in the case of crops is mostly concerned with the dates of first occurrences of bud burst, leaf expansion, flowering, fertilization, fruiting, seed dispersal and germination in their annual cycle (Fenner, 1998). One way of monitoring and predicting phonological phases is through the use of growing degree days (GDD) (McMaster and Wilhelm, 1997). GDD is a cumulative measure of heat accumulation, calculated using average daily temperatures and the baseline temperature that differs among various crops (eq. 1).

$$\mathrm{GDD}=[\frac{T_{max}+T_{min}}{2}] - T_{base} \quad (1)$$

where T_{max} and T_{min} are maximum and minimum daily air temperatures, and T_{base} is the baseline temperature for a given crop. For days when GDD was a negative value, it was set to zero instead.

1.4.4. Crop calendars

Crop calendars are an attempt at showing optimal planting and harvesting dates of crops in particular regions (FAO, 2010). Timing of sowing and harvest affects the simulation of crop growth and yields and on the impact of croplands on water and energy balance (Twine, Kucharik and Foley, 2004). The selection of crop planting dates is a balancing act; planting too early might lead to frost damage during flowering and increase the risk that the crop will use up available moisture before the reproductive stage begins, whereas planting late can lead to heat stress during the crop maturing phase (Ortiz, Tapley and Santen, 2012). Crop calendars are usually created using either satellite remote sensing (Zhang, Friedl and Schaaf, 2006; Roerink *et al.*, 2011; You *et al.*, 2013) or by compiling data from observers around the world (e.g., USDA 2006; FAO 2010). Both approaches have their limitations; in the case of remotely sensed data, the ground resolution is typically 1 km or greater, which happens to be too coarse to distinguish between individual crops in many parts of the world, whereas the scale of the observations is usually presented at a national-level, and commonly in graphic format. To the

best of the author's knowledge, there is only one global scale crop calendar to date (Sacks *et al.*, 2010). Those authors compiled data from six sources, mostly from the aforementioned FAO and USDA datasets to produce calendars covering planting and harvesting dates of 19 individual crops. The resulting calendars present data at the national level, with some large countries being divided into subnational units, and relate to the late 1990s and early 2000s.

1.5. Aim of the study

This work is focused on estimating the occurrences of maximum areas of bare soil resulting from the planting of major crops throughout the year on arable land, as well as acreages of major soil groupings that are without vegetation. Bare soil was defined as having less than 15% of the surface covered by plants. Periods of bare soil were estimated starting with the planting dates of crops obtained from the planting calendar and ending when the crop covered the aforementioned proportion of surface. The plant phenological development was estimated using GDD accumulation starting at the day of planting. The global aspect of the problem was tackled by dividing the globe into six super regions, which were further divided into subregions. The result of this work, described in a later chapter was a world divided into 33 regions, and for all of them, maps showed the location of their croplands, together with the annual variation of bare soil area, divided into soil groupings according to FAO–UNESCO classification. Additionally, for each region, the area under cultivation for each of 13 major crops was summarized while excluding areas under conservation agriculture. This, in turn, allowed the estimation of potential shortwave solar radiation that could be reflected from arable land throughout the year, according to various scenarios concerning farming practices, taking into account the α of the bare soil.

2. Study area and methods

In this chapter, the way that the study area was divided into regions and the procedure leading to obtaining annual bare soil area for each of them is explained. The procedure is also summarized in the flowchart presented below (Figure 1). Maps throughout this thesis were created using ArcGIS software by Esri.

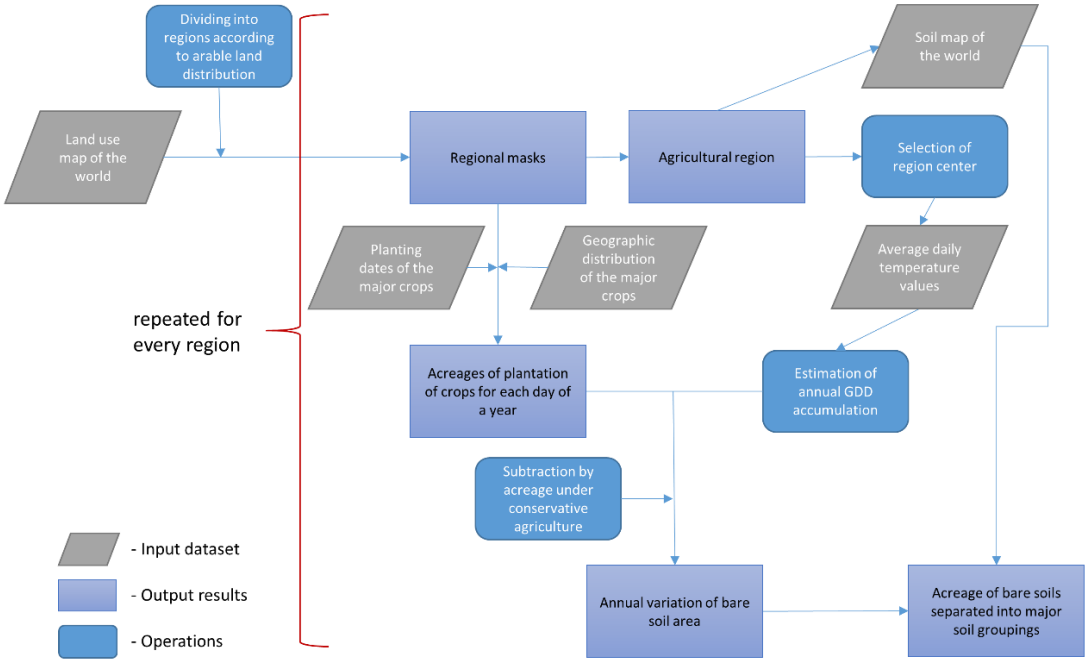

Figure 1. Flowchart illustrating the steps taken in the procedure.

2.1. Selection and creation of agricultural regions

The study area encompasses all of the arable land in the world, as delimited on "*Geographic distribution of global agricultural lands in the year 2000*" (Ramankutty *et al.*, 2008). In order to tackle the global aspect of the study, the agricultural lands were first divided into agricultural regions. That division was inspired by the division proposed by USDA in Major World Crop Areas and Climatic Profiles and was further subdivided into smaller regions. The regions were selected in such a way as to contain continuous agricultural lands. In the first step, the farmed areas related to each of the 13 major farming crops (Monfreda, Ramankutty and Foley, 2008) were summed for each pixel of the earth. Those selected crops were barley,

cassava, cotton, groundnuts, maize, millet, potato, rapeseed, rye, sorghum, soybeans, sugar beet, and wheat. The arable areas for all of those crops were stored in raster files, where each pixel was the size of 5 arc minutes. Using ArcMap software from ESRI, all of those 13 aforementioned rasters were summed, producing one raster showing a farmed area all in pixels covering the whole earth. The polygons representing the regions were drawn on top of a map of the summed farmed area. In the next step, all of the previously mentioned maps showing the farmed area of each of the selected major crops were divided by the regions in such a way that for each region one dataset for each major crop was obtained. Additionally, the geographical center of each agricultural region was selected, in order to be used in a further step. The final division encompasses 33 regions, which for ease of presentation were grouped together into six super regions on a continental scale.

2.2. Applying crop calendars to regions

The procedure performed in the following steps was repeated for all of the regions. The *Crop planting dates: an analysis of global patterns* dataset, published by Sacks et al. in 2010, was introduced in the next step, and will henceforth be called crop calendar. The crop calendar presents data about planting and harvesting dates, among other things, for 19 major crops, including the 13 that were selected for this work. The planting dates dataset that will be of use in this step was presented in the form of rasters, where each cell shows data about the average planting day of the crop of interest in a given area, separately for all of the crops. Those calendars were transformed into a vector dataset, where polygons were created spanning continuous regions with the same planting date. Using ArcMap, the farmed area of each crop was superimposed on the planting date from the crop calendar related to that crop. Then, by applying a zonal statistic tool, with each distinct planting date serving as a zone, all of the pixels with a farming area within such a zone were summarized. The example of this procedure is shown in Figure 2. As each of the pixels contained information about the farming area of a given crop within the said pixel, by summing pixels found within each zone, the number of hectares on which a crop is planted on a particular date in the region was obtained. That step was repeated for each crop present in a given region. The final result of this operation was a table, showing dates of planting together with the area being planted, separately for all of the crops.

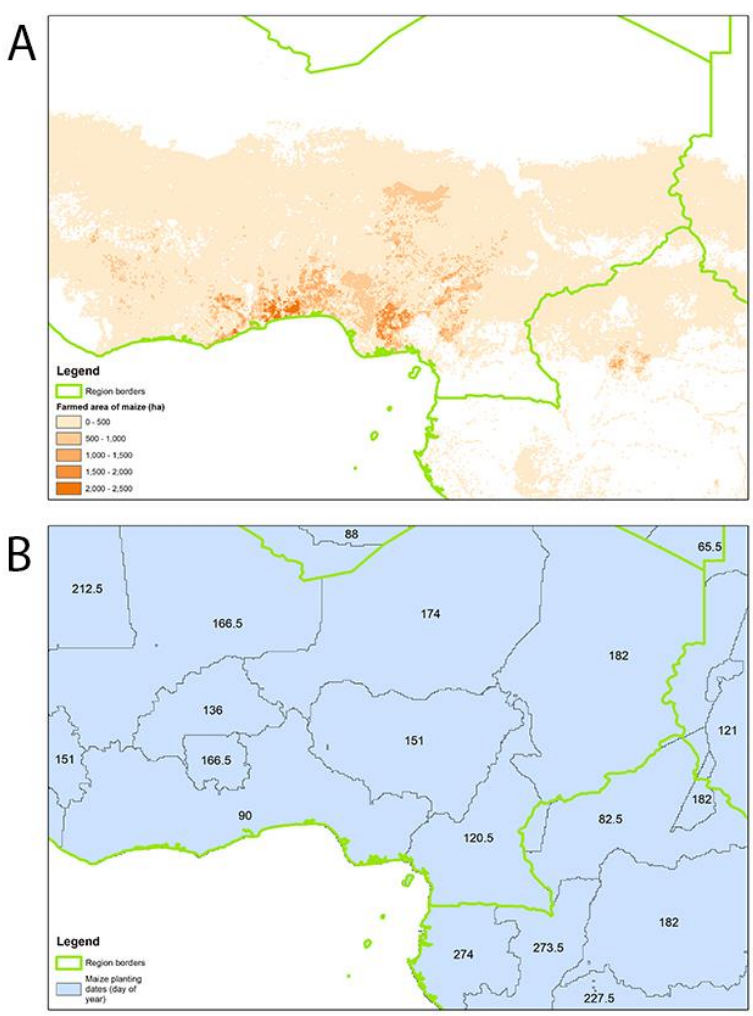

maize	Planting day	sum of hectares
1	212.5 Western Africa	9773.56
2	136 Western Africa	223869.38
3	182 Western Africa	166904.18
4	166.5 Western Africa	304449.75
5	120.5 Western Africa	309053.21
6	174 Western Africa	6050.96
7	90 Western Africa	3804958.67
8	151 Western Africa	2055052.89
9	82.5 Western Africa	228.23
10	182 Central Africa	257420.56
11	82.5 Central Africa	85922.07
12	120.5 Central Africa	6984.06
13	274 Central Africa	199172.54
14	357.5 Central Africa	174.4
15	61 Central Africa	31.87
16	227.5 Central Africa	936937.31
17	121 Central Africa	459.17
18	273.5 Central Africa	7866.41
19	335 Central Africa	73626.4
20	318 Central Africa	195.99
21	182 Eastern Africa	39538.87
22	61 Eastern Africa	66550.25
23	65.5 Eastern Africa	873.76
24	101.5 Eastern Africa	1176899.21
25	121 Eastern Africa	572292.39
26	82.5 Eastern Africa	383.19
27	357.5 Eastern Africa	122.63
28	105.5 Eastern Africa	176446.75
29	40.5 Eastern Africa	837370.45
30	274 Eastern Africa	184400.74
31	90 Eastern Africa	1552010.02
32	227.5 Eastern Africa	559.09
33	15.5 Eastern Africa	545711.67
34	88 Northwestern Africa	211.7
35	136.5 Northwestern Africa	613.08
36	61 Northwestern Africa	158.42
37	274 Northwestern Africa	100.17
38	45.5 Northwestern Africa	257281.53

Figure 2. An example of combining calendar planting dates with farming area: A—farmed area of maize in hectares, each pixel represents area being farmed; B—the crop calendar converted into polygons, the numbers inside refer to the day of year in which the maize is planted; C—export of data into tabular format, where each unique instance of planting date within region is summarized together with the total area of maize being planted on that day.

2.3. Predicting the periods of bare soil

In this work, periods of bare soil were assumed to start with planting and stay that way until a crop develops enough to cover a significant portion of the surface (15%), thereby changing the spectral properties of the field. In order to predict the rate of phenological development, growing degree days were implemented. GDD is based on heat accumulation and is calculated based on average daily temperatures. At this stage of the procedure, the average daily temperatures for each day of the year, measured over the period of ten years (1990–2000) were estimated. The temperatures were obtained from the National Center for Atmospheric Research (NCAR, 2018) for the centers of the regions, which were selected during the first step. Consequently, for each day of the year, the mean temperatures from ten-year

periods were averaged, resulting in an annual course of average daily temperatures for each region. Using the formula:

$$\mathrm{GDD}=[\frac{T_{max}+T_{min}}{2}] - T_{base} \quad (1)$$

where T_{max} and T_{min} are the maximum and minimum daily temperatures, respectively and T_{base} is a baseline temperature required for phenological processes, and is related to the crop in question and obtained from the works of Miller, Lanier, and Brandt (2001), Lee (2011) and Worthington and Hutchinson (2005). The GDD value for any day cannot be lower than zero, so for days when the average daily temperature was below the baseline, the GDD was set to zero. The annual GDD course was obtained by cumulating values for each subsequent day.

2.4. Estimating annual bare soil variation

In this step, the periods for when the agricultural land stayed bare of vegetation after planting were calculated. In the three papers mentioned in the previous paragraph, besides finding the baseline temperatures for the crops, the number of GDD required by the crops to reach their phenological phases was also found. Having the planting dates together with the farmed area for each crop, the annual accumulation of GDD was added to the table. For each unique planting date and crop combination, the number of GDD required for a crop to reach a phenological stage sufficient to cover the surface by at least 15% was added to the already accumulated GDD on that day. This value was used to find a date matching that number of accumulated GDD, which was considered as a date when soil stopped being bare due to planting the given crop on a given date. This step resulted in recording the periods of bare soil together with their areas. Performing this step for every crop present in a given region and afterward summing the farmed areas related to those periods resulted in obtaining the bare soil course for the whole region.

The impact of conservation agriculture was also taken into account. Since the database containing a farmed area of major crops makes no distinction about the type of agriculture, the impact of conservation agriculture on the area of bare soil was estimated in a three-step procedure. First, all of the farmed areas in a region were summed giving a total farmed area in a region. Next, taking the area under CA from the works of Derpsch et al. (2010), Friedrich, Derpsch, and Kassam (2012) and data from EUROSTAT the proportion of CA to total farmed area in each region was calculated. Afterward, the bare soil area was multiplied by the

proportion of the surface being farmed in a conventional way, effectively subtracting the area under CA.

2.5. Major soil grouping areas in the regions

In this step, the composition of soil used in agricultural units within each region was obtained. Two datasets were used in this procedure, the Digital Soil Map of the World (DSMW, FAO–UNESCO 2007) and the global land cover map (Arino *et al.*, 2012). The DSMW is a global soil map in vector format, presenting soil units classified according to the FAO–UNESCO system at a scale of 1:5 000 000. GlobCover is a raster map with a resolution of 300 m, containing 22 land cover types. In order to delimit soils to croplands, three classes from GlobCover were selected: Post-flooding or irrigated croplands, Rainfed Croplands and Mosaic Cropland (50–70%)/vegetation which taken together cover 12% of the land surface. Those three classes served as a mask to extract the area occupied by particular soil units within the extent of all of the regions. This was achieved in ArcMap, employing the Intersect tool; the soil units within the extent of the mask and a region were selected, then using the calculated geometry area of each, the soil units were calculated. This step was repeated for all of the regions. The proportion of FAO–UNESCO soil units at a major soil grouping level was required in further steps of the project, of which this thesis is one part.

3. Results

3.1. Regionalization of the study area

The study area was divided into 33 regions, which will be presented after aggregation into six super regions at a continental scale. The regions selected for the procedure are listed below:

- Africa (AF)— consisting of five regions: Northwestern (AFnw), Western (AFwe), Central (AFce), Eastern (AFea), Southern including Madagascar (AFsm);
- Asia (AS)—being the largest super region, this was split into ten parts: the former republics of the Soviet Union in Central Asia (Kazakhstan, Uzbekistan, Kyrgyzstan, Turkmenistan, Tajikistan) (AScr), the Middle East and Egypt (ASme), China and Mongolia (AScm), Western India (ASwi), Eastern India (ASei), Southern India (ASsi), Indonesia and Malaysia (ASim), Japan and South Korea (ASjk), the Philippines (ASph) and Southeast Asia (ASse);
- Europe (EU)—made up of four parts: the European Union and its associated countries (Switzerland and Norway), plus the countries of the former Yugoslavia outside the European Union, divided into three subregions: Western (EUwe), Central (EUce) and Southern (EUso), and the Russian Federation with the former republics of the Soviet Union (Belarus, Ukraine, Azerbaijan, Armenia, Georgia) (EUrr);
- North and Central America (NA)—divided into eight regions: Canada (NAca), the United States (West (NAwe), Midwest (NAmw), Northeast (NAne) and South (NAso)), Mexico (NAme), Central America (NAce) and the Caribbean (NAca);
- South America (SA)—covering three regions: Brazil (SAbr), the Andean States (SAas) and the Southern Cone (SAsc);
- Oceania (OC)—which includes 3 regions: Australia (East (OCae) and West (OCaw)), New Zealand (OCnz) (Figure 3).

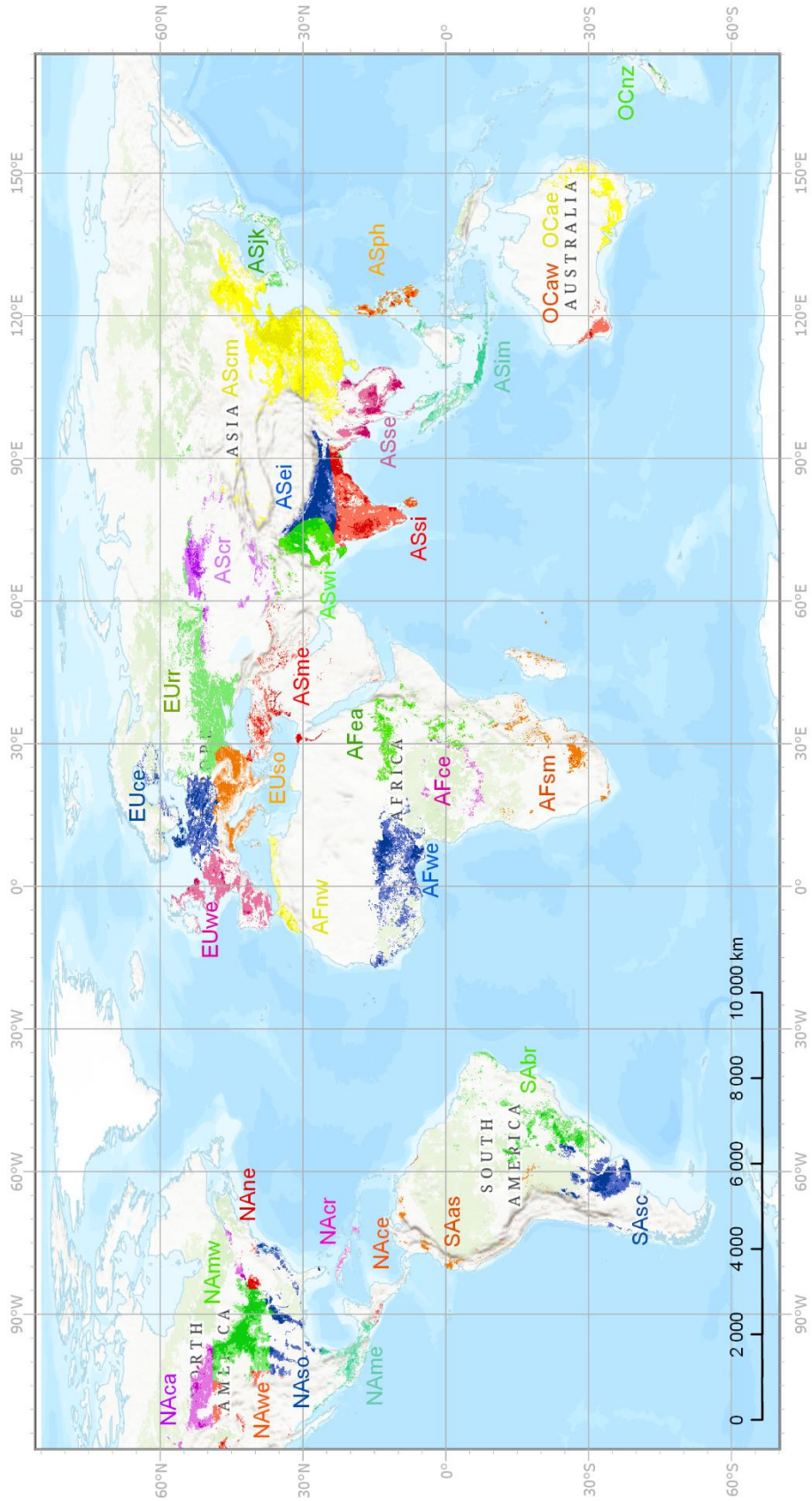

Figure 3. Division of the world into the agricultural super regions. Colored abbreviations—names of the regions as in Study Areas and Methods

3.2. Global annual variation of bare soil

The annual variation of bare soil as a result of the planting of barley, cassava, cotton, groundnut, maize, millet, potato, rapeseed, rye, sorghum, soybean, sugar beet, and wheat is presented in Figure 4. The maximum of almost 1.5 million km^2 is reached around the 140th day of the year (DOY) and is flanked by two peaks, one of around 900,000 km^2 preceding the maximum around the 95th DOY and the other one occurring after the maximum around the 180th DOY and reaching about 700,000 km^2 (Figure 4). This period, related to summer in the northern hemisphere, is then followed by a period of relatively low amount of less than 200,000 km^2 of bare soil starting around the 220th DOY and lasting until the 320th DOY, when the amount of bare soil rises again, to just short of 700,000 km^2 which is related to the planting happening mostly in the southern hemisphere.

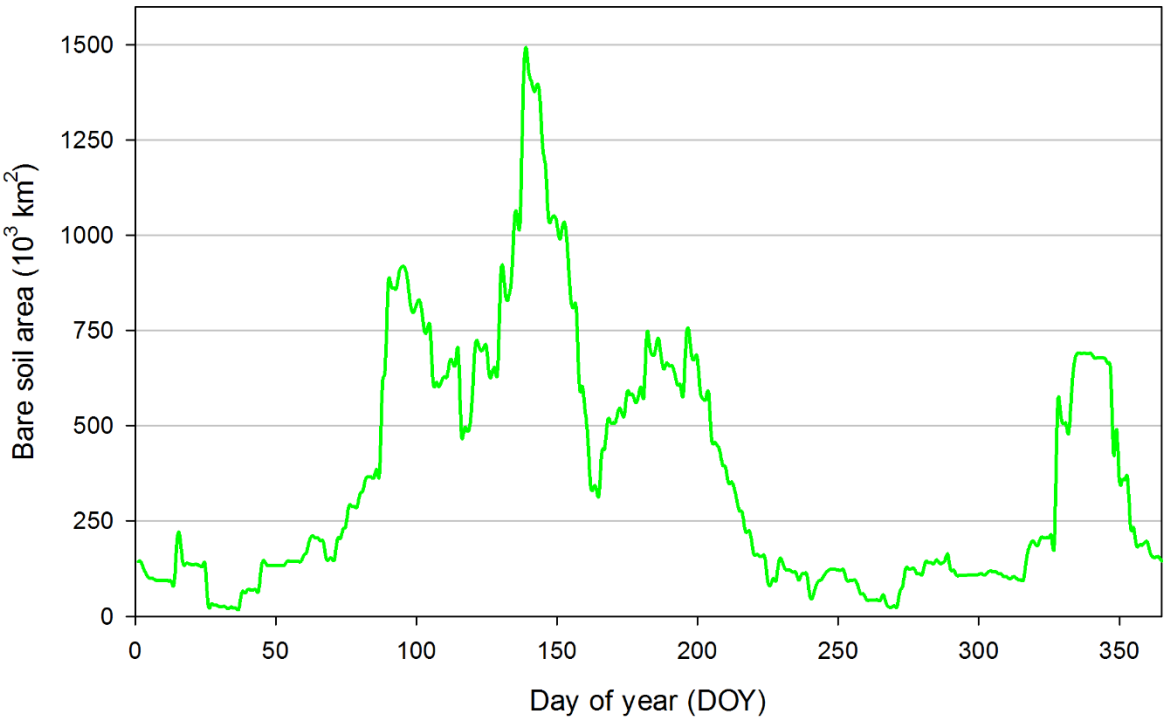

Figure 4. Annual variation of the bare soil area on a global scale.

Globally, among the 13 crops included in this work, the largest farmed area belongs to wheat, followed by maize, taking 34% and 21%, respectively (Table 2). After these, barley is farmed on 8.5% of analyzed land, sorghum and soybeans each making just short of 6%, then millet and cotton having each around 5%. Rapeseed is being farmed on shy of 4% of the area, groundnuts on a little more than 3%, followed by other crops, right up to the moment that their development covers more than 15% of the surface, which are also listed.. Note that in

cases of millet and groundnuts those periods were estimated only as a number of days, as the GDD values were not found.

Table 1. Both relative and absolute areas being farmed for 13 major crops, and baseline and target GDD values used to predict periods of bare soil after planting.

	Area		GDD	
Crop	(%)	(thousands km^2)	baseline (°C)	target
Wheat	34.6	2218.78	5	170–220
Maize	20.8	1334.02	10	264–476
Barley	8.5	541.64	5	145–184
Sorghum	5.9	376.63	10	500–575
Soybean	5.8	369.21	10	250–300
Millet	5.1	327.61	NA	35–45 (days)
Cotton	4.9	313.11	0	400
Rapeseed	3.7	240.09	8	411–463
Groundnuts	3.3	208.49	NA	21–28 (days)
Potato	3.0	190.01	8	500–600
Cassava	2.1	135.90	10	220–300
Rye	1.4	88.91	5	170–200
Sugar beet	1.0	62.62	1	335–476

The soil units used for agriculture presented here are classified according to FAO–UNESCO on the 1st level (Table 2). The soil unit most commonly used in agriculture is *Luvisol*, covering over 16% of arable land, and can be found on every continent. With its good drainage, rich nutrient content and mixed mineralogy, it is suitable for a wide range of agriculture. *Chernozems* are one of the most fertile soils, rich in humus, phosphorus, ammonia and have high moisture-storage capacity and are the second most used soil in agriculture, making up just more than 10% of arable land. The third most widely farmed type of soil is *Lithosol*, found predominantly in mountainous regions, with almost 10% coverage of arable land. Even though *Lithosols* are shallow, poorly mineralized soils, they can be productive and fertile (Tekwa and Shehu, 2011). *Cambisols* is the fourth most commonly found soil grouping, with a share of almost 10%. They are characterized by favorable aggregate structure and high quantities of weatherable minerals, making them very desirable for agriculture. They occur in

a range of climates, most notably in temperate and boreal regions that were covered by glaciers, as well as in regions with active geologic erosion. *Kastanozems* is a soil grouping characterized by rich humus and calcium content, found mostly in dry climates. Making up over 6% of arable land, they are commonly used in agriculture but usually require irrigation. *Gleysols* are an example of azonal soils present in nearly any climate, found in depressions and low landscape. Naturally occurring *Gleysols* are wet soils, but after artificial drying, they are fertile and useful for agriculture. *Arenosols* are sandy soils, characterized by poor water-holding capacity and are poor in nutrients. Nonetheless, they can be productive if treated with proper fertilization and are therefore farmed on around 5% of arable land. *Phaozems,* constituting over 4% of arable land, are valuable in agriculture for their rich content of humus and calcium. *Fluvisols* is another example of azonal soil, in this case, found in alluvial deposits along rivers and lakes, which cover short of 5% of the arable land surface. The high fertility of alluvial soil is known to humanity since the beginnings of agriculture. *Xerosols* that are found on over 4% of arable land is a soil grouping found in arid climates, with the potential to be highly fertile if proper irrigation is implemented. *Acrisols* make up about 4% of arable land, occurring mostly in humid, tropical regions. They are acidic soils rich in clay content, adopted for the farming of acid-tolerant crops. They make up around 6% of global arable land. *Vertisols* are a product of vertical mixing of soil particles due to repeating patterns of wetting and drying. With their high level of nutrients, they have potential to be fertile, but require intensive management due to high clay content. They make up less than 4% of arable land. Similar to the aforementioned *Xerosols, Yermosols,* found on about 3% of arable land, is a soil grouping found in arid climates, with high fertility if irrigated. *Ferrasols* are characteristic red soils found most often in tropical, humid climates. Their color and name are both the result of the high content of metal oxides, principally iron and aluminum. In global agriculture, they make up around 3% of arable land. *Histosols,* which is found on about 2.5% of arable land, is a soil grouping rich in organic matter. *Nitosols* is the soil group that is found mostly in tropical and subtropical areas, and perhaps the most fertile soil group in such regions; despite frequently low quantities of phosphorus, these can be productive if properly managed. The last two soil groupings that have a share in global arable land higher than 1% are *Regosols* and *Podzoluvisols.* All the other soil units were found in less than 1% of arable land globally, but their contribution to arable land in particular regions can be higher.

Table 2. Absolute and relative areas of major soil groupings found on arable land at the global scale.

Soil Grouping	Area (%)	Area (thousands km^2)
Luvisol	16.93	1078.9
Chernozem	10.12	645.2
Lithosol	10.06	641.3
Cambisol	9.43	601.15
Kastanozem	6.35	404.9
Gleysol	5.43	346.2
Arenosol	4.69	299.2
Phaeozem	4.33	276.2
Fluvisol	4.30	273.9
Xerosol	4.28	272.8
Acrisol	4.04	257.3
Vertisol	3.90	248.8
Yermosol	3.08	196.5
Ferrasol	2.85	181.5
Histosol	2.55	162.5
Nitosol	1.80	115
Regosol	1.64	104.8
Podzoluvisol	1.40	89
Solonetz	0.86	54.9
Planosol	0.76	48.4
Podzol	0.51	32.8
Rendzina	0.28	18.1
Andosol	0.20	12.7
Ranker	0.19	12.4

3.2.1. Northern hemisphere

The entirety of arable land found in the super regions of Europe and North America, all of the Asian regions except ASim, parts of the SAas from South America and the whole African region of AFnw with parts of AFce and AFea are encompassed in the northern hemisphere. The annual variation of bare soil area of arable land (Figure 5) found in that delimitation is dominated by an episode starting on the 92nd DOY and ending on the 200th DOY (beginning of April until end of July). Three distinct peaks are noticeable during that period, the highest one on the 140th DOY (second half of May) coincides with extensive planting in Europe, Asia and North America resulting in almost 1.5 million km^2 of bare soil. Almost 900,000 km^2 of arable land is bare around the 100th DOY (beginning of April) as a consequence of planting primarily in Asia and Europe. The last of the three major peaks achieves just short of 750,000 km^2 between the 185th and the 196th DOY (first half of July), caused primarily by planting in Asia and reinforced by planting in arable land located in parts of Africa lying in the northern hemisphere.

Wheat is the crop with by far the largest share of area dedicated for its cultivation, with almost 40% of analyzed land sporting this plant (Table 3). A bit over half of that area is used for maize with a share of over 20%; halving this area again gives us the share of land used for the cultivation of barley (9%). Plantations of cotton, sorghum, and millet occupied similar areas of land between them, each found on about 5% of arable land in the northern hemisphere. A significant share of the area was also dedicated to rapeseed, potatoes groundnuts and soybeans with a share of around 4%, 3%, 3%, and 2%, respectively. Rye, cassava, and sugar beet were present but each of these was farmed on less than 2% of the analyzed area.

Similar to the results for the whole globe, the most common soil grouping used in agriculture is *Luvisol*, with over 15% of arable land in the northern hemisphere belonging to that grouping (Table 4). *Chernozems* are also used extensively, with an eighth of arable land encompassed by that grouping, largely due to Europe and North America. *Cambisols* and *Lithosols* both have a share of about 11%, followed by *Kastanozems* and *Gleysols* that occupy around 7% of arable land in the northern hemisphere. Similar shares of about 4% were observed for *Xerosols, Fluvisols,* and *Acrisols*, while *Yermosols, Vertisols, Histosols, Phaozems* and *Arenosols* each occupied around 3% of that area. The remaining soil groupings had an

individual share of lower than 2%, while *Planosols* were not found at all on arable land in this hemisphere.

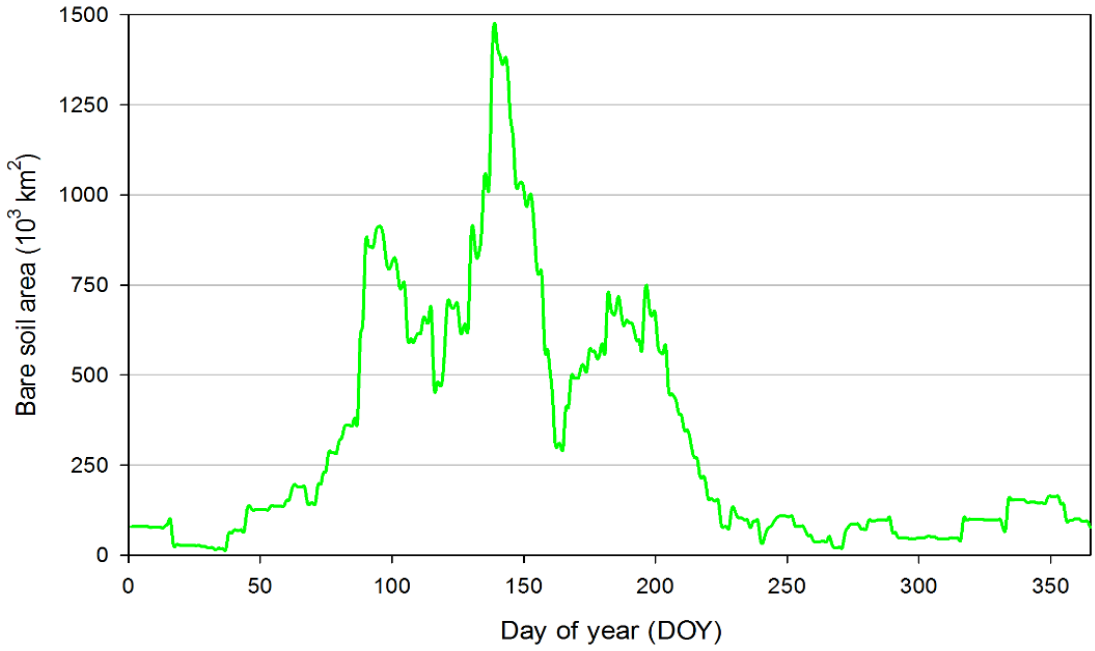

Figure 5. Annual variation of bare soil area of arable land in the northern hemisphere

Table 3. Area and share of major crops on arable land in the southern hemisphere.

Major crop	Area (thousands km^2)	Area (%)
Wheat	1960	37.6
Maize	1063.9	20.4
Barley	487.1	9.4
Cotton	279.8	5.4
Sorghum	266.6	5.1
Millet	241.6	4.6
Rapeseed	229	4.4
Potato	176.5	3.4
Groundnut	164.2	3.2
Soybean	123	2.4
Rye	87.8	1.7
Cassava	67.8	1.3
Sugar beet	61.8	1.2

Table 4. Area and share of major soil groupings on arable land in the southern hemisphere.

Soil groupings	Area (thousands km^2)	Area (%)
Luvisol	813.65	15.62
Chernozem	645.2	12.39
Cambisol	595.85	11.44
Lithosol	585.8	11.25
Kastanozem	362.35	6.96
Gleysol	345.5	6.63
Xerosol	238.45	4.58
Fluvisol	230	4.42
Acrisol	223.8	4.30
Yermosol	187.5	3.60
Vertisol	181.3	3.48
Histosol	162.5	3.12
Phaeozem	157.5	3.02
Arenosol	154.35	2.96
Podzoluvisol	89	1.71
Nitosol	82.8	1.59
Regosol	63.2	1.21
Podzol	32.8	0.63
Rendzina	18.1	0.35
Solonetz	14.1	0.27
Ferrasol	11.45	0.22
Andosol	7.9	0.15
Ranker	6.2	0.12
Planosol	0	0

3.2.2. Southern hemisphere

Arable land in the southern hemisphere spreads over the majority of the South American super region, southern parts of Africa, the whole of Oceania and the ASim region in Asia. Compared to the acreage of bare soil in the northern hemisphere, the maximal area of bare soil is over three times smaller, reaching 400,000 km^2 between the 335th and the 346th DOY (first half of December)(Figure 6). That peak is preceded by a period of increasing acreage of bare soil that starts around the 275th DOY (beginning of October) during which the area slowly rises to about 100,000 km^2 by the 327th DOY (second half of November) after which it quickly skyrockets to the aforementioned maximum, resulting primarily from the planting of maize in South America, after which it falls again. The other distinct peak occurs between the 15th and the 25th DOY (second half of January), with the bare soil area at that time just below 100,000 km^2. Other instances of bare soil were spotted around the middle of the year, between the 141st and the 170th DOY (middle of May to middle of June), caused mostly by the planting of wheat in Australia.

Three major crops dominate the agriculture of the southern hemisphere: maize, wheat and soybeans, each of them with a share of arable land of over 20% (Table 5). Maize, which is the crop with the greatest area under cultivation in this hemisphere is planted primarily in South America and Africa, while the share of wheat is elevated by extensive farming in Oceania, with large areas also in South America and Oceania. Sorghum and Millet are farmed on about 10% and 7%, respectively, both largely due to farming areas in Africa. Unlike in the northern hemisphere, significant areas are dedicated to the cultivation of cassava (about 6%), mostly in Africa but also in South America. A similar area of about 5% is used for growing barley, mostly in Oceania. The farming of groundnuts results in their share of arable land reaching about 4%, largely due to Africa. The last major crop with a significant share of arable land is cotton, farmed both in Africa and South America.

As in the case of the northern hemisphere, the *Luvisols* are the most dominant major soil grouping in agriculture, making up almost 30% of arable land in the southern hemisphere (Table 6). *Ferrasols* with a share of almost 20% is the second most common grouping, recognized for its characteristic reddish color, especially common in South America. *Arenosols* and *Phaozems* have respective shares of about 16% and 13%, the former mostly in Africa while the latter is found extensively in Argentina. *Vertisols*, *Lithosols,* and *Planosols* have each a

share of between 10% and 5%, while *Fluvisols*, *Kastanozems, Regosols,* and *Solonetz* all occupy similar areas, with a share of just below 5%. The remaining arable area is divided almost equally between *Xerosols, Acrisols* and *Nitosols,* each with a share of over 3%, and the remaining soil units have a minuscule share: *Yermosols, Rankers, Cambisols, Andosols,* and *Gleysols*. The soil groupings not listed above were not found within arable land in the southern hemisphere; those are *Chernozems, Histosols, Podzosols, Podzoluvisols,* and *Rendzinas*.

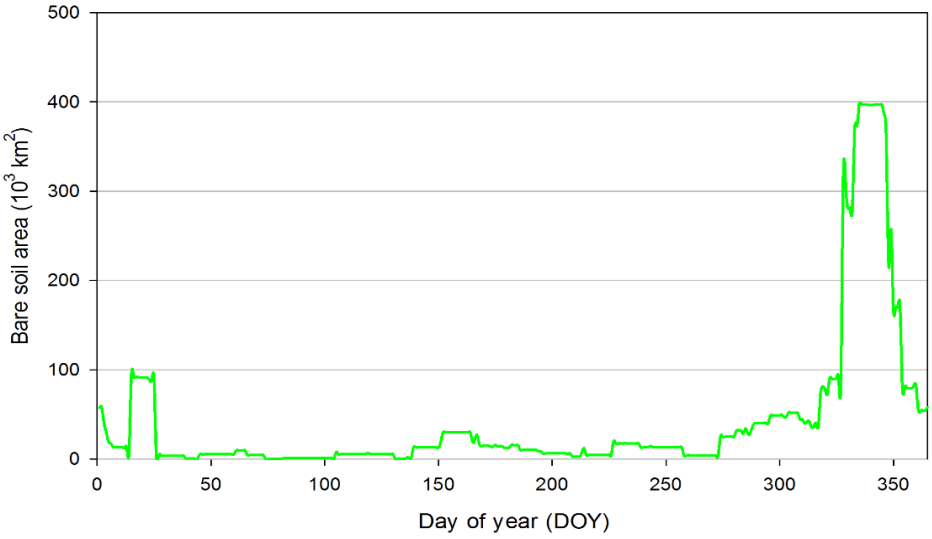

Figure 6. Annual variation of bare soil area of arable land in the southern hemisphere.

Table 5. Area and share of major crops on arable land in the southern hemisphere.

Major crop	Area (thousands km^2)	Area (%)
Maize	270.2	22.6
Wheat	258.8	21.6
Soybean	246.2	20.6
Sorghum	110	9.2
Millet	86.1	7.2
Cassava	68.1	5.7
Barley	54.6	4.6
Groundnut	44.3	3.7
Cotton	33.4	2.8
Potato	13.5	1.1
Rapeseed	11.1	0.9
Rye	1.2	0.1
Sugar beet	0.8	0.1

Table 6. Area and share of major soil groupings on arable land in the southern hemisphere.

Soil groupings	Area (thousands km^2)	Area (%)
Luvisol	265.25	29.47
Ferrasol	170.05	18.89
Arenosol	144.85	16.09
Phaeozem	118.7	13.19
Vertisol	67.5	7.50
Lithosol	55.5	6.16
Planosol	48.4	5.37
Fluvisol	43.9	4.87
Kastanozem	42.55	4.72
Regosol	41.6	4.62
Solonetz	40.8	4.53
Xerosol	34.35	3.81
Acrisol	33.5	3.72
Nitosol	32.2	3.57
Yermosol	9	1.00
Ranker	6.2	0.68
Cambisol	5.3	0.58
Andosol	4.8	0.53
Gleysol	0.7	0.07
Chernozem	0	0
Histosol	0	0
Podzol	0	0
Podzoluvisol	0	0
Rendzina	0	0

3.3. Africa

The continent of Africa is a great landmass that comprises an area of around 30 million km^2, of which 38% is used for agriculture; however, most of that is used as pasture for grazing of cattle and other animals, and just 8% of Africa's land is arable. The north–south extent of the continent is over 8,000 km, spanning both northern and southern hemispheres, resulting in a diverse range of climates. The African continent was divided into five agricultural regions (Figure 7):

- Northwestern (AFnw)—also called the Maghreb, concentrated around the northwestern coast of Africa. The farming areas in this region are found along the Atlantic and Mediterranean coasts, and in the south are bordered by the immense Sahara desert;
- Western (AFwe)—the western region consists of land found along the Gulf of Guinea, bordered in the north by the Sahara, and is flanked in the east by the tropical rain forest of central Africa;
- Central (AFce)—this region is occupied predominantly by tropical rain forests and is therefore not favorable for agriculture. The notable exception to this is the Congo River and arable land can be found along it;
- Eastern (AFea)—a region spanning eastern Africa, bordered by the Sahara in the north, and in the south by the lakes Tanganyika and Malawi;
- Southern, including Madagascar (AFsm)—the southernmost region delimited in Africa. Bordered in the north by the central and eastern regions, it is the only African region located fully in the southern hemisphere.

The variation of bare soil in the whole of the African region (Figure 8) is dominated mostly by the major crops farmed on the continent (Table 3). Those are maize, sorghum, and millet, each consisting of about 20% of the analyzed crops in the region. Other crops farmed in significant numbers include cassava, groundnuts, and wheat, with shares of 10%, 9%, and 8%, respectively. Cotton and barley are farmed on around 4% of arable land each, while soybeans and potato on about 1%. Due to the continent stretching over northern and southern hemispheres, as well as the equatorial region, there are three distinct peaks of bare soil throughout the year. The most notable one reaches around 350,000 km^2 and starts around the 150th DOY, increases until the 190th DOY and then decreases until the 230th DOY,

together lasting for more than two and a half months, with the largest area of bare soil lasting for around three weeks from the 180th to the 193rd DOY. Another considerably smaller peak of around 120,000 km^2 lasts for close to a month, from the 90th to the 115th DOY. The last notable peak is the smallest of the three, reaching close to 60,000 km^2, and was found starting around the 318th DOY and lasting all the way to the 3rd day of the following year. This last peak is attributed mostly to the southern region and to spring planting around that time. The contribution of particular crops to those values is presented while analyzing each region in detail.

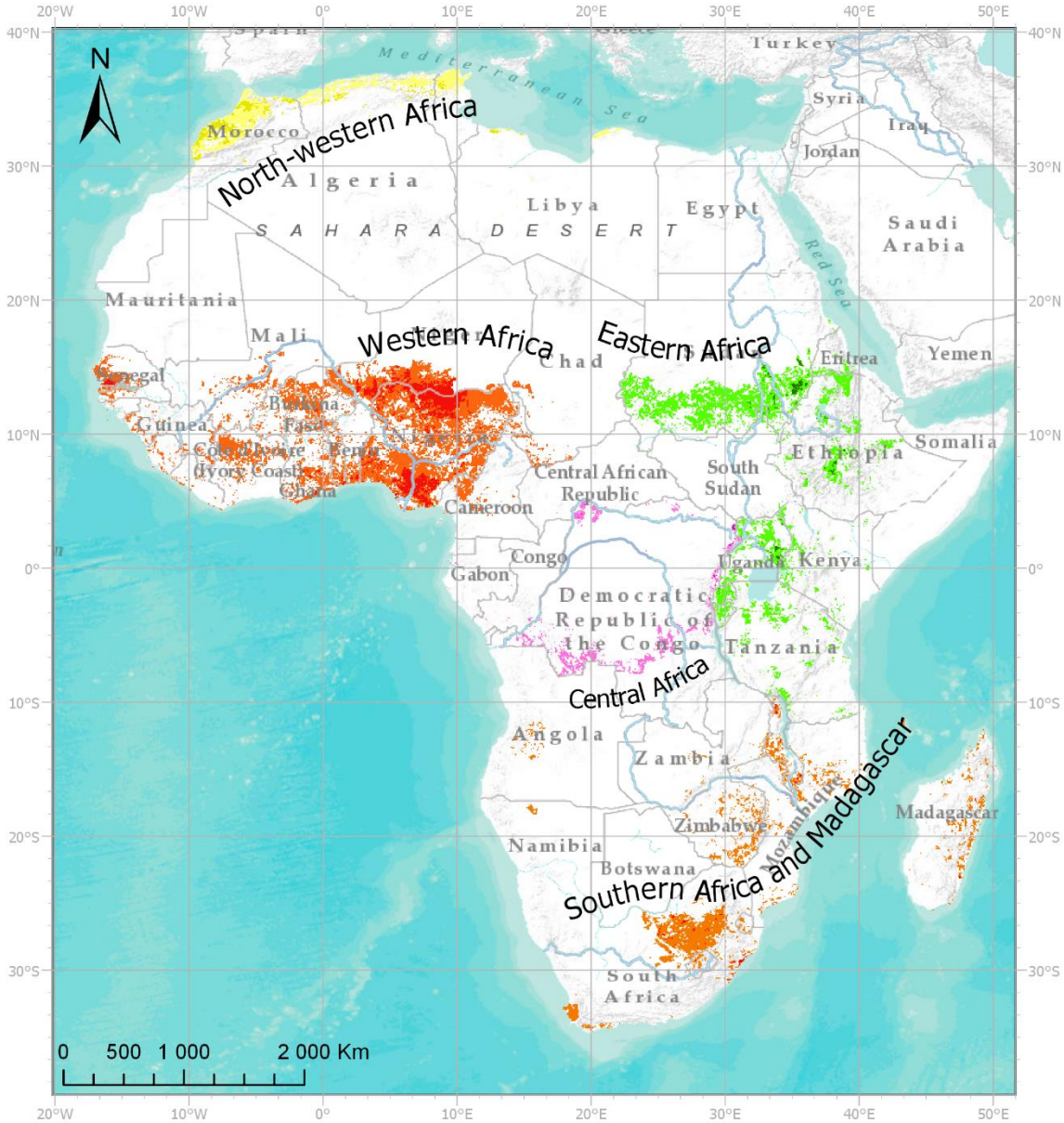

Figure 7. Arable land in Africa super region divided into regions.

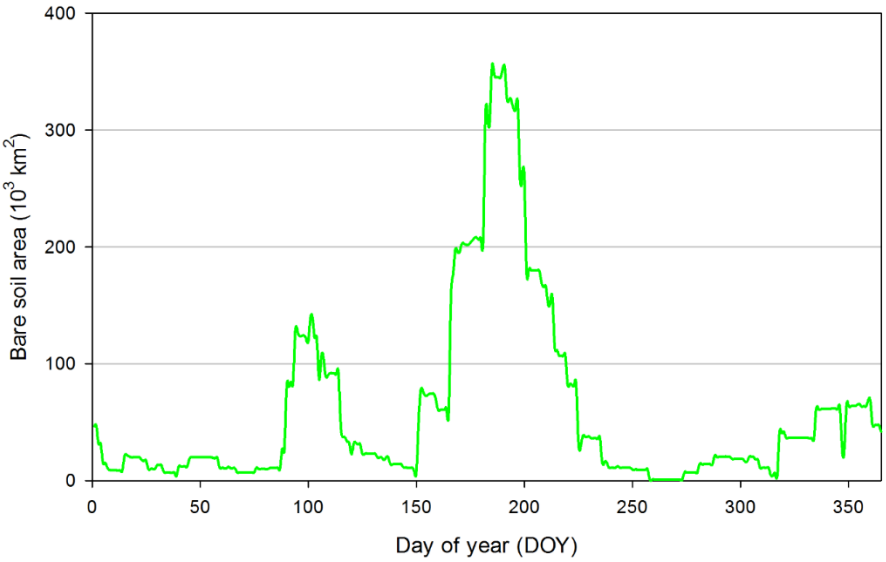

Figure 8. Annual variation of bare soil area in Africa super region.

Table 7. Area and share of arable land of major crops farmed in Africa.

Major crop	Area (thousands km^2)	(%)
Maize	211.1	23.4
Sorghum	190.8	21.1
Millet	171.5	19
Cassava	93.2	10.3
Groundnut	79.9	8.8
Wheat	68.4	7.6
Cotton	34.9	3.9
Barley	34.7	3.8
Soybean	9	1
Potato	8.4	0.9

3.3.1. Northwestern Africa

Agriculture is limited in northwestern Africa, found only along the Mediterranean and Atlantic coasts in any significant acreage, being limited by the Sahara Desert and Atlas Mountains (Figure 9). Most of the arable land in this region belongs to either Morocco or Tunisia, with both countries practicing CA, but only on 8,000 and 4,000 ha, respectively, so it has no significant influence on the bare soil variation (Figure 10).

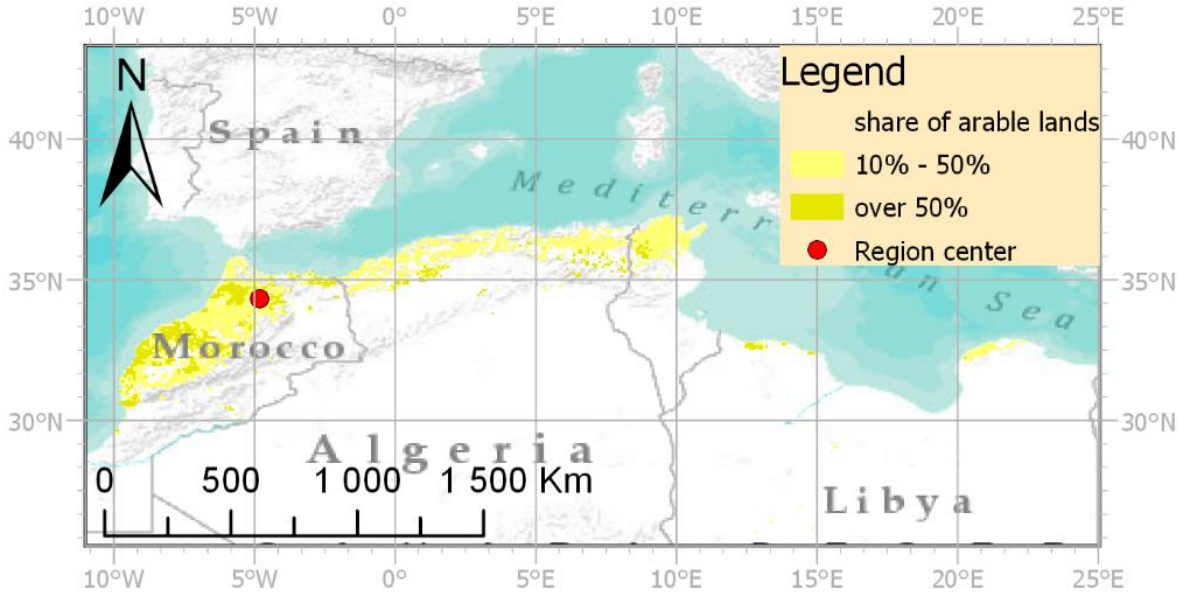

Figure 9. Distribution of arable land in the Northwestern Africa region.

The major soil groupings used for agriculture in AFnw are *Cambisols*, occupying almost a third of arable land, followed by *Luvisols* and *Kastanozems*, each taking about 14%, then *Xerosols*, *Fluvisols,* and *Vertisols* with 11%, 8%, and 6% area coverage, respectively (Figure 11). The remaining 15% is split between nine more soil groupings, none of which occupy a significant portion of arable land in the region. Among the analyzed crops, all but cassava was found being farmed (Figure 12). The overwhelming majority of arable land is used for farming of two cereals, wheat (60%) and barley (33%), followed by much smaller areas of maize (3%) and potatoes (2%). The remaining 2% is split between all the other crops except cassava. The point used for obtaining average daily temperatures used to calculate GDD was located at 34° north and 5° east, which is located in the Moroccan agricultural heartland, some 150 km south of the Strait of Gibraltar. Those daily T_{avg} (average daily temperatures) oscillate between 15°C in winter and 25°C in summer, making the accumulation of GDD quite rapid, therefore

resulting in brief periods of bare soil (Figure 13). The biggest share of the area is dedicated to farming wheat, which is sown as early as the 45th DOY; however, the majority of wheat is sown between the 91st and the 94th DOY, resulting in almost 70,000 km^2 of bare soil at that time. The planting days of barley are similar to those of wheat, with some barley being planted around the 46th DOY, but most barley is planted between the 80th and the 88th DOY, one to two weeks before the planting of wheat. Those two crops explain most of the bare soil variation in the region, with the wheat taking longer to develop. Around the time the crops are planted, wheat requires around three weeks to cover bare soil, while barley takes around two weeks. The first bump of bare soil found around the 45th DOY is slightly reinforced by the sowing of maize, which happens mostly around the 46th DOY with the crop taking around eight weeks to cover the surface. The majority of potatoes are planted around the 76th DOY, and with them taking about ten weeks to cover the surface, they raise the bare soil maximum found on the 95th DOY slightly. The effect of the remaining crops on regional bare soil variation is almost negligible. The region's overall contribution to global or even continental bare soil variation is relatively small.

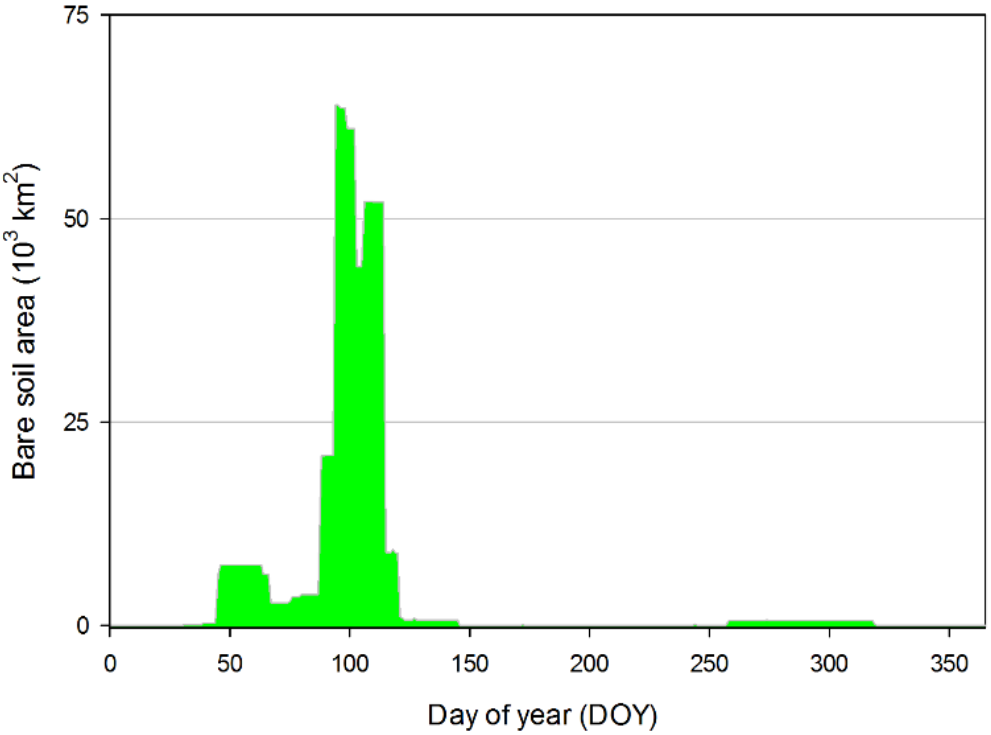

Figure 10. Annual variation of bare soil area in Northwestern Africa region.

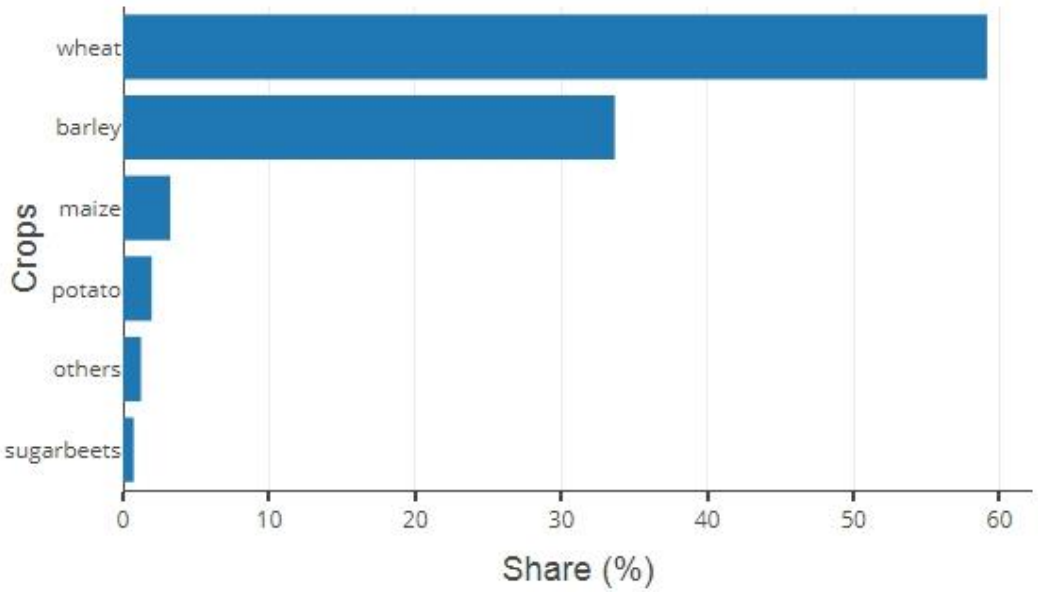

Figure 11. Share of major crops in the Northwestern Africa region.

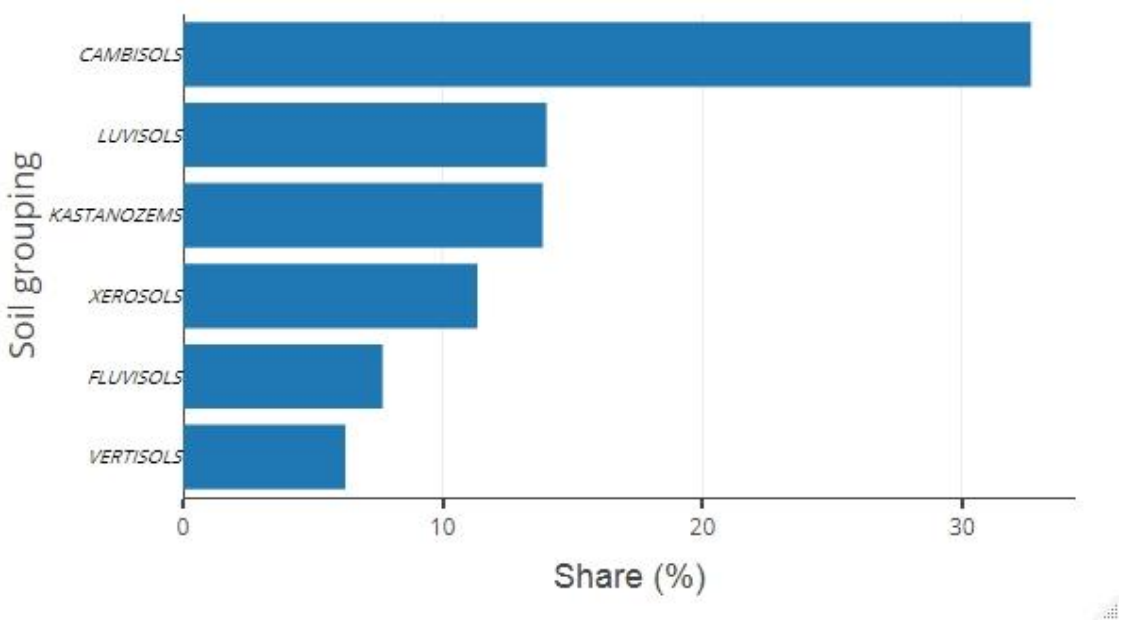

Figure 12. Share of major soil groupings in the Northwestern Africa region.

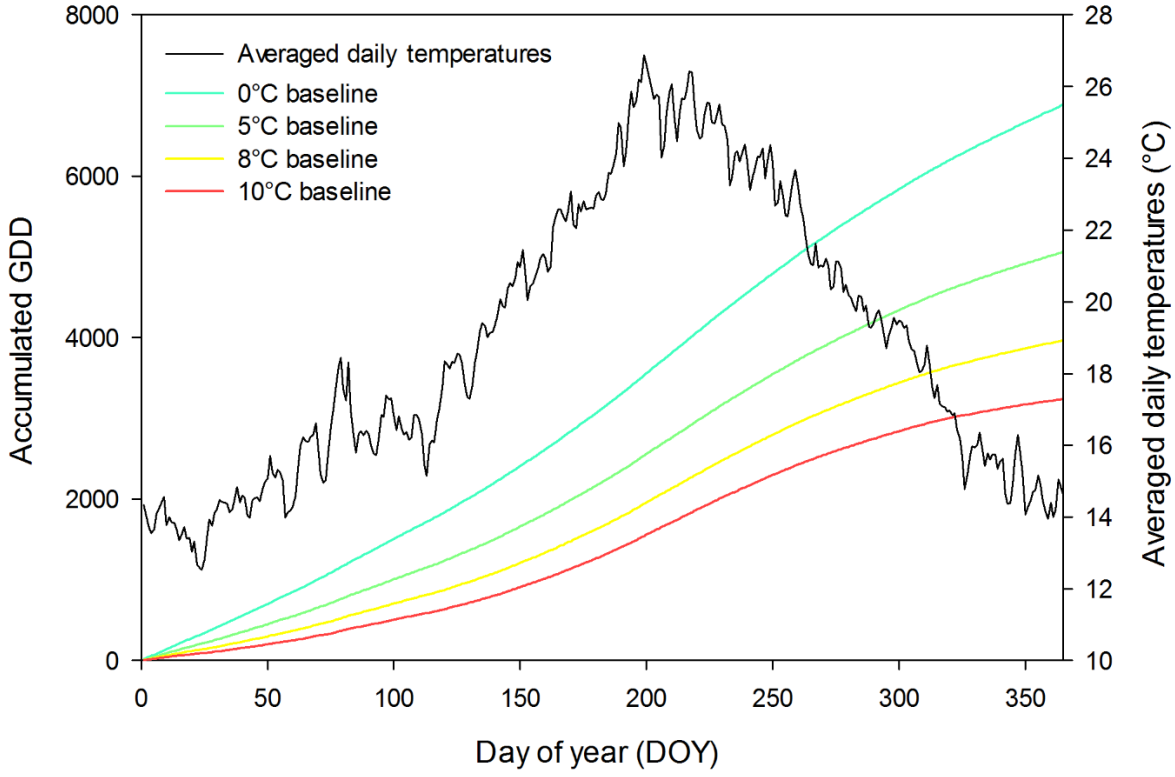

Figure 13. Average daily temperatures and resulting annual GDD accumulation calculated for four baselines in the Northwestern Africa region.

3.3.2. Western Africa

The AFwe has the highest acreage of arable land of all the African regions, having almost as much land dedicated to agriculture as all the other African regions combined. Separated from the AFne region by the Sahara Desert, arable land can be found in the general vicinity of the Gulf of Guinea, along the Niger River, in the northern parts of Nigeria and along the Gambia River in the western part (Figure 14). No instances of CA were reported in this region.

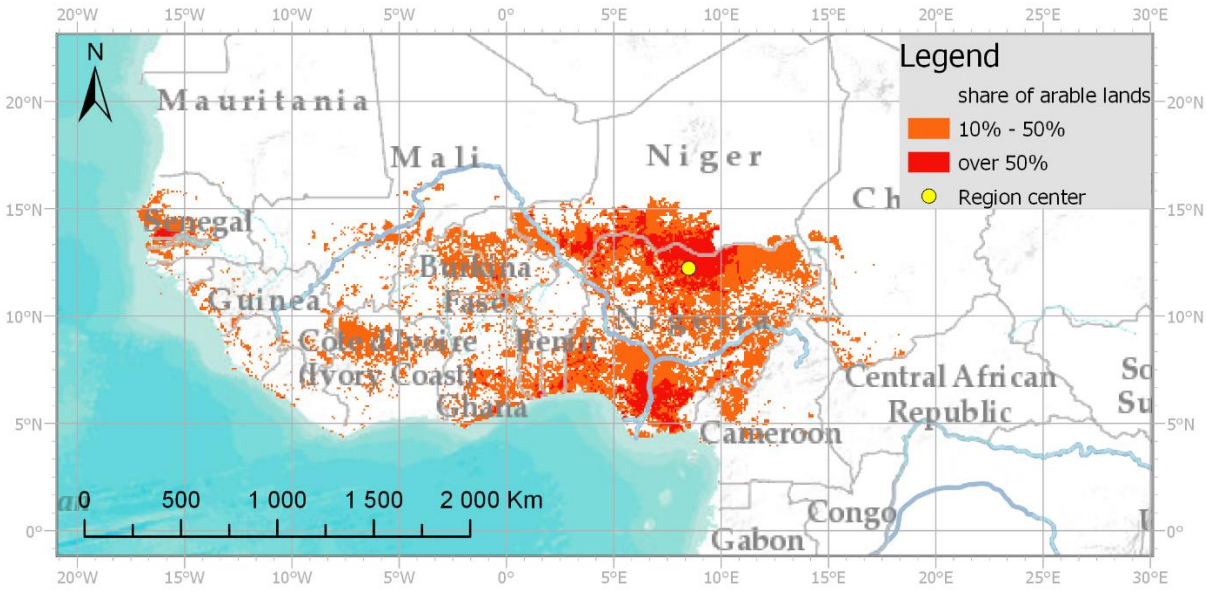

Figure 14. Distribution of arable land in the Western Africa region.

The most common soil groupings used in agriculture in AFwe (Figure 15) are *Luvisols*, followed by *Arenosols* and *Regosols*, which occupy around 37%, 19% and 14% of arable land in the region, respectively. The other two notable soil units are *Lithosols* and *Vertisols*, covering 9% and 6%. The other soil units were only found to occupy small areas. Between the major crops analyzed, two that are farmed on the most arable land are millet and sorghum, farmed on 30% and 26% of analyzed arable land. Both crops are cereals that are well suited to the subtropical climate, characterized by decent drought resistance and tolerance for high-temperature conditions. About 15% of arable land is dedicated to the cultivation of maize, followed by groundnuts and cassava, both with a 10% share of the area. The area used for planting cotton makes up around 5%, and soybeans and wheat, with a share of about 1% each, round up the list (Figure 16). The average daily temperatures were obtained from a spot located at 12° north and 8° east, which correlate to the extensive agricultural region located

in northern Nigeria. With the region located so close to the equator, the temperatures were somewhat stable throughout the year, ranging between 22°C and 32°C, which resulted in rapid GDD accumulation (Figure 17). The variation of bare soil in the AFwe region (Figure 18) is dominated by two crops: millet and sorghum. The main period when soils are bare as a result of planting occurs between the 150th and the 230th DOY, reaching its peak around the 187th DOY, reaching 255,000 km^2 at its maximum. The beginning of that period is marked with the planting of maize and cassava, as well as first batches of millet and sorghum. The planting of millet occurs on various days during that period, with the latest planting observed on the 212th DOY, with the majority of millet being planted between the 167th and the 185th DOY, and requiring from 35 to 40 days to cover the surface. The planting pattern of sorghum in the region is similar to that of millet, with planting occurring between the 152nd and 213th DOY, the biggest share is planted on the 167th DOY. Sorghum was found to take similar, albeit slightly less time to grow than millet, with the field staying bare between 28 and 34 days after planting. That big area of bare soil is preceded by a smaller peak found between the 90th and the 112th DOY, reaching almost 50,000 km^2, or around 20% of the biggest peak. That earlier period of bare soil is caused primarily by the planting of maize, groundnuts, and cassava.

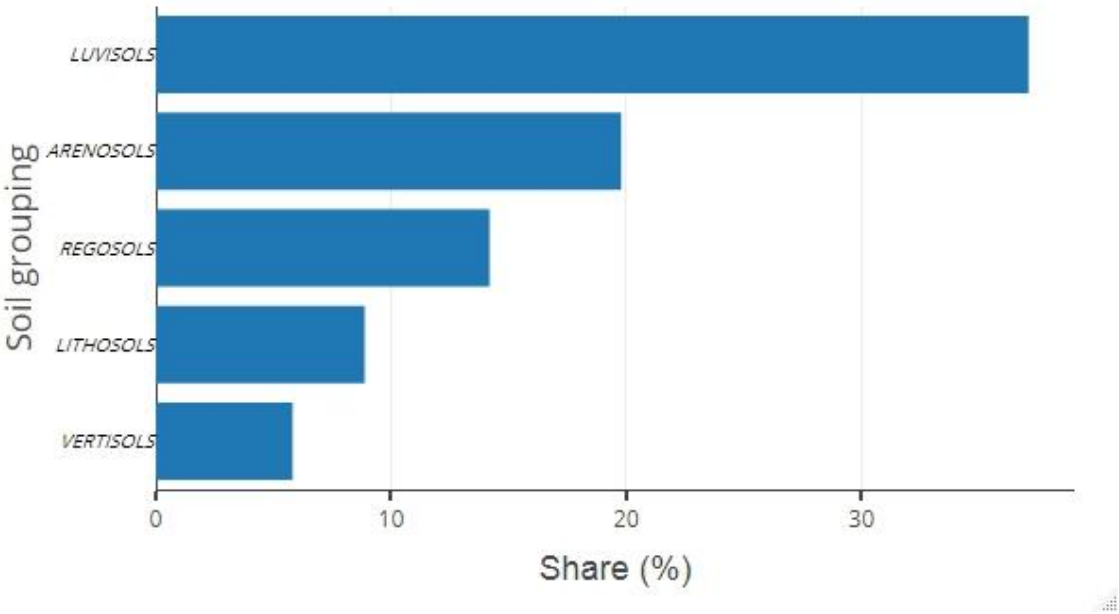

Figure 15. Share of major soil groupings in the Western Africa region.

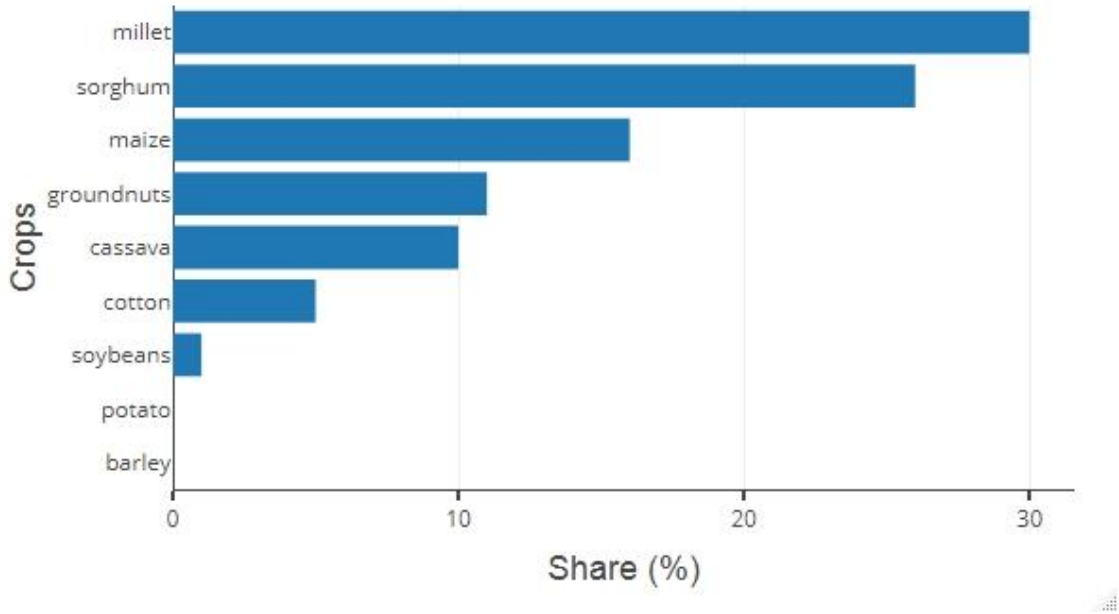

Figure 16. Share of major crops in the Western Africa region.

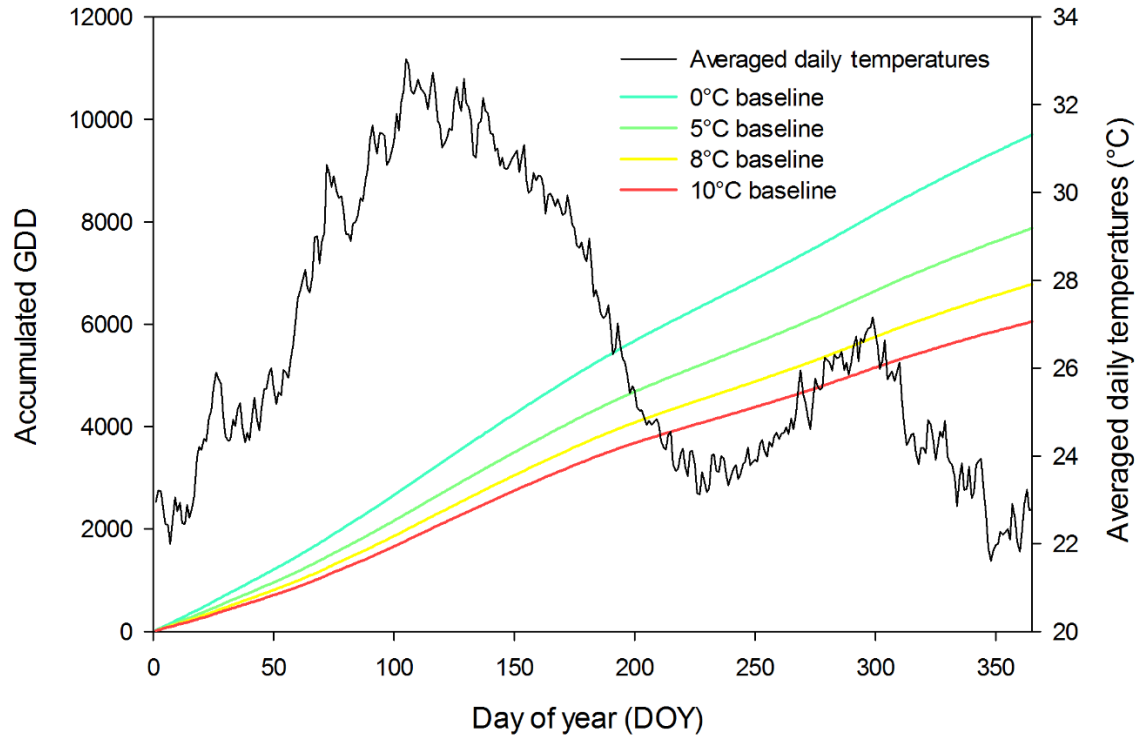

Figure 17. Average daily temperatures and resulting annual GDD accumulation calculated for four baselines in the Western Africa region.

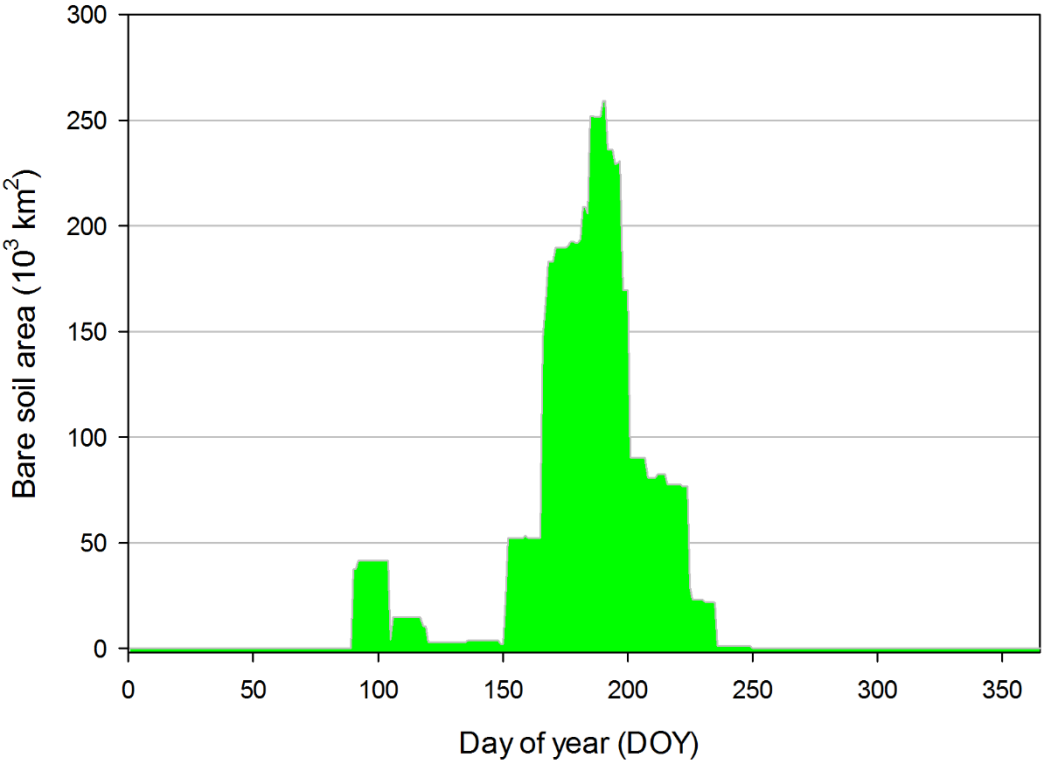

Figure 18. Annual variation of bare soil area in the Western Africa region.

3.3.3. Central Africa

The AFce has the smallest acreage of arable land found among the African regions. The region is located around the equator and almost entirely covered by tropical rain forest. Most of the arable land is found around the Congo River and its tributaries, with a notable concentration around the cities of Kinshasa, Mbuji-Mayi, and Bangui (Figure 19). CA was not found to be practiced in the region.

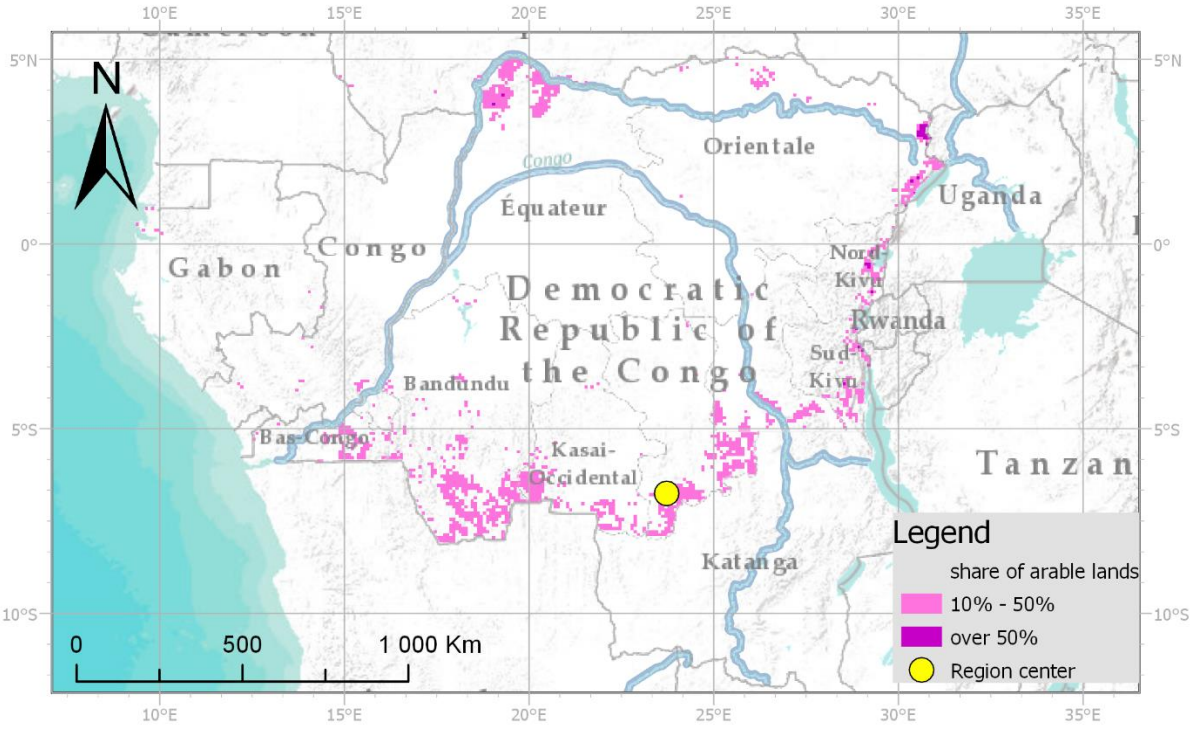

Figure 19. Distribution of arable land in the Central Africa region.

Over half of the arable land in the region is composed of *Nitosols*, with their share of 51% of arable land, the highest of any region. Rankers are the next soil unit, constituting 21% of arable land; worth noting is the fact that AFce is the only agricultural region where Rankers were found to be farmed. The composition of soils is rounded off by *Ferrasols*, *Lithosols*, *Luvisols*, and *Gleysols*, whose contribution to arable land is around 6% for *Ferrasols* and 5% for each of the remaining three (Figure 20). Among the analyzed crops, almost half of the arable land was dedicated to the cultivation of cassava, which has a share of 47%. About a third of arable land is occupied by maize, a share of 33%. Groundnuts are farmed on about 13% of arable land in the region, with a remaining couple of percent split between cotton, sorghum, and millet, taking around 3%, 2% and 1%, respectively (Figure 21). The point which served for the acquisition of average daily temperatures was located at 7° south and 24° east,

which is in the southern part of the region in the middle of the biggest concentration of arable land. With its location so close to the equator, average daily temperatures are very stable throughout the year, oscillating between 22°C and 28°C; therefore the accumulation of GDD has a very linear shape (Figure 22). In the annual variation of bare soil in the region three peaks can be distinguished (Figure 23). The biggest area of bare soil occurs between the 349th DOY and 3rd day of the following year, reaching up to 16,000 km^2, and is caused primarily by the planting of cassava, which takes about three weeks to develop and end the bare soil period. The other two significant peaks occur around the middle of the year. The first lasts between the 160th and the 186th DOY and is caused mostly by sowing cassava, and reinforced by the sowing of groundnuts, maize and sorghum. Together, the bare soil area in this period reaches up to 11,000 km^2. The last significant peak occurs around a month and a half later, between the 213th and the 258th DOY. At that time, the soil stays bare after the planting of groundnuts on the 213th DOY, followed by the planting of maize around the 227th DOY. When those two periods overlap, the area of bare soil reaches 14,000 km^2.

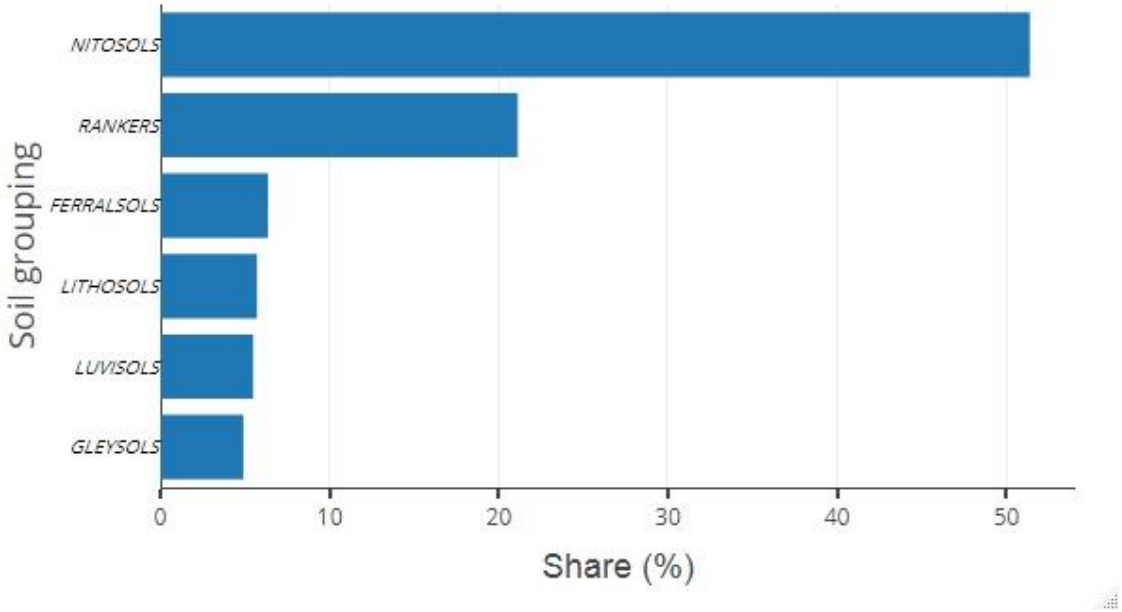

Figure 20. Share of major soil groupings in the Central Africa region.

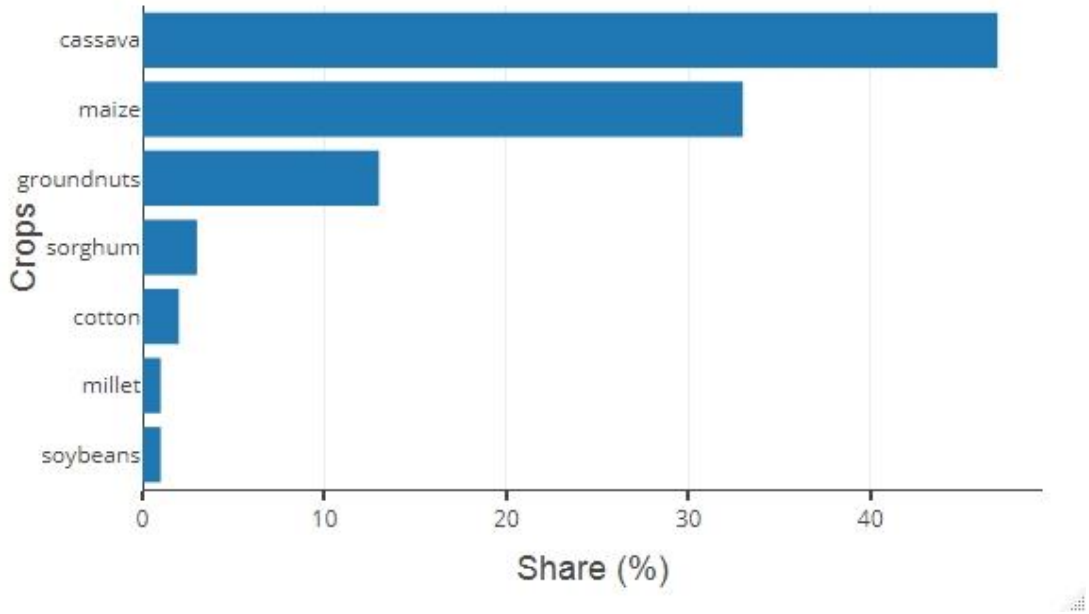

Figure 21. Share of major crops in the Central Africa region.

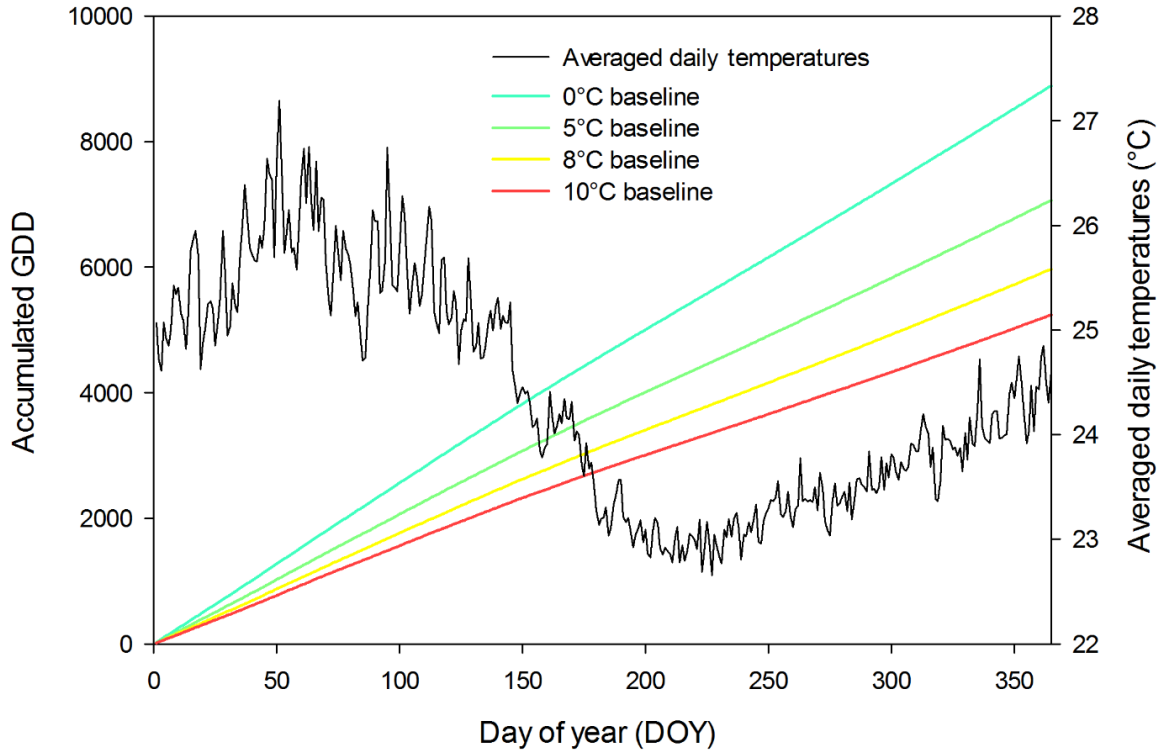

Figure 22. Average daily temperatures and resulting annual GDD accumulation calculated for four baselines in the Central Africa region.

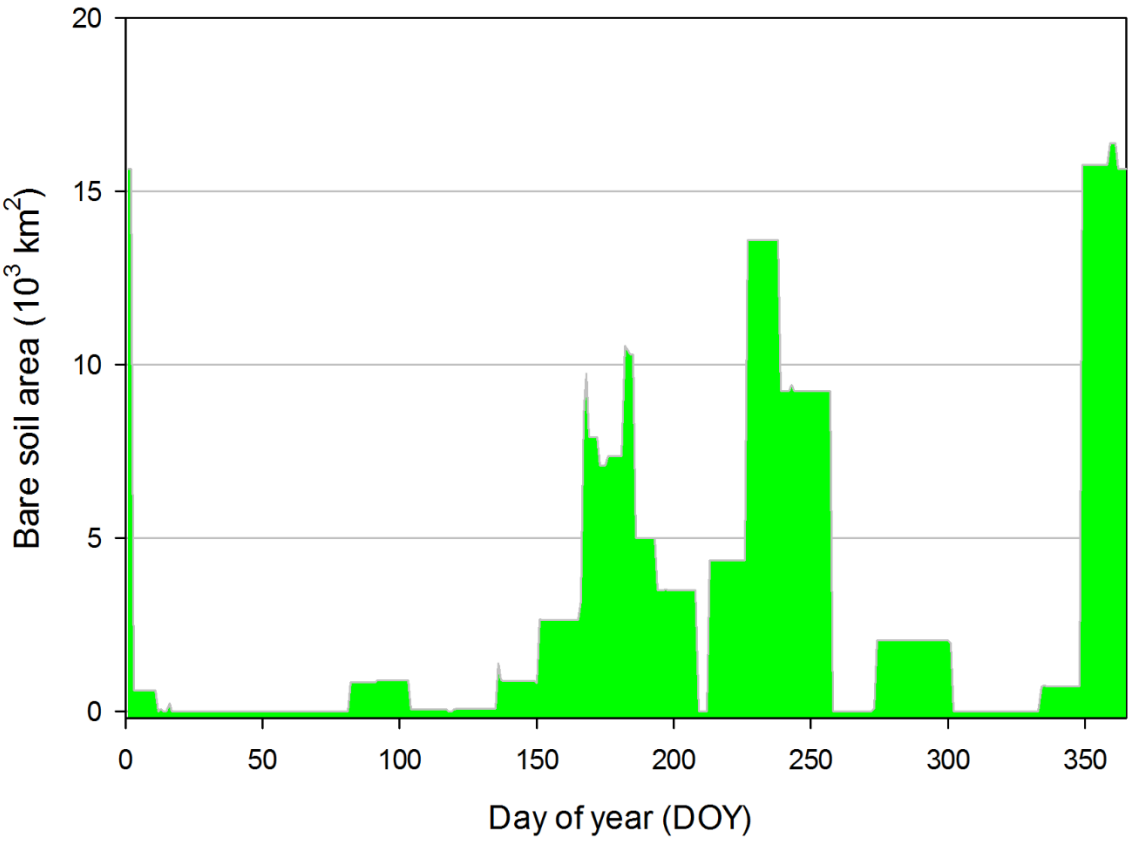

Figure 23. Annual variation of bare soil area in the Central Africa region.

3.3.4. Eastern Africa

The acreage of agriculture in the AFea region is second only to AFwe in the continent. The region stretches from the arable land of southern Sudan in the north all the way to Lake Malawi in the south. The western border rests on the line of lakes, from Lake Albert in the north to Lake Tanganyika in the south. The arable land is more dispersed in the region, the highest concentration is found in a belt spanning southern Sudan and Ethiopia, with other significant concentrations located around the African Great Lakes, primarily around Lake Victoria. Arable land also occupies eastern parts of the region, along the Somali Basin, however in lesser concentration that previously mentioned zones (Figure 24).

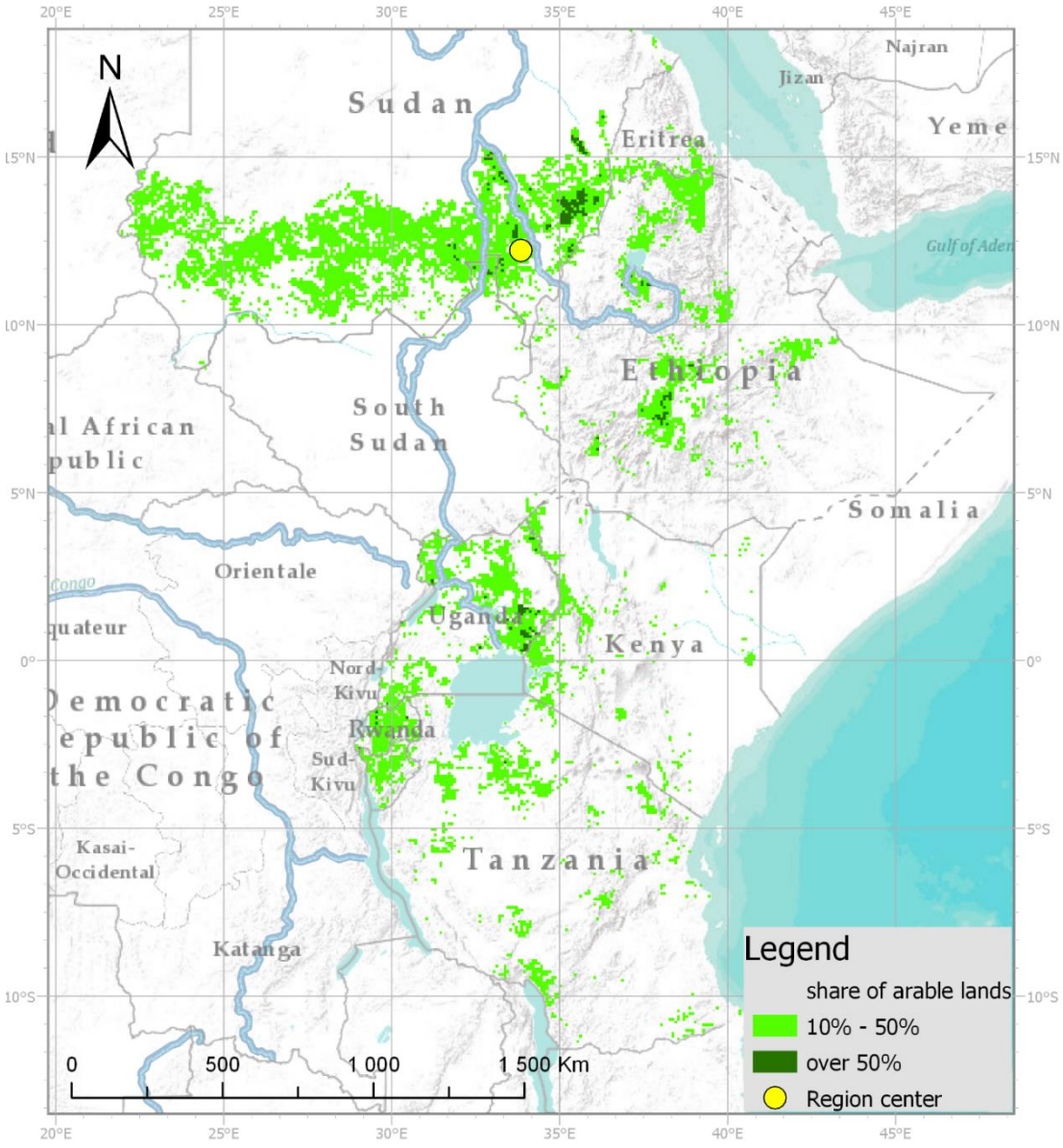

Figure 24. Distribution of arable land in the Eastern Africa region.

Among the soil units found in arable land (Figure 25), the most widespread are *Arenosols* and *Vertisols*, with a share of 22% and 19%, respectively. *Nitosols* occupy around 10%, while *Cambisols* and *Lithosols* are both found on 8% of arable land. The remaining soil units that have significant shares are *Luvisols*, *Acrisols,* and *Ferrasols*, with their respective shares of 6%, 6%, and 5%. Between the analyzed crops (Figure 26), the largest area was dedicated to farming sorghum, making up 33% of arable land in the region. A quarter of the area was used for planting maize (24%), followed by millet with a share of 15%. The remaining crops were farmed on a smaller area; those were 8% groundnuts, followed by wheat and cassava with 5% each, and cotton and barley rounding off the list, each occupying close to 3%. Average temperatures used for estimating annual GDD accumulation were extracted from a point located at 12° north and 33° east, right in the middle of the biggest concentration of agriculture in the region. The mean daily temperatures ranged between 22°C and 32°C, very similar to ones in AFwe. The accumulation of GDD was therefore rapid and stable throughout the year (Figure 27). The shape of the annual variation of bare soil in the region (Figure 28) consists of one big and sharp peak, as well as a period of a gradual increase in bare soil area. The maximum peak reaches about 90,000 km^2 and occurs between the 182nd and the 214th DOY. The peak is caused by the planting of sorghum, millet, and groundnuts, all of which occur at a similar time. Out of those, the biggest area was covered by sorghum, which takes around 32 days to cover the surface, followed by millet, which takes one week longer, and groundnuts taking a similar time to sorghum. The other period of bare soil spans around three months, between the 75th and the 160th DOY, and has an irregular shape, rising and falling repeatedly, reaching around 40,000 km^2 at the maximum. The majority of crops farmed in the region are planted on various days throughout this period.

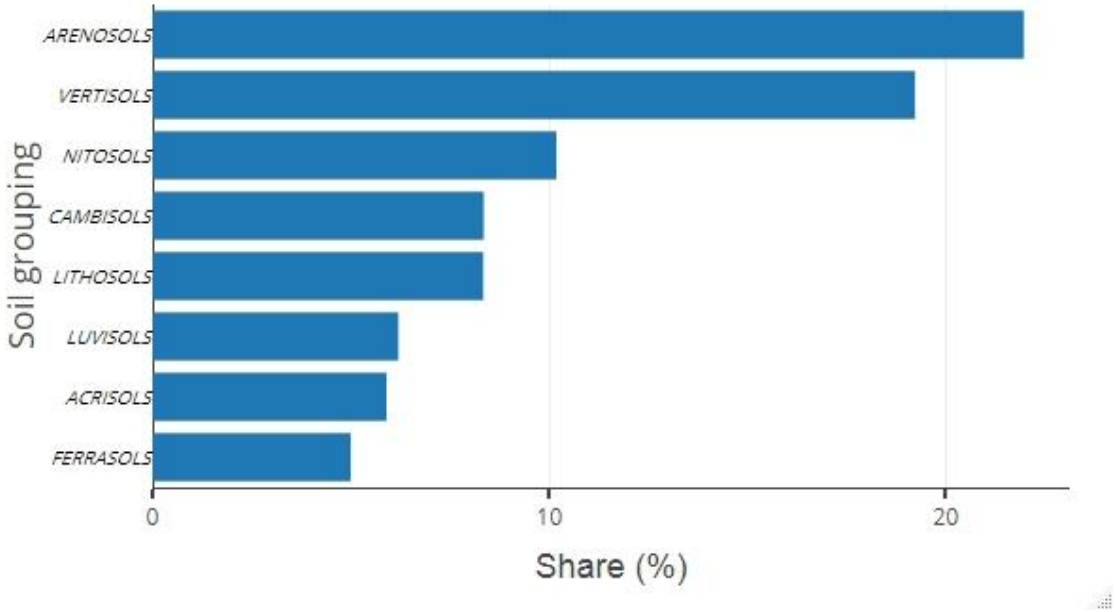

Figure 25. Share of major soil groupings in the Eastern Africa region.

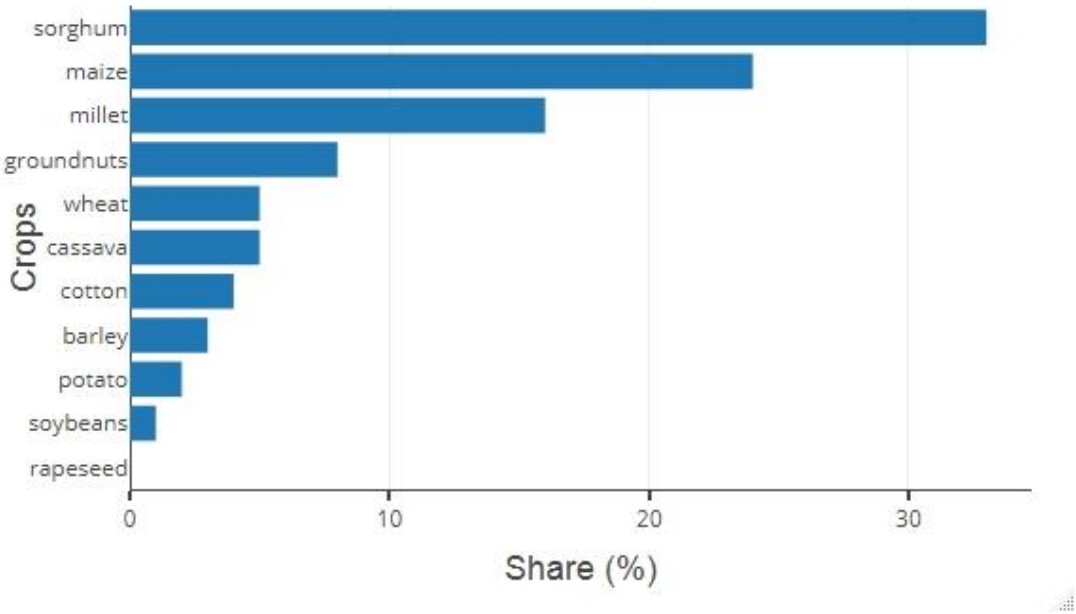

Figure 26. Share of major crops in the Eastern Africa region.

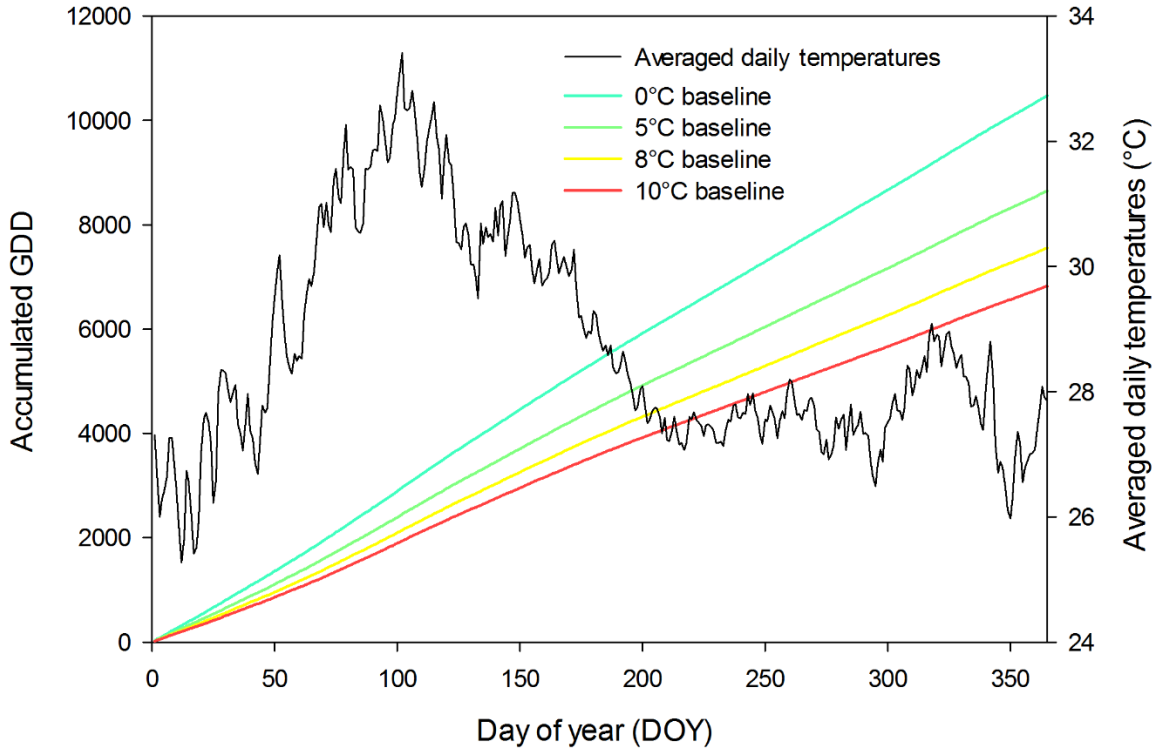

Figure 27. Average daily temperatures and resulting annual GDD accumulation calculated for four baselines in the Eastern Africa region.

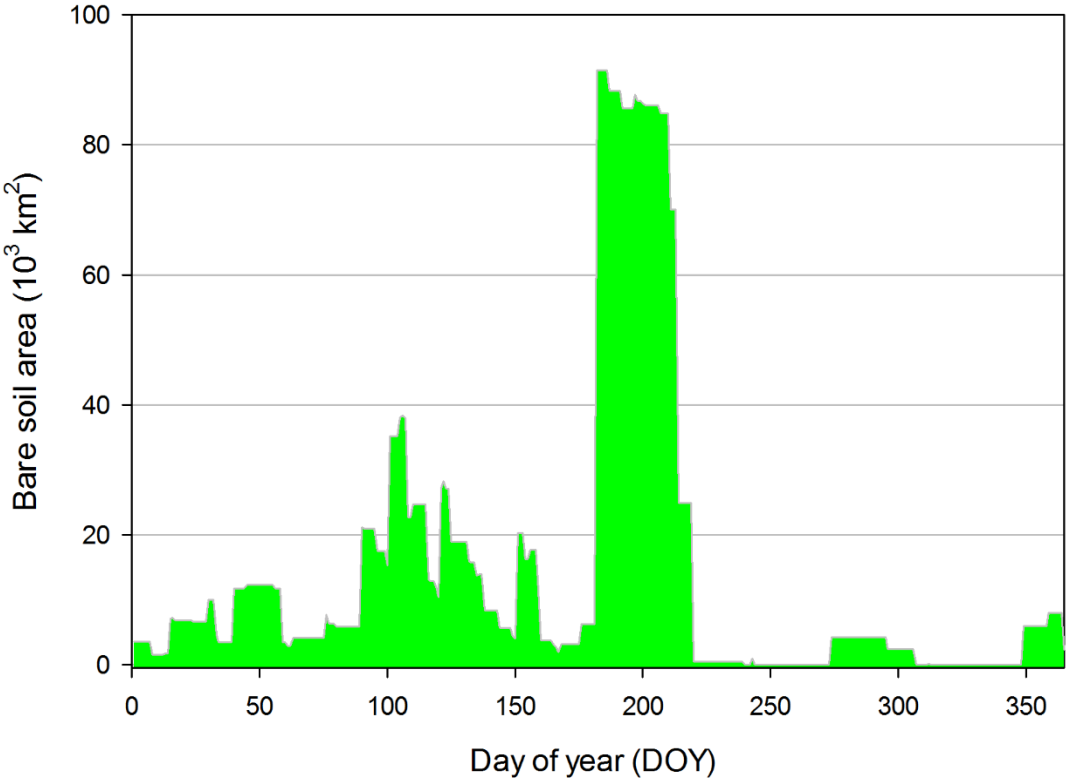

Figure 28. Annual variation of bare soil area in the Eastern Africa region.

3.3.5. Southern Africa and Madagascar

AFsm is the last region included in the African super region. The borders of AFwe and AFea limit the northern extent, while oceans envelop the region from the other sides. Compared to other African regions, the area of arable land is in the middle, smaller than in AFea and larger than in AFnw. The arable land is spread around the region, with the higher concentration found in the eastern parts of South Africa, close to the capital of Pretoria. Other significant regions include the southwestern tip of the continent, around the city of Cape Town, at the Zimbabwean highlands, around Lake Malawi. In Madagascar, agriculture is concentrated around eastern and northern coasts (Figure 29).

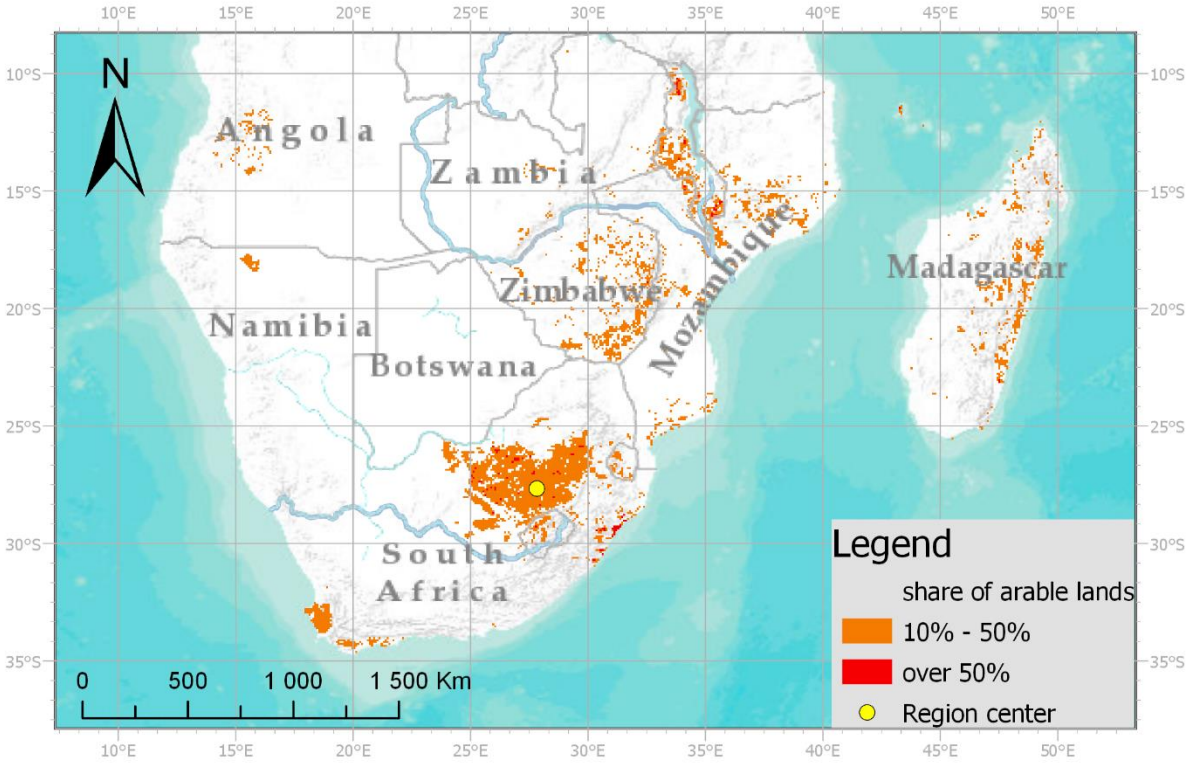

Figure 29. Distribution of arable land in the South Africa and Madagascar region.

The most commonly farmed soil unit in the region (Figure 30) is *Luvisols*, which occupies 34% of arable land, followed by *Arenosols* that are present on 20%. *Fluvisols* can be found on around 16% of farmed land, with *Ferrasols* and *Cambisols* rounding off the list of major soil units with their shares of 8% and 7%, respectively. Over half of the analyzed arable land in the region is dedicated to the cultivation of maize, which occupies 55% of it. No other crop in the region comes even close to that value, with the next being cassava with its 13% share. Shares of the remaining crops are expressed in single digit values, those are wheat 7%,

groundnuts and sorghum 6% each, millet 5% and cotton 4% (Figure 31). Mean daily temperatures were extracted from a point located at 27° south and 28° east, which relates to the biggest agricultural concentration found within the region, between Pretoria and Lesotho. The average daily temperatures range between 11°C and 26°C (Figure 32). The annual variation of bare soil (Figure 33) is characterized by a stable rise in area, starting around the 281st DOY, reaching its maximum around the 335th DOY, and steady falling until bare soil disappears around the 40th day of the following year. The beginning of this period correlates to the planting of maize on the 281st DOY and is regularly reinforced by additional batches of maize planting, happening all the time until the 15th day of the following year. The peak, occurring on the 335th DOY results from the planting of maize and sorghum on this date. A significant portion of arable land is bare following the planting of cassava on the 350th DOY. Maize planted on the aforementioned dates was found to take between four and five weeks to cover the surface, sorghum taking a bit longer, between five and six weeks, and for cassava planted at the end of the year it was two and a half weeks.

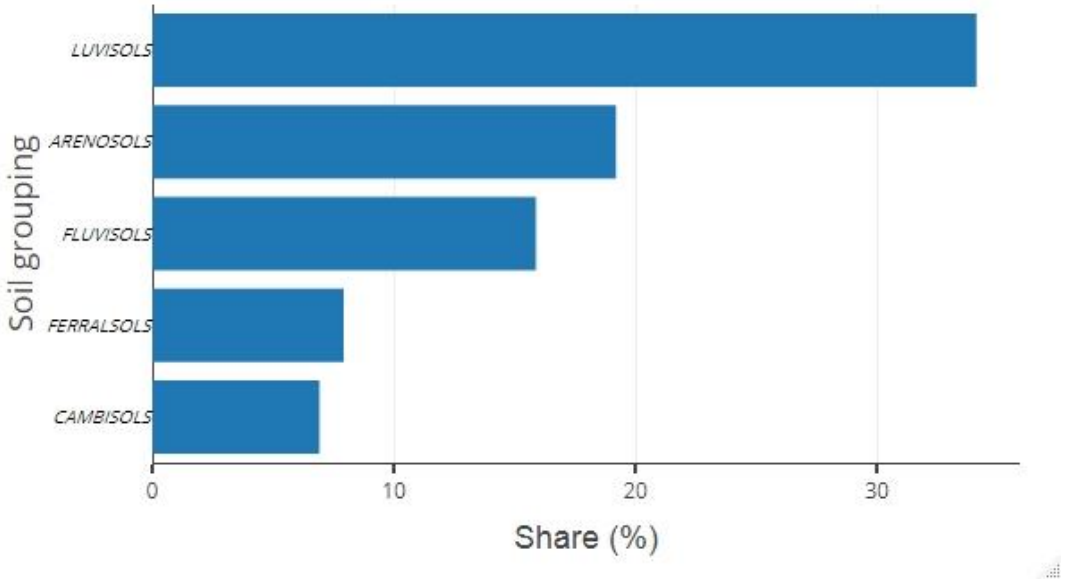

Figure 30. Share of major soil groupings in South Africa and Madagascar region.

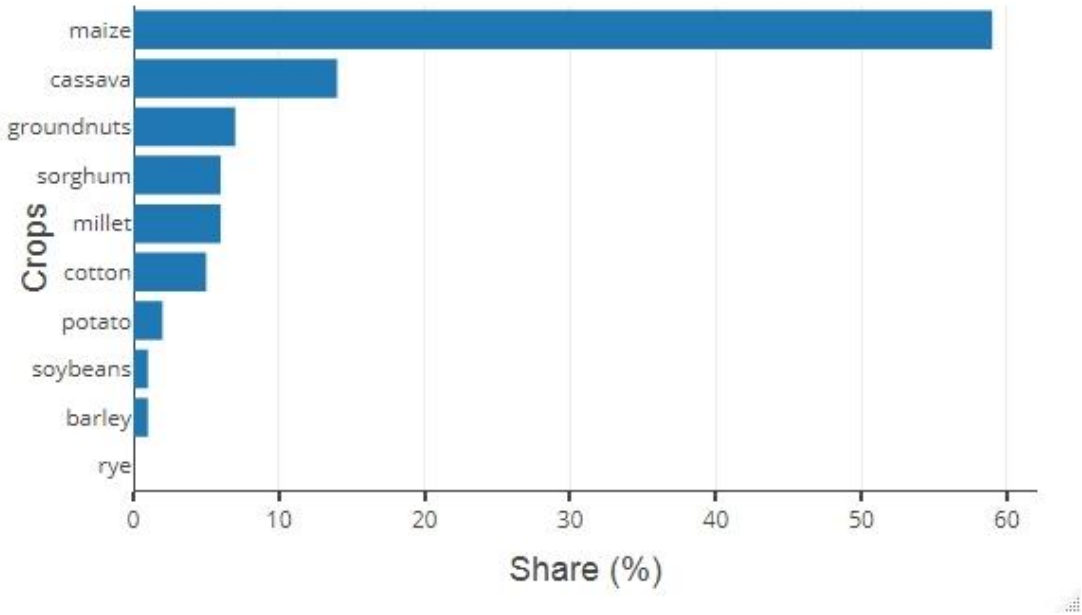

Figure 31. Share of major crops in South Africa and Madagascar region.

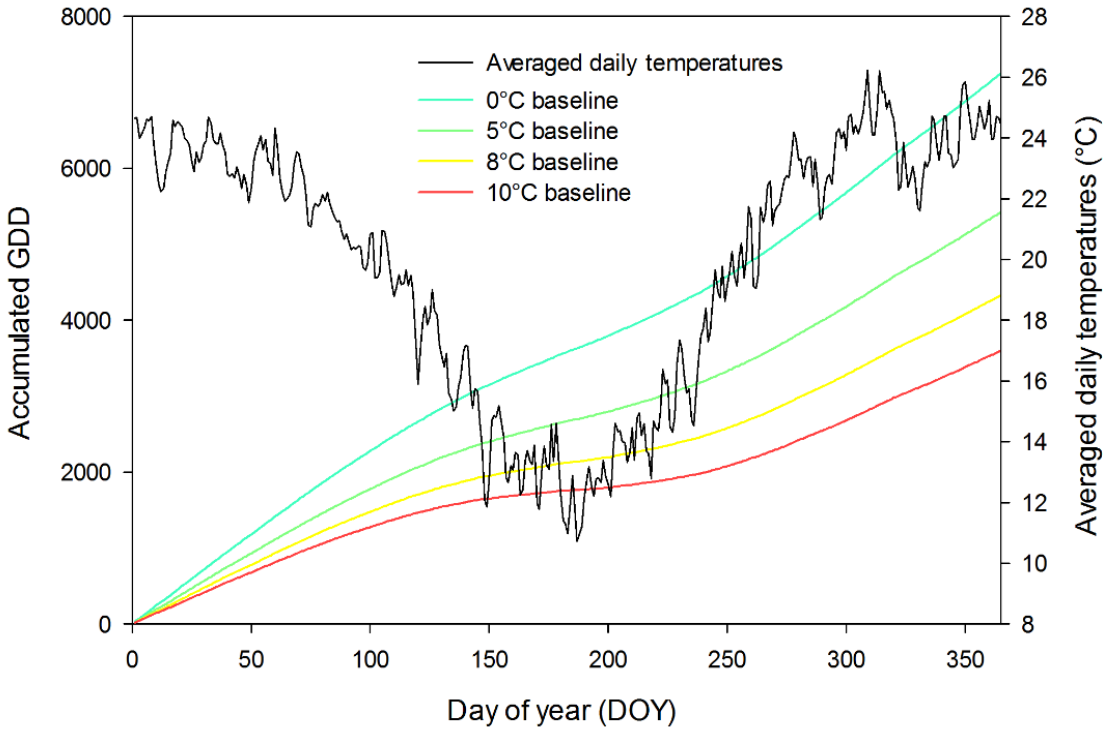

Figure 32. Average daily temperatures and resulting annual GDD accumulation calculated for four baselines in South Africa and Madagascar region.

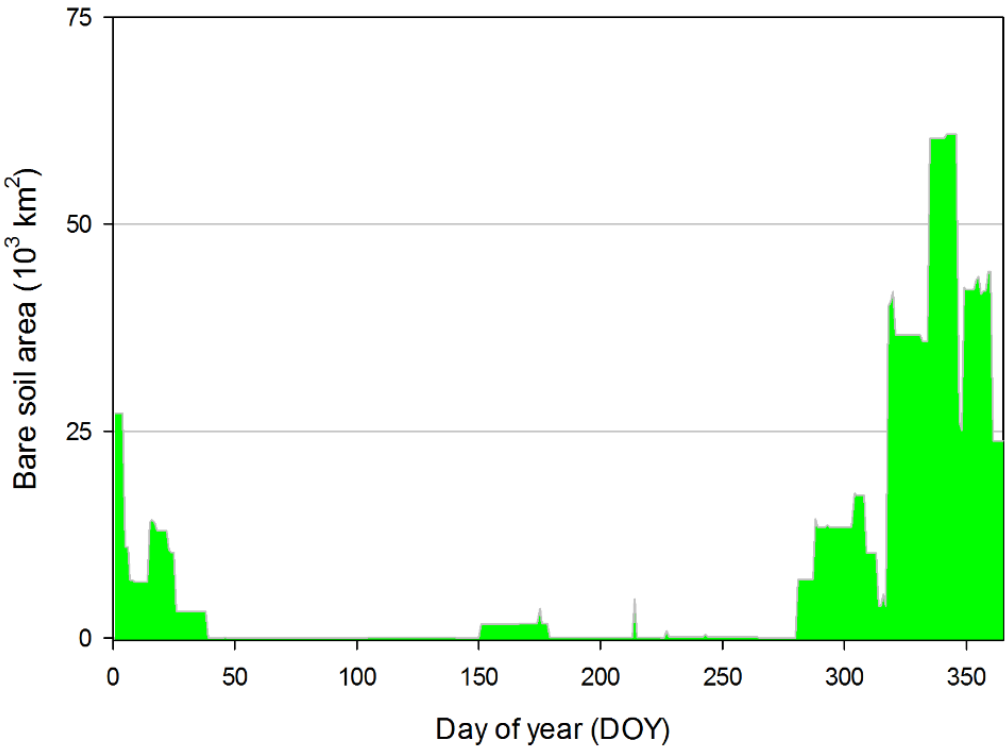

Figure 33. Annual variation of bare soil area in South Africa and Madagascar region.

3.4. Asia

The Asian continent is by far the largest super region and contains the highest area of arable land required to support its humongous and constantly growing population. The continent extends 8,700 km from north to south and 9,700 km from west to east, spanning a range of environments and climates. Over half of the land surface (53%) is dedicated to some kind of agricultural activity, divided into pastures, permanent crops and arable land. The latter occupies around 30% of agricultural land or 15% of the total land area. The Asian continent was divided into ten agricultural regions (Figure 34):

- Former republics of the Soviet Union in Central Asia (AScr)—a landlocked region, consisting of arable land belonging to "stan" countries other than Afghanistan and Pakistan;
- Middle East and Egypt (ASme)—which technically encompasses parts of northern Africa, but Egyptian agriculture is geographically closer to Middle Eastern than to Northwestern Africa;
- China and Mongolia (AScm)—a region with extensive acreage of arable land, especially in the eastern parts;
- Western India (ASwi)—a region including western parts of the Indian subcontinent, Afghanistan and Pakistan, characterized by a hot and dry climate;
- Eastern India (ASei)—the eastern part of the Indian subcontinent, including countries situated on the southern slopes of the Himalayan Mountains; the climate here is predominantly humid, subtropical;
- Southern India (ASsi)—this region encompasses parts of the Indian subcontinent south of ASwi and ASei, including the countries of Bangladesh and Sri Lanka. The effect of the monsoon on climate is strongest in this region;
- Indonesia and Malaysia (ASim)—the arable land in this region is dispersed between numerous islands, dominated by the tropical season with rain all year round;
- Japan and South Korea (ASjk)—agriculture in Japan suffers from land shortage; however, what arable land is available is intensively cultivated;
- Philippines (ASph)—was distinguished as a separate agricultural region, as the climate is divided into wet and dry periods. The arable land is disjointed, as the country is situated on more than 7,000 islands;

- Southeast Asia (ASse)—this region focused around the Indochinese Peninsula includes mainland parts of southeastern Asia.

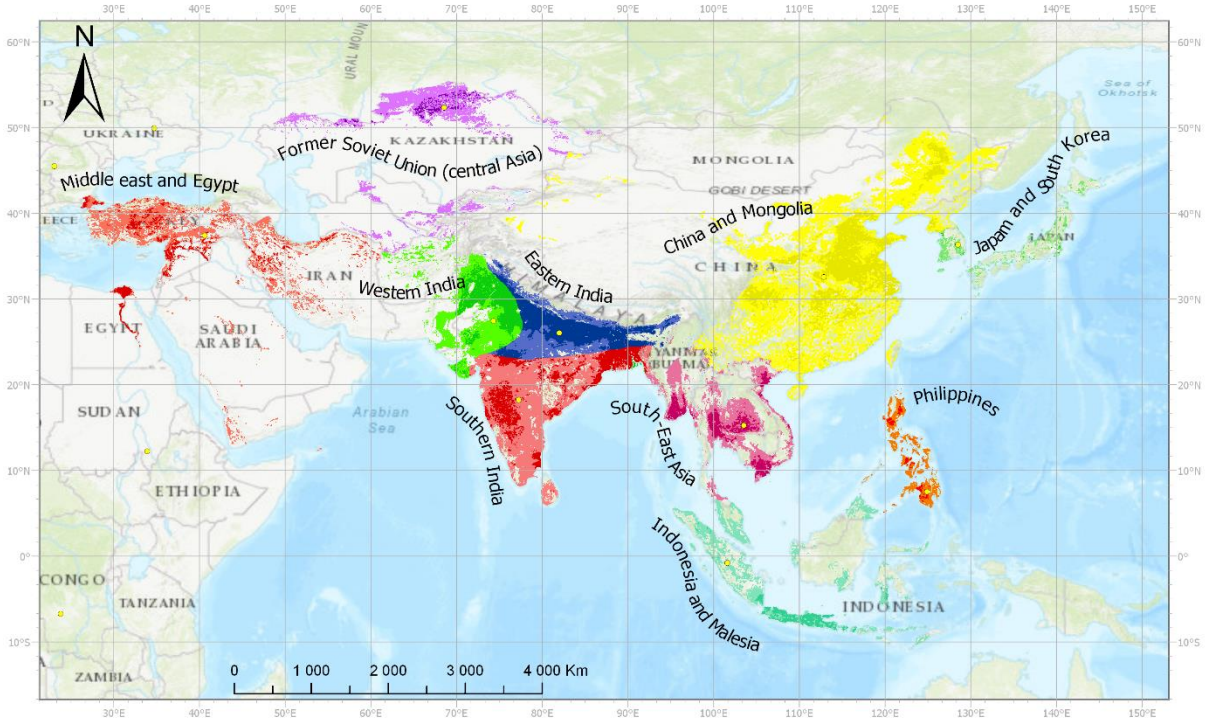

Figure 34. Arable land in the Asian super region divided into regions.

Each of the major crops analyzed was found to be cultivated in the Asian super region (Table 8). Among them, the largest share of the area was dedicated to wheat, which occupied almost 40% of analyzed arable land. The area occupied by maize is about twice as low, as it is cultivated on 18% of arable land. The next two crops occupy significantly lesser areas; those are cotton and millet, with a share of about 8% and 6%, respectively. Areas, where groundnuts, barley, rapeseed, sorghum, and soybeans are sown are similar, each of them occupying around 5% of arable land. The list is closed off by crops that have a share of area lower than 1%; those are cassava, sugar beet, and rye. The planting days of those crops are responsible for the variation of bare soil area within the super region (Figure 35). The Asian super region stretches both into the northern and southern hemispheres; however, the majority of arable land is located in the northern one. When analyzed as a whole, there are only around three months during the year when bare soil resulting from planting crops is almost nonexistent, in the period between the 231st and the 318th DOY. Three peaks of the area of bare soil were found between the spring and summer period, the biggest one around the 140th DOY, preceded by one around a month and a half earlier, on the 90th DOY and

followed by a smaller one two months later, around the 196th DOY. One, although way smaller peak can be distinguished on the 334th DOY, relating to planting around that time in southern parts of the region, including the Indian subcontinent.

Table 8. Area and share of arable land of major crops farmed in Asia**.**

Major Crop	Area (thousands km^2)	(%)
Wheat	943.3	39.5
Maize	428.5	17.9
Cotton	184.9	7.7
Millet	143.4	6
Rapeseed	132	5.5
Groundnut	117.2	4.9
Sorghum	115.4	4.8
Barley	115.3	4.8
Soybean	102.7	4.3
Potato	72.3	3
Cassava	19.1	0.8
Sugar beet	11.9	0.5
Rye	1.9	0.1

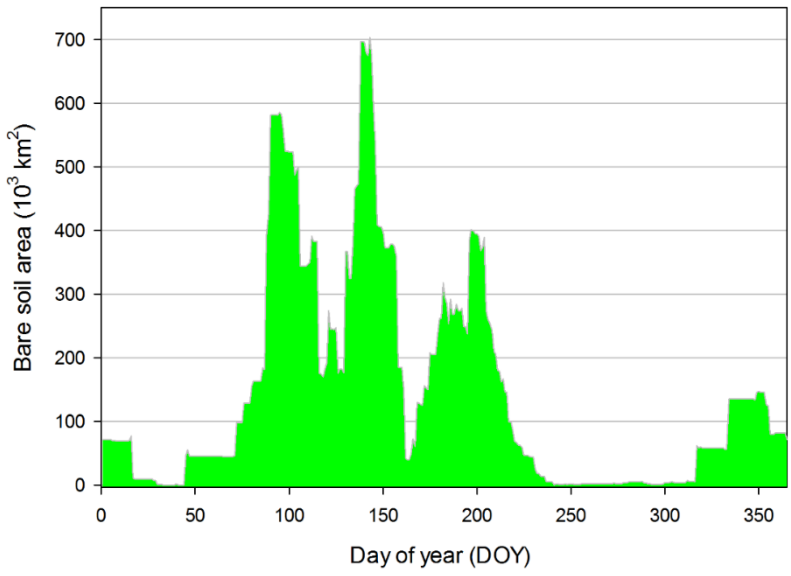

Figure 35. Annual variation of bare soil area in Africa super region.

3.4.1. The former republics of the Soviet Union in Central Asia

The AScr is one of the few completely landlocked regions, and a unique region in the Asian super region. Such conditions result in a low amount of annual rainfall and big amplitude of temperatures throughout the year. The arable land situated in northern Kazakhstan suffered erosion and nutrient loss as a consequence of the Virgin Lands Campaign initiated by Nikita Khrushchev in the 1950s. The climate conditions make the region more favorable for herding cattle than farming, and so the majority of the agricultural area in the region is used as pastures. Nonetheless, there are still considerable amounts of arable land, especially in northern Kazakhstan, but smaller areas can be found in each of the countries (Figure 36).

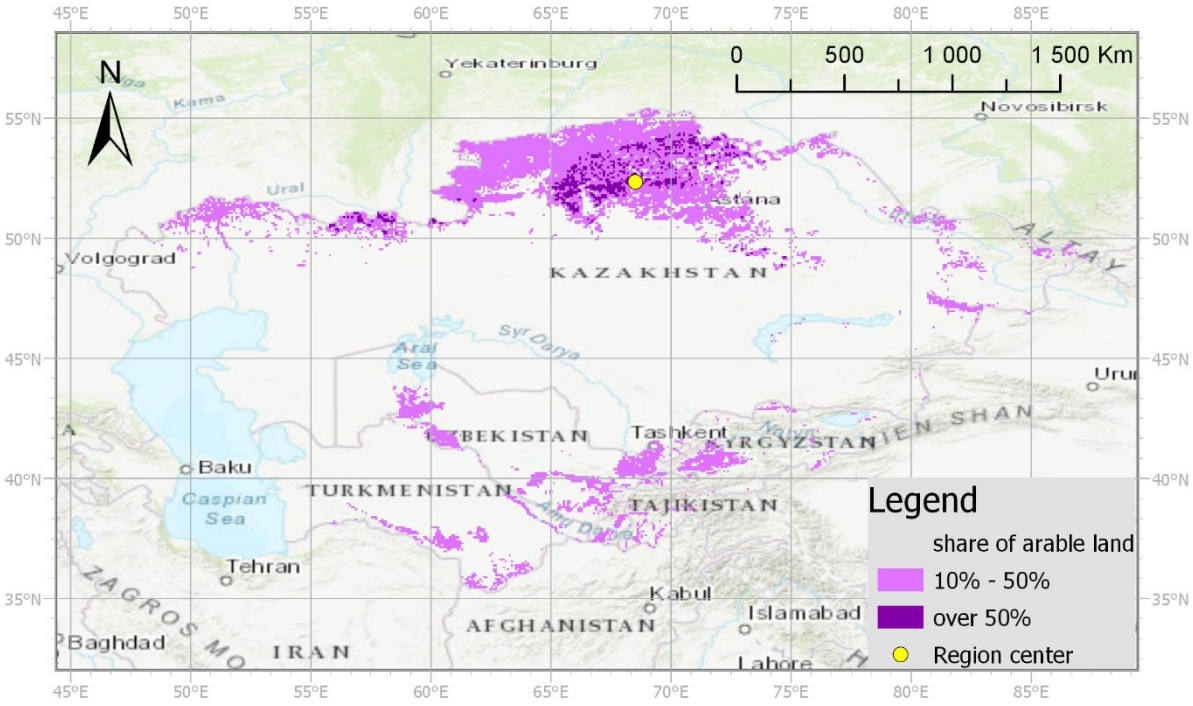

Figure 36. Distribution of arable land in the Asian region of Former republics of the Soviet Union.

There is no soil unit used in farming that has an overwhelming majority in the region (Figure 37); rather there are five soil groupings that have a share of between 13% and 20%; those are, ordered by decreasing shares: *Chernozems, Kastanozems, Gleysols, Lithosols*, and *Xerosols*. Together, those soil units have a share of about 80%. Two more soil units were distinguished, *Yermosols* and *Fluvisols*, each with a share of around 7%. Among the cultivated major crops (Figure 38), the biggest area by far is dedicated to the cultivation of wheat, which is almost 70%. The other crops farmed in the significant area are cotton and barley, with a share of almost 15% and 12%, respectively. Potatoes and maize are each farmed on less than

2% of arable land. All the other crops' individual share is lower than 1%. The average daily temperatures were extracted from the point located at 52° north and 68° east, which is located in northern Kazakhstan. During the coldest months, mean temperatures can be as low as -17°C, while in the summer they reach about 21°C. The annual accumulation of GDD is therefore uneven (Figure 39), commencing in April, growing quite rapidly during summer, and stopping between the middle of September and October. After that, it is nonexistent until it starts again in the April of the following year. The annual variation of bare soil area (Figure 40) is dominated by wheat and is very focused. The peak, of almost 150,000 km^2, occurs around the 138th DOY and lasts for around three weeks. That maximum peak is preceded by a lesser one, around five times smaller, occurring around the 120th DOY and caused mostly by earlier planting of barley and cotton a few days later.

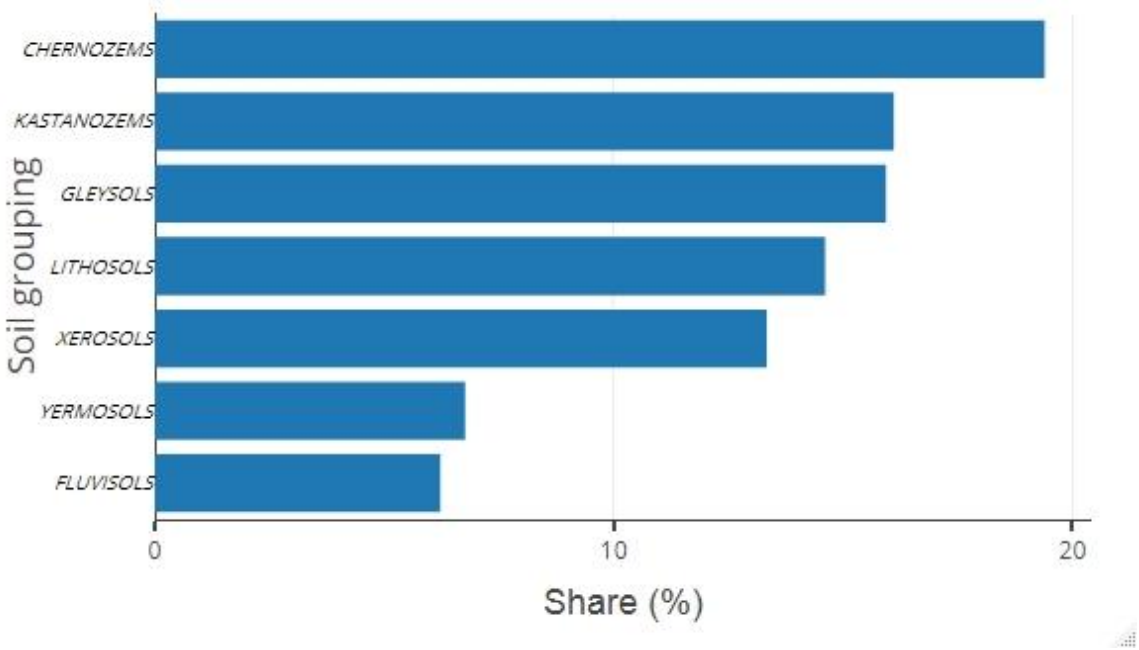

Figure 37. Share of major soil groupings in the Asian region of Former republics of the Soviet Union.

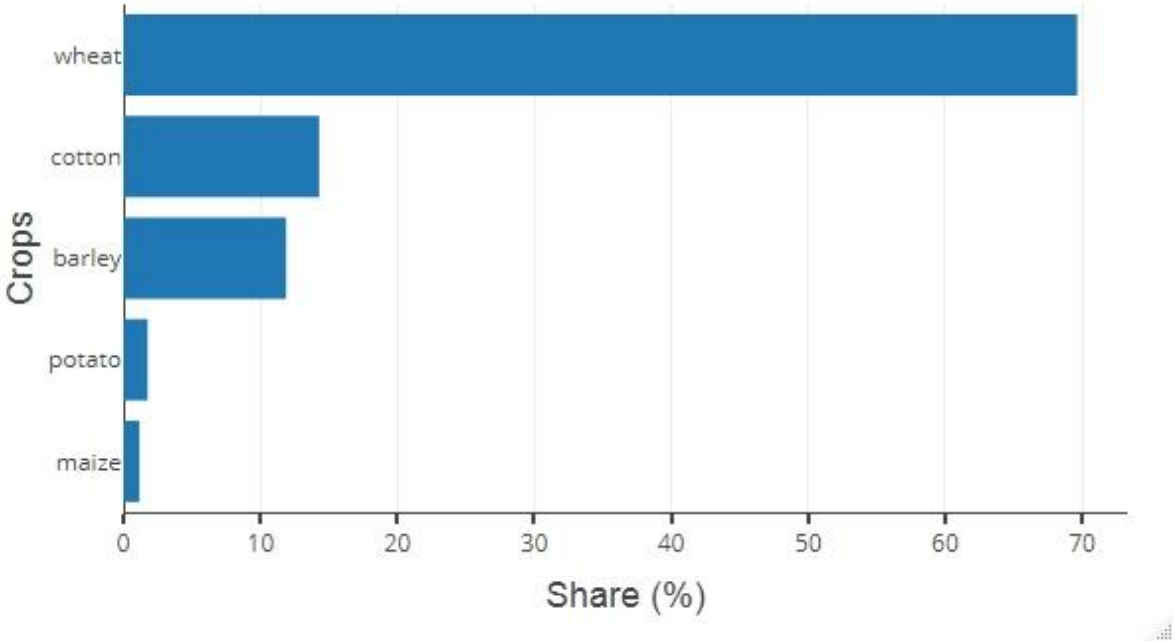

Figure 38. Share of major crops in the Asian region of Former republics of the Soviet Union.

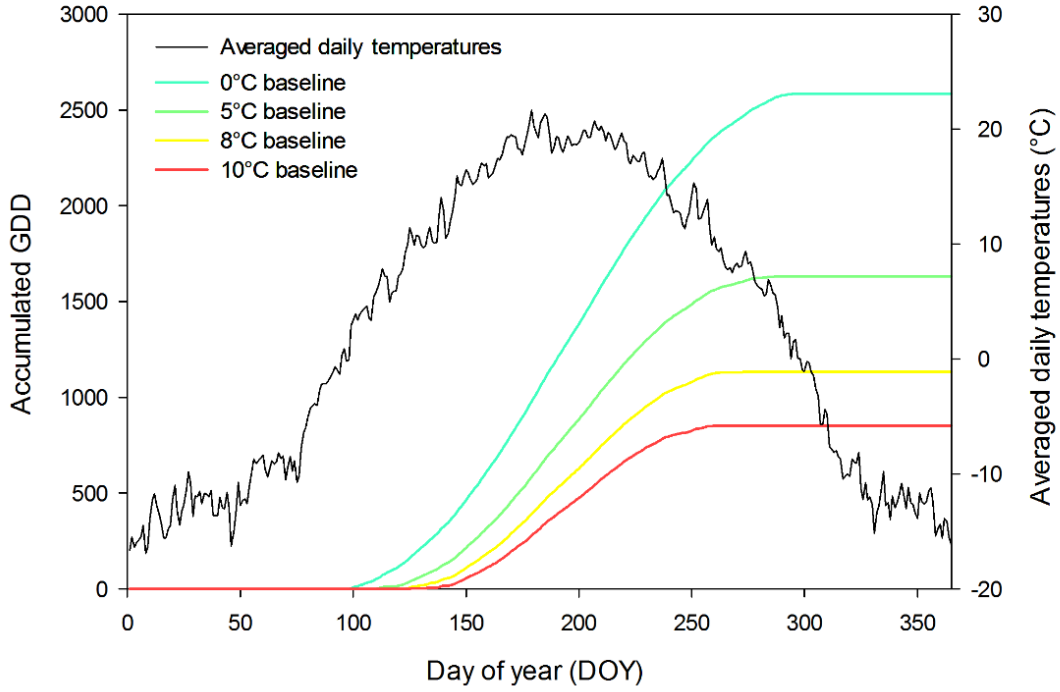

Figure 39. Average daily temperatures and resulting annual GDD accumulation calculated for four baselines in the Asian region of Former republics of the Soviet Union.

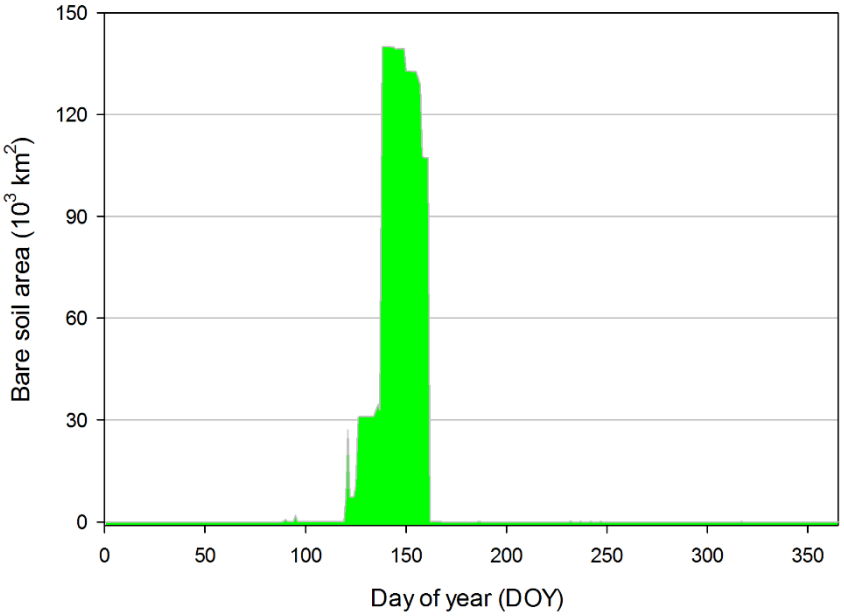

Figure 40. Annual variation of bare soil area in the Asian region of Former republics of the Soviet Union.

3.4.2. Middle East and Egypt

This agricultural region stretches from the floodplains of the Nile in the west, to the Anatolian Peninsula in the north, all the way to eastern parts of Iran in the east and the Arabian Peninsula in the south. The agriculture in this region has a long history; in fact, the region was among the first where agriculture began. The concentration of arable land is found along the Nile, as well as at its delta, on the Anatolian Peninsula, in western and northern parts of Iran and along the eastern Mediterranean coast, including Syria, Lebanon, and Israel. Arable land is scarce and dispersed in the Arabian Peninsula (Figure 41).

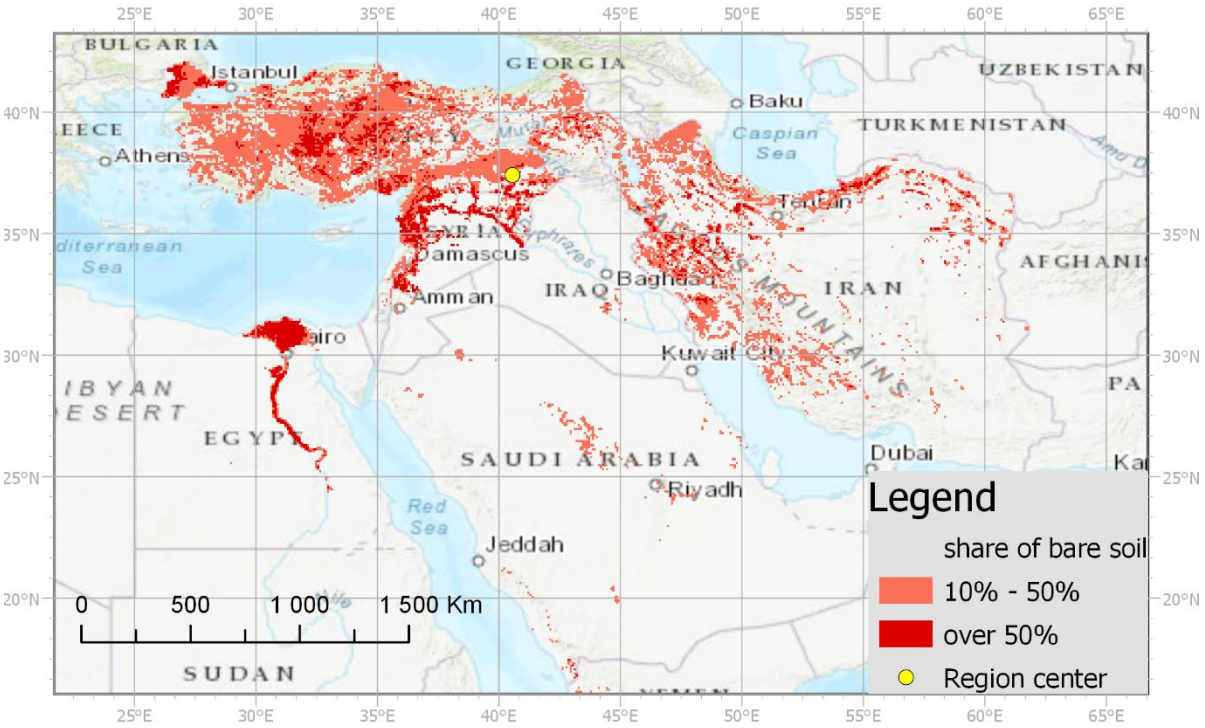

Figure 41. Distribution of arable land in the Middle East and Egypt region.

Of all the arable land in the region (Figure 42), a quarter comprises *Xerosol* soil units. Other soil units that are widespread in the region are *Fluvisols* and *Lithosols*, each constituting about 20% of the arable land. *Luvisols*, with their share of around 10%, exist in half of the area where the aforementioned ones are present. The list is rounded off by *Cambisols* that were found on 6%, followed by four soil units that each occupy close to 3%; those are *Yermosols, Vertisols, Regosols* and *Solonchaks*. Agriculture is dominated by the cultivation of cereals (Figure 43), especially wheat, which is farmed on over 60% of the land analyzed, followed by barley that was found on around three times less. Maize and cotton are other significant crops in the region's agriculture, each occupying around 5% of arable land. Among the remaining

crops farmed in the region, a noticeable area of around 2% each was used for the cultivation of sugar beet, sorghum, and potatoes. The mean daily temperatures used for the calculation of GDD were extracted from a point situated at 37° north and 40° east, close to the border between Turkey and Syria. The temperatures showed seasonality, oscillating between 10°C and 28°C, which caused GDD accumulation to vary in intensity throughout the year (Figure 44). With such a heavy share of wheat compared to other crops, the annual variation of bare soil (Figure 45) was dominated by its planting. The maximum amount of bare soil occurs around the 90th DOY and reaches over 220,000 km^2. Due to the rapid accumulation of GDD at that period and the general rapid phenology of wheat, the majority of soils just stayed bare for a period of between two and three weeks. A smaller peak, reaching just over 30,000 km^2, occurred around the 120th DOY and was caused by the later planting of wheat in eastern parts of the region, as well as the planting of maize. Barley was found to be planted on similar days as wheat and reinforced those peaks.

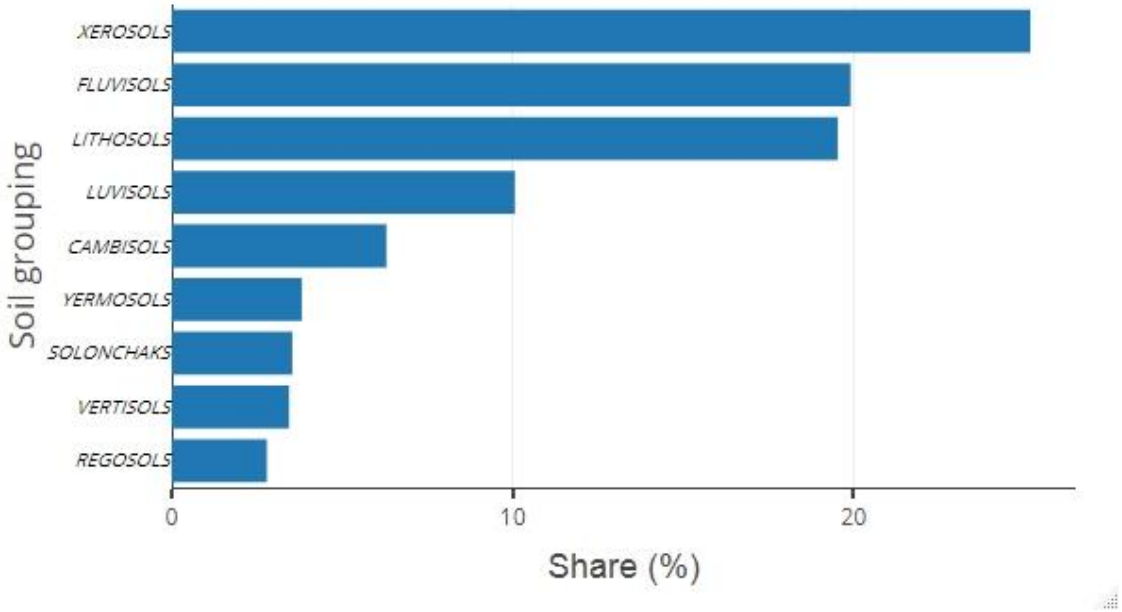

Figure 42. Share of major soil groupings in the Middle East and Egypt region.

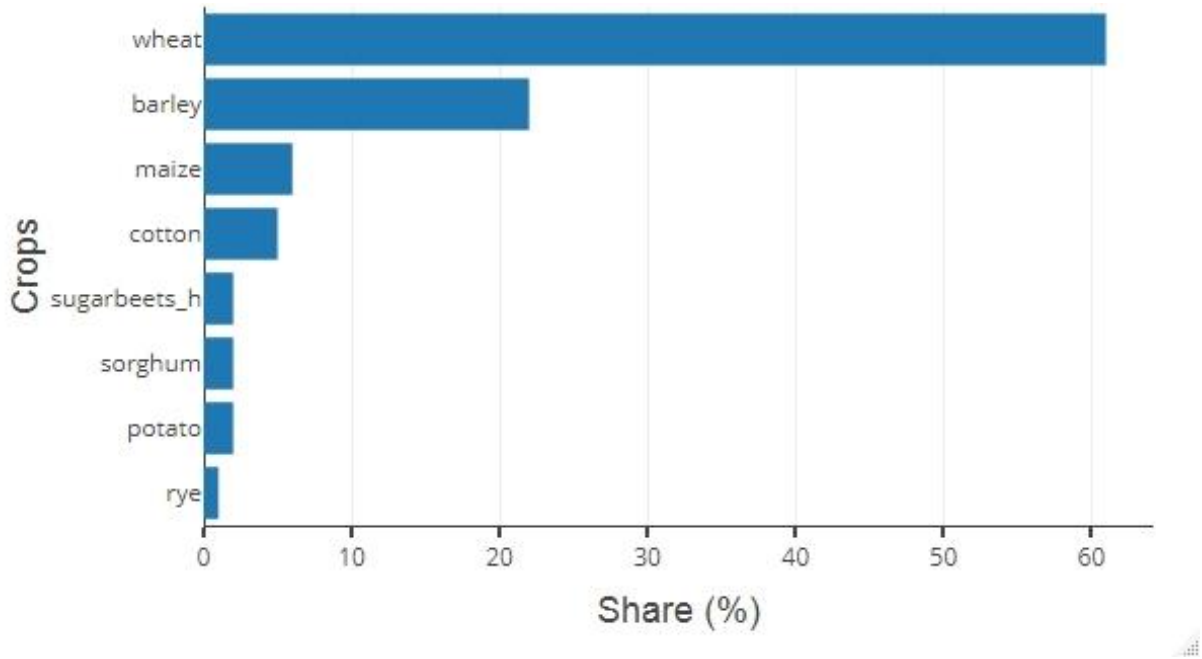

Figure 43. Share of major crops in the Middle East and Egypt region.

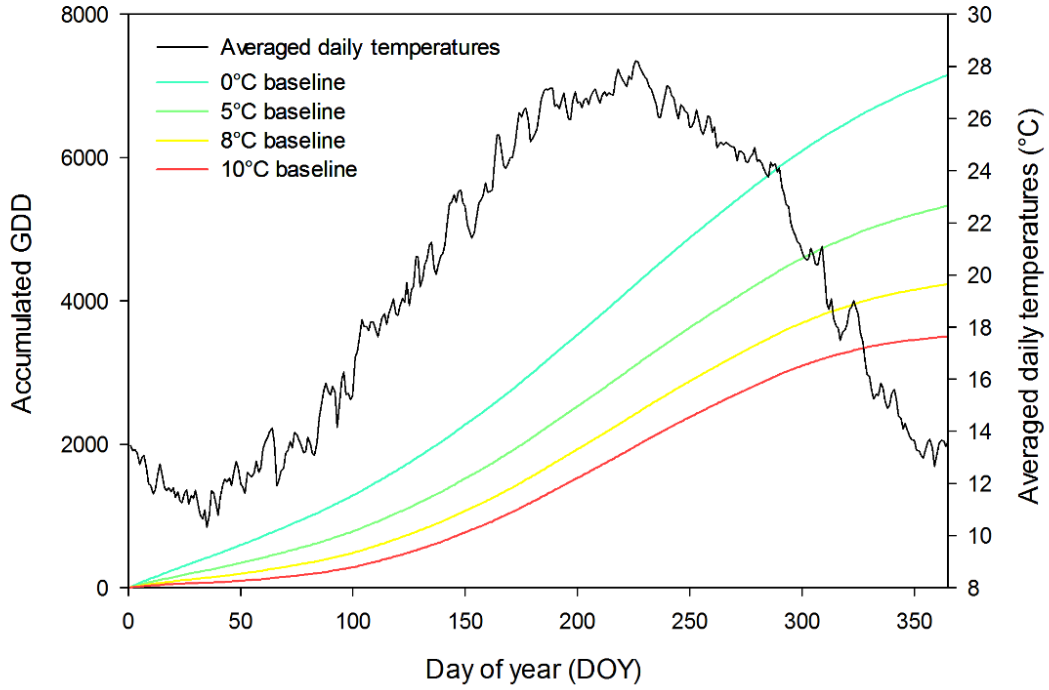

Figure 44. Average daily temperatures and resulting annual GDD accumulation calculated for four baselines in the Middle East and Egypt region.

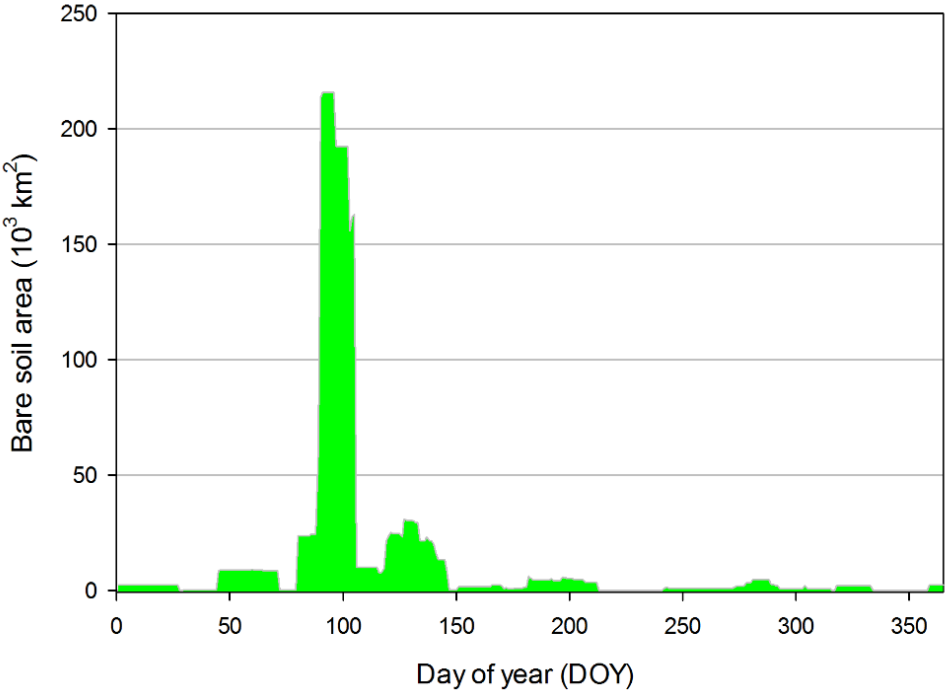

Figure 45. Annual variation of bare soil area in the Middle East and Egypt region.

3.4.3. China and Mongolia

As of the day of writing, China is still the most populous country in the world, and its arable land is accordingly extensive. Among the regions delimited inside the Asian super region, it has by far the largest area classified as arable land; however, if the Indian subcontinent was not split into three regions, it would have a larger area. Nonetheless, arable land found in China represents around 10% of all arable land in the world. Traditionally, Chinese agriculture was focused in the eastern parts of the country, with efforts made to extend it to the west and the north. Two great rivers, the Yellow and Yangzi Rivers, support that intensive agriculture. Smaller pockets of arable land were also located in western parts of China, and in Mongolia; however, those regions are more suited for pastures and herding (Figure 46). The practice of CA was reported on over 65,000 km^2, which makes up around 8% of analyzed arable land.

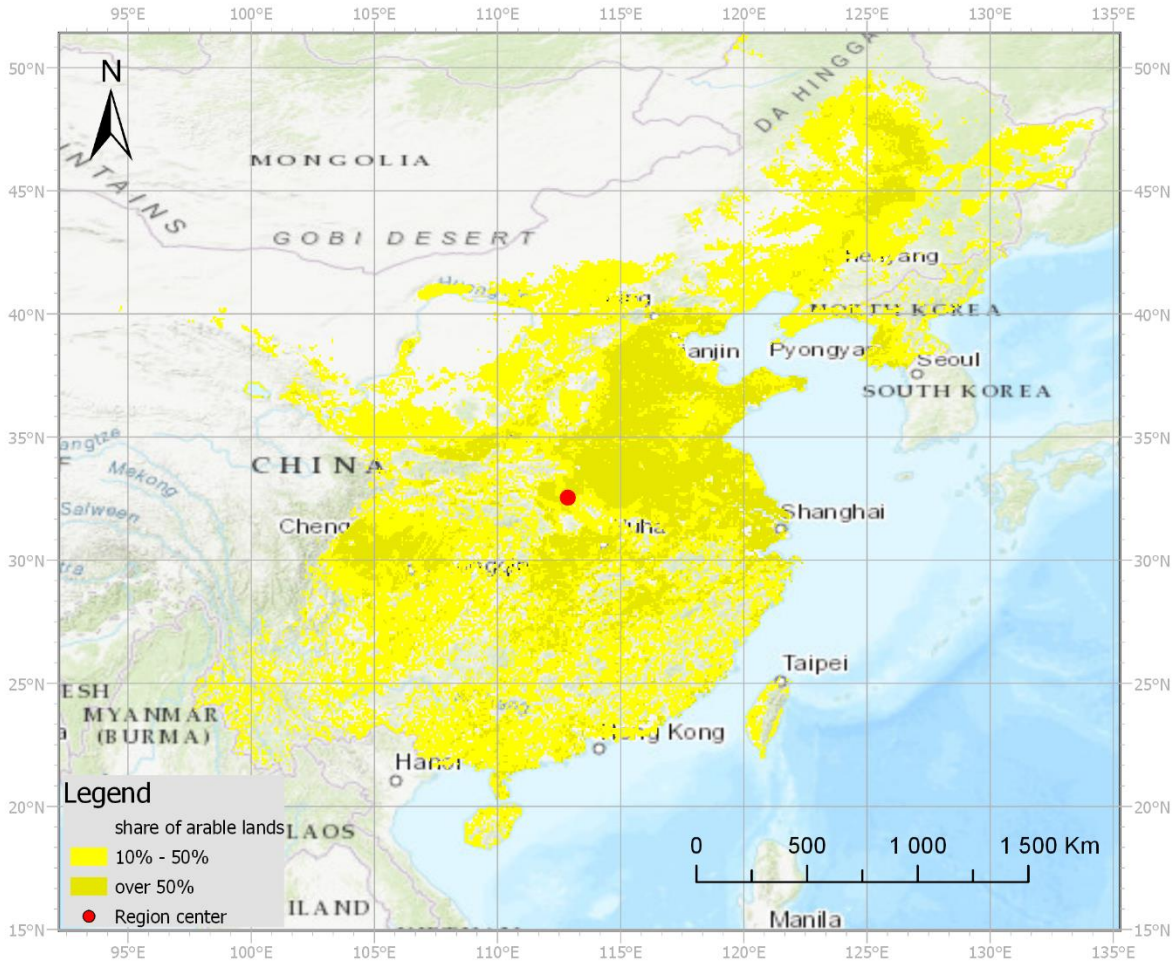

Figure 46. Distribution of arable land in the China and Mongolia region.

The soil unit that is found most commonly in arable land (Figure 47) in the region is *Lithosols*, occupying roughly a third of the area. A slightly smaller share of the area is taken by *Gleysols*, which have a share of almost 27%. The next two soil units combined occupy a similar area; those are *Acrisols* and *Cambisols* that make up around 15% and 11%, respectively. The remaining area is split between *Yermosols, Vertisols, Fluvisols* and *Kastanozems*, each of them occupying roughly 3%. Among analyzed crops (Figure 48), the biggest farmed areas were occupied by wheat and maize, each of them had a share of just short of a third of arable land. Soybeans and rapeseed were each found on around 10%. Following that, three crops were cultivated each on about 5% of analyzed land; those crops are potatoes, groundnuts, and cotton. The average daily temperatures were extracted from a point located at 32° north and 113° east. The obtained temperatures ranged between -3°C in the coldest period and 27°C in the warmest. The rate of accumulation of GDD throughout the year was increasing toward the warmest month and decreasing toward winter (Figure 49). The annual variation of bare soil shows the major periods during the first half of the year (Figure 50). The peak amount of bare soil occurs around the 112th DOY and reaches more than 375,000 km^2. The first major wave of planting occurs between the 72nd and the 88th DOY and the majority of bare soil in this period is a result of sowing wheat and maize. Soils tend to stay bare until around the 158th DOY when the majority of maize, cotton, and potatoes that were planted later start to cover the fields.

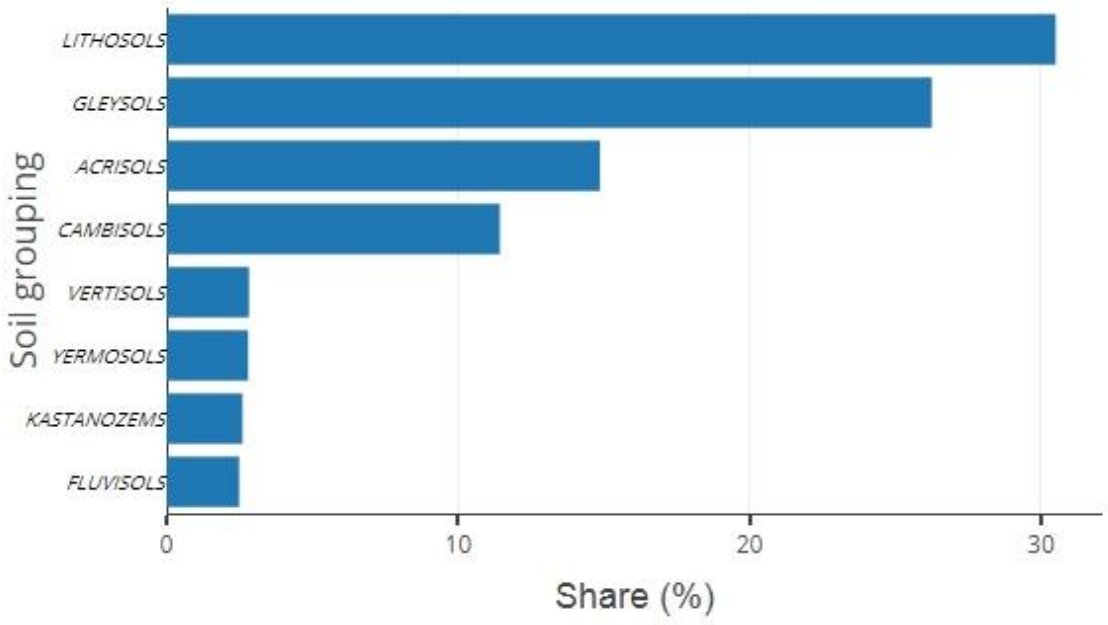

Figure 47. Share of major soil groupings in the China and Mongolia region.

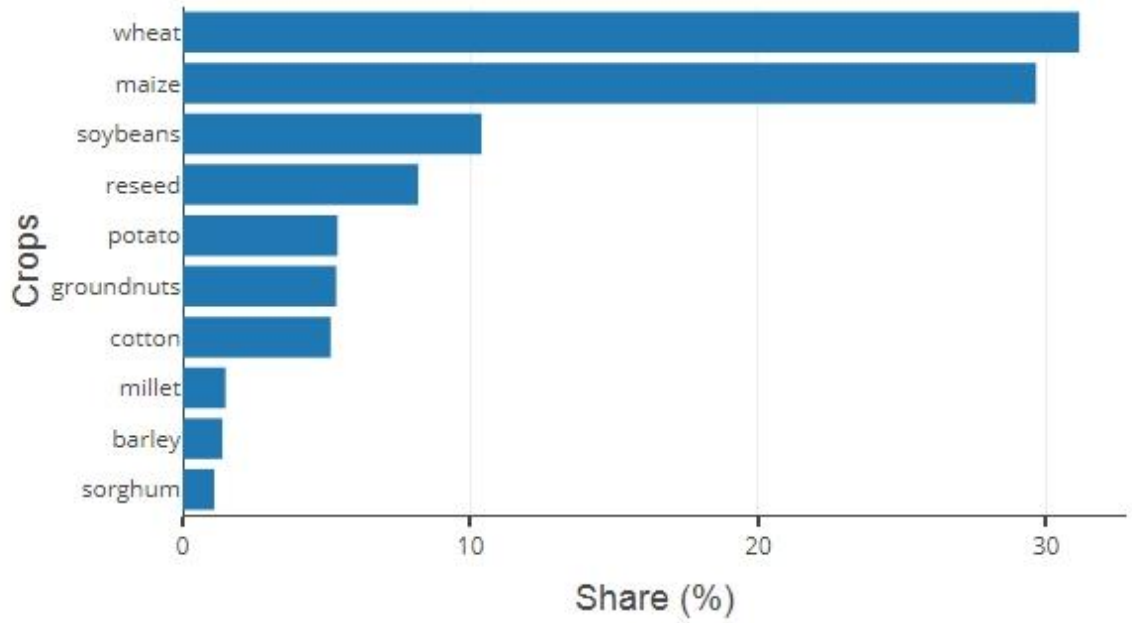

Figure 48. Share of major crops in the China and Mongolia region.

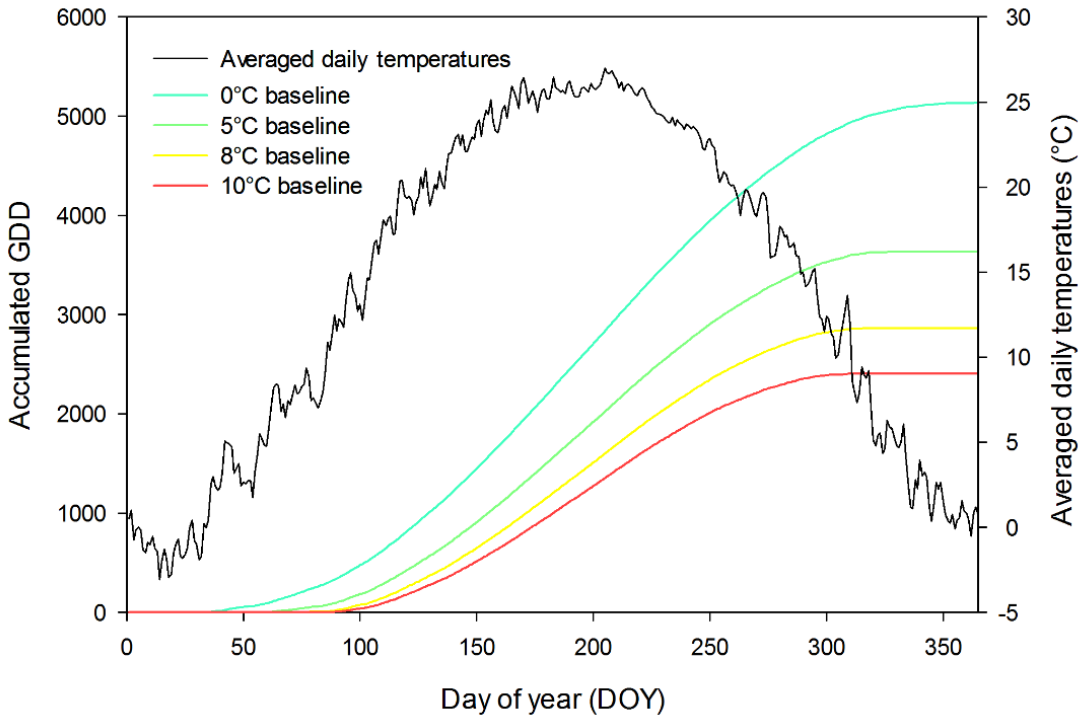

Figure 49. Average daily temperatures and resulting annual GDD accumulation calculated for four baselines in the China and Mongolia region.

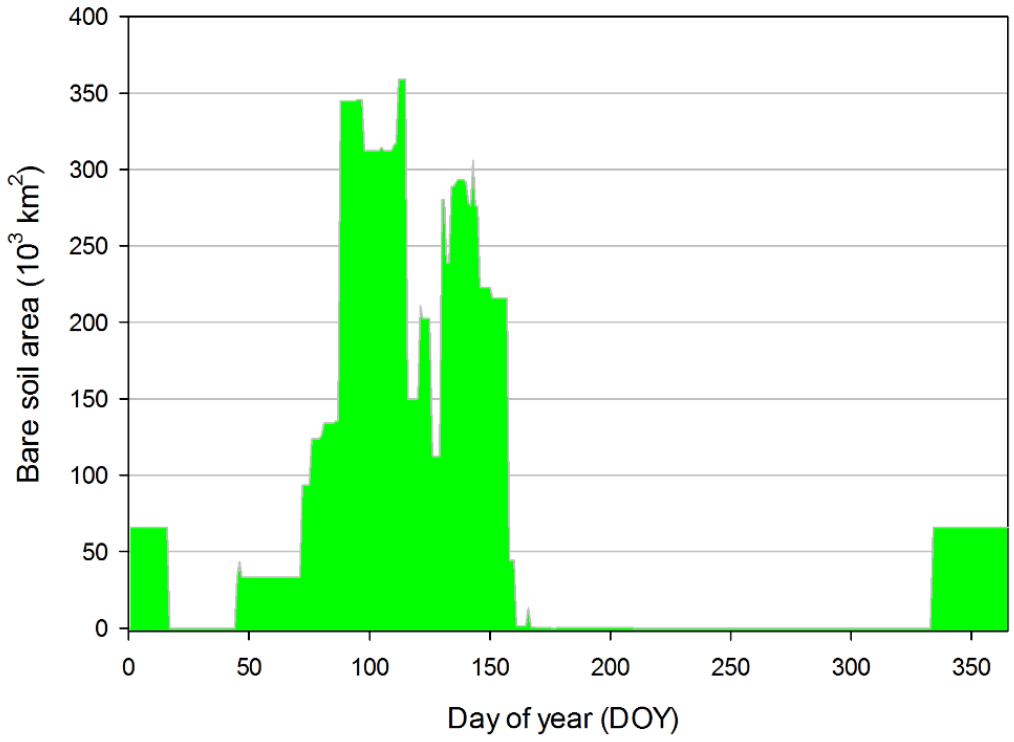

Figure 50. Annual variation of bare soil area in the China and Mongolia region.

3.4.4. Western India

Western India is the first of three regions that make up the Indian subcontinent; the region constitutes western parts of India, together with Pakistan and Afghanistan. As in those other regions, there is a significant quantity of arable land. In the western parts, located in Afghanistan, agriculture is dispersed and less intensive due to the mountainous terrain; in the central parts of the region, situated in Pakistan, arable land can be found all along the Indus River Valley; and in the remaining part of the region, which is located in western India, agriculture is omnipresent, with the exception of the Thar Desert (Figure 51). Around 15,000 km^2 of CA were reported around India, and most of them were found in this western region.

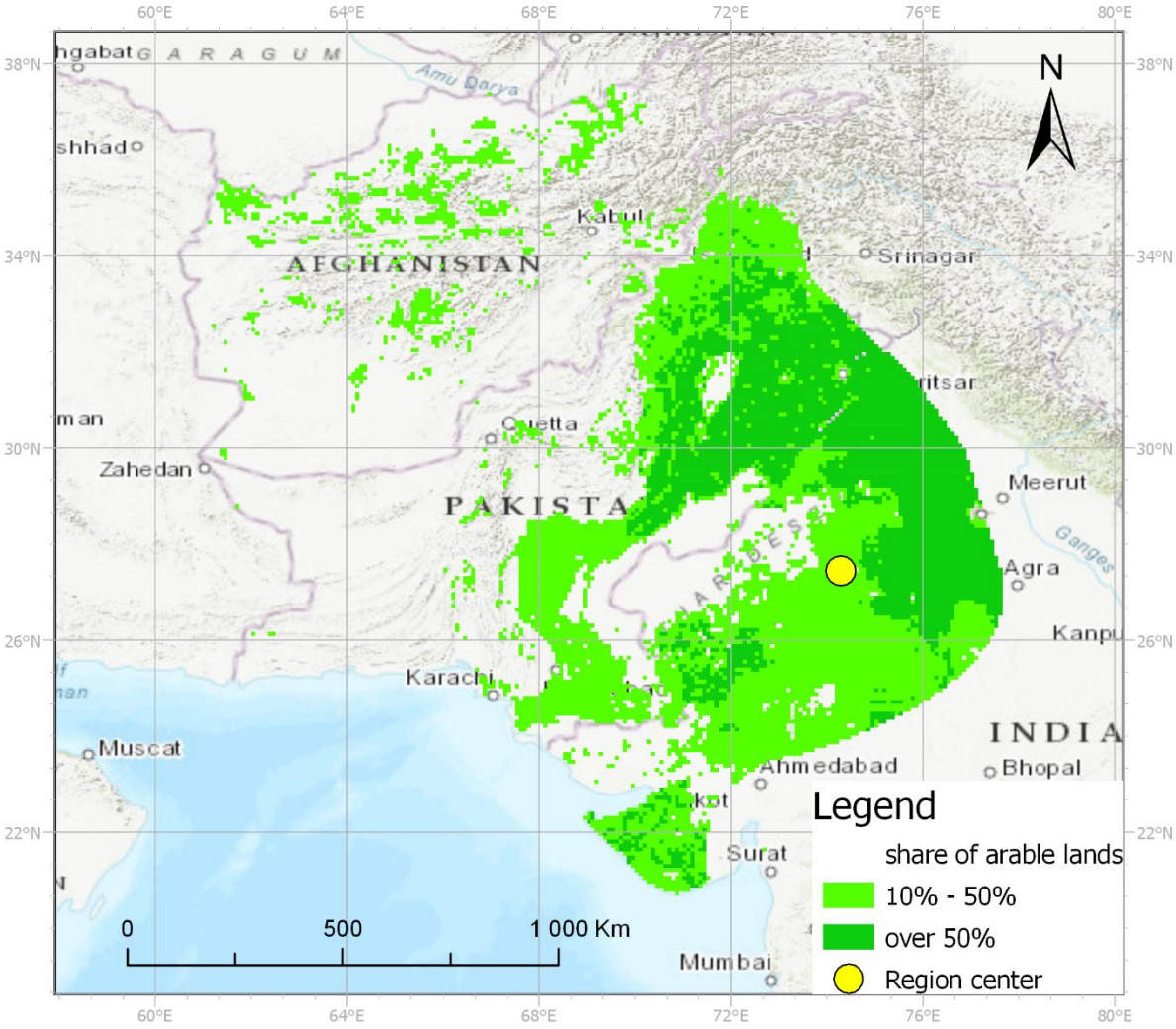

Figure 51. Distribution of arable land in the Western India region.

The share of soil units in arable land in the region (Figure 52) shows that the dominant soil unit was found to be *Yermosols*, with a share of below 30%. A similar area is occupied by

the next two soil units, *Cambisols* and *Xerosols*, each occupying between 15% and 17%. *Lithosols* were found on more than 10% of arable land, and the remaining soil units with notable shares are *Arenosols* and *Fluvisols,* with 9% and 7%, respectively. Among the analyzed major crops (Figure 53), the biggest area in the region was dedicated to wheat, which was farmed on almost half of the arable land. Areas three times smaller were dedicated to millet and cotton, each of them farmed on roughly 16%. Rapeseed was cultivated on around 8% of the area, and another 9% was split evenly between maize and groundnuts. The temperatures used for the estimation of GDD were obtained from a point located at 27° north and 74° east (Figure 54). In this dry and warm region, the mean daily temperatures ranged between 15°C during the coldest days and 36°C during the hottest. The annual variation of bare soil in the region (Figure 55) shows the first and the highest peak occurring around the 138th DOY. The peak is caused by the sowing of wheat; however, in that condition, the soil stayed bare for only a week and a half. Another period of bare soil occurs around a month later, starting around the 168th DOY and gradually increasing until it reaches a maximum around the 186th DOY. After that, the amount of bare soil decreases until the 217th DOY. Most of the crops cultivated in the region are planted during this extended period. The last notable occurrence of bare soil is noted between the 317th and the 252nd DOY and relates to the late planting of rapeseed.

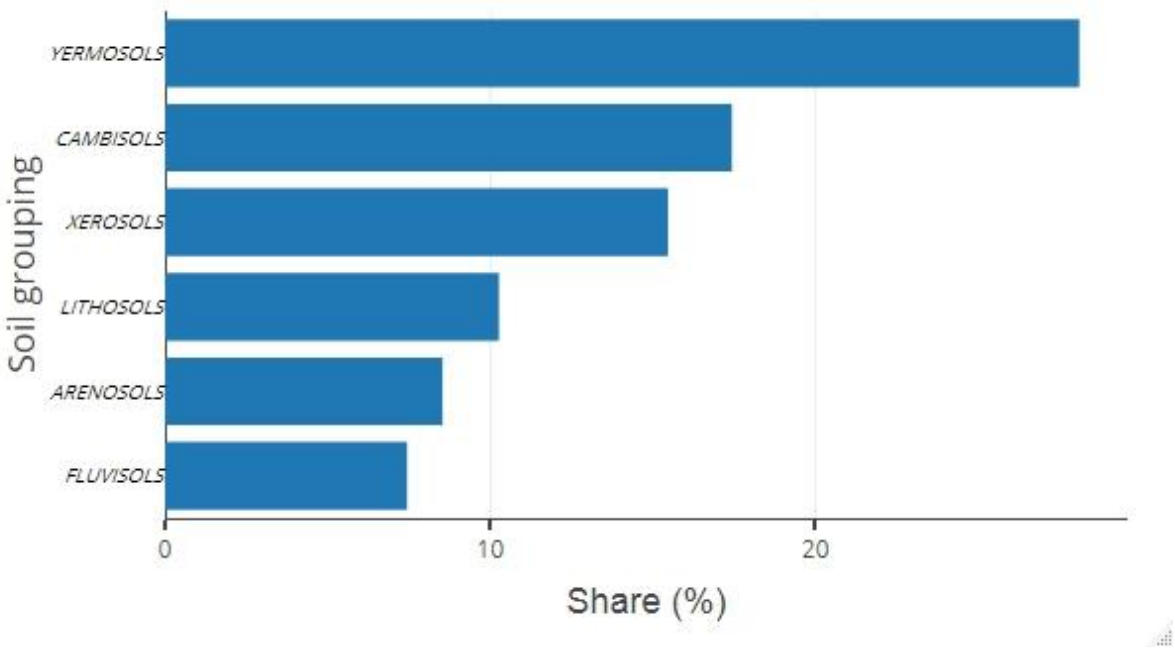

Figure 52. Share of major soil groupings in the Western India region.

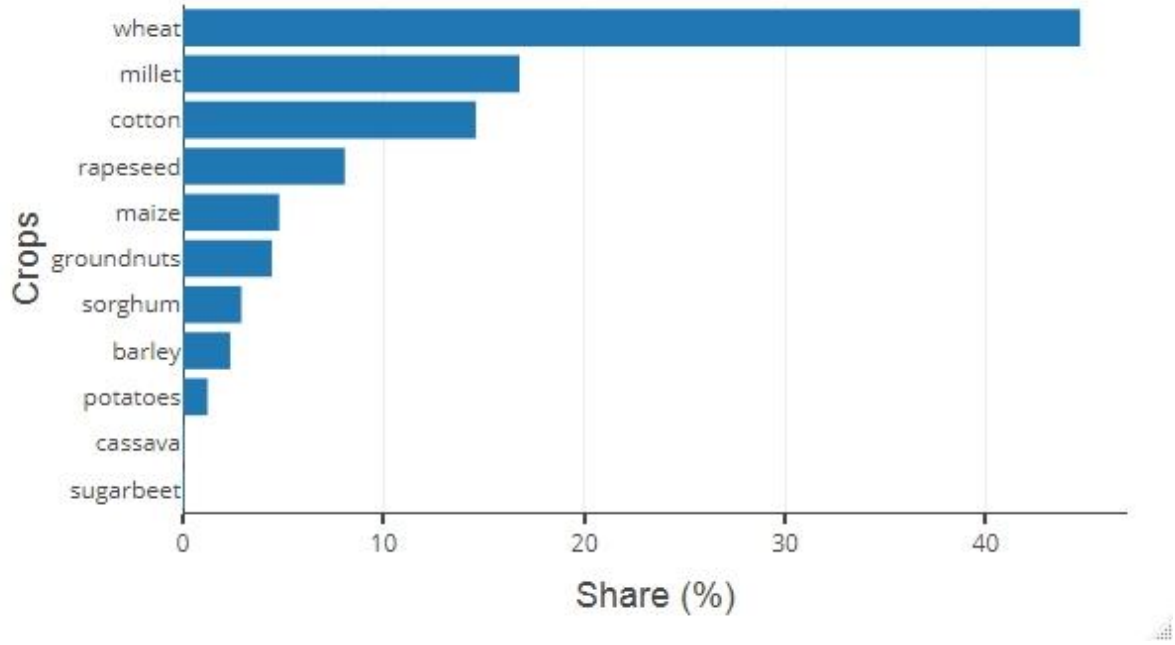

Figure 53. Share of major crops in the Western India region.

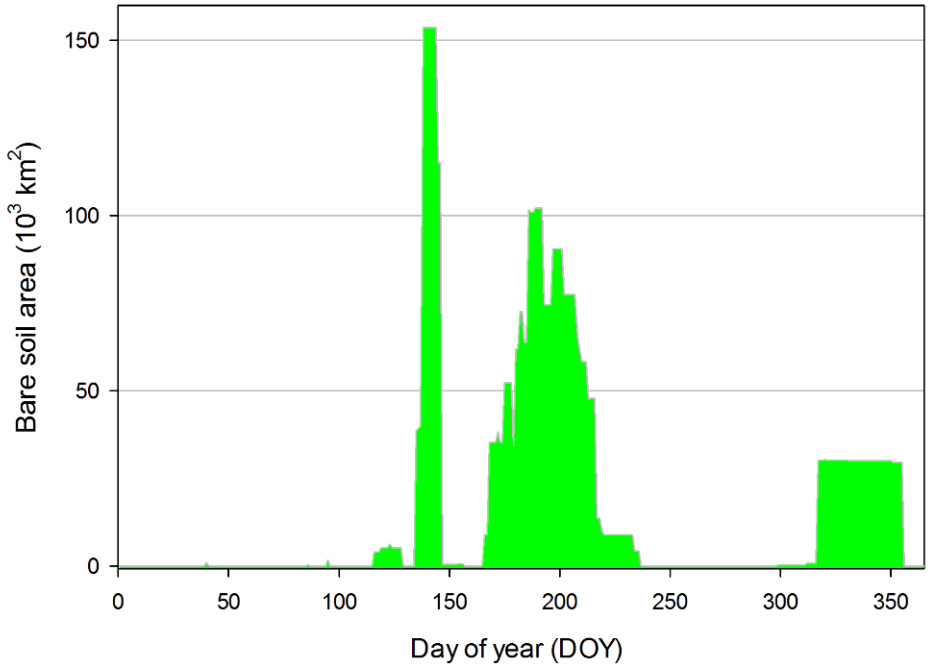

Figure 54. Average daily temperatures and resulting annual GDD accumulation calculated for four baselines in the Western India region.

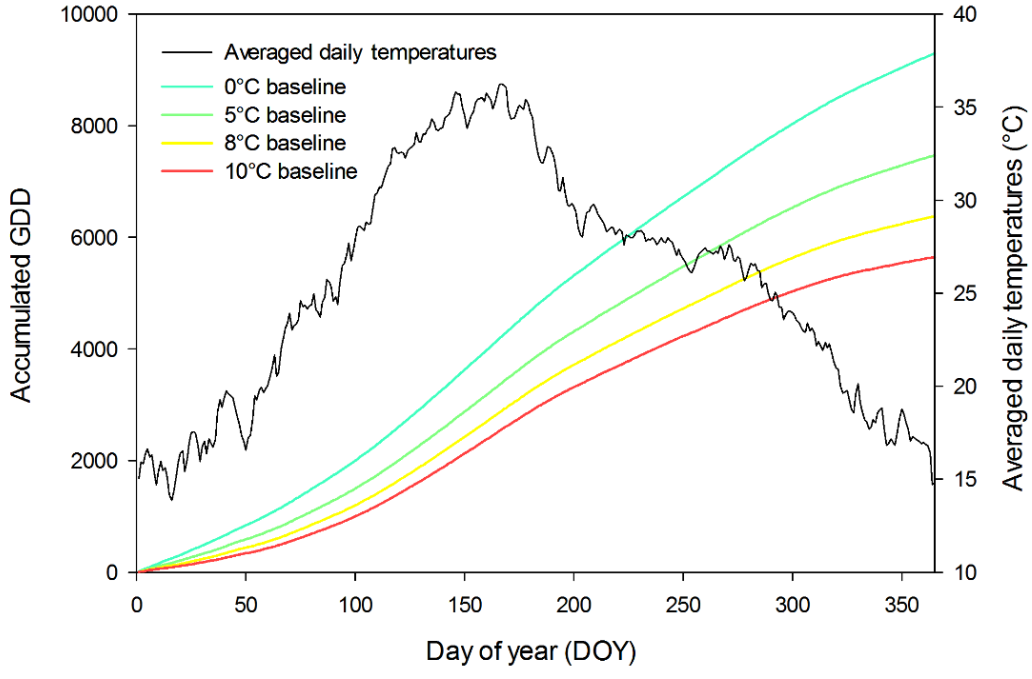

Figure 55. Annual variation of bare soil area in the Western India region.

3.4.5. Eastern India

The second region distinguished on the Indian subcontinent contains land east of the previous region; besides parts of India, it includes the countries of Nepal, Bhutan and northern parts of Bangladesh. In contrast to the previous region, the climate is more humid, being situated on the Himalayan foothills. Arable land is found around the whole region, most notably along the Ganges and Brahmaputra Rivers and the fertile plains of Uttar Pradesh (Figure 56).

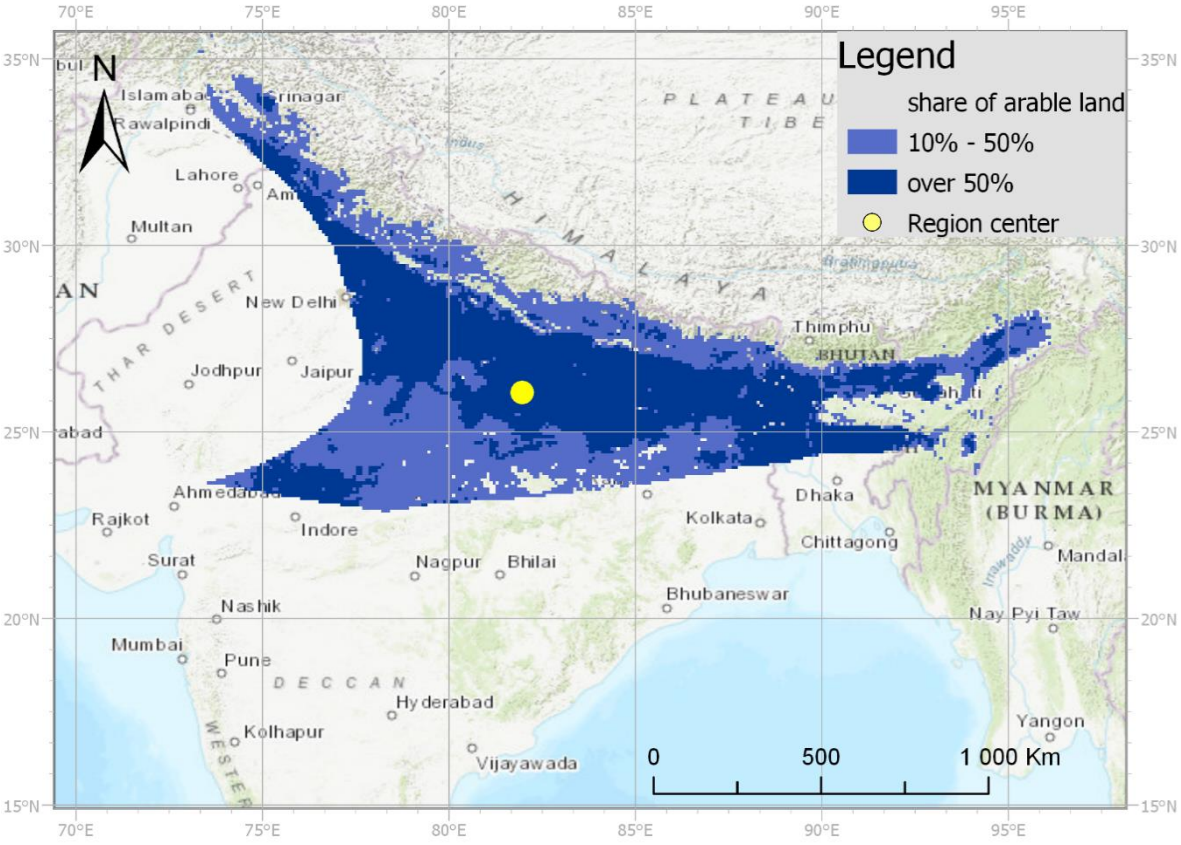

Figure 56. Distribution of arable land in the Eastern India region.

Not surprisingly for a region that depends on major rivers for its agriculture, the two most commonly farmed soil units (Figure 57) are *Cambisols* and *Luvisols*, having a share of 37% and 25%, respectively. The share of *Vertisols* and *Fluvisols* is roughly 10% for each of them. The other notable soil units include *Gleysols* and *Acrisols,* each of them with a share of over 5% of arable land. Similar to the previous Indian region, the major crop that was most commonly farmed was wheat (Figure 58), which was found on over 60% of arable land. An area roughly four times smaller was dedicated to maize, with its share short of 15%. Almost one-tenth of arable land was used for the cultivation of rapeseed, followed by around 7% for

the cultivation of millet. Barley, potatoes, and sorghum were each found on a bit more than 2% of arable land. The central point used for obtaining annual mean daily temperatures was located at 26° north and 82° east. The obtained temperatures were similar to the ones in ASwi, ranging between 16°C and 36°C, resulting in similar GDD accumulation (Figure 59). One maximum peak of bare soil can be observed around the 196th DOY, with over 140,000 km^2 of soil being bare, mainly after the planting of wheat (Figure 60). This area stayed bare for around a week and a half, due to wheat's rapid phenology at this time caused by warm temperatures. Two smaller peaks were observed preceding the main one, both of around 50,000 km^2, around the 135th and the 182nd DOY. Planting of wheat at an earlier date caused the first of them, while the second one was caused primarily by the planting of millet. One delayed period of bare soil was also found between the 317th and the 350th DOY, this one reaching up to 25,000 km^2 and resulting from the sowing of rapeseed.

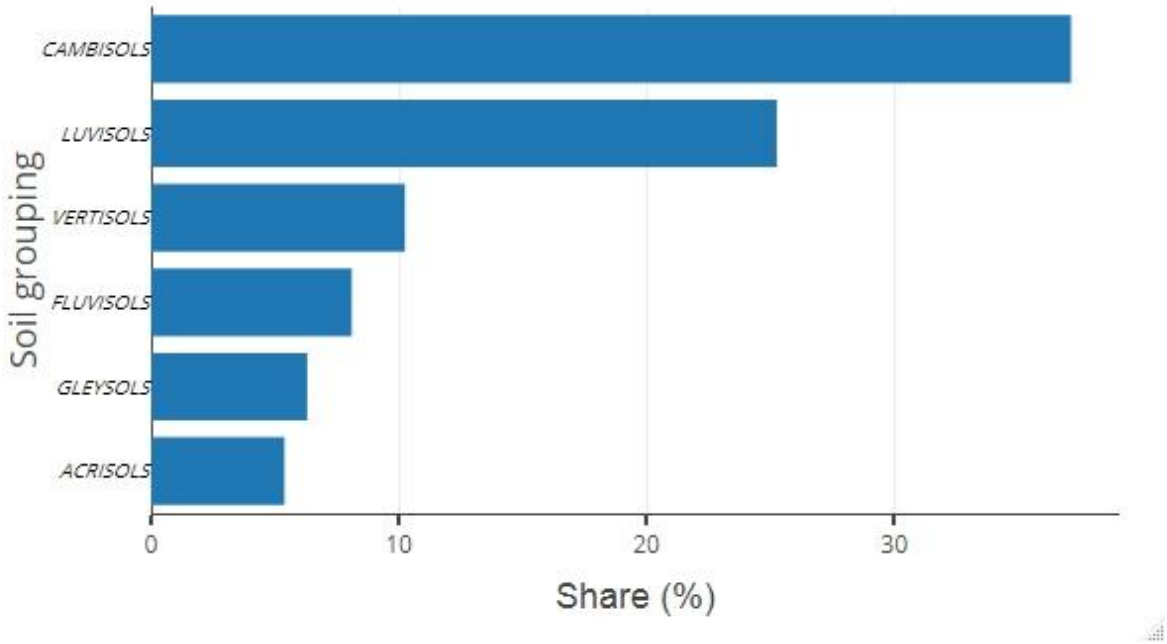

Figure 57. Share of major soil groupings in the Eastern India region.

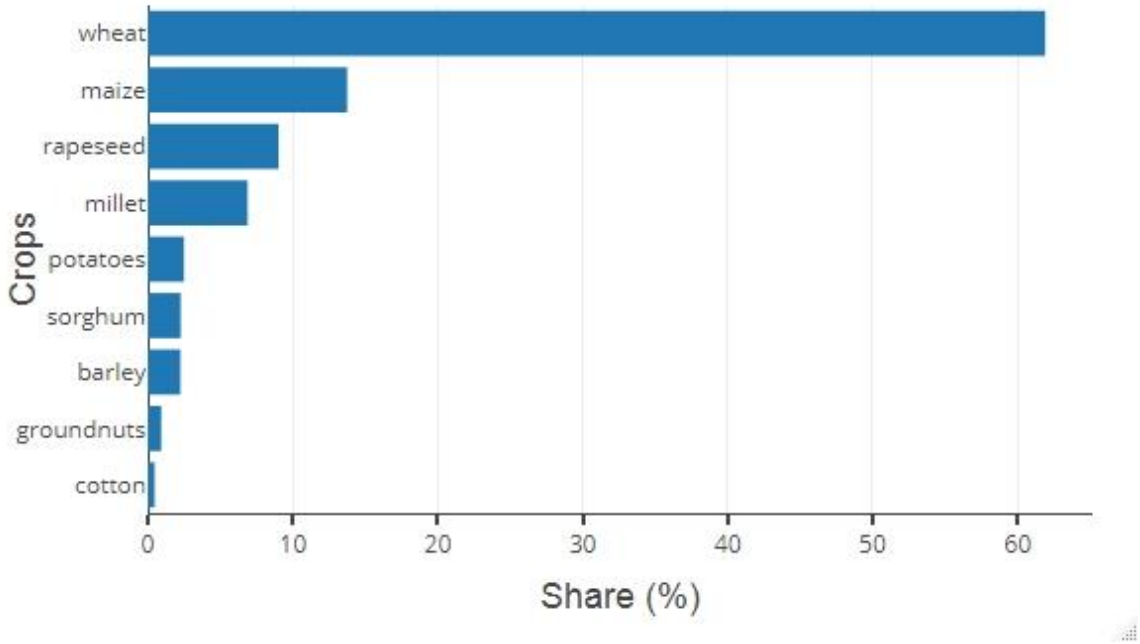

Figure 58. Share of major crops in the Eastern India region.

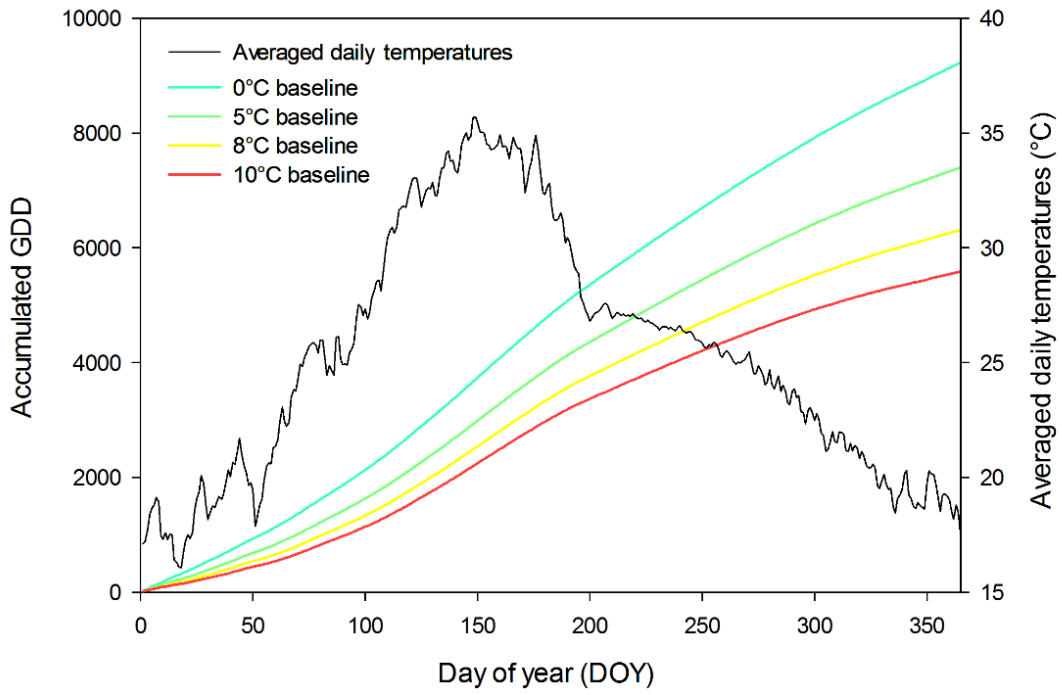

Figure 59. Average daily temperatures and resulting annual GDD accumulation calculated for four baselines in the Eastern India region.

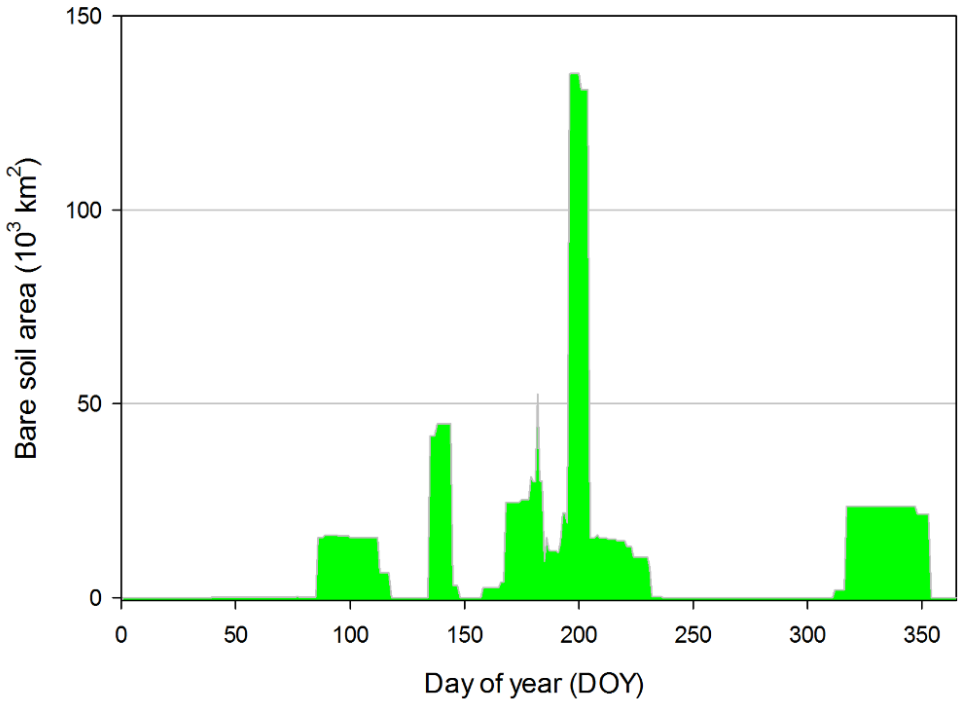

Figure 60. Annual variation of bare soil area in the Eastern India region.

3.4.6. Southern India

The third and last of the regions delimited from the Indian subcontinent, the ASsi, is bordered in the north by ASwi and ASei, and from other directions by the Indian Ocean. The southern parts of Bangladesh and the island country of Sri Lanka are also included in the region. Compared to the other two regions comprising the Indian subcontinent, ASsi experiences the greatest influence of monsoon seasons on its climate. The arable land is found across the whole region, intermixed with patches of forests and shrubs. Huge agricultural concentrations were observed in western parts of the region, in the states of Karnataka and Maharashtra, another one along the Krishna River that flows into the ocean through the eastern part of the region. Huge swaths of terrain are also adopted for agriculture in the eastern parts of the region, including Bangladesh, which is a result of the high fertility of soils along the Brahmaputra and Ganges Rivers. The most notable inland concentration of arable land in the region is found around the state of Chhattisgarh, located in the northern part of the region (Figure 61).

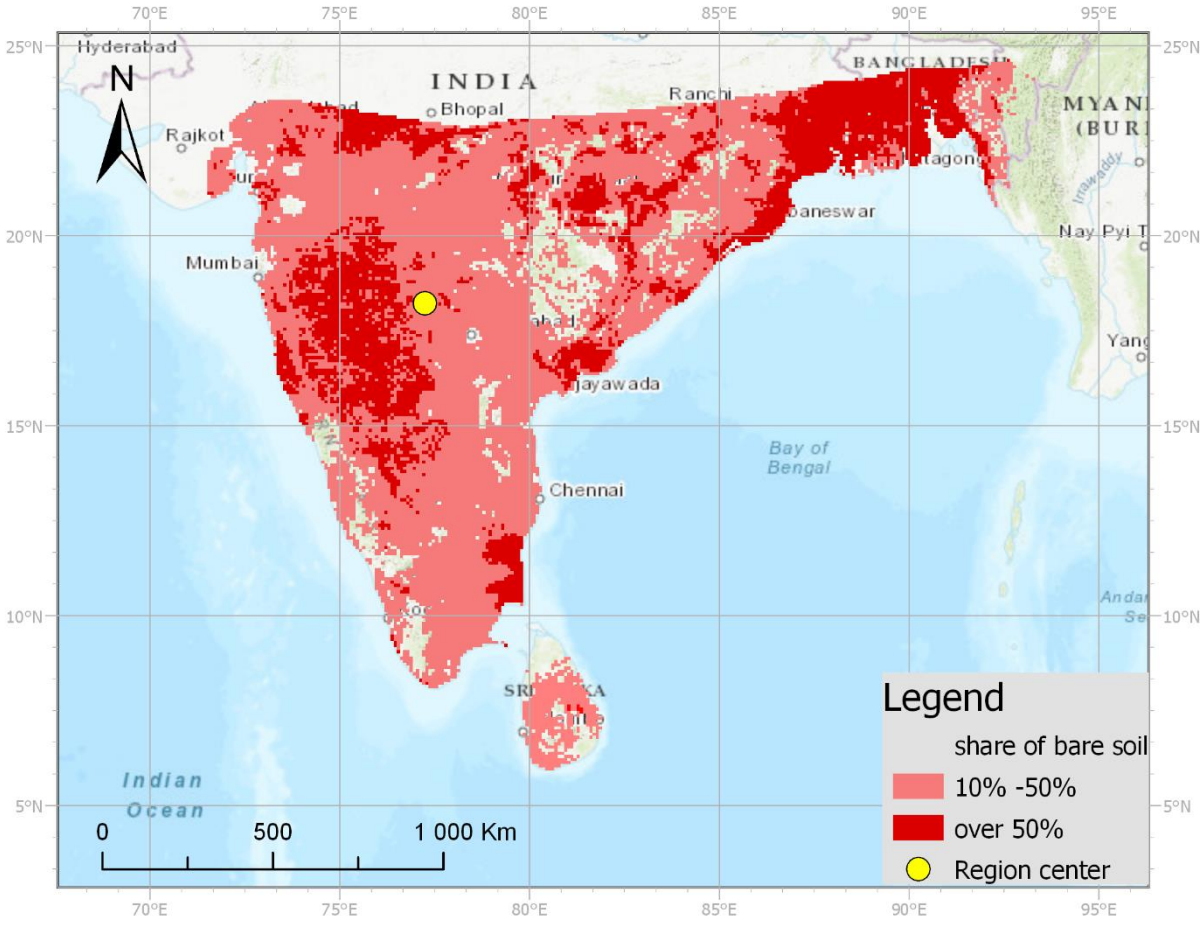

Figure 61. Distribution of arable land in the Southern India region.

Just four soil units constitute more than 80% of arable land in the region; those are: *Luvisols* with a share of over 40%, *Vertisols* that have roughly 25%, *Nitosols* found on about 10%, followed by *Cambisols* occupying around half of the area of *Nitosols* (Figure 62). Among other notable soil units are *Lithosols* with a share close to 5%, and *Fluvisols* and *Gleysols,* each having a share of roughly 4%. The composition of major farming crops in the region differs from those of other Indian regions (Figure 63). The most commonly farmed crop was sorghum, which was cultivated on almost one-third of analyzed land. The areas dedicated to millet, groundnuts, and cotton were all similar and each of them made up close to 15% of arable land. The areas occupied by wheat and maize were also similar to each other, with 11% and 9% dedicated to them, respectively. The last crop with significant acreage was rapeseed, found on almost 3% of arable land. The average daily temperatures were extracted from the point located at 18° north and 77° east. Those temperatures were significantly different than ones found in two other Indian regions. Having a location closer to the equator, the annual temperatures showed a much smaller amplitude, ranging between 22°C and 32°C, resulting in quite smooth GDD accumulation throughout the year (Figure 64). The annual variation of bare soil in the region shows a simpler structure than other Indian regions (Figure 65). The maximum acreage of bare soil is reached around the 182nd DOY when it reaches almost 190,000 km^2. Prior to that peak, the increase in bare soil starts around the 158th DOY, which is when examples of the planting of every major crop in the region occur. After the aforementioned peak, the amount of bare soil decreases steadily until around the 225th DOY, when the areas of the late sowing of sorghum and millet are covered by developed vegetation. The overall shape of bare soil variation is almost symmetrical, centered on the peak on the 182nd DOY.

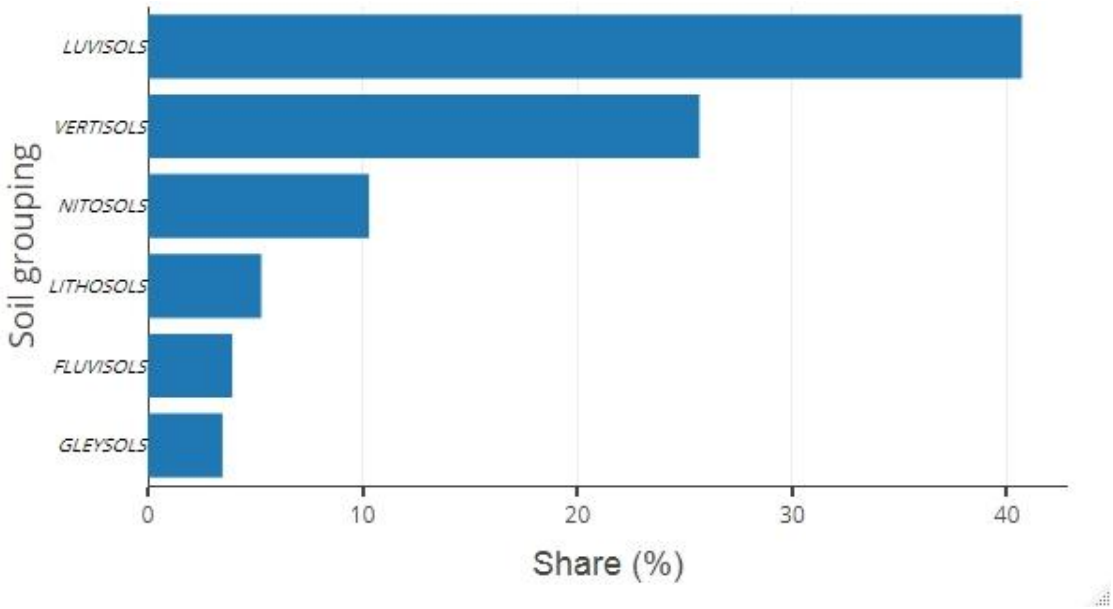

Figure 62. Share of major soil groupings in the Southern India region.

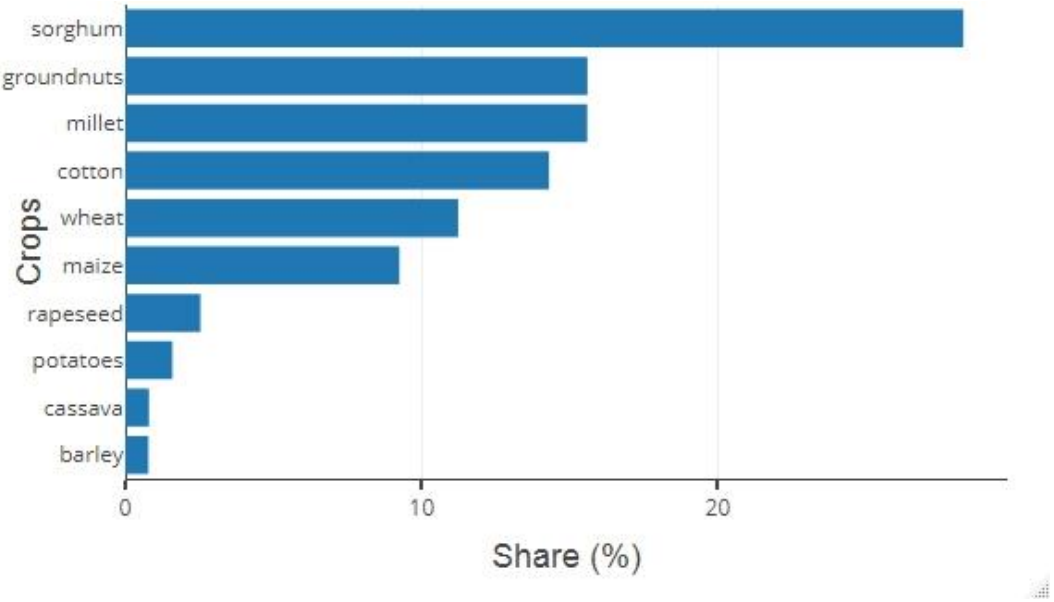

Figure 63. Share of major crops in the Southern India region.

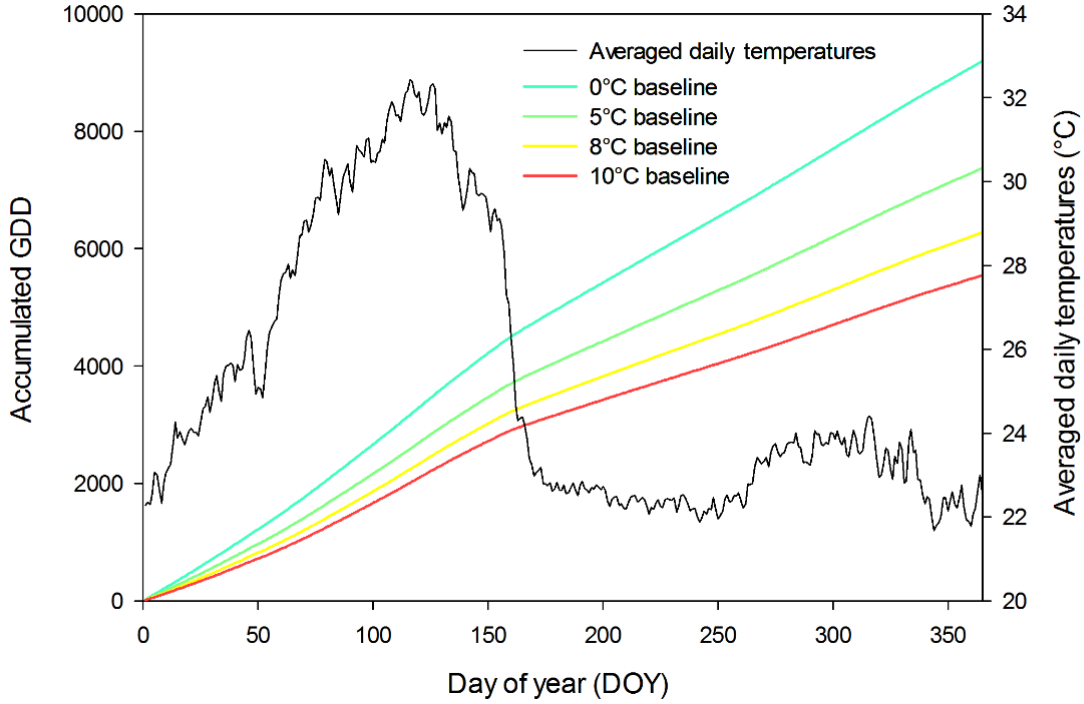

Figure 64. Average daily temperatures and resulting annual GDD accumulation calculated for four baselines in the Southern India region.

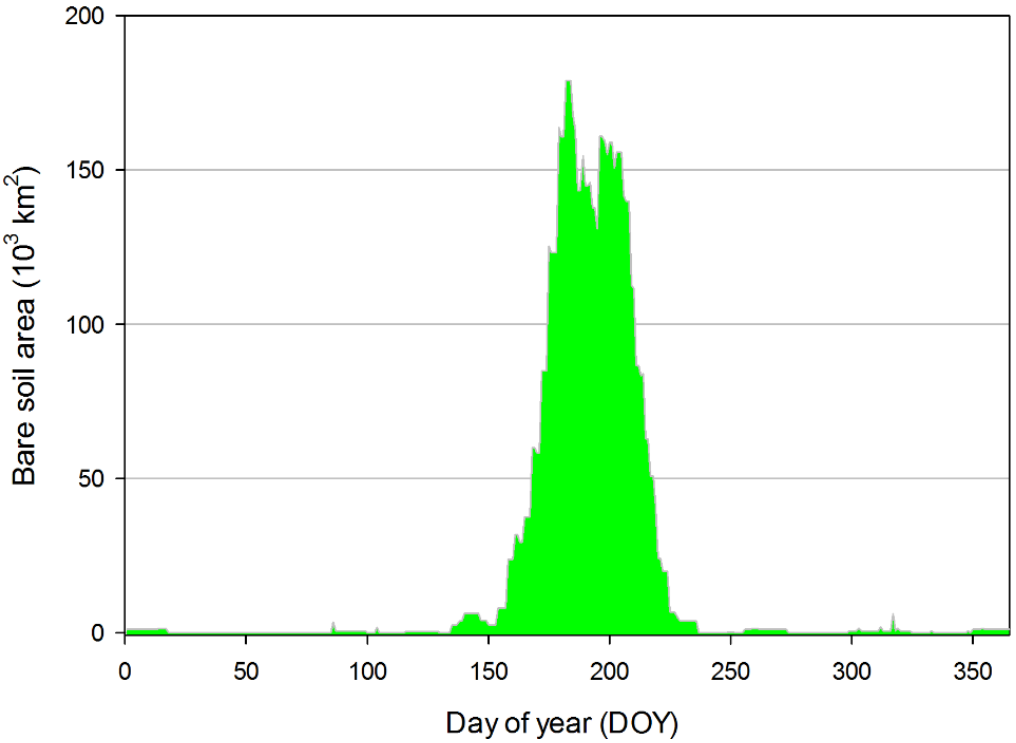

Figure 65. Annual variation of bare soil area in the Southern India region.

3.4.7. Indonesia and Malaysia

The ASim is an archipelago region, consisting of over 13 thousand islands belonging to Indonesia and almost a thousand Malaysian ones, and the country of East Timor. The region is circled by seas from all directions: by the South China Sea from the north, the Pacific Ocean from the northeast, and from the south and west by the Indian Ocean. The region also includes the Strait of Malacca, linking both oceans and being one of the most important shipping channels in the world. The arable land found in this region was spread between the numerous islands, with the biggest concentration on the island of Java. On the island of Sumatra, the arable land is located especially in the south and north, with the interior parts covered by rain forests. Agriculture is less developed on the island of Borneo, where arable land was found in pockets at the southern, western and northeastern tips, with the majority of the interior occupied by tropical rain forests. Arable land was also found on the southern tip of the island of Sulawesi and on the chain of small islands located in southeastern parts of Indonesia and in East Timor (Figure 66). However, the overall acreage of arable land is quite small compared to mainland Asian regions.

Figure 66. Distribution of arable land in the Indonesia and Malaysia region.

The most commonly found soil unit in agriculture (Figure 67) was *Acrisols*, which is a soil associated with humid and tropical regions. Almost 15% of arable land was located on *Fluvisols*, followed by another 15% split almost evenly between *Histosols* and *Luvisols*. The last

two notable soil units are *Cambisols* and *Ferrasols*, each of them found on around 5% of arable land. Out of the 13 analyzed major crops, only six were reported as being planted in the region (Figure 68). Over half of the arable land was dedicated to farming maize, followed by cassava that was sowed on one-fifth of analyzed land. Relatively similar areas were used for soybeans and groundnuts, which had a share of 13% and 10%, respectively. The values used for the estimation of annual GDD accumulation were extracted from a point centered at 1° south and 101° east, which is located on the island of Sumatra. With the region located at the equator, the mean daily temperatures showed very low annual variability, ranging by only 2°C, between 26°C and 28°C, resulting in a very stable accumulation of GDD (Figure 69). The resulting annual variation of bare soil possesses three distinct peaks (Figure 70). The biggest one reaches almost 28,000 km^2 and occurs around the 349th DOY, and results from the planting of maize around the 334th DOY, followed by the sowing of cassava. The second largest peak is smaller by around 25%, reaching a bit more than 21,000 km^2, and is found between the 204th DOY and the 231st DOY. The surface remains uncovered due to the planting of maize followed by groundnuts. The last and the smallest significant peak reaches only around 7,500 km^2. That last period occurs between the 16th and the 30th DOY as a result of the planting of soybeans.

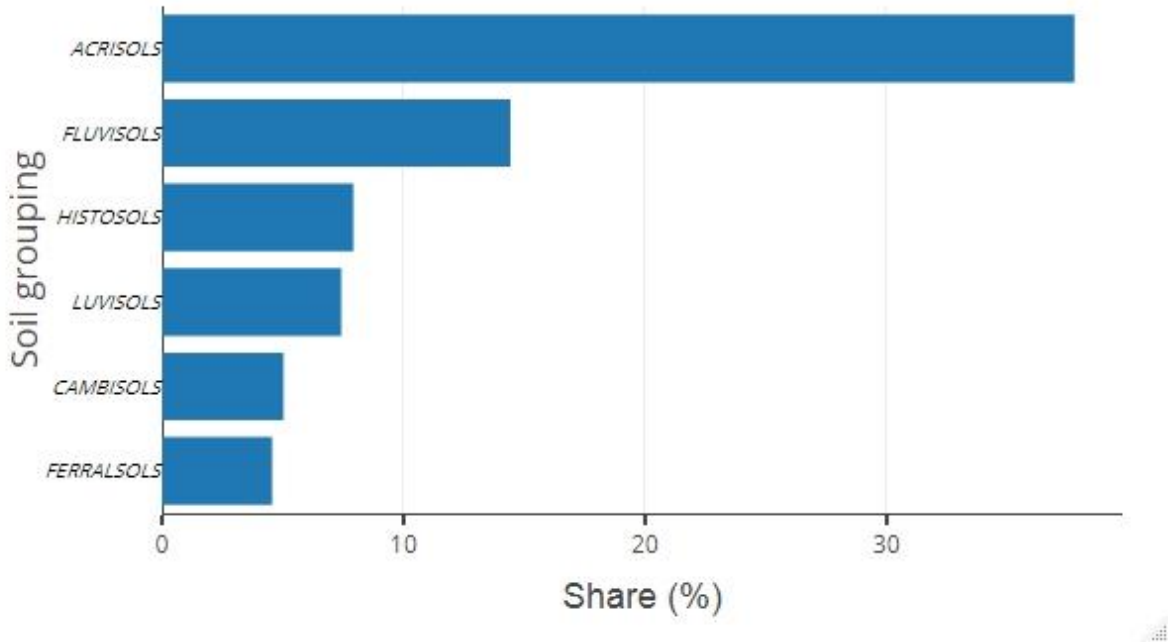

Figure 67. Share of major soil groupings in the Indonesia and Malaysia region.

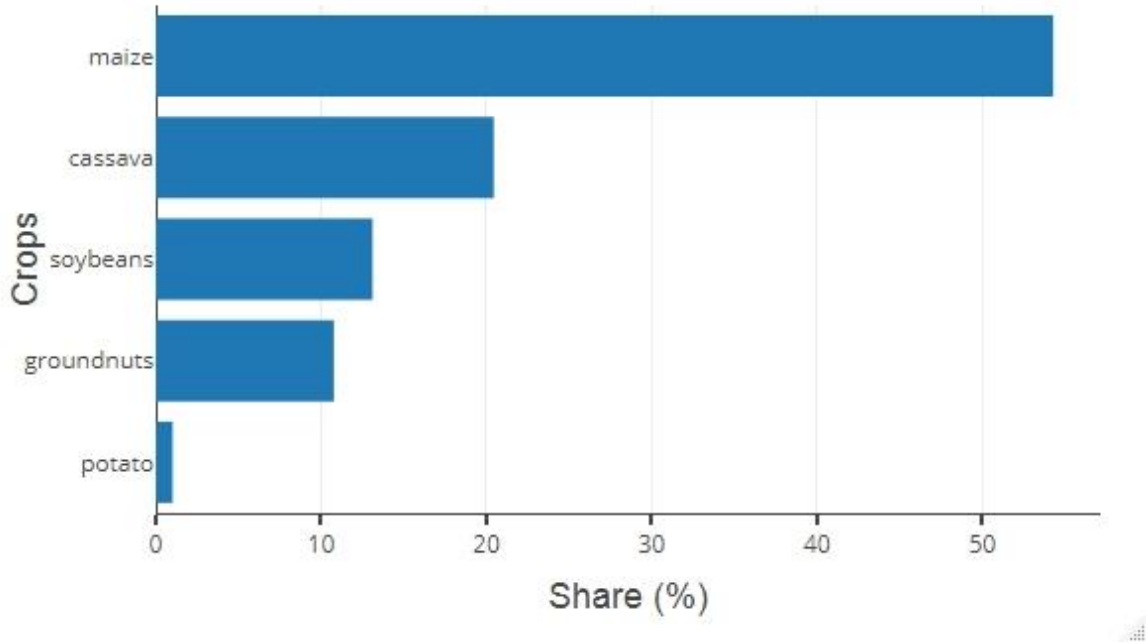

Figure 68. Share of major crops in the Indonesia and Malaysia region.

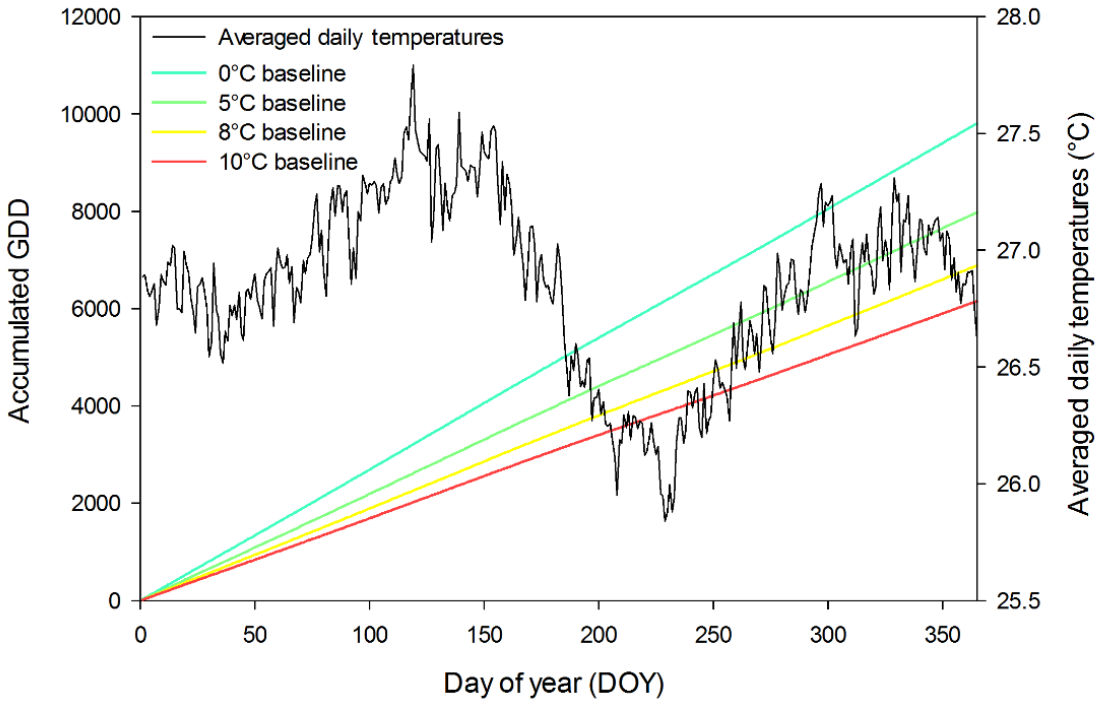

Figure 69. Average daily temperatures and resulting annual GDD accumulation calculated for four baselines in the Indonesia and Malaysia region.

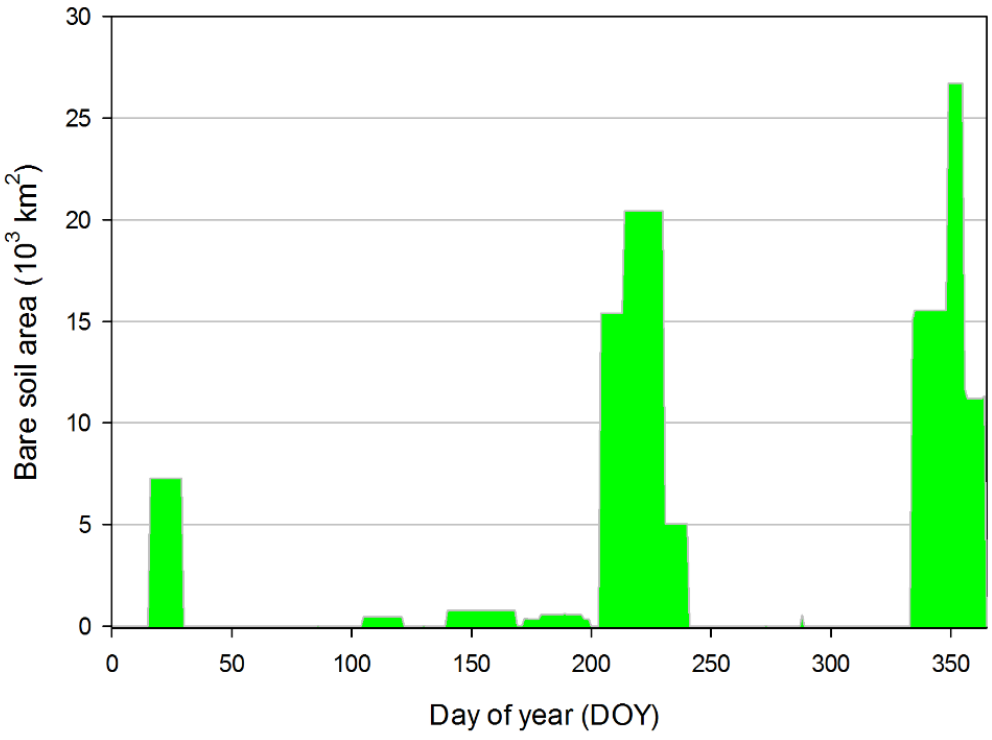

Figure 70. Annual variation of bare soil area in the Indonesia and Malaysia region.

3.4.8. Japan and South Korea

The ASjk region is another Asian region located predominantly on islands. The Japanese islands are of volcanic origin, resulting in fertile soil; however, over 70% of the country is mountainous, leaving mostly just the coastline for agriculture and urbanization. The geographical characteristics of South Korea are similar, with two-thirds of the land area covered by mountains. The quantity of arable land in this region is the lowest compared to all other Asian regions. In South Korea, the biggest concentration of arable land is found along the western coast and a significant pocket of agriculture exists in the southeastern parts of the country, along the Nakdong River. In Japan, most agriculture is found in Honshu Island, especially on the lowlands along the western and eastern coast. Another pocket of agriculture was located on the northern tips of the island of Kyushu and in eastern parts of the island of Hokkaido (Figure 71).

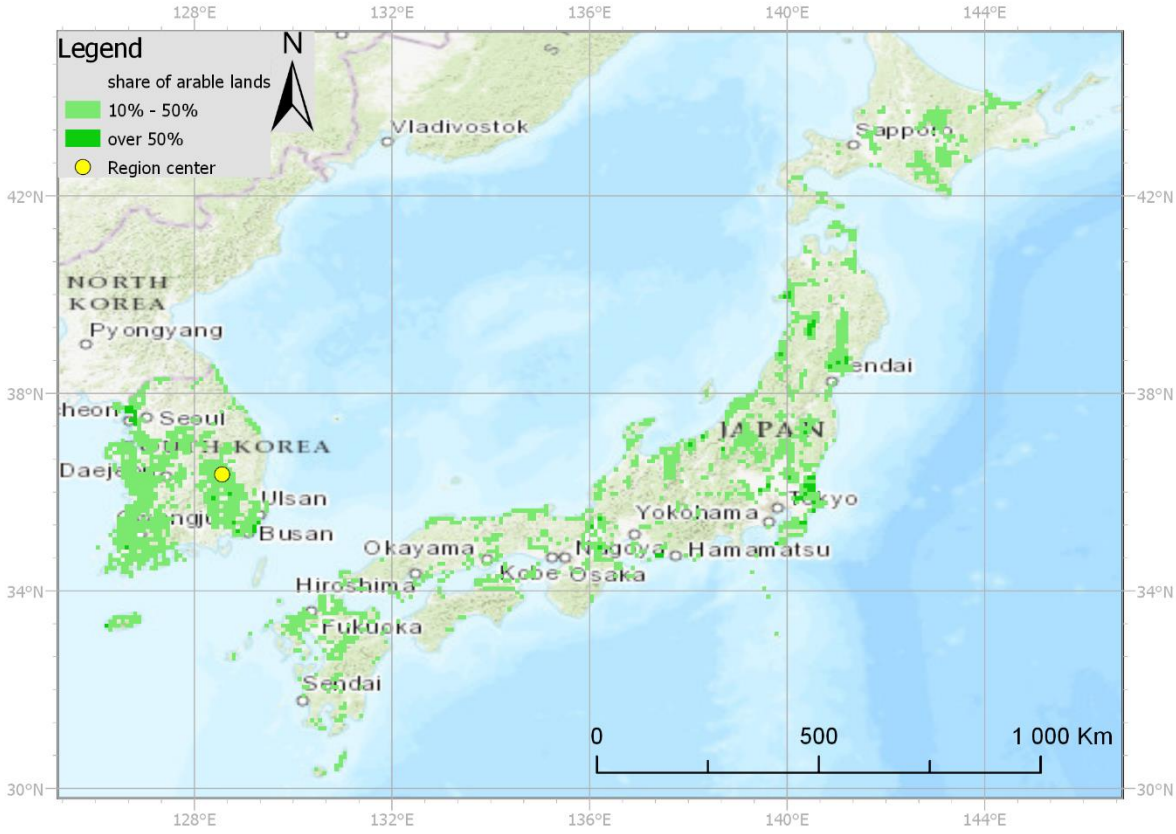

Figure 71. Distribution of arable land in the Japan and South Korea region.

Three soil units occupy similar proportions of arable land within the region (Figure 72), *Lithosols, Acrisols* and *Solonetz*, each of them with a share of around 25%. The remaining quarter is divided into *Fluvisols* with a share of about 13% and *Cambisols* and *Gleysols* that

each occupy around 6%. The two major crops farmed on most of the arable land are soybeans and wheat, which both combined constitute more than 50% of analyzed land (Figure 73). Similar areas were also found for barley and potatoes, with a share of 18% and 16%, respectively. Around one-tenth of arable land was sowed with sugar beet, while a share of maize was just a bit more than 2%. The point used to extract temperatures for GDD estimation was located in South Korea, at 36° north and 128° east (Figure 74). The mean daily temperatures were above freezing point throughout the year, ranging between 1°C and 24°C. The annual variation in the acreage of bare soil has a compact shape (Figure 75). The first occurrences of bare soil in the year were observed around the 45th DOY, after the planting of wheat and barley. The amount of bare soil stays stable until around the 105th DOY when acreage increases due to the planting of potatoes, maize, and sugar beet. The maximum amount of bare soil almost reaches 5,000 km^2 around the 111th DOY. After that day, the bare soil area steadily decreases until the 166th DOY, when it reaches its second peak of a bit more than 3,000 km^2, caused by the sowing of soybeans.

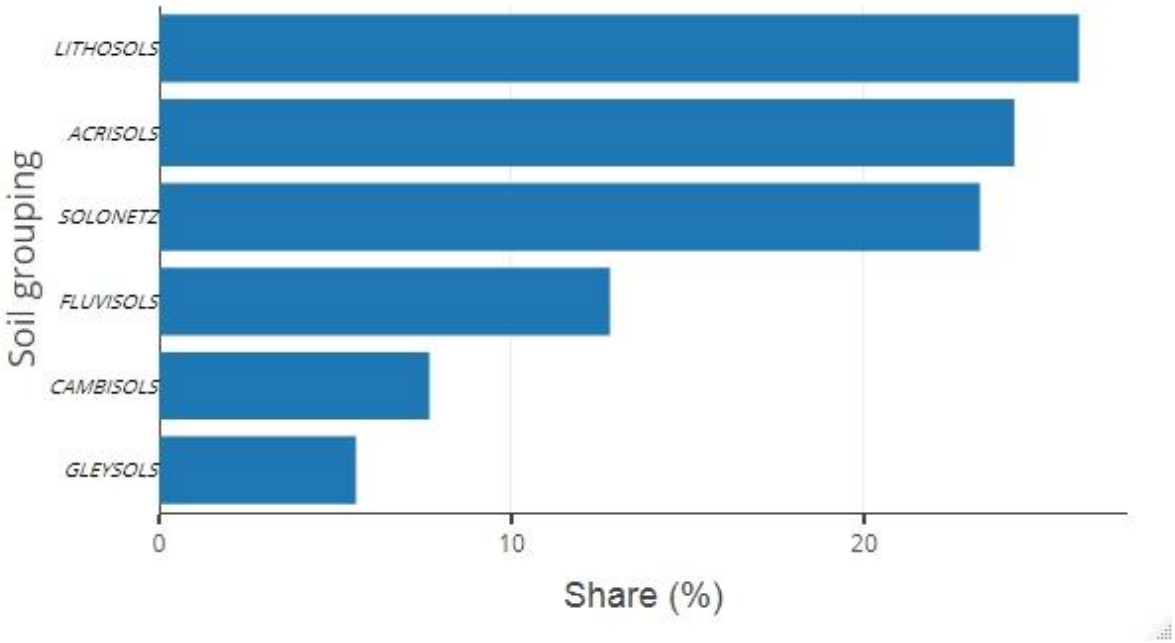

Figure 72. Share of major soil groupings in the Japan and South Korea region.

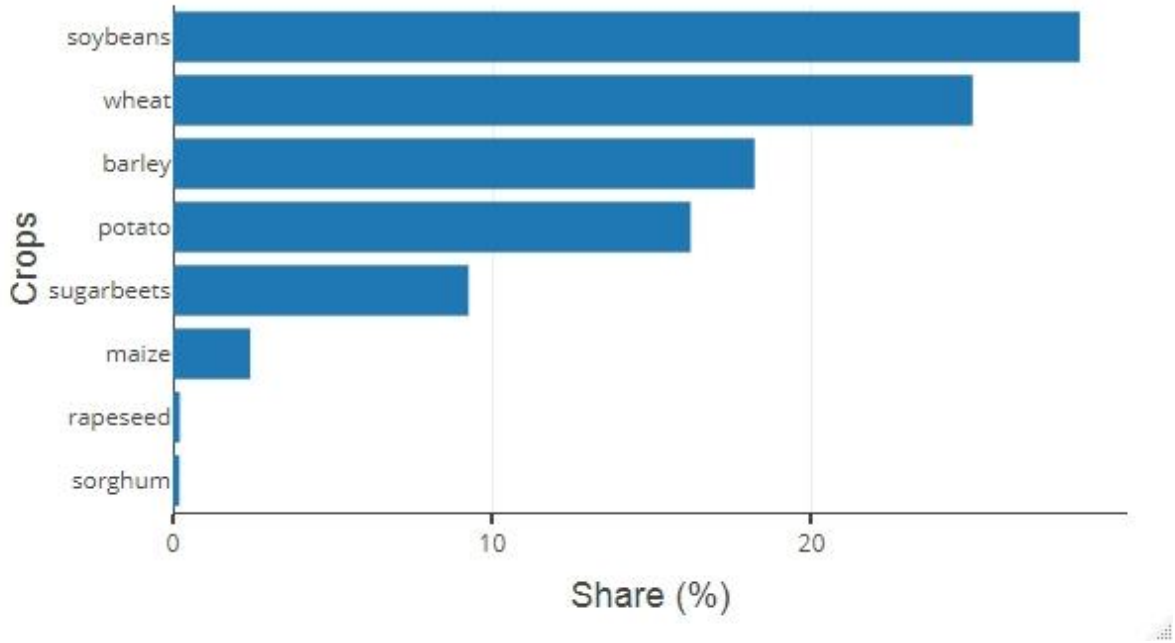

Figure 73. Share of major crops in the Japan and South Korea region.

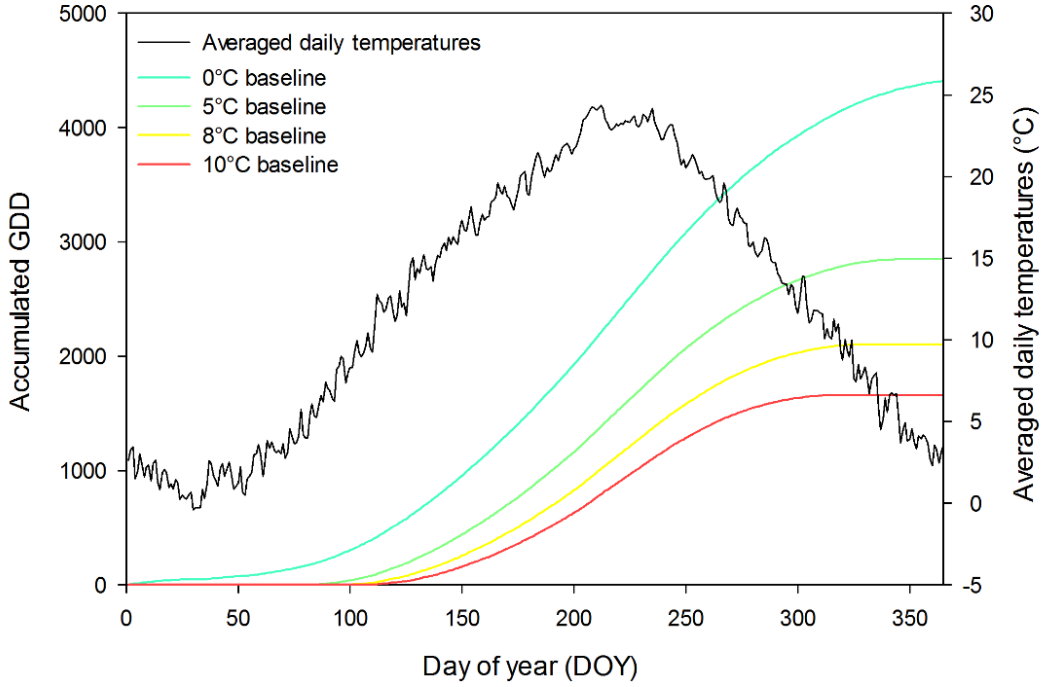

Figure 74. Average daily temperatures and resulting annual GDD accumulation calculated for four baselines in the Japan and South Korea region.

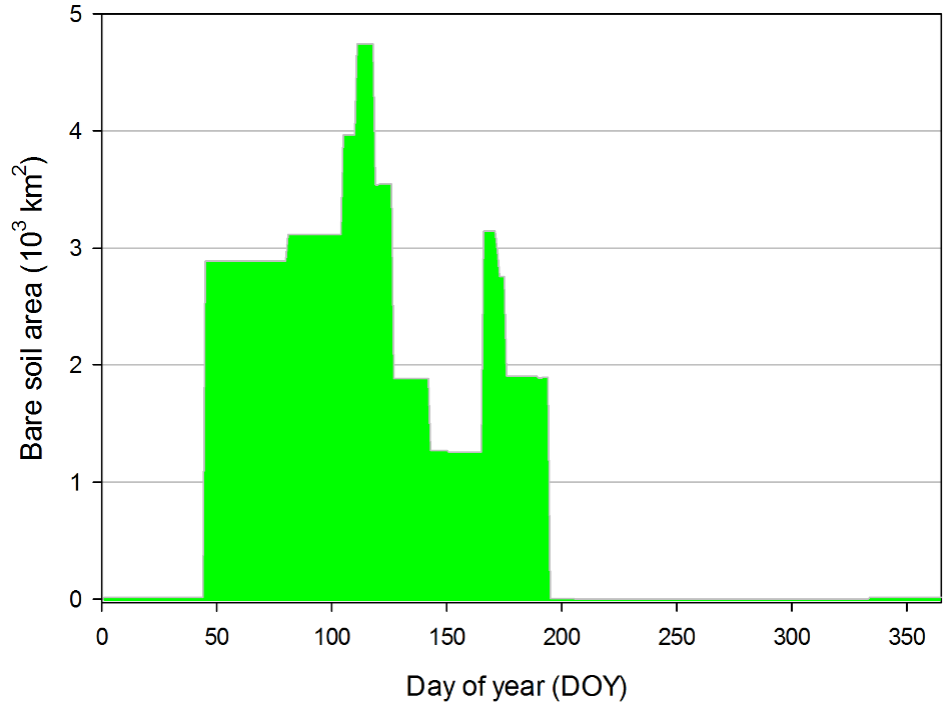

Figure 75. Annual variation of bare soil area in the Japan and South Korea region.

3.4.9. Philippines

The Philippines region is yet another island region, consisting of over 7,500 islands. Most of those are mountainous and covered by tropical rain forests of volcanic origin. Nonetheless, around one-fourth of the country's land is used for agriculture. The biggest concentration of arable land was found on the northern island of Luzon, especially in western parts around the capital city of Manila and on the southern island of Mindanao, especially on the western side. Another significant pocket of arable land was found on the Visayas islands, especially on Cebu, Panay, and Leyte (Figure76).

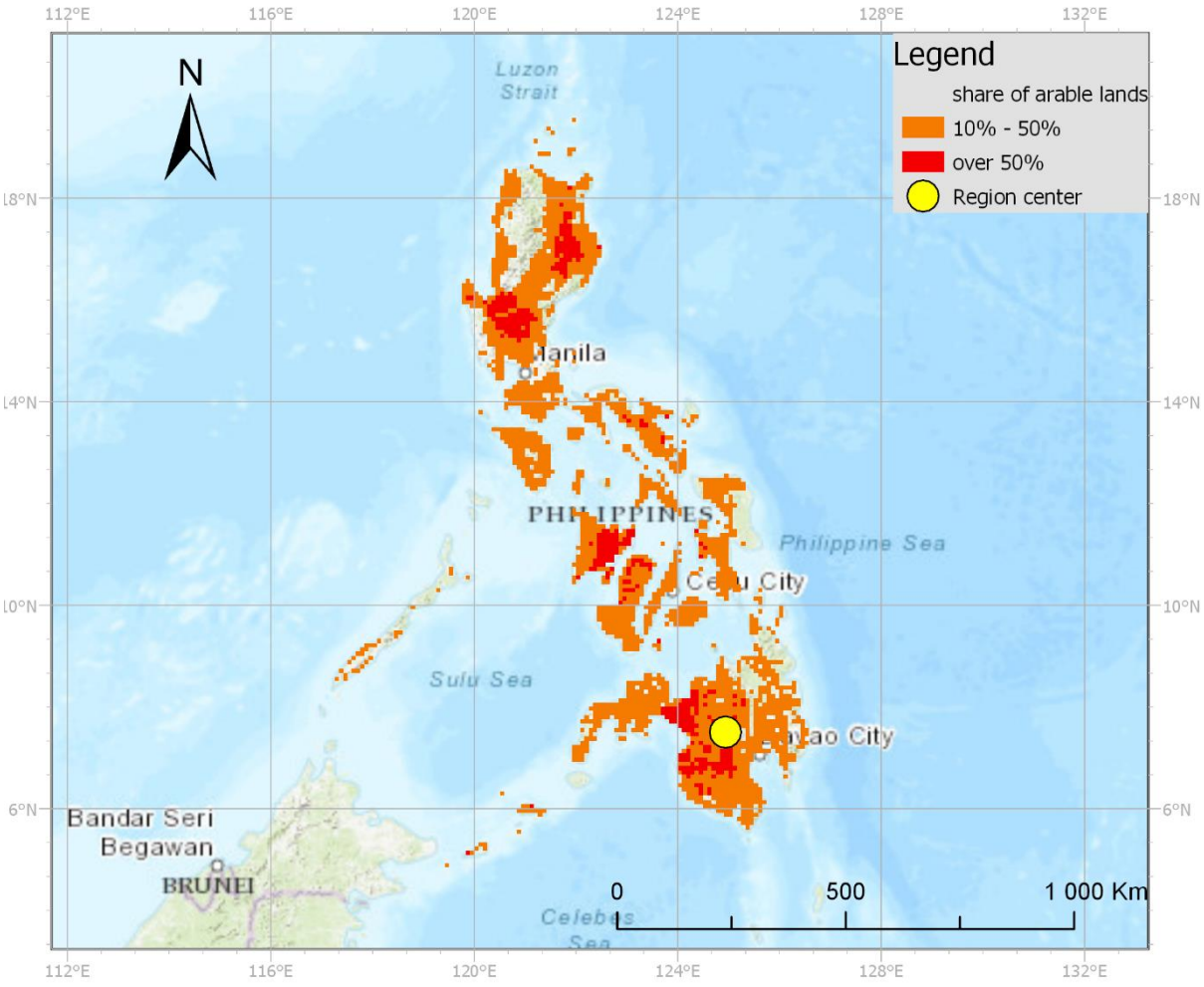

Figure 76. Distribution of arable land in the Philippines region.

The most commonly found soil unit used in agriculture was *Nitosol,* which was found on over 40% of arable land (Figure 77). *Cambisols* and *Acrisols* occupied similar areas of over 15% each. Areas covered by *Luvisols* and *Vertisols* were also alike, each of them of about 7%. The areas obtained for other soil units were much smaller, around 3% for *Andosols* and 2% each for *Gleysols* and *Arenosols.* Even less diversity was found among the major crops

analyzed (Figure 78). The vast majority of analyzed arable land was dedicated to the cultivation of maize, which had a share of more than 90%. Most of the remaining land were used for sowing cassava, with an almost 8% share. Token areas under cultivation of potatoes, groundnuts, cotton and soybeans were found, none of which had even a 1% share. The central point for the extraction of temperatures was located at 7° north and 125° east, on Mindanao Island. The ASph is located close to the equator, and therefore the annual variation of mean daily temperatures is very low, ranging between 25°C and 28°C, resulting in a very linear accumulation of GDD throughout the year (Figure 79). Since over 90% of analyzed land was under the cultivation of maize, the annual variation of bare soil (Figure 80) was also dominated by the planting of this crop. The peak, of almost 25,000 km^2 of exposed soils, happens around the 130th DOY and lasts until the 151st DOY, as the maize was estimated to take around three weeks to cover the surface again.

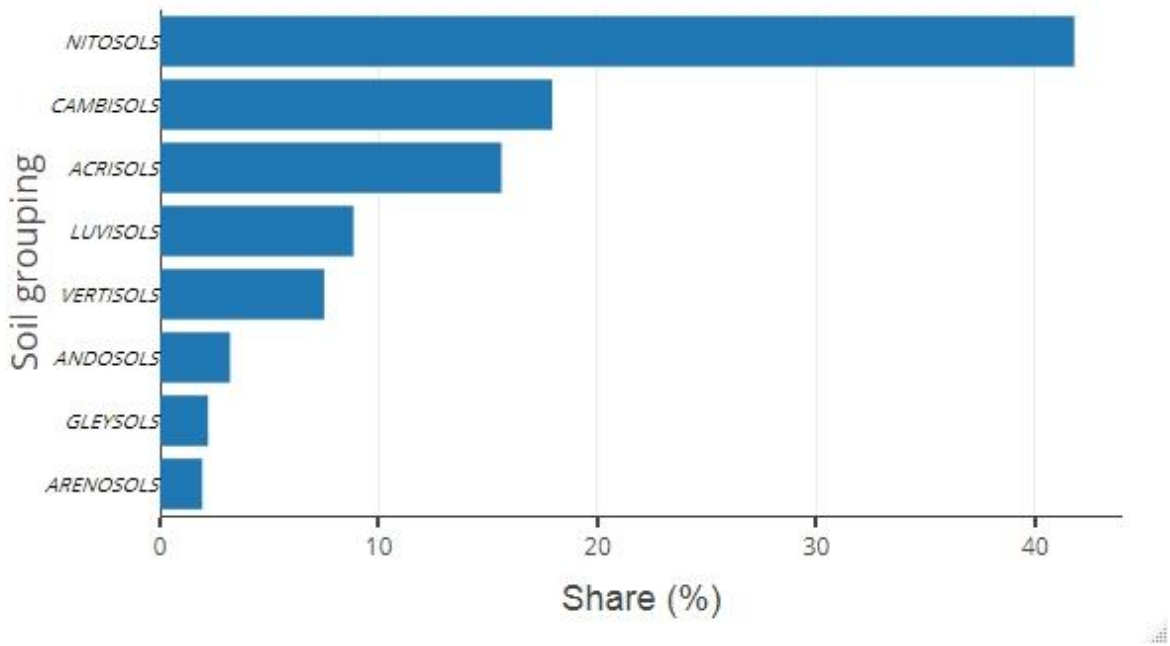

Figure 77. Share of major soil groupings in the Philippines region.

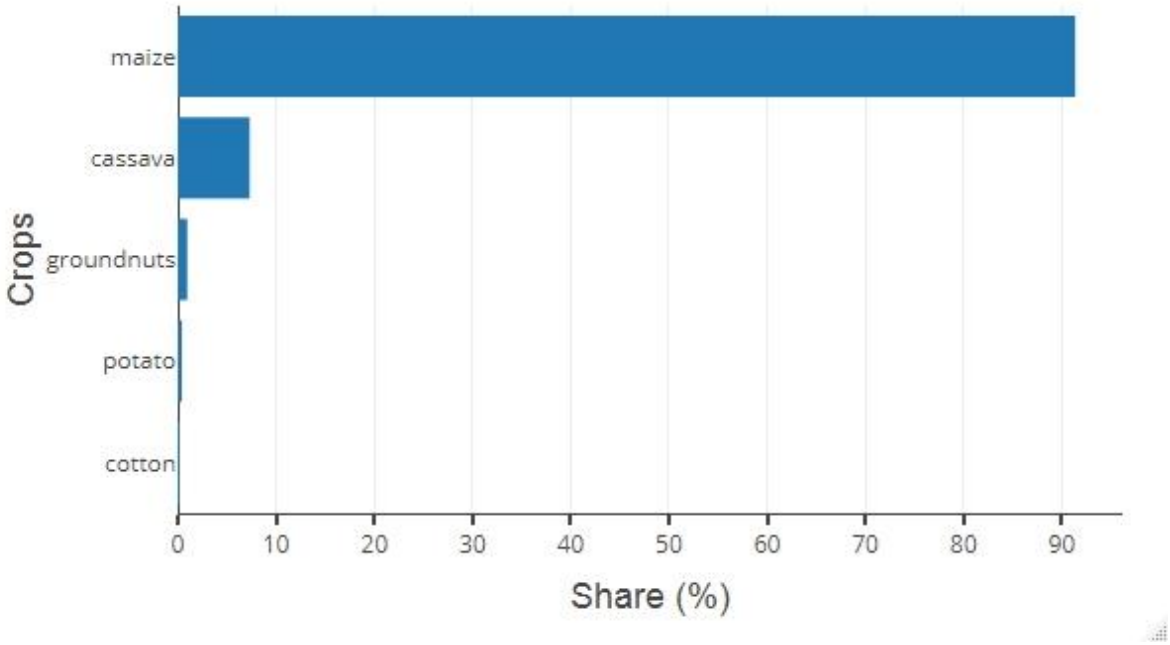

Figure 78. Share of major crops in the Philippines region.

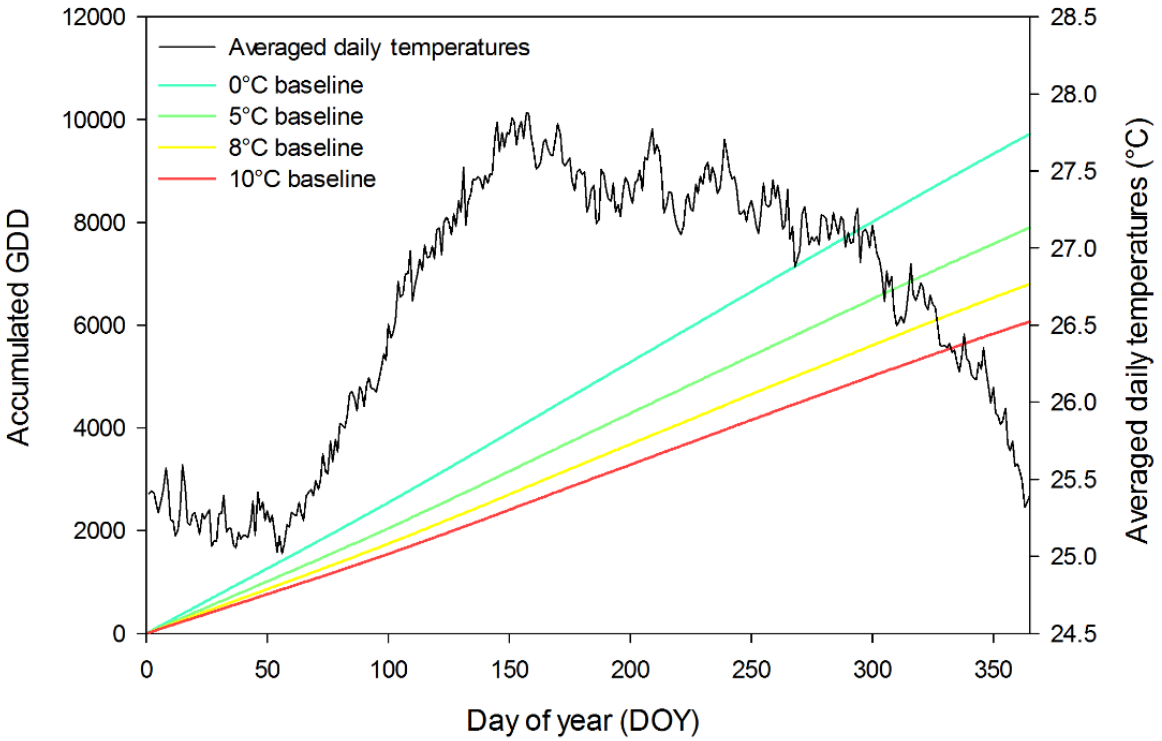

Figure 79. Average daily temperatures and resulting annual GDD accumulation calculated for four baselines in the Philippines region.

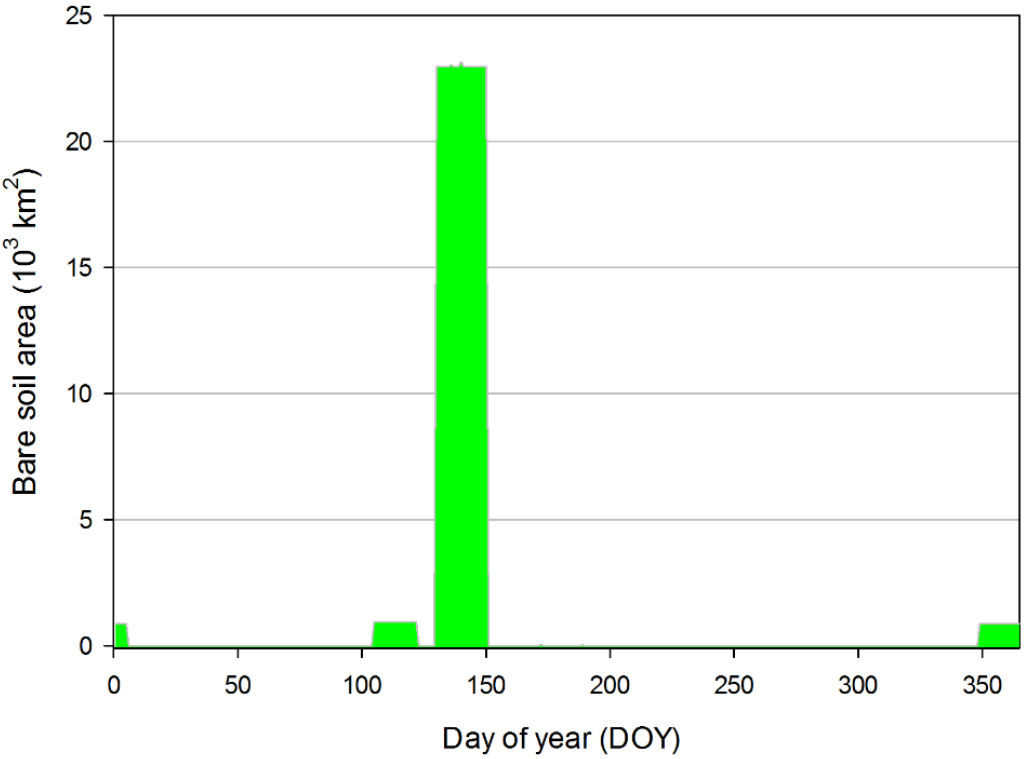

Figure 80. Annual variation of bare soil area in the Philippines region.

3.4.10. Southeast Asia

The ASse is the tenth and last region included in the Asian super region. This region, located on the mainland of the southeastern part of the Asian continent, consists primarily of the Indochinese Peninsula, including parts of the Malay Peninsula belonging to Thailand. The region includes mountain ranges that begin on the Tibetan Plateau, separated by lowlands. As the region is subdivided by the aforementioned mountains, the pockets of agriculture are spread out. The most notable ones are located along the major rivers of the peninsula: Irrawaddy, Mekong, Chao Phraya and Red River. The overall quantity of arable land is however low, comparable to ASph (Figure 81).

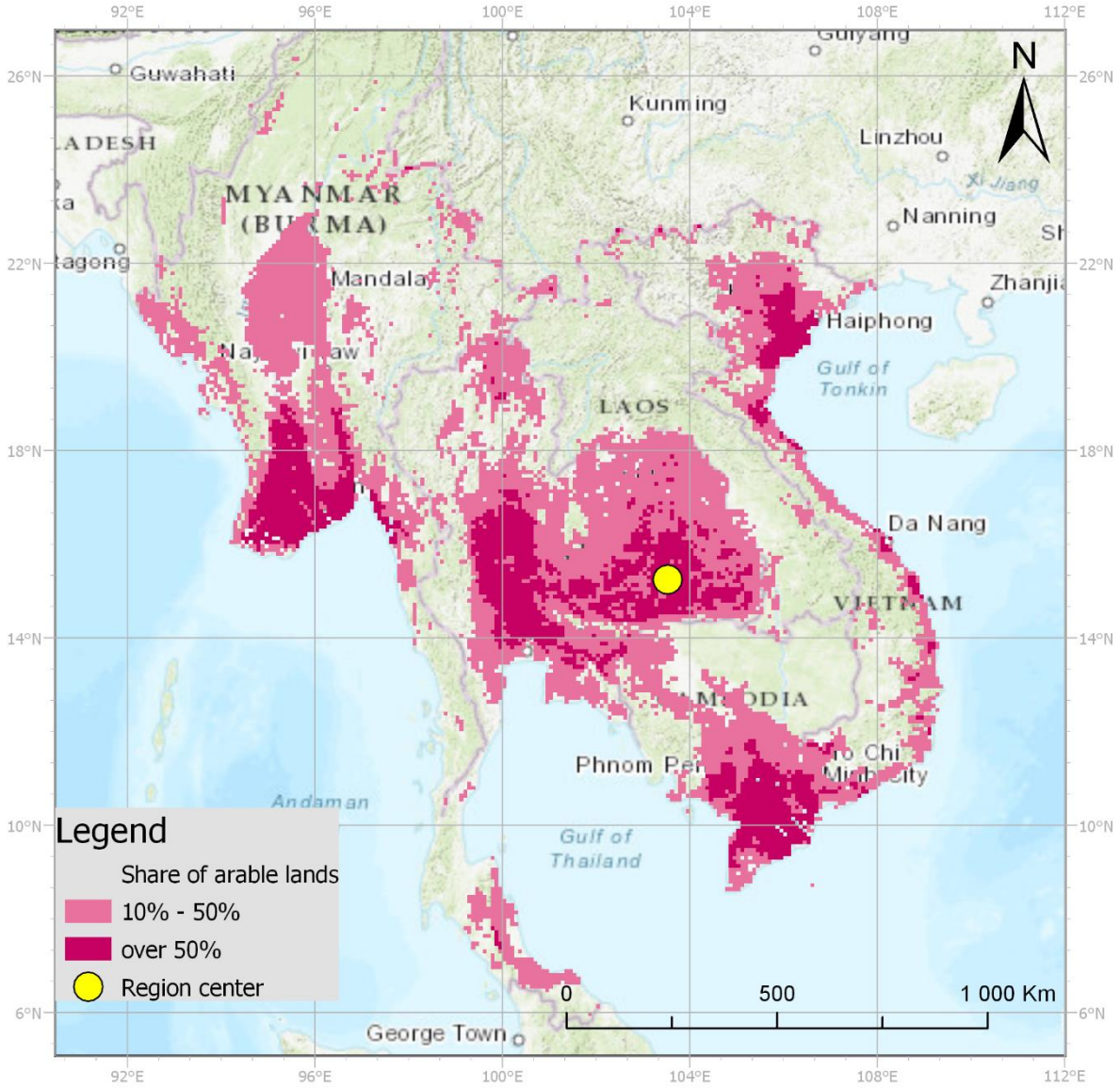

Figure 81. Distribution of arable land in the Southeast Asia region.

Over half of the analyzed areas under cultivation were located on *Acrisols* (Figure 82), which is quite a common soil unit in tropical climates. The next most commonly farmed soil unit was *Gleysols,* a soil unit associated with wet environments, with a share of around 20%. Around 8% was covered by *Luvisols* and the same percentage for *Fluvisols*. The last soil unit covering a significant portion of arable land was *Nitosols*, which had a share of almost 5%. Between the analyzed major crops cultivated in the region, two-thirds of the area was dedicated to maize (Figure 83). Much smaller but still significant areas were used for growing soybeans and cotton, with a share of around 15% and 10%, respectively. The last three major crops each had a share of between 2% and 3%, and those were wheat, sorghum, and potatoes. Temperatures used to calculate annual GDD accumulation were obtained from the point located in the eastern part of Thailand, at 15° north and 103° east (Figure 84). The tropical location of the region resulted in a relatively low variation of mean daily temperatures, which ranged between 19°C and 23°C. The annual variation of bare soil is dominated by one big peak, followed by a smaller one (Figure 85). The biggest peak reaches almost 18,000 km^2 at around the 151st DOY and is a result of the planting of maize between the 134th and the 151st DOY. The soil stayed bare for about three weeks after planting maize at that time. The second, smaller peak occurs around a month and a half after the biggest one and reaches almost 9,000 km^2. This second peak is caused primarily by the planting of soybeans and cotton. Around the 300th DOY a smaller batch of maize planting occurred, resulting in a period of over three weeks with about 2,000 km^2 of bare soil.

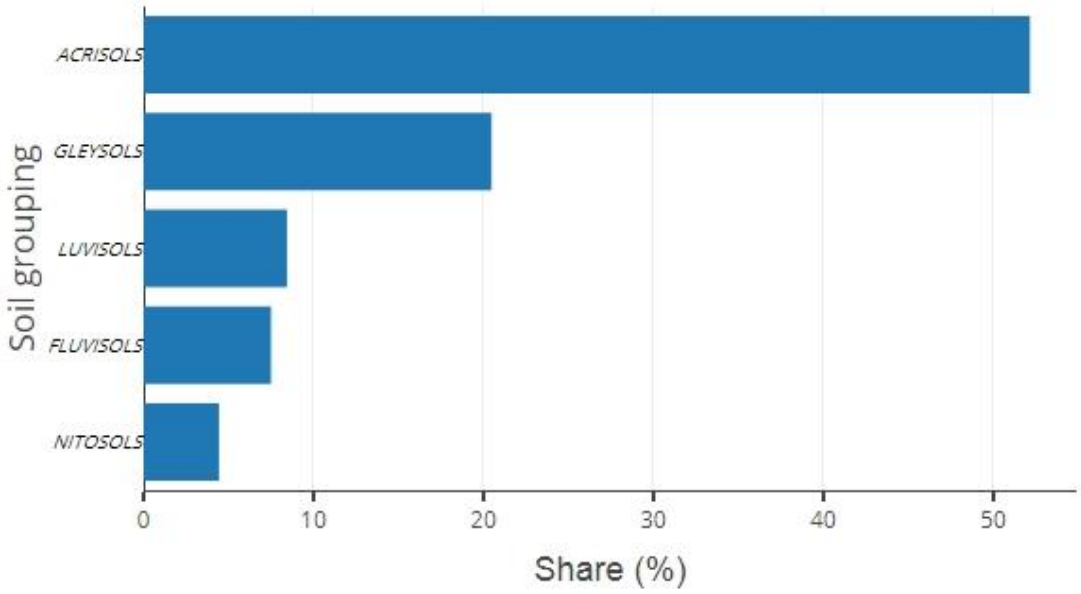

Figure 82. Share of major soil groupings in the Southeast Asia region.

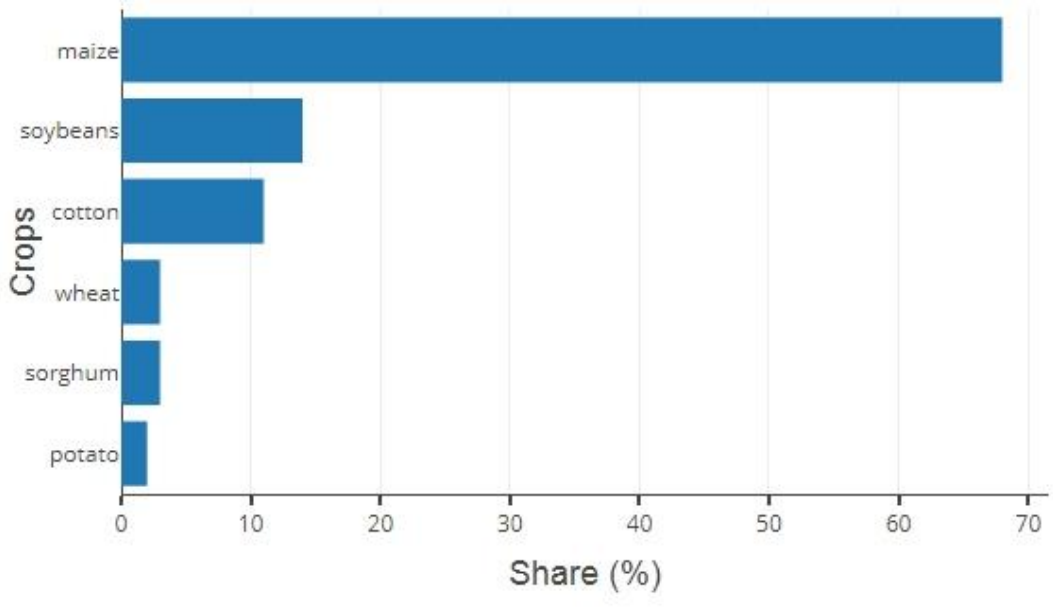

Figure 83. Share of major crops in the Southeast Asia region.

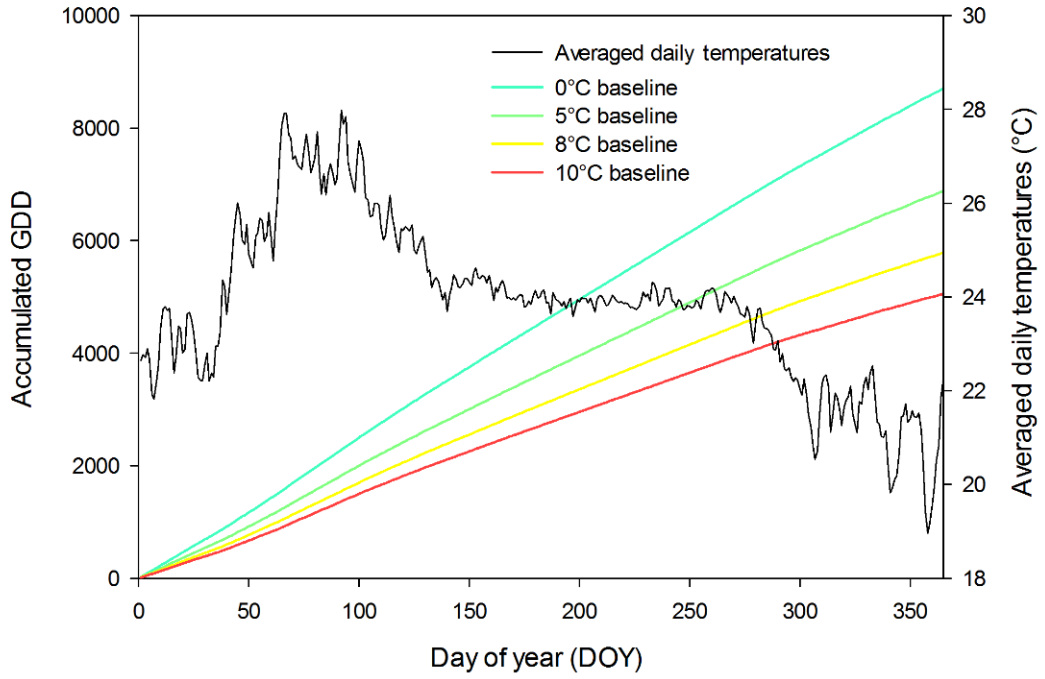

Figure 84. Average daily temperatures and resulting annual GDD accumulation calculated for four baselines in the Southeast Asia region.

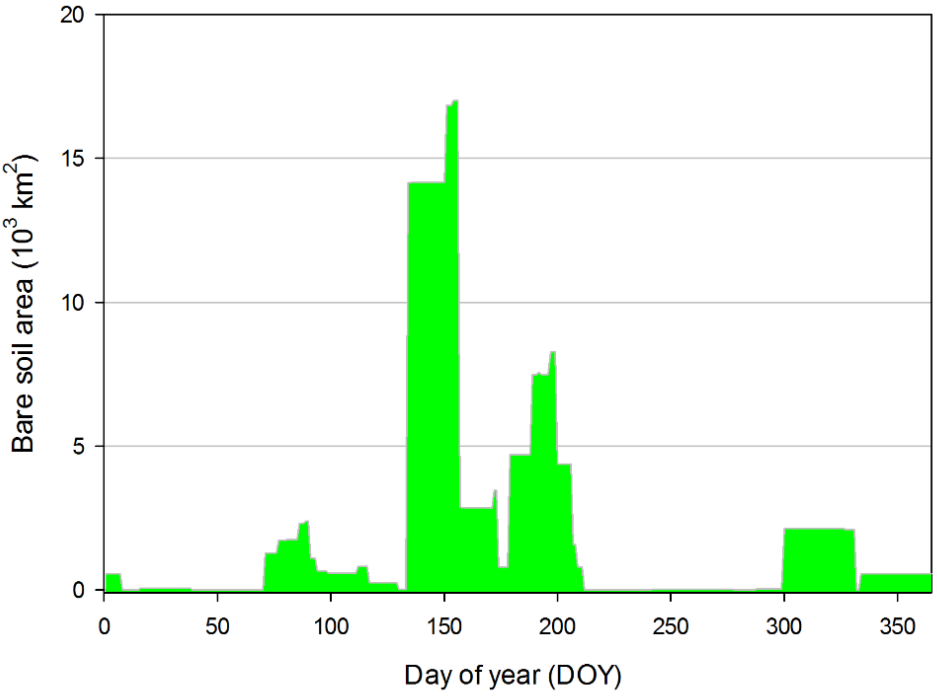

Figure 85. Annual variation of bare soil area in the Southeast Asia region.

3.5. Europe

Europe is the second smallest continent after Australia, with only around 20% of land used for some kind of agricultural activity, which is the lowest among all the continents. On the other hand, almost 60% of those agricultural land is arable, which is the highest percentage by far. Broadly speaking, the European continent is divided into three climate zones; western parts influenced mostly by the ocean, eastern Europe with its continental climate and southern parts belonging to the Mediterranean climate. This climate split has led to the distinguishing of four regions within the continent, those are (Figure 86):

- Western (EU)—including France and everything to the west of it; the region is dominated by a temperate oceanic climate, with Mediterranean influences in parts of the Iberian Peninsula;
- Central (EUce)—located to the east of EUwe; the western parts of the region are influenced by the hybrid oceanic/continental climate, that turns more continental towards the eastern part;
- Southern (EUso)—includes areas south of the Alpine Mountains and the Balkans; the region experiences a Mediterranean climate;
- Russian Federation with the former republics of the Soviet Union (Belarus, Ukraine, Azerbaijan, Armenia, Georgia) (EUrr)—even though most of Russia's land area lies in Asia, the majority of its agriculture is located to the west of the Ural Mountains.

Figure 86. Arable land in the Europe super region divided into regions.

The annual variation of bare soil in the European super region was used to estimate the dynamics of the shortwave radiation of those soils (Cierniewski, Ceglarek and Kazmierowski, 2018b; Cierniewski, Ceglarek, Kaźmierowski, *et al.*, 2018c). In that work, however, only areas of the European Union together with its associated countries were taken into account, without the EUrr region. Agricultural production in Europe is dominated by two cereals, wheat and barley, that together occupy two-thirds of the arable land analyzed (Table 9). Two crops brought over from the Americas are important in today's European agriculture; those are maize and potatoes farmed on around 10% and 6% of arable land, respectively. A similar area to the one occupied by potatoes is dedicated to the cultivation of rye. Rapeseed and sugar beet were each farmed on over 3% of land. The annual variation of bare soil in the region (Figure 87) is dominated by planting in EUrr as it has the biggest arable area. The first occurrence of arable land was spotted around the 39th DOY, and for over three months the bare soil area is steadily increasing, up to the maximum of over 450,000 km^2 around the 140th DOY. After that day there was a sharp decline in the bare soil area, which disappeared completely around the 165th DOY. Two months later another period of bare soil was noted, lasting for about two and a half months, between the 230th and the 285th DOY. During that period, bare soil was noted on up to almost 100,000 km^2.

Table 9. Area and share of arable land of major crops farmed in Europe**.**

Major Crop	Area	
	(thousands km^2)	(%)
Wheat	650.38	46.9
Barley	293.34	21.2
Maize	135.82	9.8
Potato	92.11	6.6
Rye	84.31	6.1
Rapeseed	46.09	3.3
Sugar beet	44.12	3.2
Cotton	24.81	1.8
Millet	10.71	0.8
Soybean	4.61	0.3
Sorghum	0.53	0
Groundnut	0.09	0

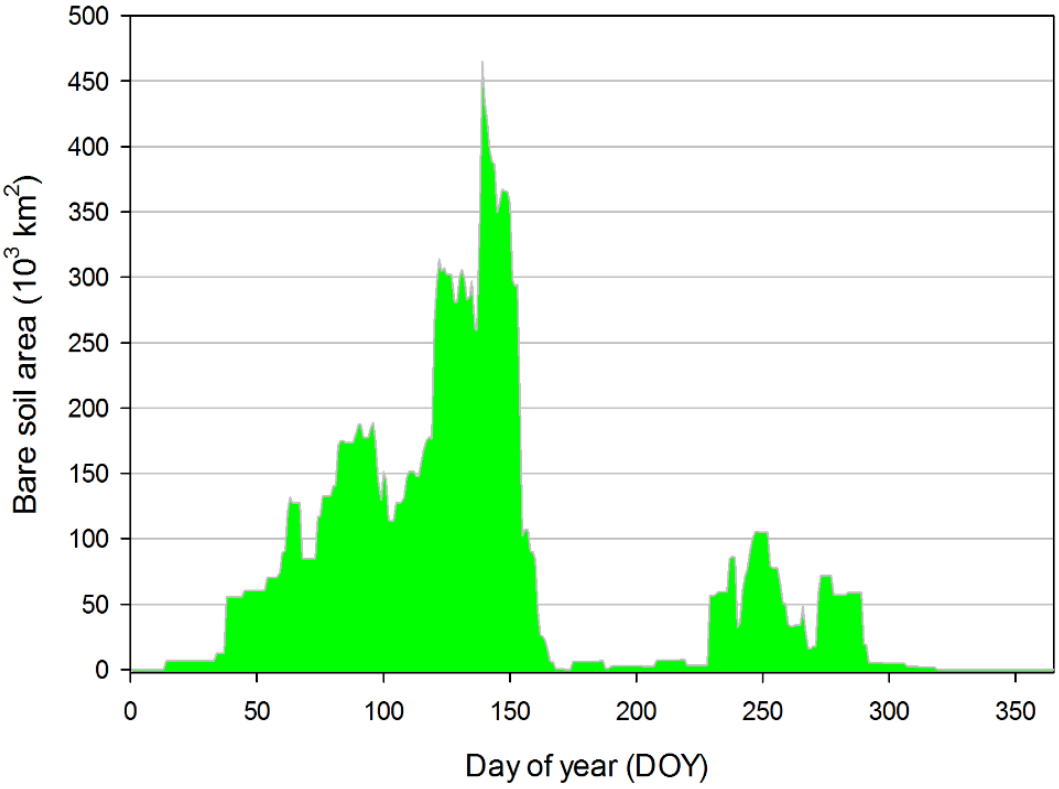

Figure 87. Annual variation of bare soil area in the Europe super region.

3.5.1. Western Europe

The westernmost region of Europe experiences a relatively mild climate compared to what would be expected at the same latitude, thanks to the influence of the Gulf Stream. The agricultural production of this region is concentrated around inland areas of Spain, central and northern France and southern and eastern parts of the United Kingdom. The average farm size varies within the region, with the smallest found in Portugal and Spain; in France the average area was three times larger than in Spain, and in the United Kingdom it was bigger still. Out of the three regions belonging to the European Union, the practice of CA was the most widespread, especially in Spain where almost 8,000 km^2 were reported, and a quarter of that in France (Figure 88).

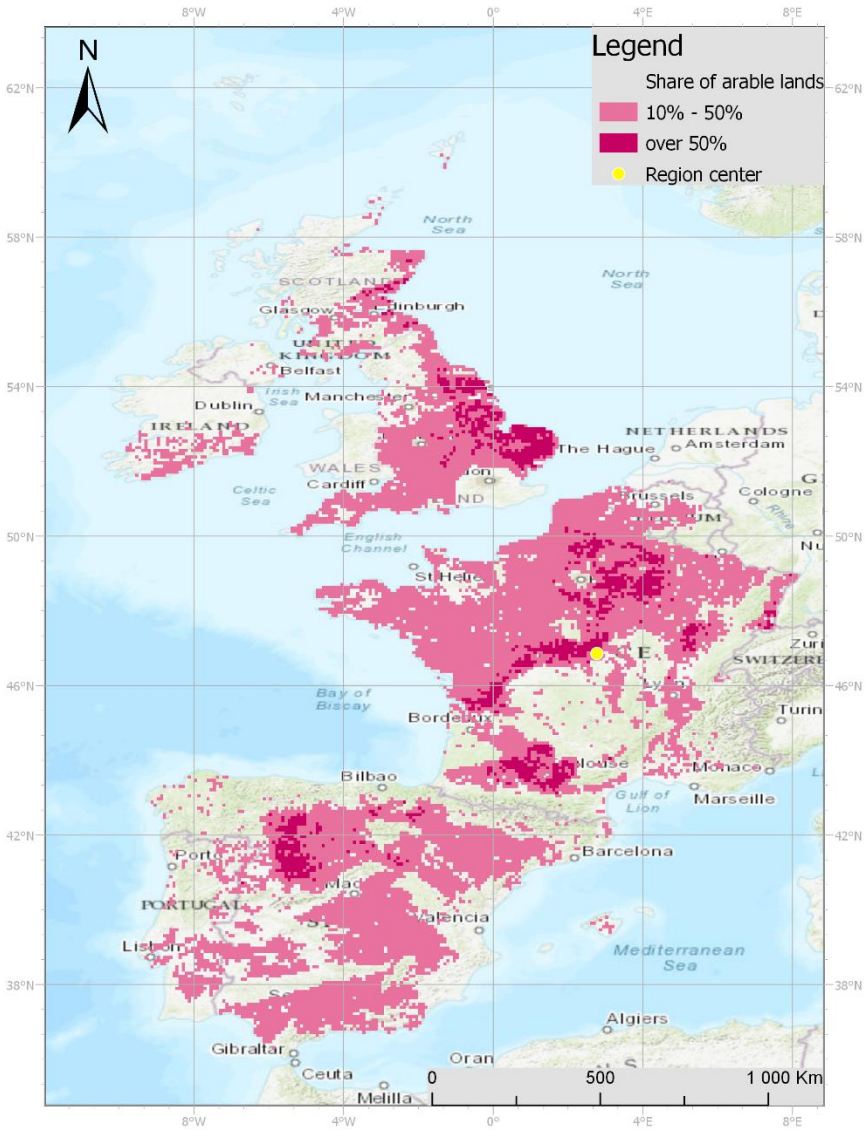

Figure 88. Distribution of arable land in the Western Europe region.

The dominant soil unit used in arable land was *Cambisols*, found on almost half of them (Figure 89). Almost a third of the land is occupied by *Luvisols*, while the areas occupied by *Fluvisols* and *Rendzinas* equate to around 8% for each. Over 70% of arable land is dedicated to either wheat or barley, with wheat dominating in northern parts of the region, while barley dominated in the Iberian Peninsula (Figure 90). A bit more than a tenth of the area was used for growing maize, while areas with rapeseed occupied almost 8%. Half of that area was used for farming sugar beet, around 4%. Average daily temperatures were extracted from a location in central France, situated at 47° north and 3° east, midway between the northern and southern extremities of the region. The annual mean daily temperatures showed seasonality, but never dipped below freezing point, ranging between 0°C and 21°C, resulting in a somewhat linear GDD accumulation through most of the year (Figure 91). The annual variation of bare soil is dominated by a huge peak, reaching almost 130,000 km^2 and occurring around the 120th DOY (Figure 92). Two main crops contributing to that maximum are wheat, planted around the 95th DOY, followed by maize around the 116th DOY, each taking between five and six weeks to develop and cover the surface. Another peak, around three times smaller, was found starting about the 206th DOY, after the planting of barley, followed by a period between the 230th and the 306th DOY, when the bare soil area reaches about 25,000 km^2 as a result of sowing primarily rapeseed, barley and rye on relatively smaller areas.

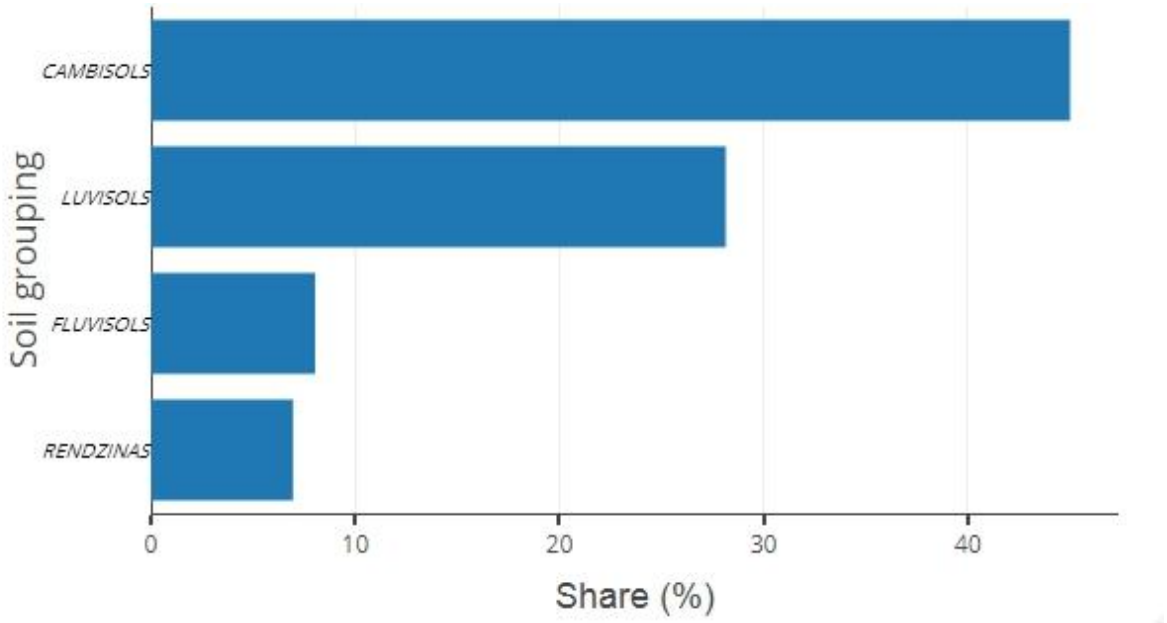

Figure 89. Share of major soil groupings in the Western Europe region.

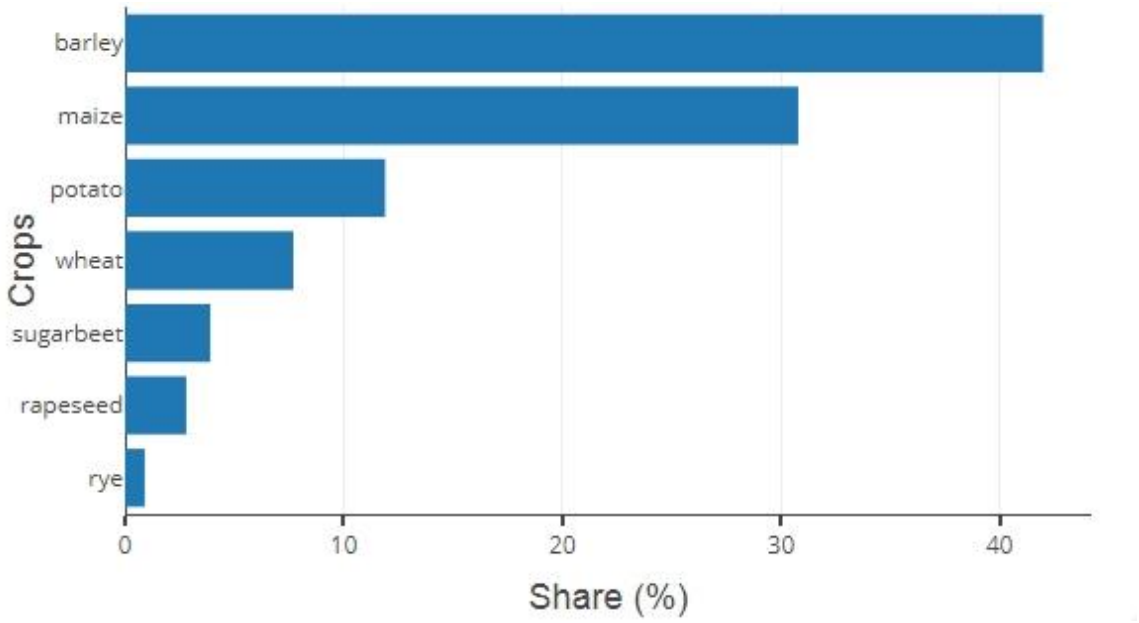

Figure 90. Share of major crops in the Western Europe region.

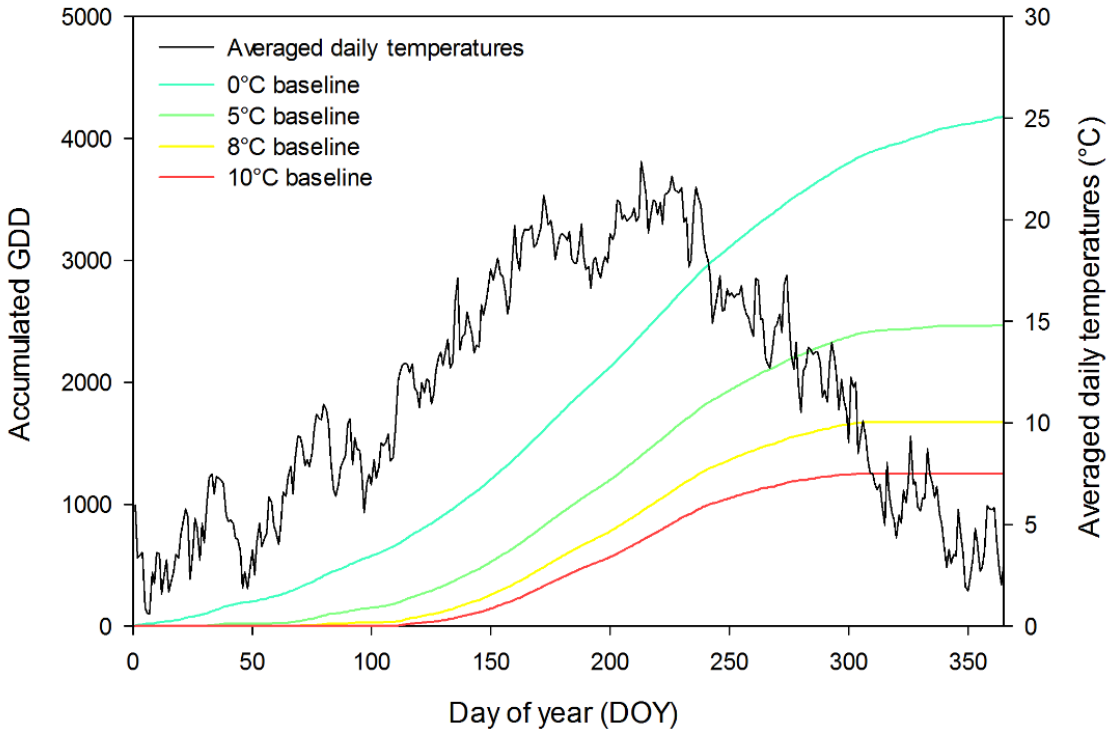

Figure 91. Average daily temperatures and resulting annual GDD accumulation calculated for four baselines in the Western Europe region.

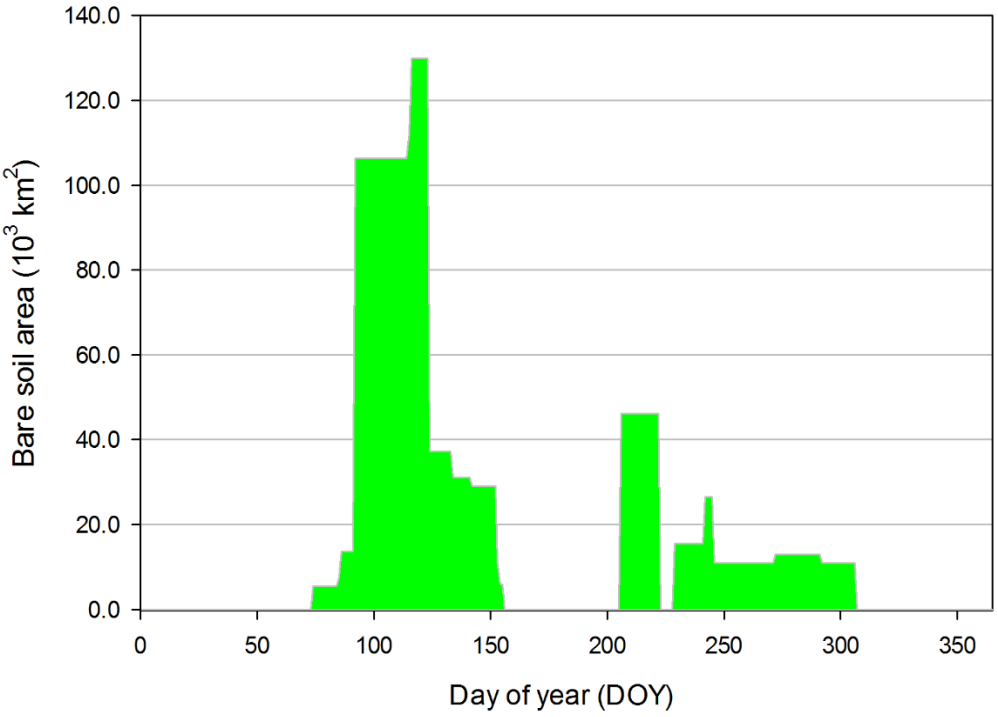

Figure 92. Annual variation of bare soil area in the Western Europe region.

3.5.2. Central Europe

Located between the oceanic climate zone to the west and heavy continental influences from the east, EUce experiences a hybrid climate, with very distinct seasons. Among the countries found in this region, Czechia, Denmark, and Germany have some of the largest average farmland sizes in the European Union, while those in Poland lie toward the smaller end of the spectrum. Arable land is spread around the whole region, with obvious exceptions for forests and mountains. The most intensely farmed parts are located in central and northern Germany, western and northern Poland, and throughout Denmark and the Netherlands. Some arable land was also present in southern parts of Sweden and Finland, close to the Baltic Sea. The practice of CA was noted on around 2,000 km^2 in Germany and on token areas in the Netherlands (Figure 93).

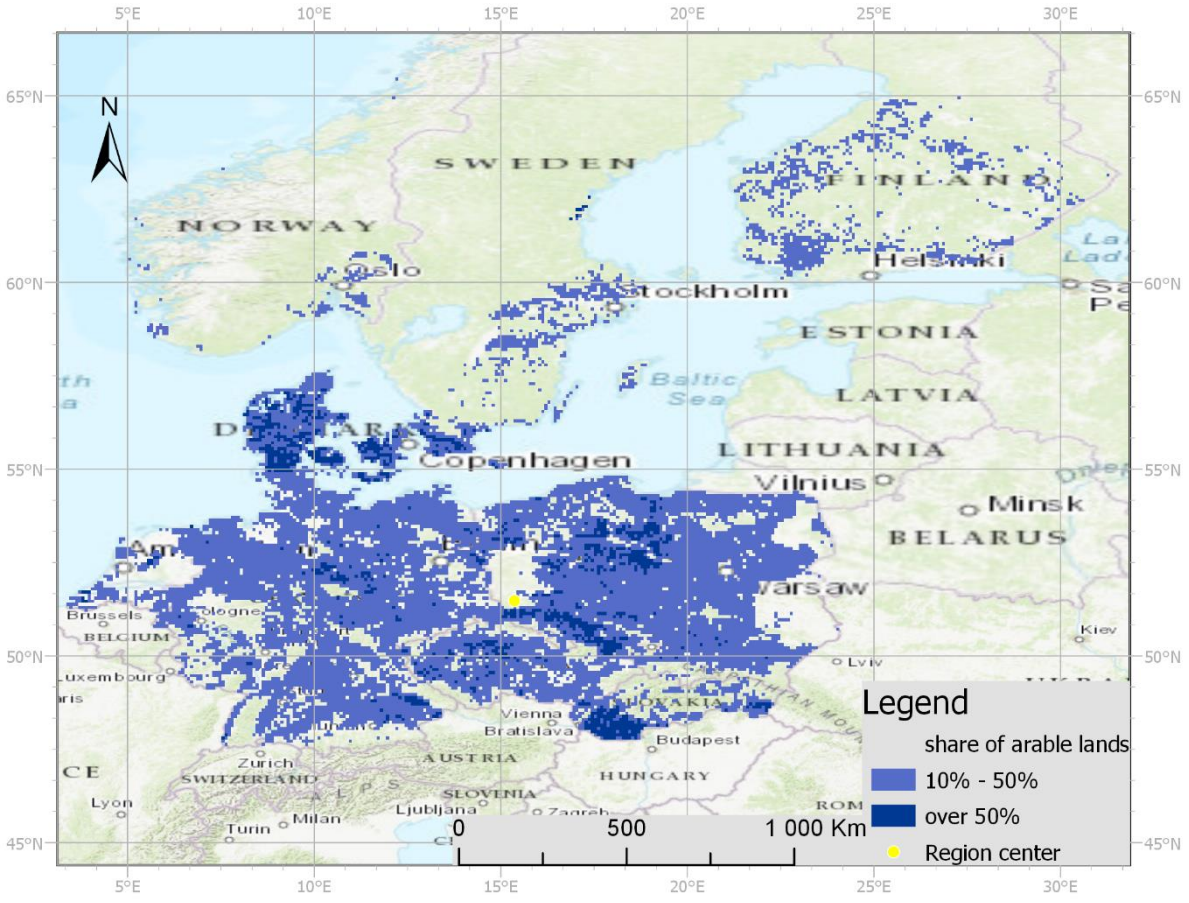

Figure 93. Distribution of arable land in the Central Europe region.

The two most dominant soil units are the same as in EUwe, however with switched positions (Figure 94). Over a third of arable land contains *Luvisols* and another fifth *Cambisols*, with those two soil units together found on almost 60% of arable land. Another widespread

soil unit was *Podzols* found on over 15% and followed by *Podzoluvisols* and *Fluvisols*, each of them located on around 6% of the analyzed surface. Almost 5% was occupied by *Chernozems*, one of the most fertile soil units. The two most dominant crops were also the same as in EUwe, those being wheat and barley (Figure 95). However, their combined share (around 60%) is lower than in EUwe (over 70%), as a third cereal is farmed on a significant area; this is rye which is found on almost 15%. Other crops with a great significance in the region are rapeseed and potato occupying almost 10% each, then sugar beet and maize farmed each on about 5%. The central point of the region was designated at 52° north and 15° east, close to the border between Germany and Poland, and in the central part of the region. The mean daily temperatures dipped below freezing point, ranging between -3°C and 20°C, resulting in quite rapid GDD accumulation throughout more than half the year, with a long period without any increase (Figure 96). In the annual course of bare soil variation, two main periods can be distinguished (Figure 97). The first begins around the 74th DOY, coinciding with the planting of potatoes, followed by maize and sugar beet around two weeks later, and then by wheat one week after that. The peak of almost 60,000 km^2 was reached around the 136th DOY. The second period occurs around three months later, starting about the 215th DOY and lasts until the 290th DOY, reaching almost 40,000 km^2 maximum. The start of the second period is caused by the planting of barley and extended by rapeseed planted around the 240th DOY.

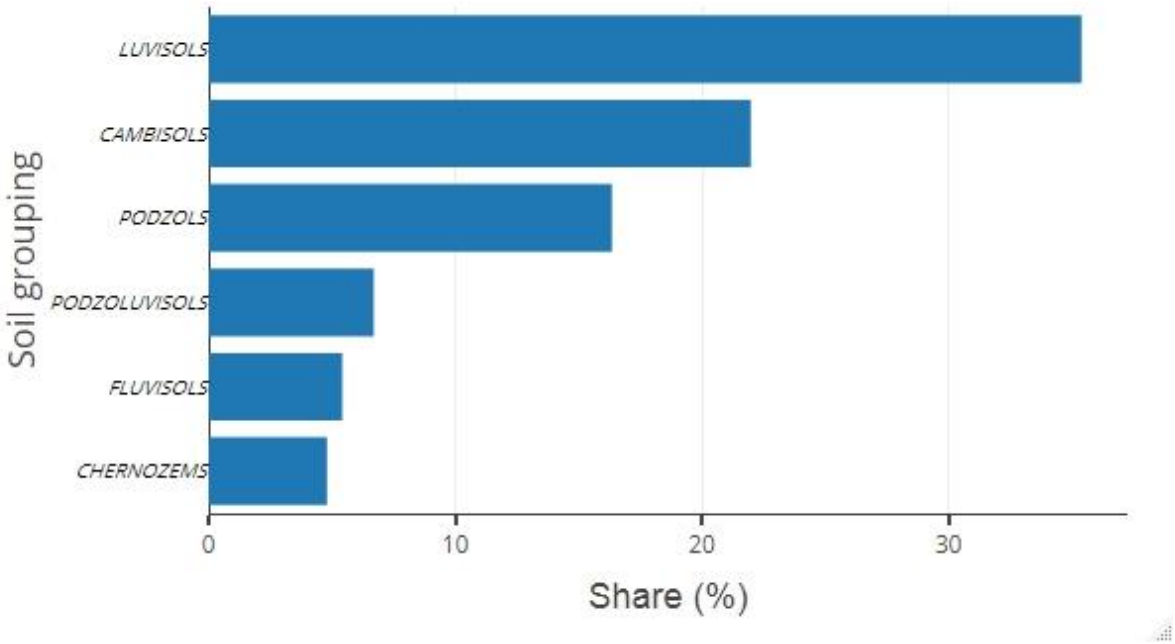

Figure 94. Share of major soil groupings in the Central Europe region.

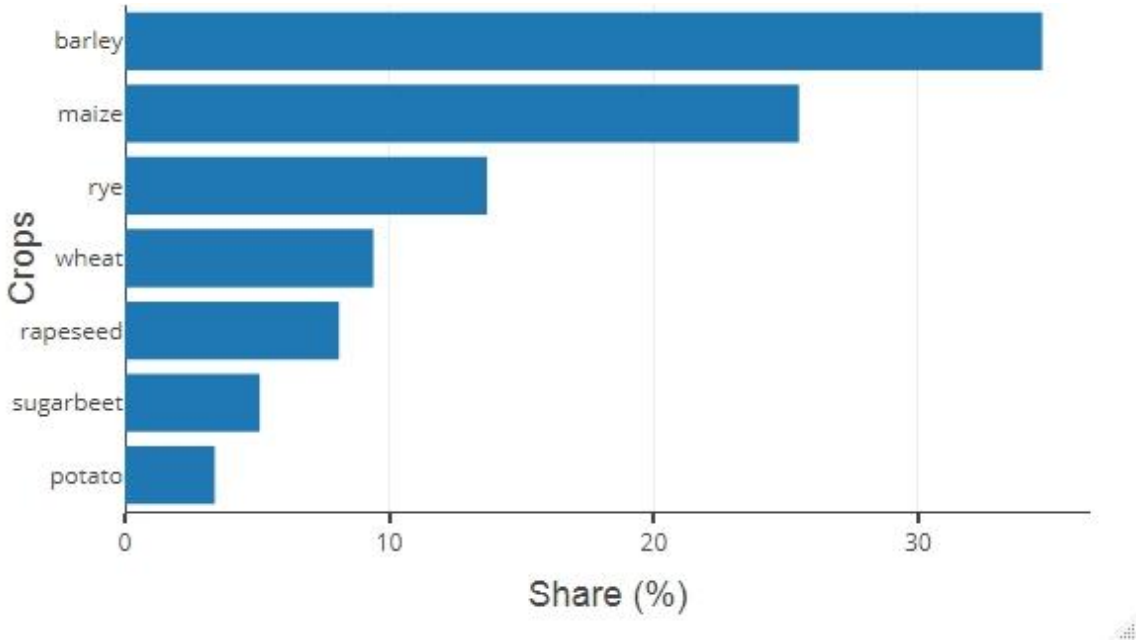

Figure 95. Share of major crops in the Central Europe region.

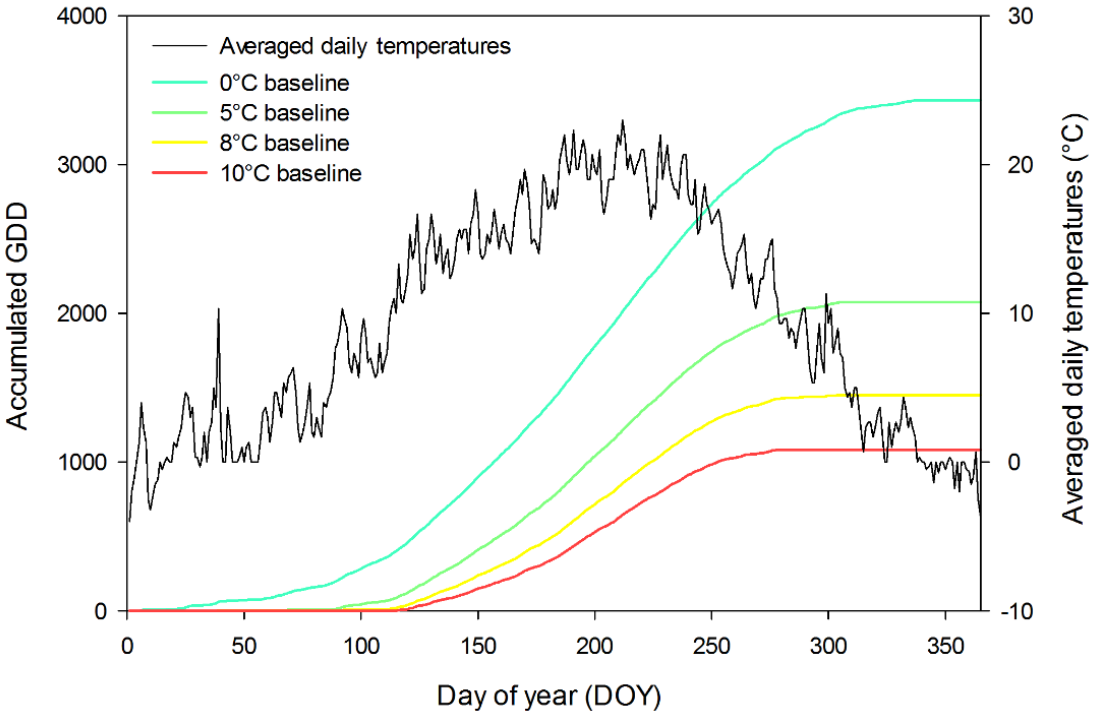

Figure 96. Average daily temperatures and resulting annual GDD accumulation calculated for four baselines in the Central Europe region.

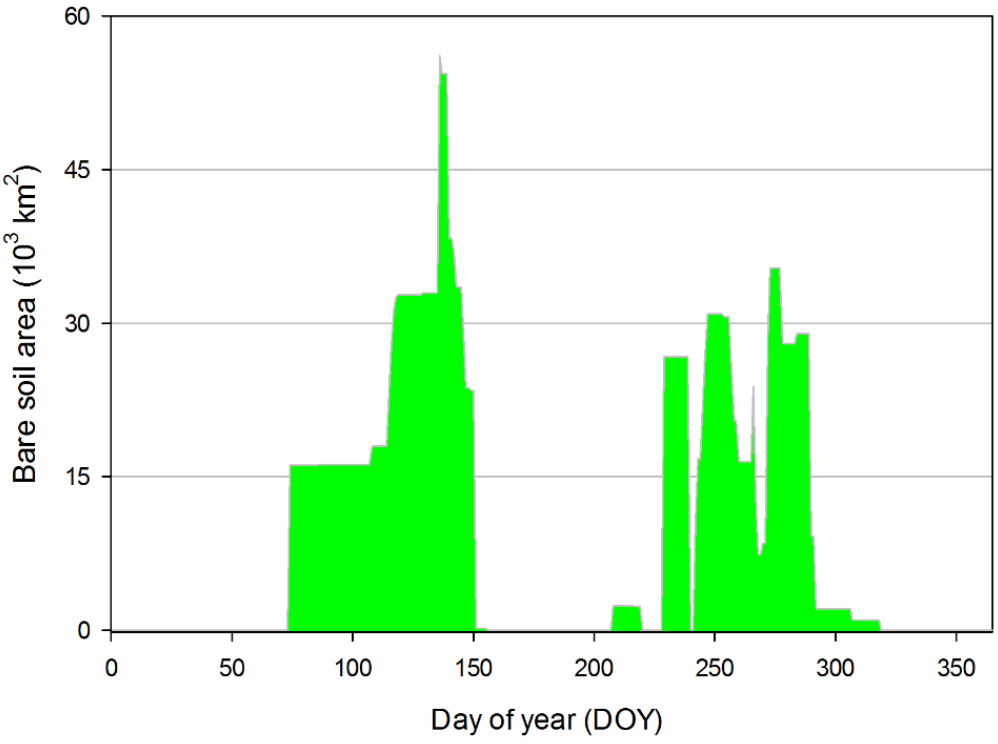

Figure 97. Annual variation of bare soil area in the Central Europe region.

3.5.3. Southern Europe

The last of the European regions consists mainly of countries of the European Union; the region is located to the east of EUwe and to the south of EUce. The main centers of agriculture in the region are located to the south of the Alpine Mountains and along the coasts of the Apennine Peninsula in Italy, in the central Balkans, along the Black Sea coast and spread out in Greece (Figure 98). Compared to other European regions, the share of arable land in agriculture is smaller, relatively, due to more widespread permanent crops, especially vines, olive trees, and citrus fruits. The biggest area dedicated to CA in the region was found in Italy, where it was practiced on almost 4,000 km^2, with minuscule areas reported also in Hungary and Greece.

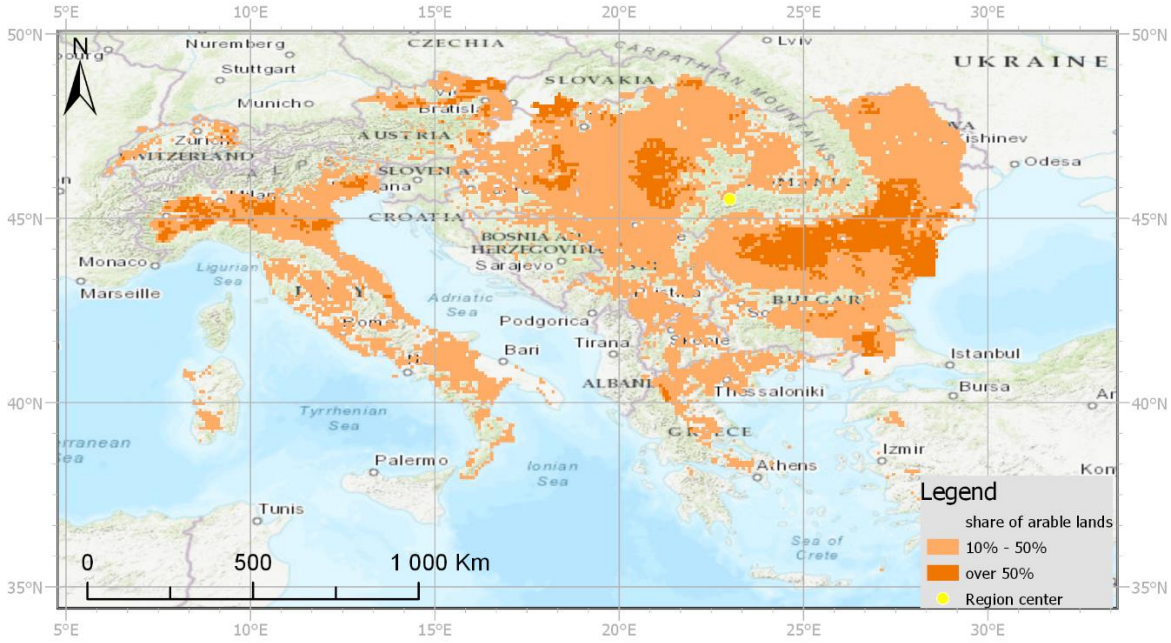

Figure 98. Distribution of arable land in the Southern Europe region.

The contribution of soil units to arable land in the region shows somewhat balanced proportions, with no soil unit dominating (Figure 99). The biggest share of the area was observed for *Cambisols* and *Luvisols*, each of those soil units occupying around a fifth of the arable land. The relatively high percentage of fertile *Chernozems* soil, of almost 15%, is the highest among European regions, and second only to AScr. A similar area to *Chernozems* was occupied by *Phaozems*. Almost 10% of analyzed land was *Fluvisols,* and half of that belonged to *Regosols*. Similar to other European regions previously described, wheat was the dominant major crop in the region, constituting over two-fifths of arable land (Figure 100). However,

contrary to the other European regions, the second most widespread crop was maize, found on almost 40% of the surface, and barley in the third spot had a share of just 10%. The remaining 10% was spread between potatoes, sugar beet, rapeseed, and rye. The annual accumulation of GDD (Figure 101) was calculated using mean daily temperatures extracted from a point located at 45° north and 23° east, at the heart of agricultural land in the Balkans. The obtained temperatures were similar to the ones in EUce, but a bit warmer, ranging between -1°C and 21°C. In comparison with other European regions, the main period of bare soil overshadows any other occurrences (Figure 102). Significant acreages of soil turn bare around the 61st DOY, when the first instances of the planting of rye are noted, followed by the planting of barley and then wheat on the 80th DOY, and reinforced by the sowing of maize starting after the 100th DOY. Areas of bare soil sharply diminish after the 124th DOY when earlier planted wheat covers the fields again and almost completely disappears after the 153rd DOY. The maximum area of bare soil in this period reaches almost 100,000 km^2 around the 120th DOY.

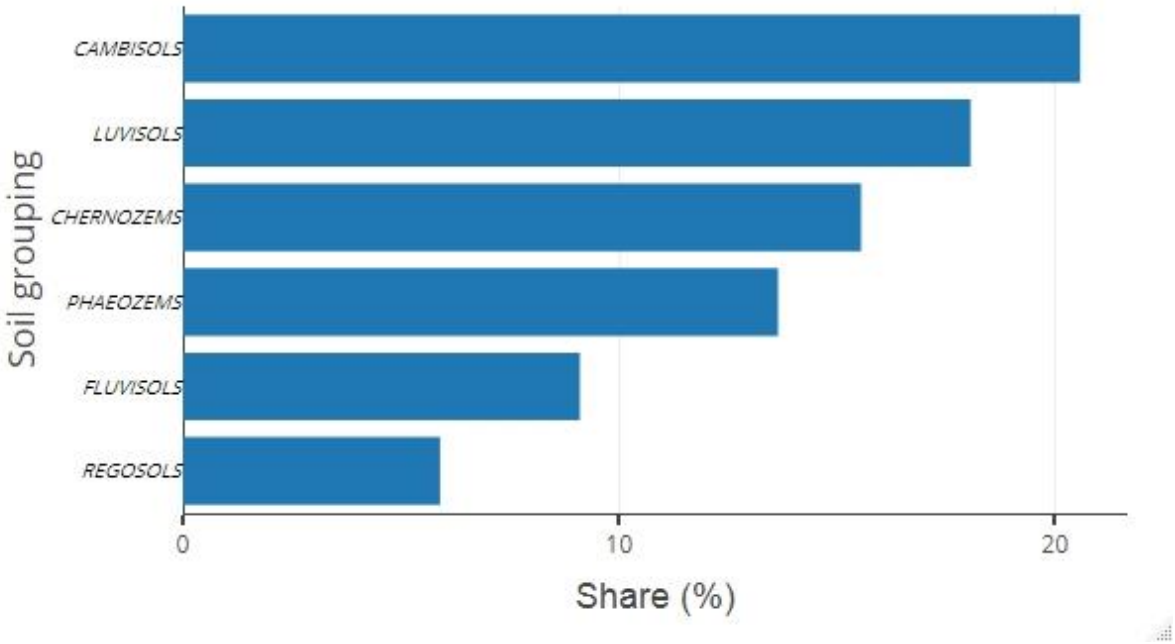

Figure 99. Share of major soil groupings in the Southern Europe region.

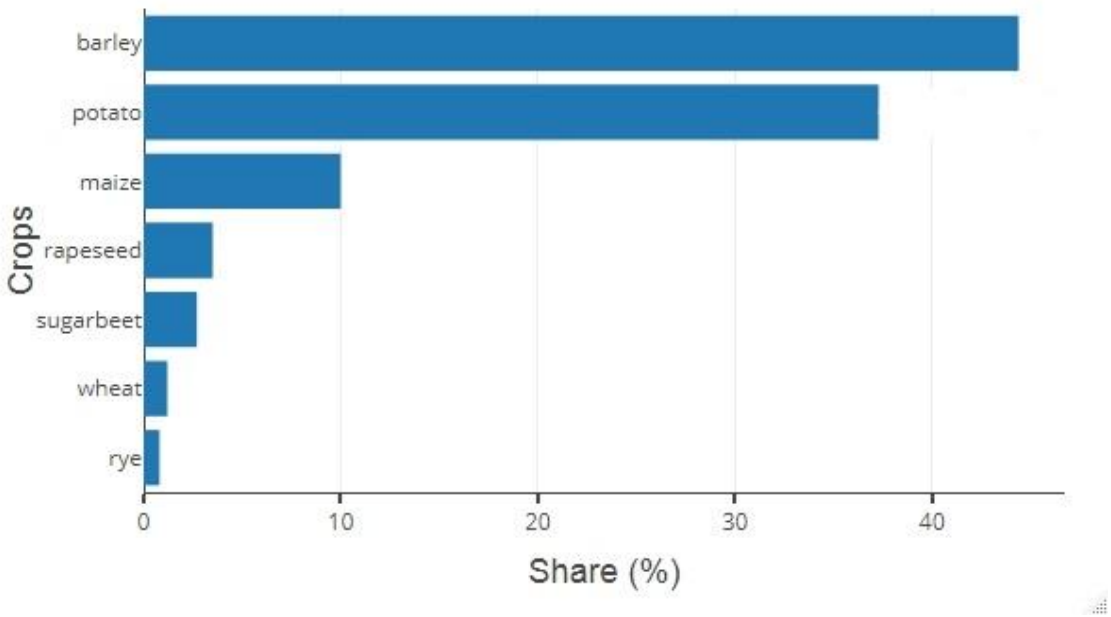

Figure 100. Share of major crops in the Southern Europe region.

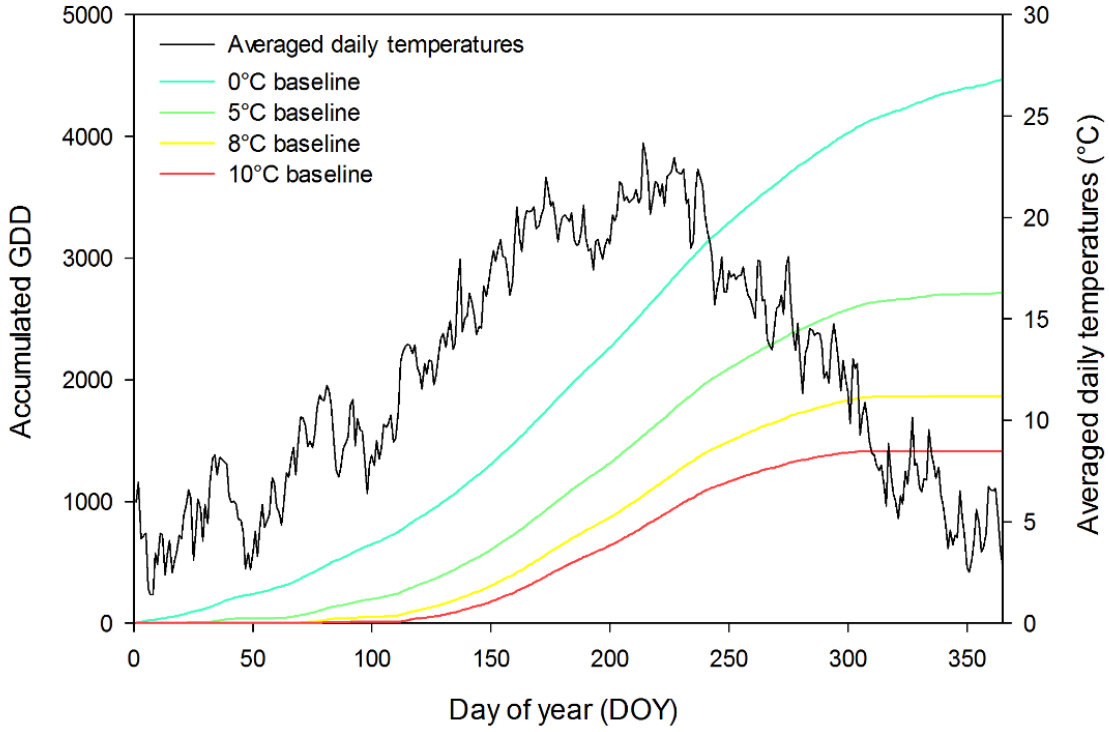

Figure 101. Average daily temperatures and resulting annual GDD accumulation calculated for four baselines in the Southern Europe region.

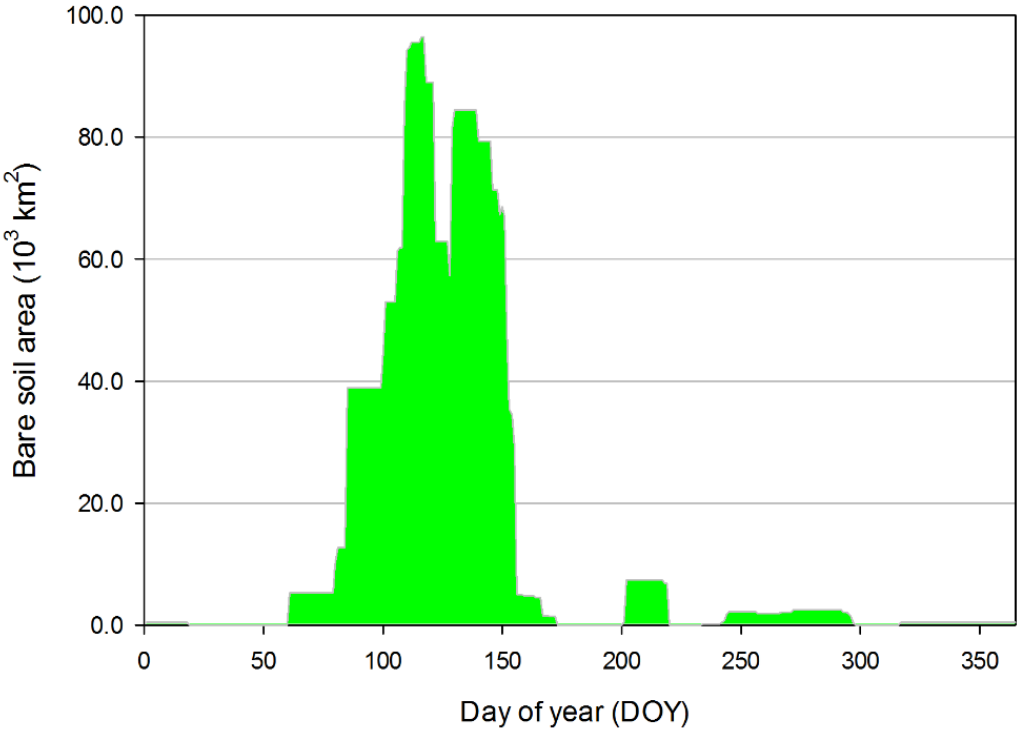

Figure 102. Annual variation of bare soil area in the Southern Europe region.

3.5.4. Former Soviet Union

Located to the east of both EUce and EUso, this region experiences the most continental climate compared to other European regions. Agriculture in this region underwent quite radical changes following the fall of the Soviet Union, transiting to a more privatized structure, accompanied by a general increase in productivity. The biggest concentration of arable land found in this region is in a belt stretching from the eastern Balkans, along the northern coast of the Black Sea and then splitting with one part continuing to the east, and the other going south to the Caucasian Mountains. Other big pockets of arable land are located in Belorussia and Lithuania (Figure 103). The acreage of arable land in this region is higher than in all other European regions combined. Relatively large areas of CA were found in the Russian Federation and in Ukraine, about 45,000 km^2 and 7,000 km^2, respectively.

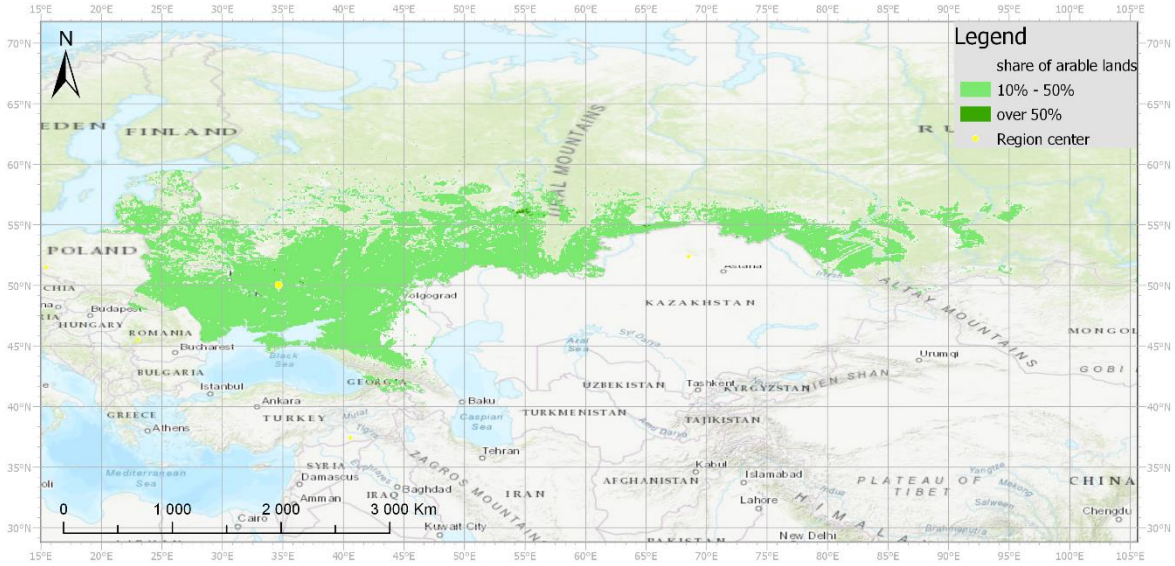

Figure 103. Distribution of arable land in the Former Soviet Union region.

Almost half of the arable land in EUrr sport the *Chernozems* soil unit, with such a high proportion of this fertile soil found nowhere else in the world (Figure 104). An area about three times smaller is occupied by *Kastanozems*, followed by three soil units sporting similar proportions of about 8% each, those are *Lithosols*, *Podzoluvisols,* and *Luvisols*. When it comes to major crops, over half of the arable land was dedicated to the growing of wheat, followed by another crop, barley, which had shares of around 53% and 20%, respectively (Figure 105). Potatoes were the next most common major crop with their share of almost 10%, and then rye having around a 7% cut of arable land. Between 1% and 4% were reserved for each of the following crops: maize, cotton, sugar beet, and millet. The annual variation of mean daily

temperatures was obtained from a point located in Ukraine, at around 50° north and 35° east. Those temperatures were as low as -9°C in the coldest months and reached 21°C in summer. The resulting accumulation of GDD was rapid between around the 100th and the 260th DOY, and nonexistent outside of that period (Figure 106). The annual variation of bare soil is dominated by a period starting in early spring and extending into summer (Figure 107). The first significant observations of bare soil are noted around the 70th DOY, resulting from the planting of wheat and potatoes, followed by the sowing of potatoes starting about two weeks later. The area of bare soil steadily increases all the way until the 122nd DOY, when it reaches a first, smaller peak of about 260,000 km^2. Around three weeks later the biggest peak was observed, reaching almost 375,000 km^2 and lasting for about two weeks. Areas of every major crop contributed to that biggest peak, especially of maize and wheat. The last period of bare soil occurs around two and a half months later, caused by late sowing of potatoes and rye. The bare soil area during that last period reaches almost 50,000 km^2.

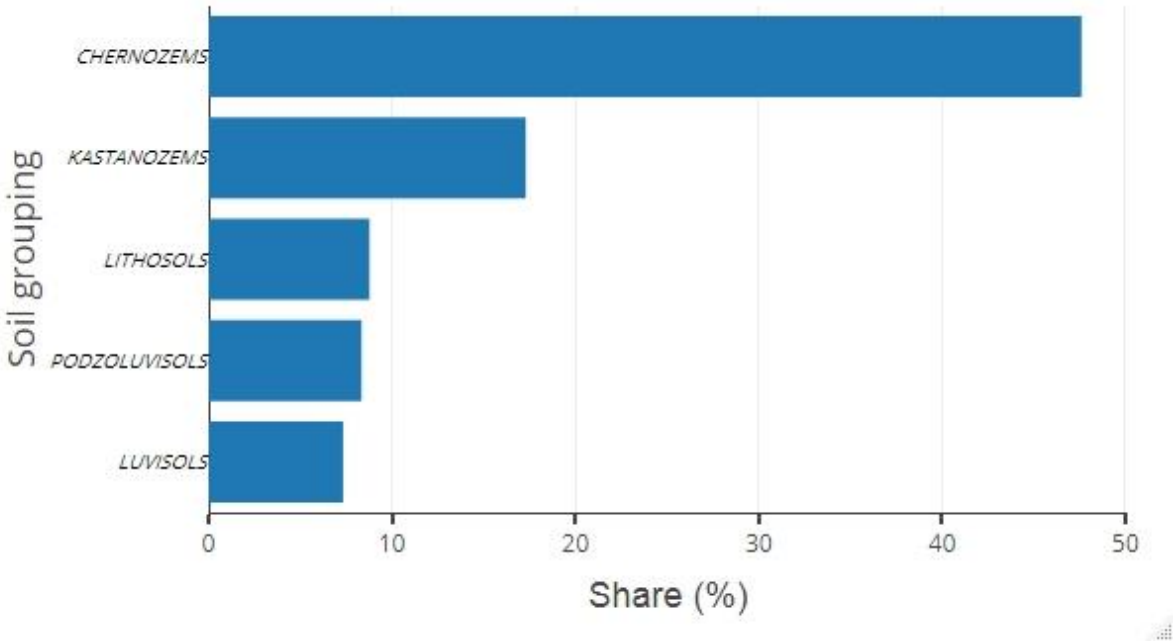

Figure 104. Share of major soil groupings in the Former Soviet Union region.

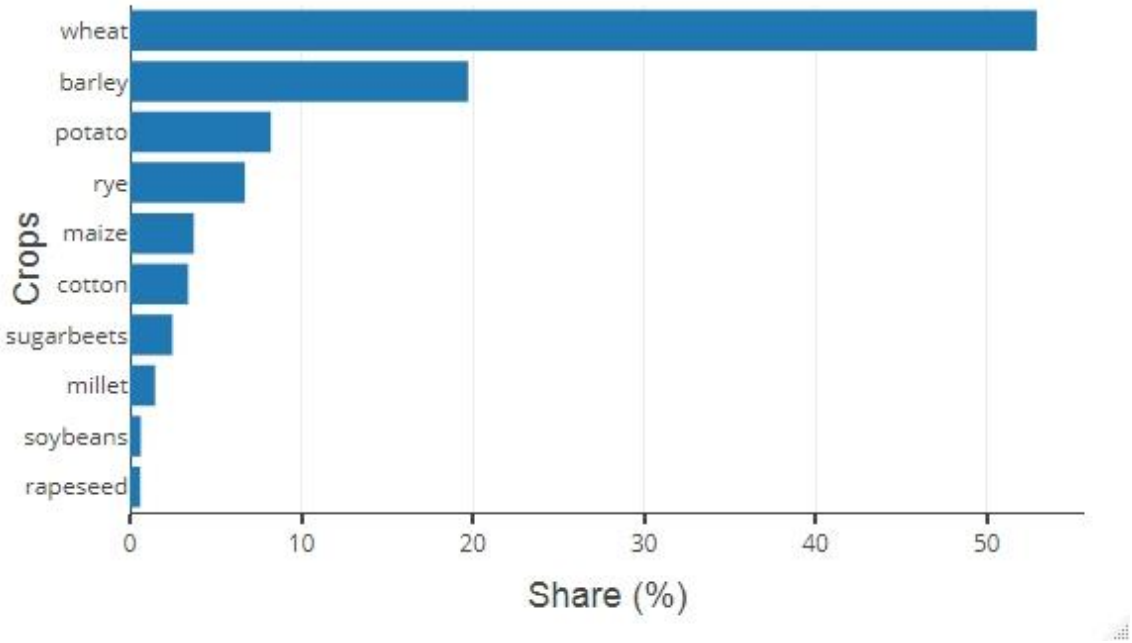

Figure 105. Share of major crops in the Former Soviet Union region.

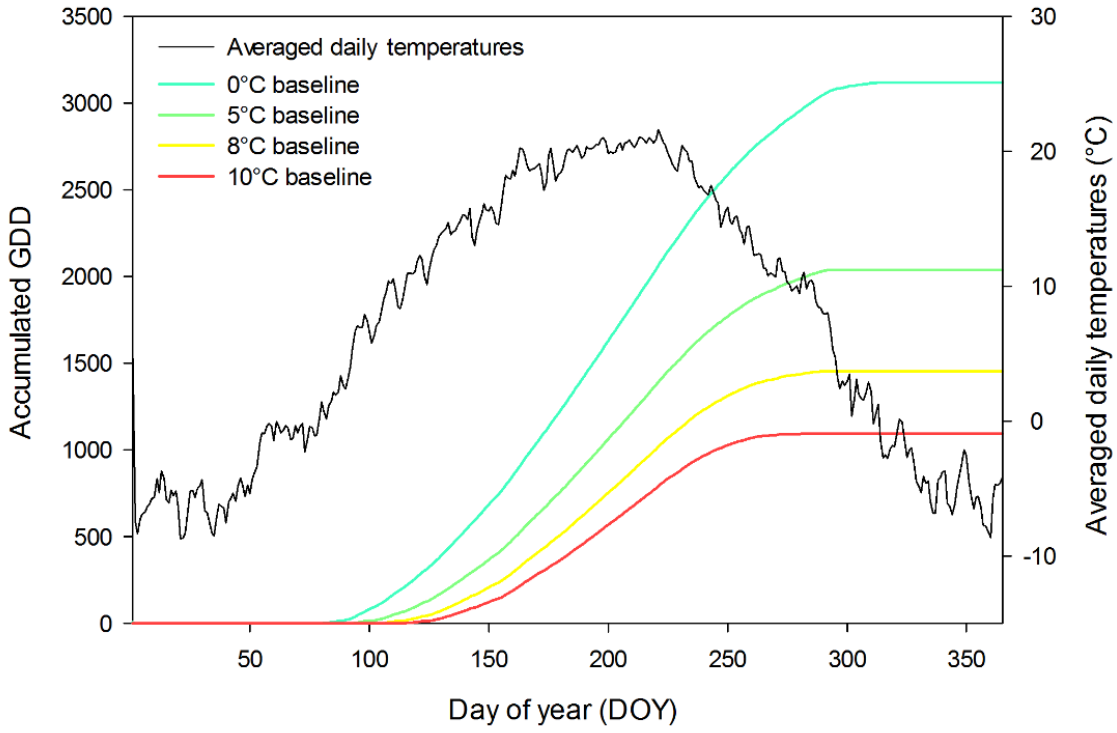

Figure 106. Average daily temperatures and resulting annual GDD accumulation calculated for four baselines in the Former Soviet Union region.

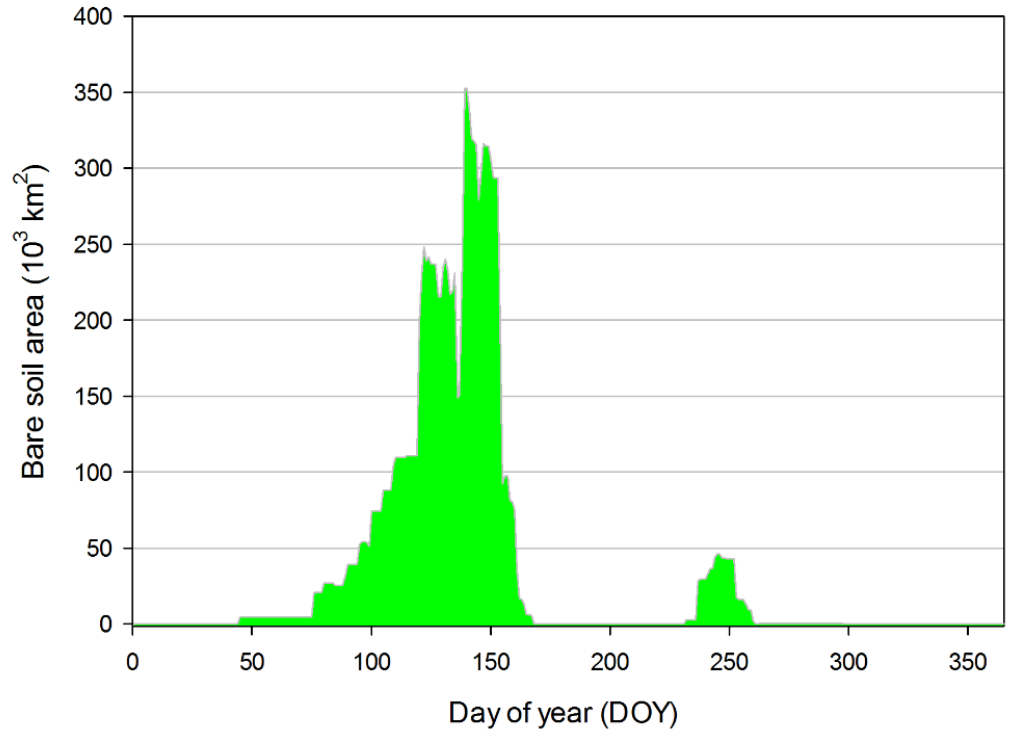

Figure 107. Annual variation of bare soil area in the Former Soviet Union region.

3.6. North and Central America

The agricultural land in this super region is found from Canada in the north to Panama in the south and in the Caribbean islands in eastern parts, spanning a multitude of climate zones. The overwhelming majority of arable land in this region is concentrated in three countries, the United States (US), Canada and Mexico. However, even though huge amounts of arable land were found in those countries, the share of arable land compared to the total land area was relatively small for each of those countries. Following the importance of the aforementioned countries, six out of eight regions making up this super region are dedicated to those countries (Figure 108):

- Canada (NAca)—the majority of arable land is located in close proximity to the borders with the US;
- Western United States (NAwe)—the region encompasses western parts of the US, with arable land spread out in various locations;
- Midwestern United States (NAmw)—the vast majority of arable land in the US is included in this region;
- Northeastern United States (NAne)—a relatively small region, located to the east of the Great Lakes;
- Southern United States (NAso)—includes the region of the Mississippi River and other southern states;
- Mexico (NAme)—arable land is concentrated in southern parts of the country, and along the east and west coasts;
- Central America (NAce)—formally the southernmost part of the North American continent, this isthmian region is surprisingly agriculturally productive;
- Caribbean (NAcr)—the biggest concentration of agriculture can be found in Cuba and Haiti.

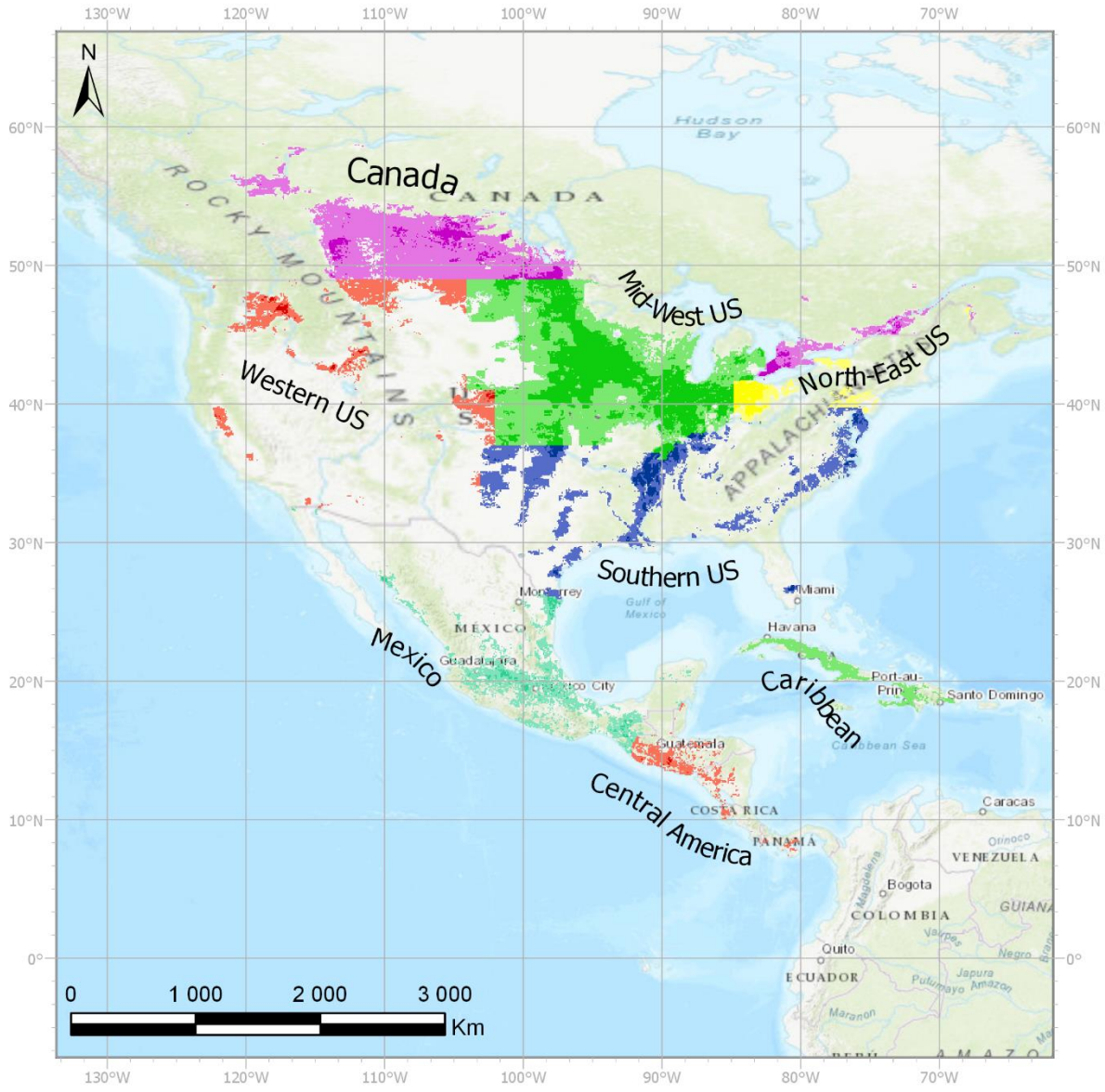

Figure 108. Arable land in the North and Central America super region divided into regions.

Not surprisingly, maize is a dominant farmed crop in the region of its origins, farmed on over 40% of analyzed land (Table 10). Wheat is the second major crop and was found on about a third of arable land. Four crops: barley, cotton, sorghum, and rapeseed have a similar share of around 5%. A trace amount of every type of major crop was found, but no other had a share larger than 1%. The annual variation of bare soil in the region was dominated by the planting of crops in the US (Figure 109). One main period of bare soil was found, and it lasted for over three months, reaching almost 300,000 km^2 around the 130th DOY. Arable land within every NA region were bare during that period. One much smaller occurrence of bare soil was found later, starting after the 280th DOY and lasting for almost two months, resulting from the planting of rapeseed in Canada.

Table 10. Area and share of arable land of major crops farmed in North and Central America**.**

Major Crop	Area	
	(thousands km²)	(%)
Maize	394	40.1
Wheat	332.1	33.8
Barley	61.1	6.2
Sorghum	55.3	5.6
Cotton	52.6	5.4
Rapeseed	50.8	5.2
Soybean	11.2	1.1
Potato	7.9	0.8
Groundnut	7	0.7
Sugar beet	5.5	0.6
Cassava	2.1	0.2
Millet	1.7	0.2
Rye	1.4	0.1

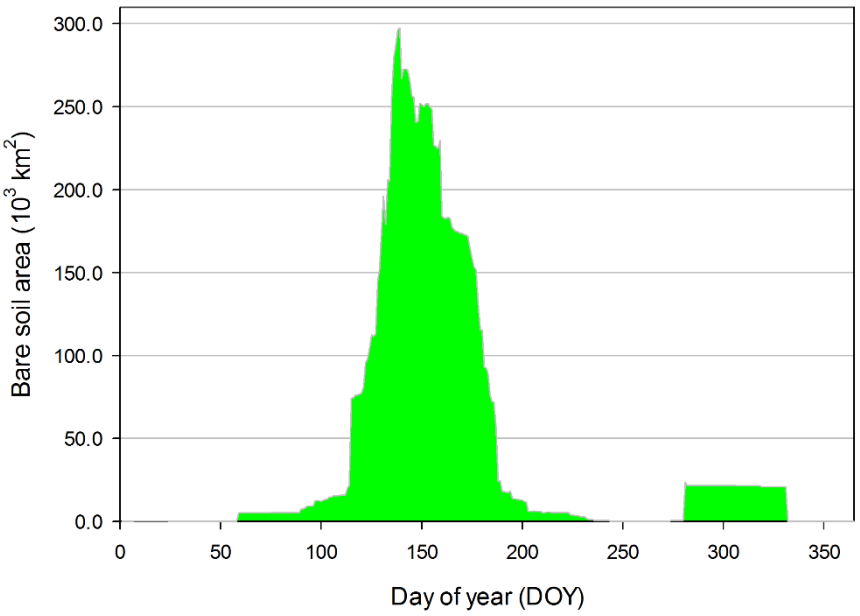

Figure 109. Annual variation of bare soil area in the North and Central America super region.

3.6.1. Canada

As the northernmost country in the Americas and the likewise northernmost region in the NA super region, Canada has the second largest land area after Russia. Even though most of Canada's land is not suitable for agriculture, it still has one of the most expansive arable land areas in the world. The majority of arable land in Canada is found along the border with the US, especially toward the western side, with another significant pocket of arable land between Lakes Huron and Erie, continuing along the Saint Lawrence River all the way to the eastern coast. The adoption of CA is widespread in Canada, with almost 200,000 km^2 being farmed in no-till or reduced-till systems, which is about half of all arable land in the country.

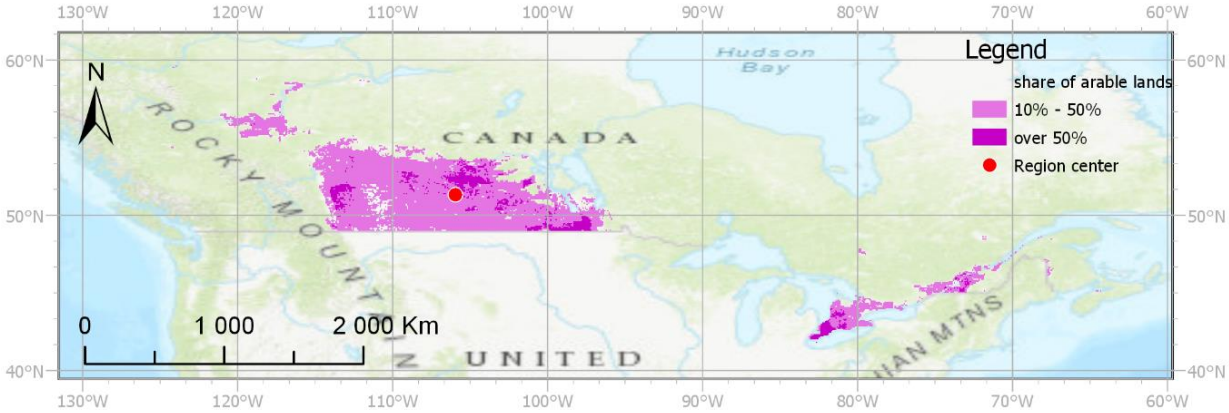

Figure 110. Distribution of arable land in the region of Canada.

Two of the most widely used soil units for agriculture in Canada are both fertile and rich in humus, those are *Chernozems* found on over 40% of arable land, followed by *Kastanozems* that are present on a quarter of arable land (Figure 111). *Luvisols* occupy about half as much land as *Kastanozems* and the last two soil units that have a significant share of land are *Gleysols* and *Solonetz,* each of them about 5%. Wheat is a staple crop in Canada, with almost half of the analyzed land being dedicated to its cultivation (Figure 112). Another 40% is split almost evenly between barley and rapeseed. The remaining 10% of arable land is used for the cultivation of maize and soybeans, that have a share of about 5% each. The region's center, used for extracting average daily temperatures, was located at 51° north and 106° west, right in the middle of its biggest concentration of agriculture. Those temperatures ranged between -14°C and 21°C, resulting in rapid GDD accumulation for about half of the year, and nonexistent in the other half (Figure 113). Two main periods of bare soil can be distinguished in the Canadian region (Figure 114). The bigger one occurs earlier in the year,

starting around the 120th DOY when huge areas are planted with wheat and barley, followed by maize and then soybeans. During that maximum period, the area of bare soil exceeds 70,000 km^2, such a state lasting for about two weeks. The other period of bare soil was delayed by about four months compared to the main one, resulting from planting of rapeseed around the 280th DOY, which resulted in almost 20,000 km^2 being bare for about six weeks.

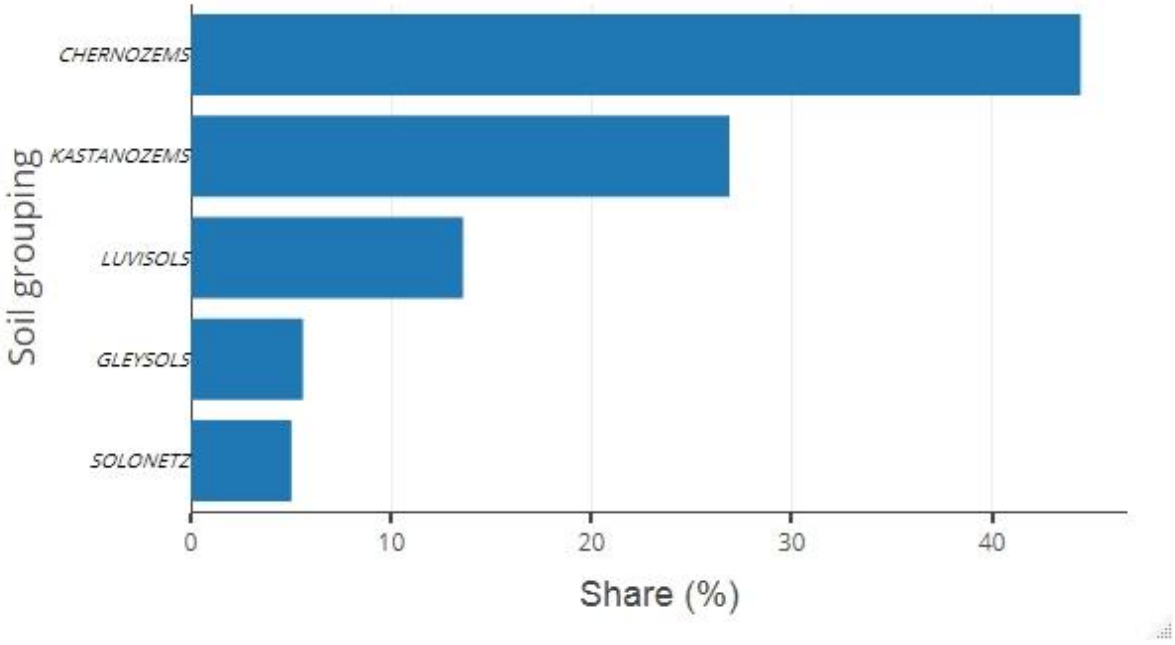

Figure 111. Share of major soil groupings in the region of Canada.

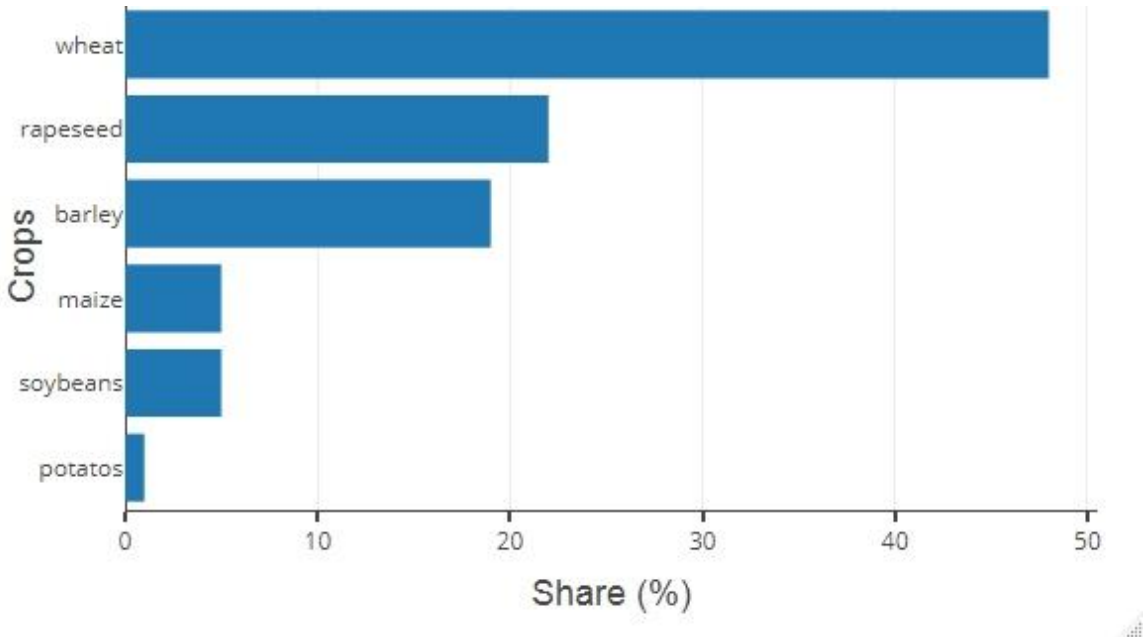

Figure 112. Share of major crops in the region of Canada.

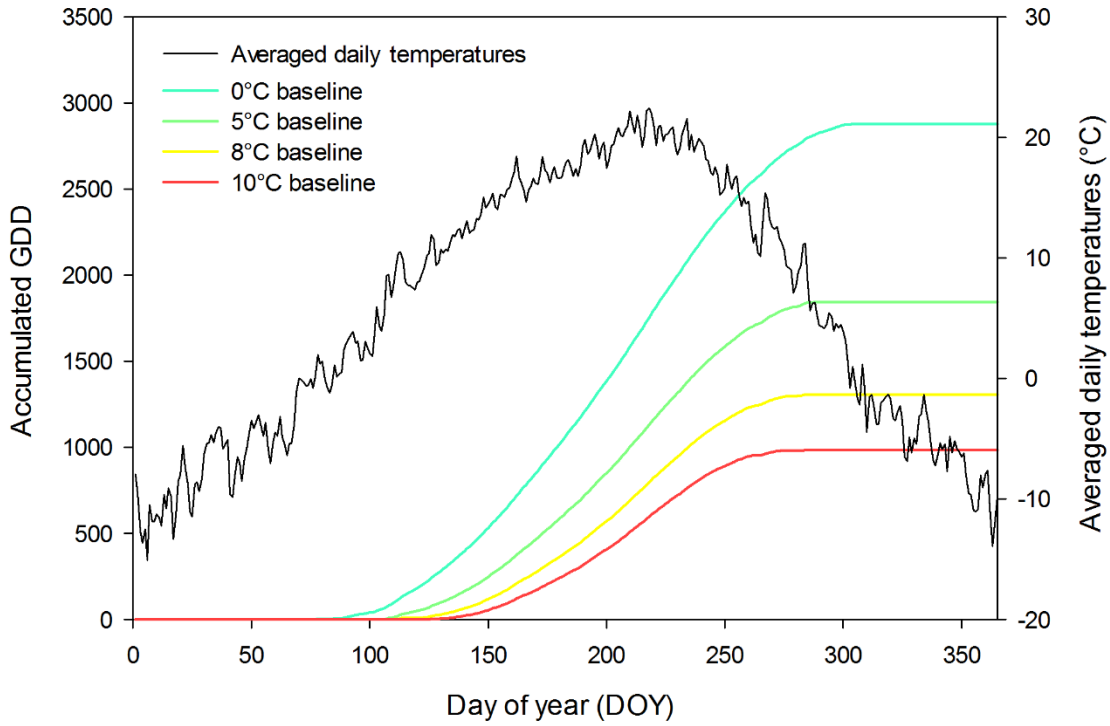

Figure 113. Average daily temperatures and resulting annual GDD accumulation calculated for four baselines in the region of Canada.

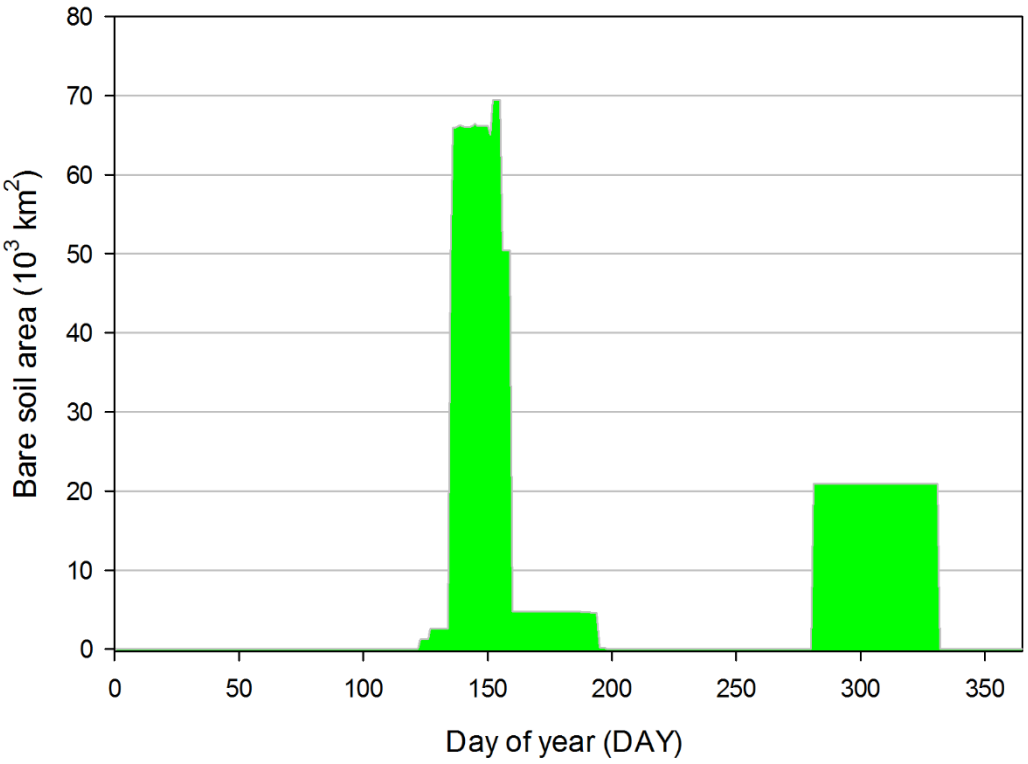

Figure 114. Annual variation of bare soil area in the region of Canada.

3.6.2. Western United States

The NAwe region includes land located to the west of the Great Plains; the region resides between two mountain ranges, the Rocky Mountains to the east and the Cascade Range and the Sierra Nevada to the west. The main geographic feature of the region is the Great Basin, which experiences a mostly arid climate, lying in a rain shadow of the mountain ranges located in the west. Large parts of the region are therefore not suitable for agriculture. The arable land is located in a couple of pockets: along the Columbia River and its biggest tributary, the Snake River in the northern parts of the region; along the Missouri River; and around the San Francisco area in southwestern parts (Figure 115).

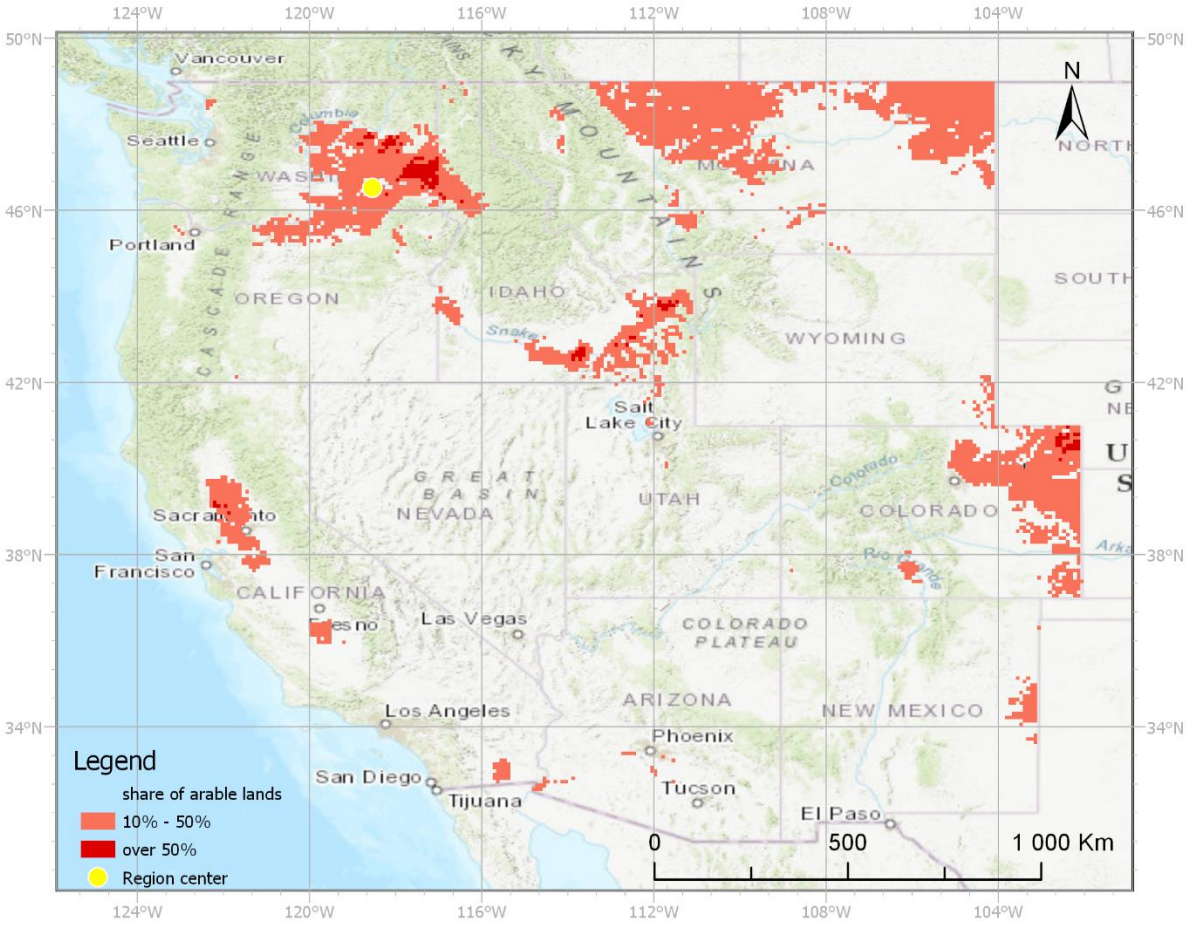

Figure 115. Distribution of arable land in the Western United States region.

No soil unit dominates over others in the NAwe region, with the three main units having a similar share (Figure 116). Those three units are *Kastanozems*, *Yermosols,* and *Xerosols*, each of them possessing a share of between 20% and 25%. Curiously, the next group of soil units is constituted from three units that have a similar share between them; those are *Regosols, Luvisols,* and *Phaozems*, with a share of around 8% to 9% each. The last two notable

soil units were *Fluvisols* and *Solonetz*, found on about 5% and 3% of analyzed land, respectively. No other soil unit had a share in arable land of even 1%. The overwhelming majority of arable land in NAwe was used for growing wheat, which was spotted on over 70% of analyzed land (Figure 117). Significant acreages were dedicated to the cultivation of barley, maize and cotton, each of them occupying between 6% and 8% of analyzed land. Almost 4% of that land was used for growing potatoes, and half of that area was reserved for sugar beet. The accumulation of GDD (Figure 118) was calculated using average daily temperatures extracted from a spot located at 47° north and 119° west, by the Snake River in the middle of the northern concentration of agriculture. Located just 4° closer to the equator than the Canadian region's center, the average daily temperatures in the winter were noticeably warmer, ranging between -4°C and 22°C, which resulted in longer periods of GDD accumulation than in the aforementioned region. Soils in the region stayed bare for a significant portion of the year, starting around the 85th DOY and lasting until the 230th DOY (Figure 119). The maximum during that period was observed around the 120th DOY, reaching over 30,000 km^2, and lasting for just over a week. The first crops planted, starting the increase of bare soil, was barley, soon followed by potatoes and then cotton. The maximum is reached soon after the planting of maize and especially wheat, starting after the 110th DOY.

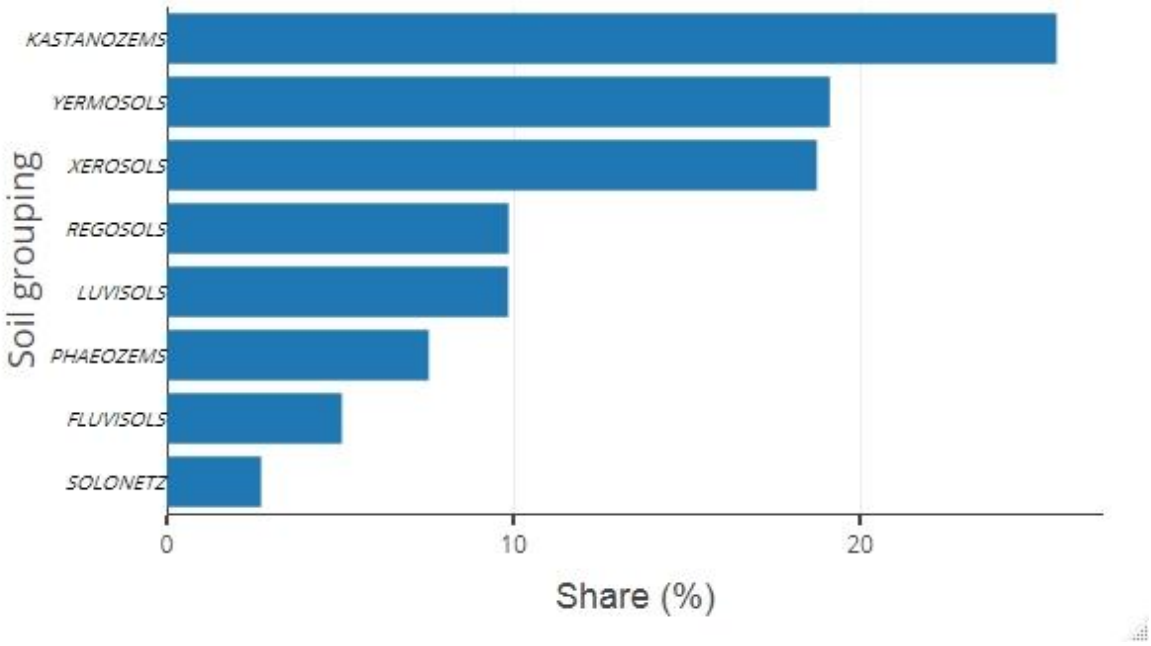

Figure 116. Share of major soil groupings in the Western United States region.

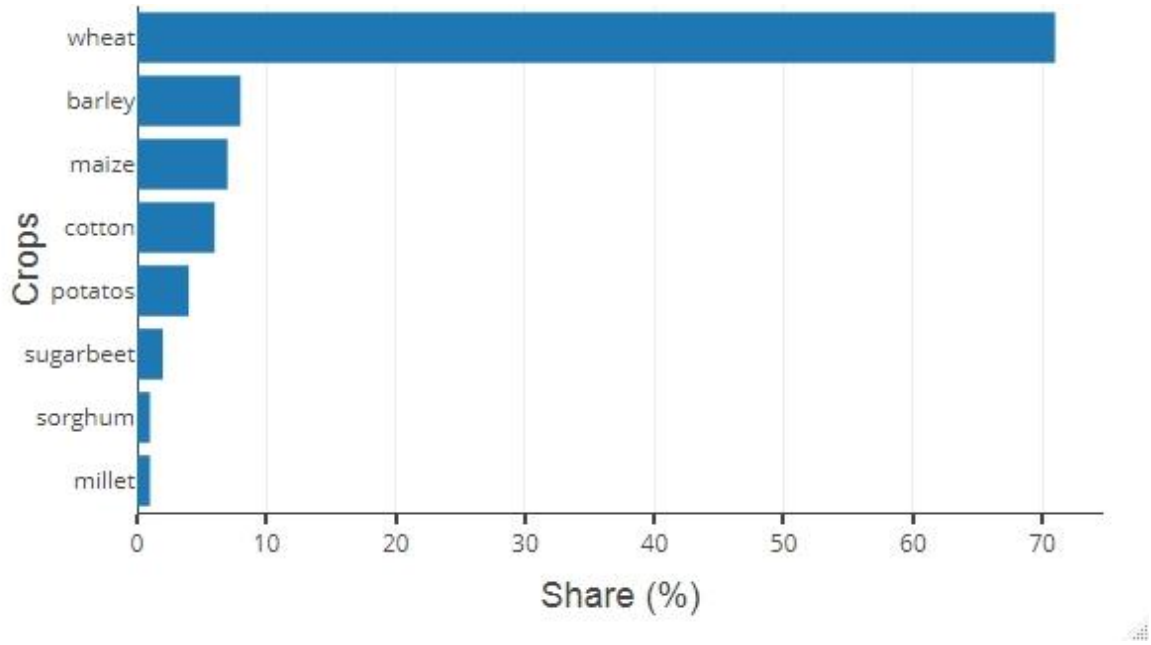

Figure 117. Share of major crops in the Western United States region.

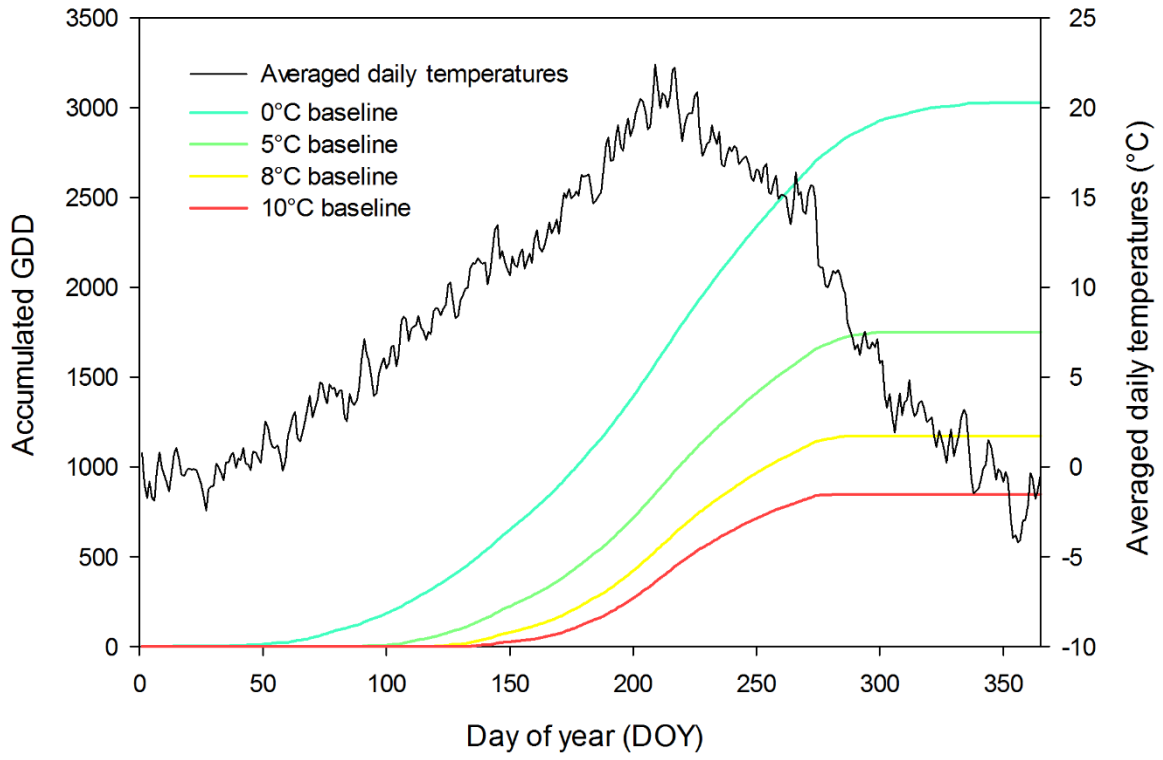

Figure 118. Average daily temperatures and resulting annual GDD accumulation calculated for four baselines in the Western United States region.

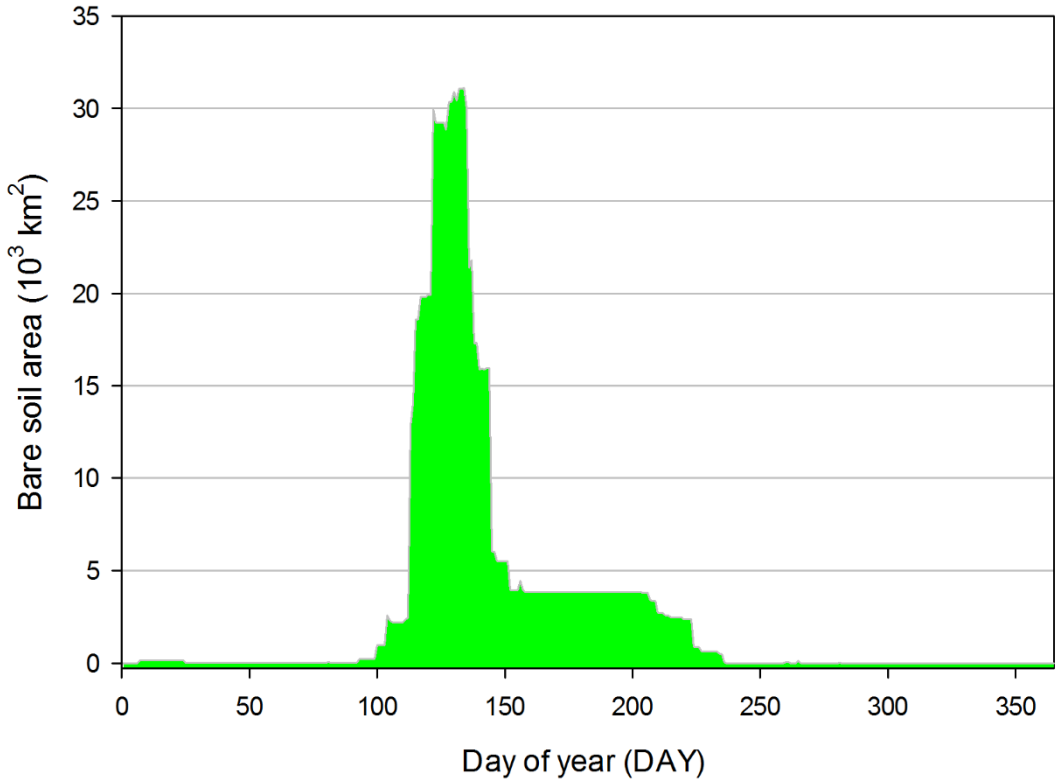

Figure 119. Annual variation of bare soil area in the Western United States region.

3.6.3. Midwestern United States

The majority of agricultural production of the US is located in this region which has more arable land than the three other regions combined. The region is located in inland US, to the east of NAwe, bordered by the Great Lakes to the northeast and limited by the Arkansas River in the south. The most notable geographical feature of the region is the Great Plains, which contain the famous Wheat Belt and Corn Belt. The arable land within the region is located almost everywhere, with the exception of the Sandhills in Nebraska, the Ozark Plateau, land located between Lakes Michigan and Huron and areas around Lake Superior (Figure 120).

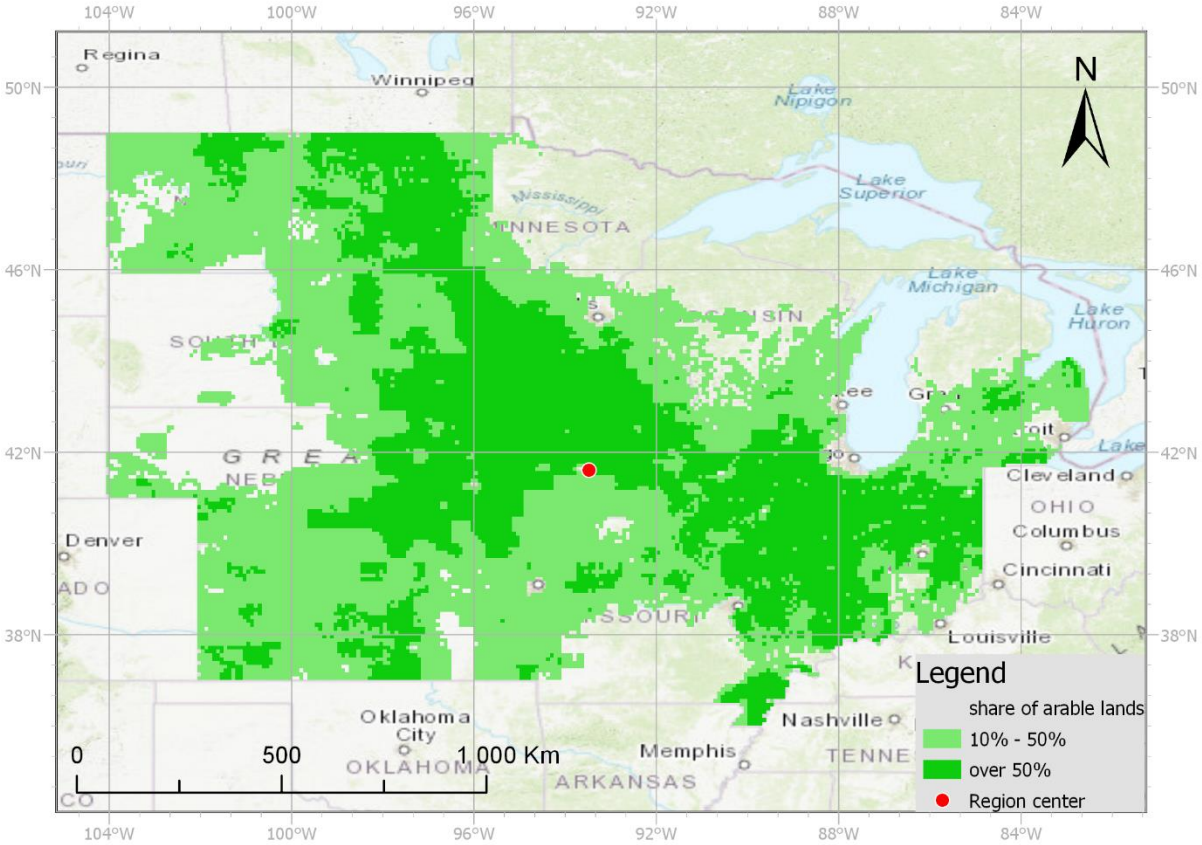

Figure 120. Distribution of arable land in the Midwestern United States region.

The immense concentration of agriculture in this region is partially explained by its soil makeup (Figure 121). The main soil units found in the region are all fertile and rich in organic matter; *Kastanozems, Luvisols* and *Phaozems* each occupy about a third of arable land within the region. *Chernozems*, another highly fertile soil unit was found on over 6% of the analyzed surface, and the last 10% is split evenly between *Regosols* and *Planosols.* Not surprisingly, the two main crops farmed in the region are maize and wheat, which together constitute around

90% of the analyzed land (Figure 122), with there being two times as much land dedicated to maize compared to wheat, making this region the largest producer of maize in the world. Crops farmed on the remaining arable land include sorghum, barley, and rapeseed, having a share of around 4%, 2%, and 1%, respectively. The center of agricultural production, used to extract daily mean temperatures, was located at 41° north and 93° west, near Des Moines in the state of Iowa. With its inland location, the annual temperatures showed a high amplitude, ranging between -12°C and 24°C, resulting in rapid GDD accumulation during a good portion of the year, but completely stopping in another part (Figure 123). Like other regions that have crops that are as dominating as maize and wheat in NAmw, the occurrences of bare soil are concentrated in one period (Figure 124). The first spike of bare soil area was noted around the 115th DOY, after the planting of wheat, followed by maize one week later. The maximum is reached around 138th DOY, when examples of every crop found in the region but sorghum are already planted, and covers over 150,000 km^2. The last areas of bare soil disappear after the 200th DOY.

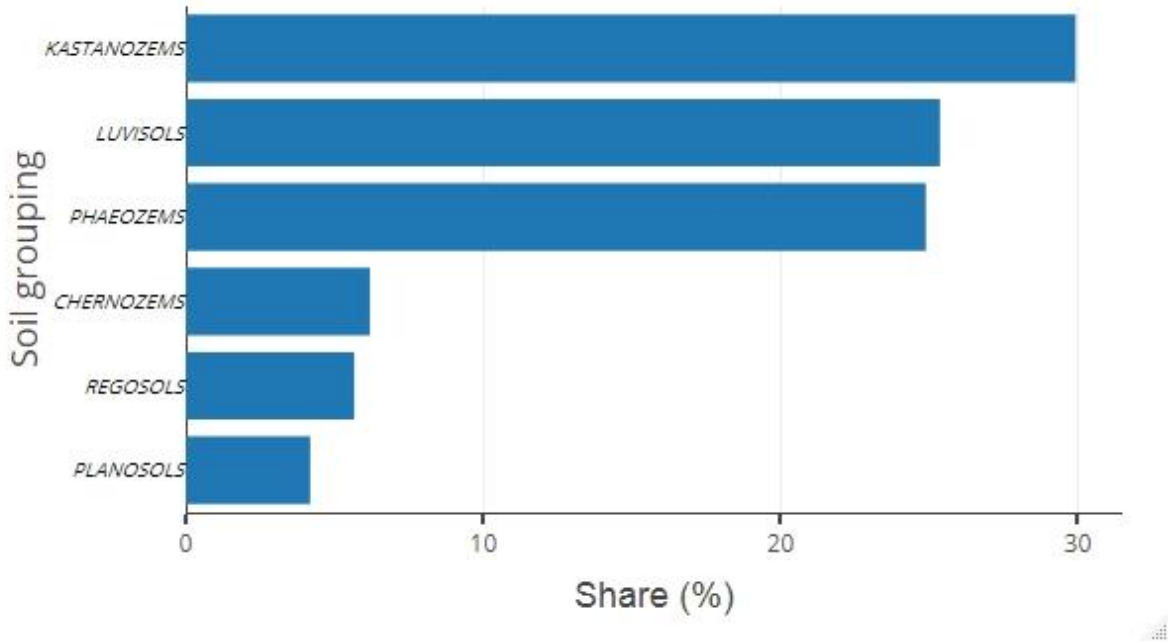

Figure 121. Share of major soil groupings in the Midwestern United States region.

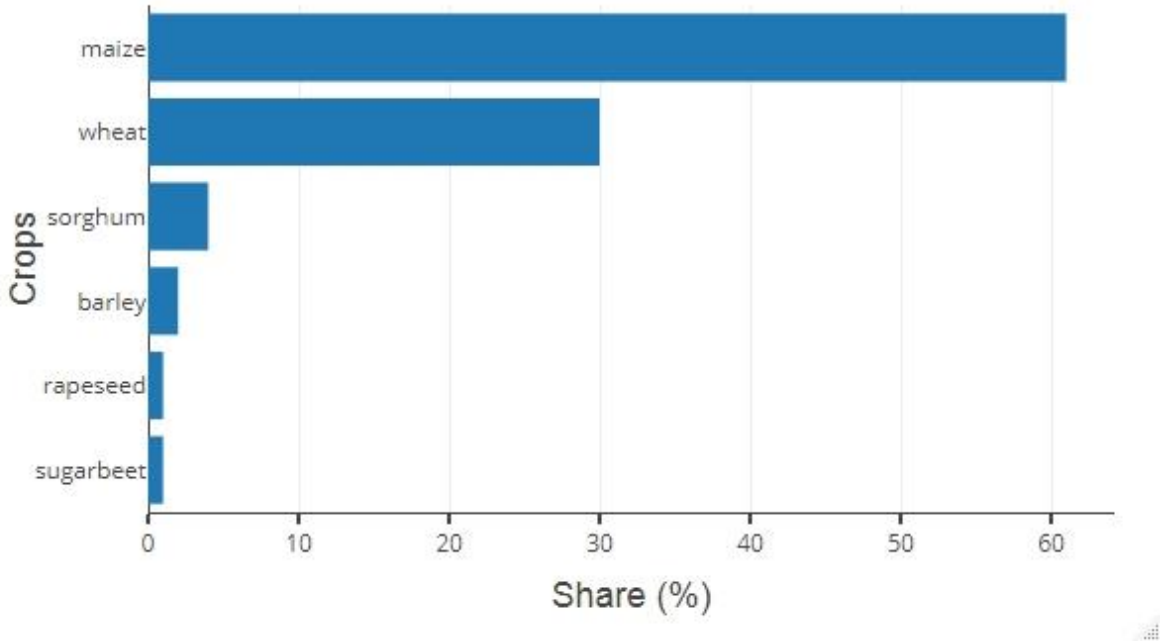

Figure 122. Share of major crops in the Midwestern United States region.

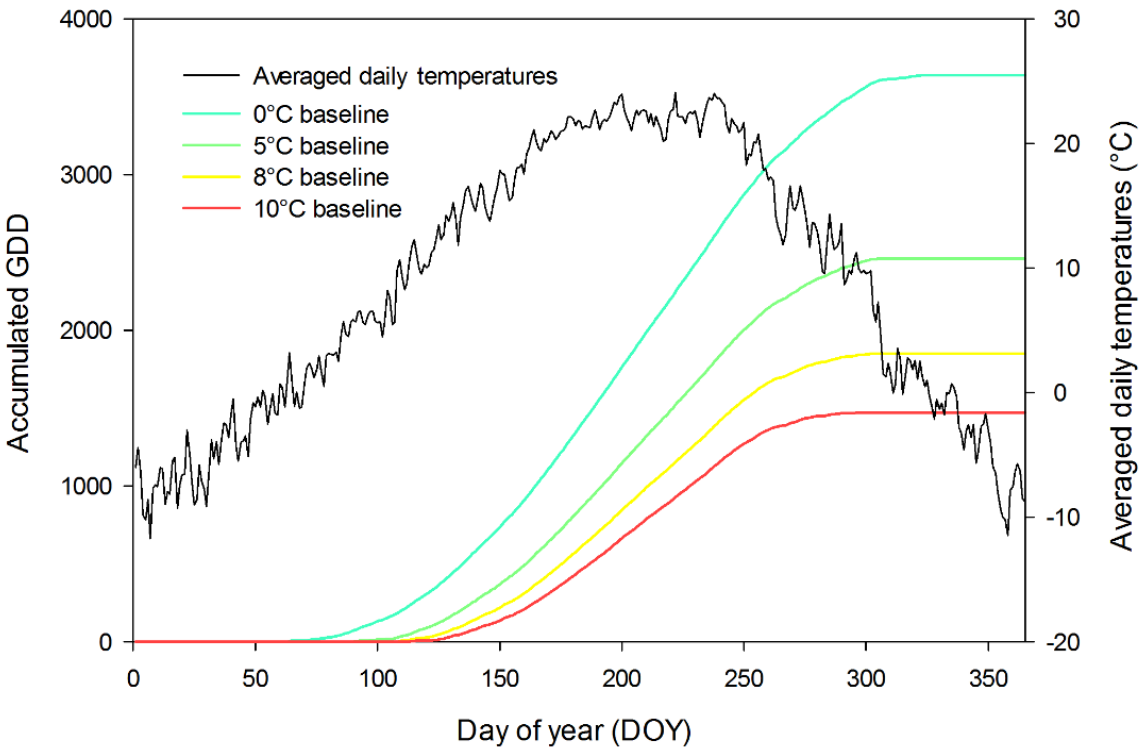

Figure 123. Average daily temperatures and resulting annual GDD accumulation calculated for four baselines in the Midwestern United States region.

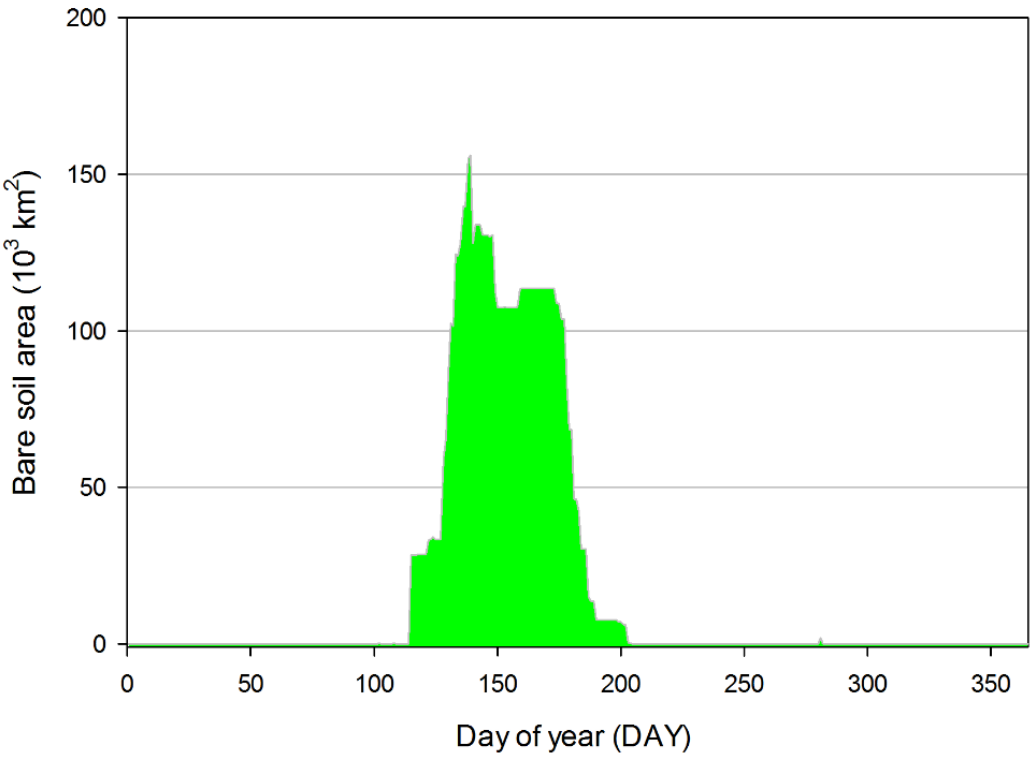

Figure 124. Annual variation of bare soil area in the Midwestern United States region.

3.6.4. Northeastern United States

In contrast to the NAmw described above, this region is the smallest of the regions that comprise the United States. The NAne is bordered in the north by the Great Lakes, to the east by the Atlantic Ocean and to the south by the state of Maryland. The Allegheny Mountains run through the middle of the region, from southeast to northwest. The arable land is located south of Lakes Ontario and Erie, in southern Pennsylvania and in northern extremes of the region, in the state of Maine (Figure 125).

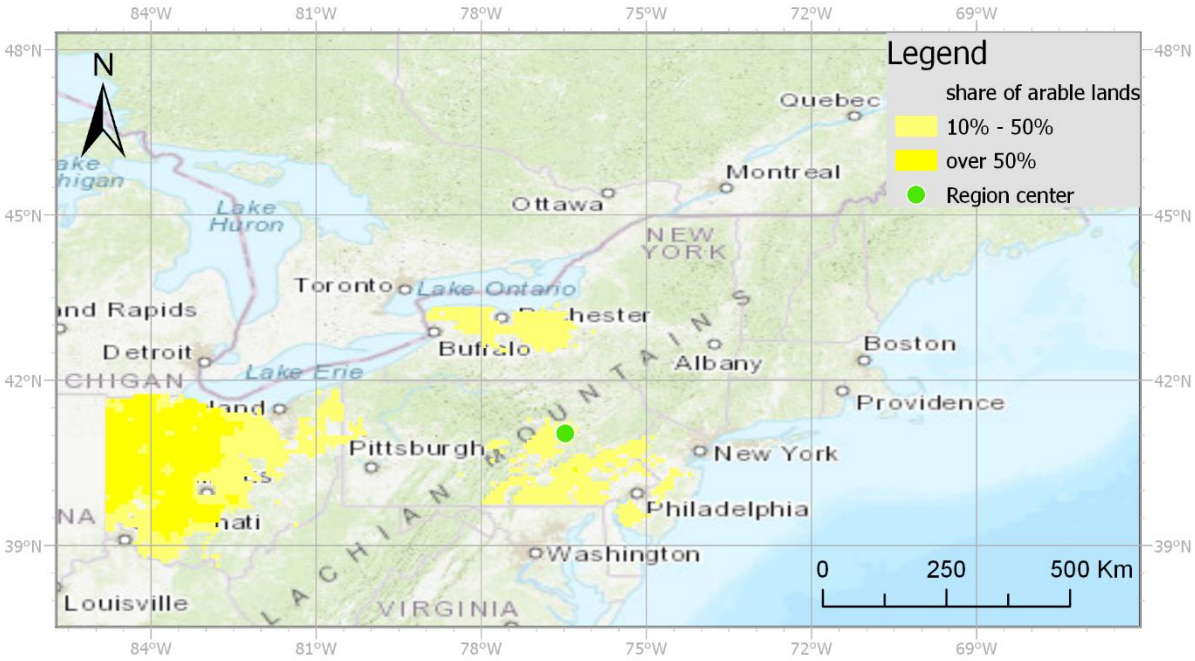

Figure 125. Distribution of arable land in the Northeastern United States region.

Luvisols were by far the most dominant soil unit in the region, found on more than 95% of arable land (Figure 126). The remaining 5% is comprised of *Cambisols, Acrisols* and *Podzols,* each of them occupying between 1% and 2%. Among the major crops cultivated in the region, the greatest area is dedicated to maize, which was found on over three-quarters of analyzed land (Figure 127). Wheat, which is the second most widely grown crop in the region was cultivated on almost a fifth of arable land. Barley and potatoes had less than a 2% share each, while other major crops were found only in token areas. Mean daily temperatures were extracted from the point located at 41° north and 77° west. Compared to NAmw, which had its center located at a similar latitude but much further from the ocean, temperatures are milder during winter and the annual amplitude is lower; mean daily temperatures ranged between -6°C and 23°C, resulting in a smoother and longer accumulation of GDD throughout

the year (Figure 128). Just like in the case of NAmw, one main period of bare soil can be distinguished (Figure 129). The planting of wheat after the 128th DOY starts that period, which is soon reinforced by the sowing of maize around a week later. After planting, wheat would develop and start covering fields after roughly three weeks, while maize took almost twice as long in this climate. At the peak, the acreage of bare soil was found to be just under 12,000 km^2, and the period lasted for about two months; the bare soil disappears after the 182nd DOY.

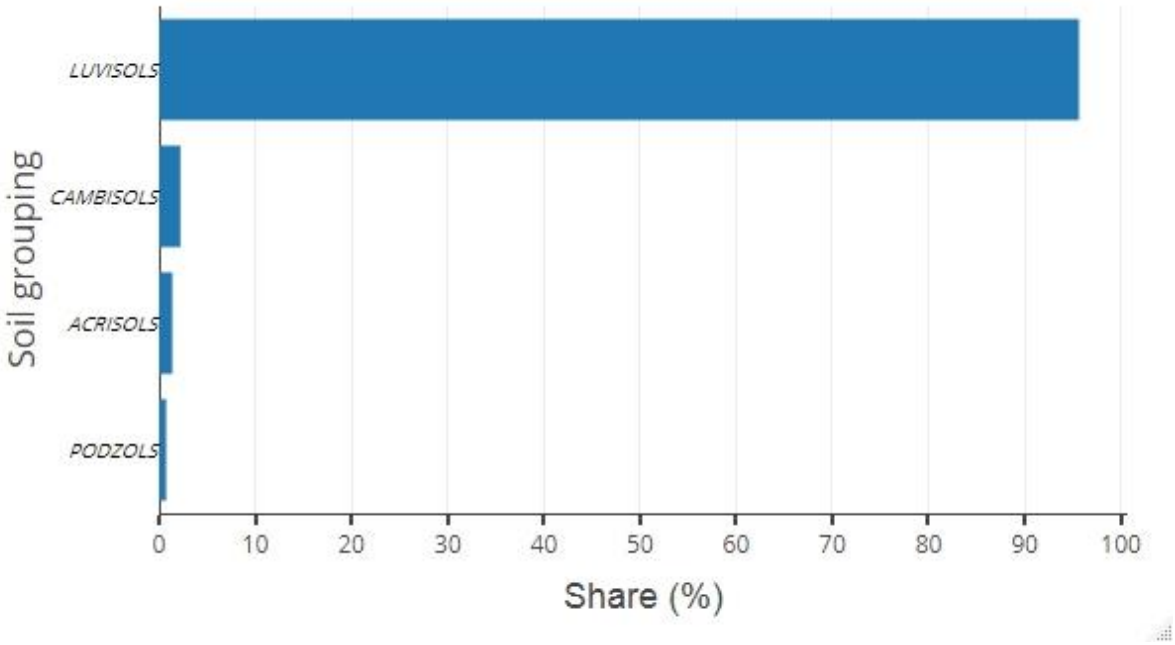

Figure 126. Share of major soil groupings in the Northeastern United States region.

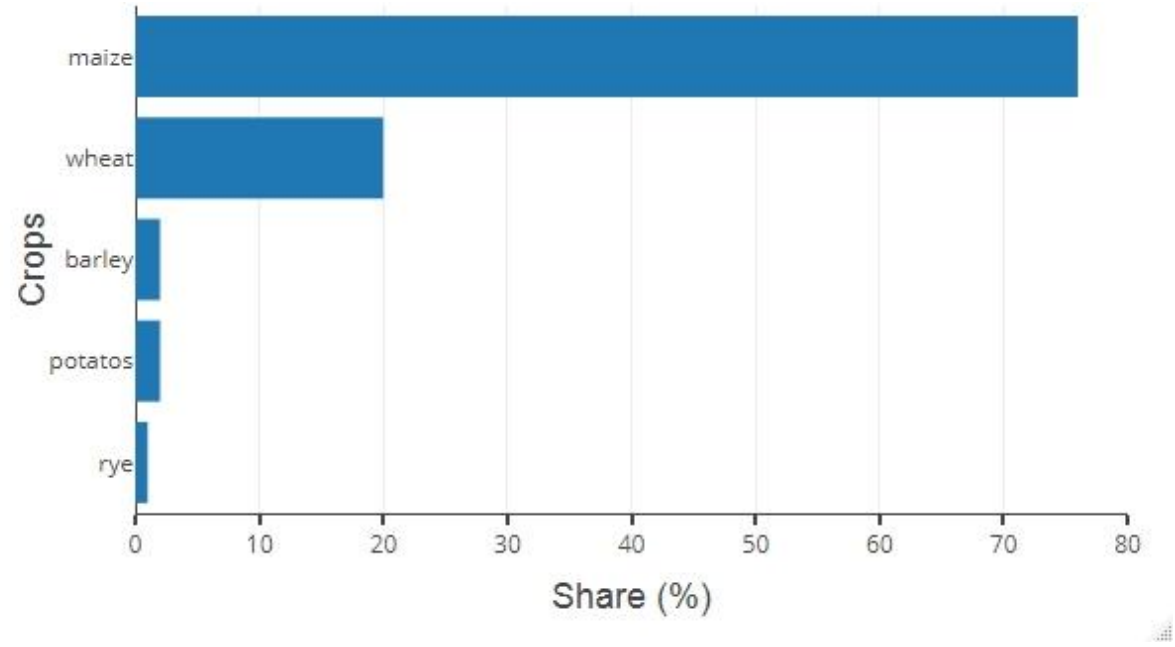

Figure 127. Share of major crops in the Northeastern United States region.

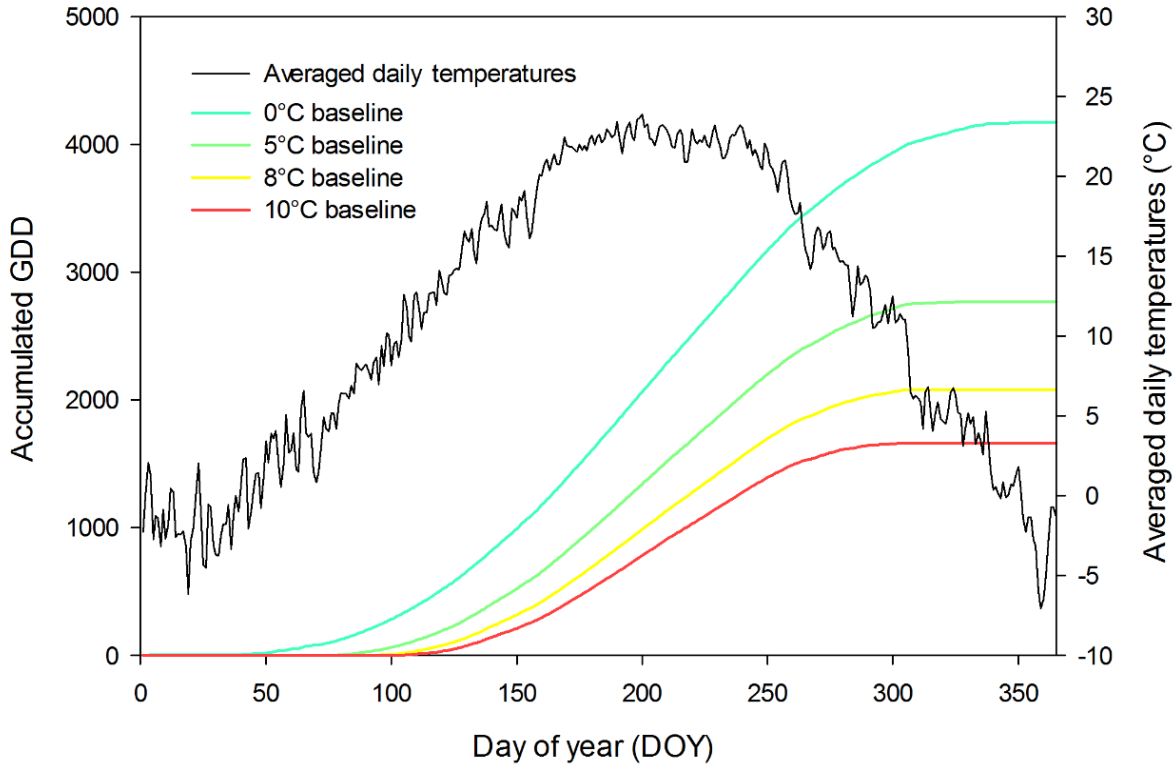

Figure 128. Average daily temperatures and resulting annual GDD accumulation calculated for four baselines in the Northeastern United States region.

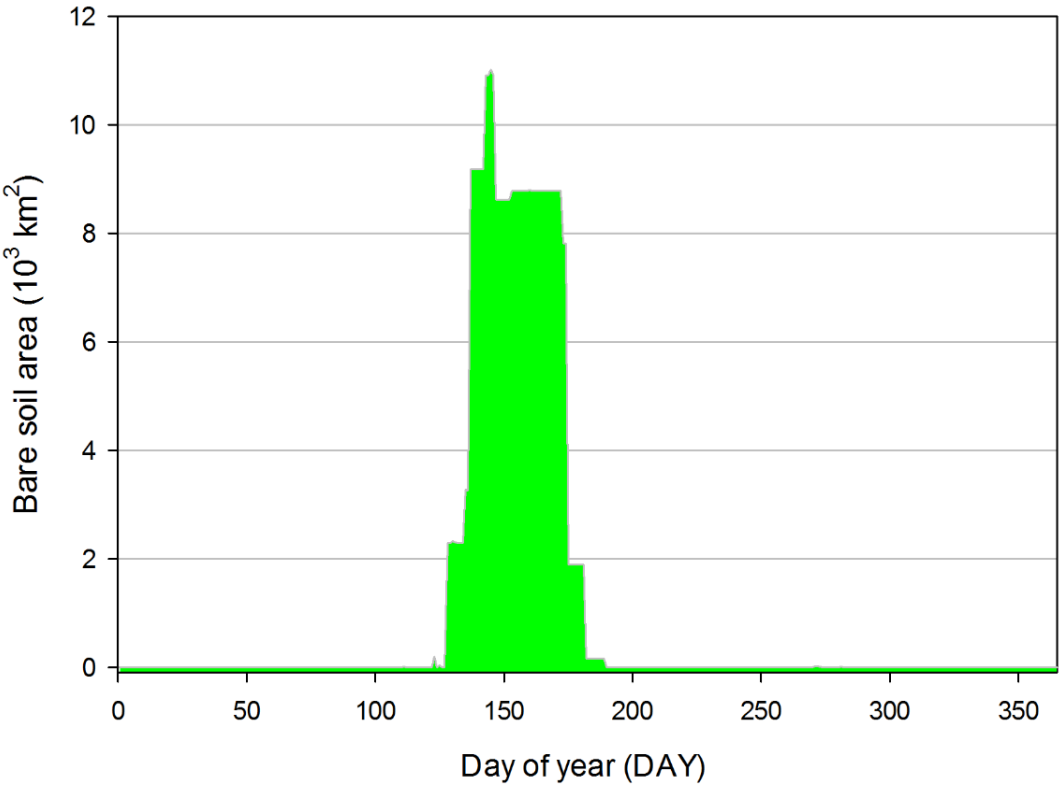

Figure 129. Annual variation of bare soil area in the Northeastern United States region.

3.6.5. Southern United States

The last of the regions comprising the United States, extends from the Staked Plains in the west to the Atlantic coast in the east. Significant parts of the Mississippi River flow through this region to its mouth in the Gulf of Mexico, supporting a significant area of arable land along its banks. Another significant concentration of arable land was found in the Coastal Plain, running along the length of the Atlantic, from Florida in the south to the Delmarva Peninsula in the north. Southern parts of the Wheat Belt are located in the western extremities of the region, and the last noteworthy concentration is located along the coast of the Gulf of Mexico (Figure 130).

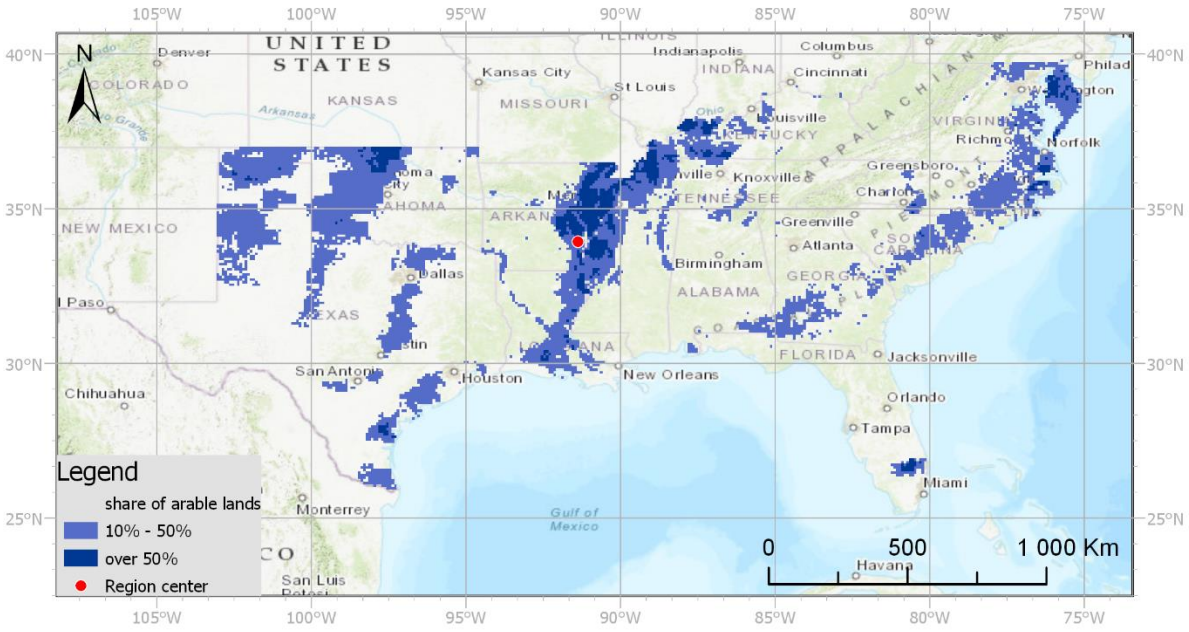

Figure 130. Distribution of arable land in the Southern United States region.

Over half of the arable land in the region lies on *Kastanozems* and another quarter on *Luvisols* (Figure 131). The remaining 25% of the analyzed land was split between *Acrisols, Phaozems,* and *Gleysols*, with a share of between 3% and 7% for each of them. Three of the main crops dominated agricultural production in the region; those were wheat, cotton, and maize, with a share of over 30% for the first two and over 20% for maize (Figure 132). Significant areas were also dedicated to the cultivation of sorghum, found on over 10% of arable land. The point used to extract mean daily temperatures was located at 34° north and 91° west, in the middle of the agricultural pocket along the Mississippi River. The annual variation of those temperatures showed a lower amplitude than in other regions of the US, dipping below 0° for just a few days, ranging between -2°C and 27°C. The resulting

accumulation of GDD was therefore smooth throughout the year, with only around three months when the accumulation stops (Figure 133). The annual variation of bare soil has a similar shape to the one in other US regions, where one main period of bare soil can be distinguished (Figure 134). The first instances of bare soil start to appear after the 85th DOY, resulting from the planting of maize commencing at that date and lasting until the 140th DOY. Wheat and cotton are planted after the 120th DOY, and it's around that date when the peak of bare soil is reached, with over 50,000 km^2 of soil exposed. Afterward, that acreage gradually decreases when major crops started successively covering the fields, until bare soil all but disappears.

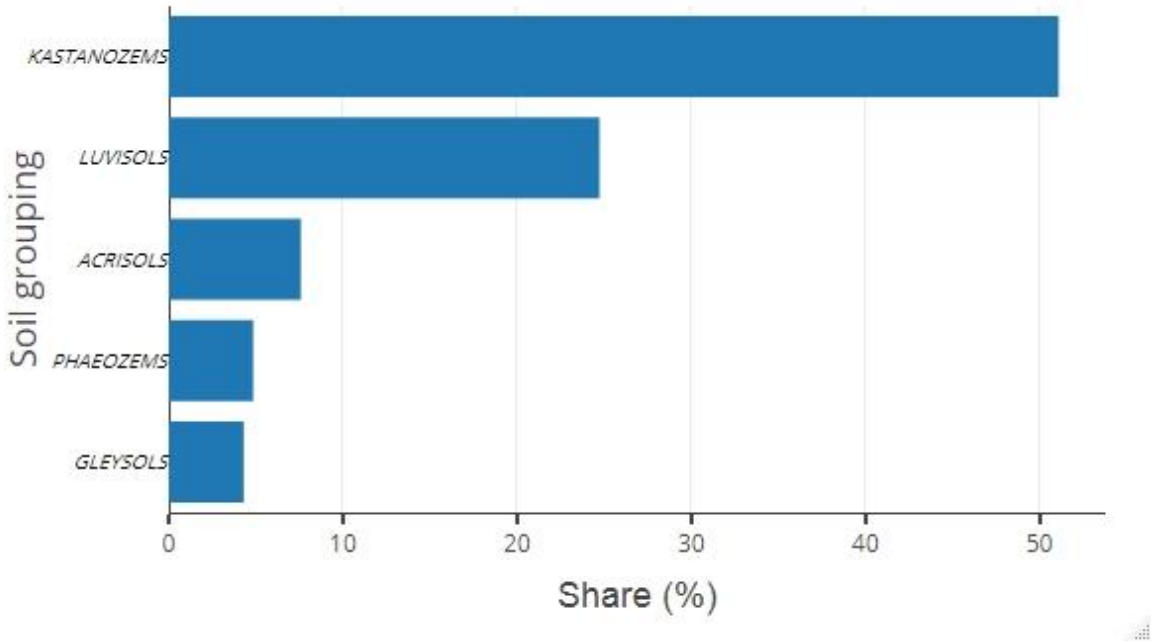

Figure 131. Share of major soil groupings in the Southern United States region.

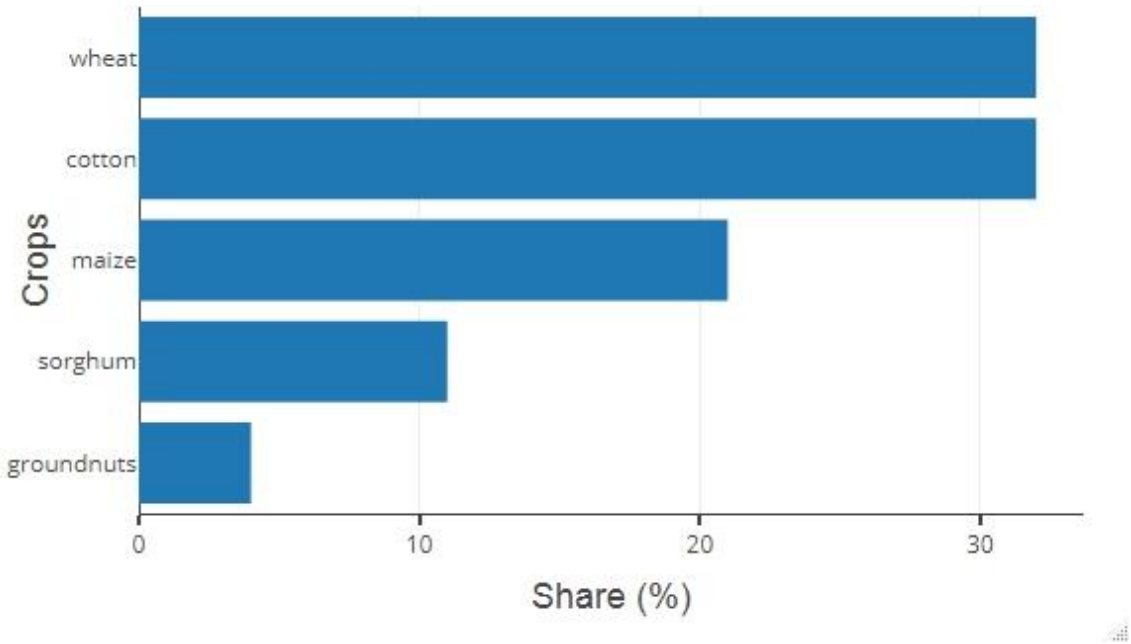

Figure 132. Share of major crops in the Southern United States region.

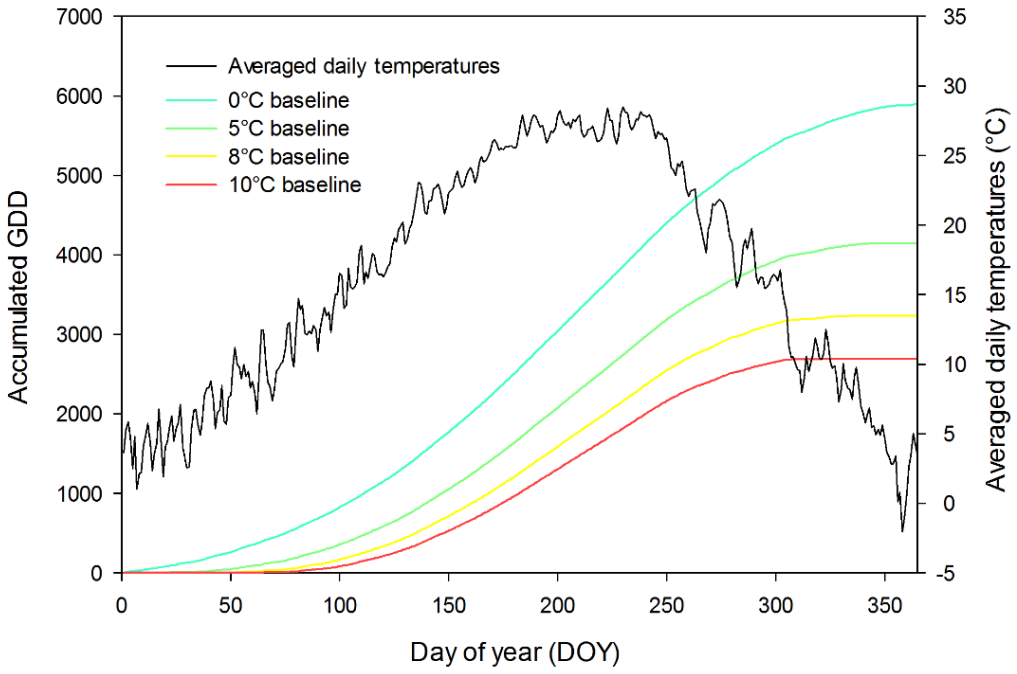

Figure 133. Average daily temperatures and resulting annual GDD accumulation calculated for four baselines in the Southern United States region.

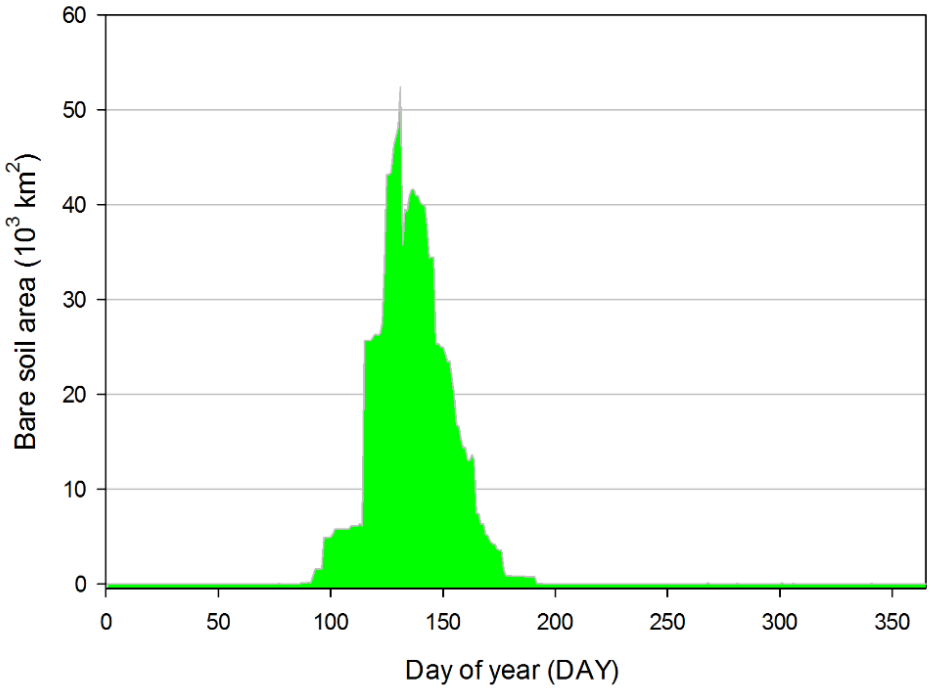

Figure 134. Annual variation of bare soil area in the Southern United States region.

3.6.6. Mexico

One of the cradles of agriculture, it was here that the first domestication of maize occurred some 7,000 to 12,000 years ago. Stretching over 3,000 km in a north–south direction, the territory of Mexico is rightly divided into two climate zones: temperate in the north and tropical in the south, with northern parts receiving less rainfall throughout the year. The majority of arable land is therefore located in the southern part of the region, especially along the coast of the Gulf of Mexico and in the Valley of Mexico, around the capital city. In northern parts of the region, arable land is sparse and concentrated mostly around the continental coast of the Gulf of California, while in the Yucatan Peninsula only scarce arable land was found, especially in its northern parts. The practice of CA was reported on just over 4,000 km^2 (Figure 135).

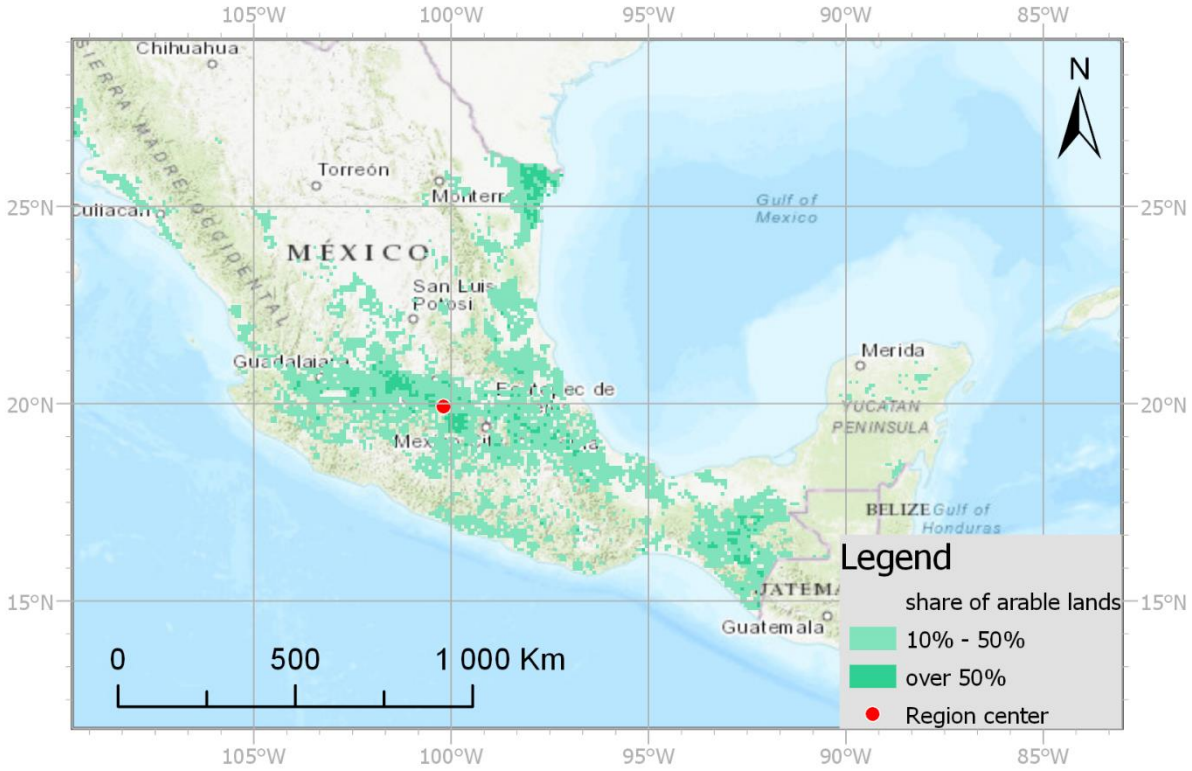

Figure 135. Distribution of arable land in the Mexico region.

Around half of the arable land is split evenly between two major soil groupings, *Xerosols* and *Yermosols* (Figure 136). Almost a fifth of that land contains *Kastanozems*, followed by three soil groupings that each have a share of around 7%: *Vertisols, Andosols* and *Gleysols*. Another three soil groupings contribute to around 2%; those are *Regosols, Cambisols,* and *Lithosols.* Maize is by far the most important crop cultivated in Mexico, with

about 70% of analyzed land dedicated to its production (Figure 137). A quarter of arable land is shared between the cultivation of two crops, sorghum and wheat, followed by barley that is sown on almost 3% of that land. The areas dedicated to the growing of cotton, groundnuts, soybeans, and rapeseed don't exceed 1% for any of them. The central point used to extract mean daily temperatures was located at 20° north and 100° west, in the middle of the biggest concentration of agriculture, not far from Mexico City. The temperatures obtained showed very little variability, oscillating around 19°C throughout the year and ranging between 17°C and 23°C, so the accumulation of GDD has a very linear shape (Figure 138). One main period of bare soil was observed, preceded by a smaller one (Figure 139). That main peak occurred after the 149th DOY and lasted for about a month and a half, almost reaching 35,000 km^2 at its maximum level. That maximum is reached after the first batch of the planting of maize when the surface was still bare after planting sorghum and wheat. The earlier bare soil period reached a little more than 5,000 km^2 and lasted between the 59th and the 113th DOY, as a consequence of sowing of sorghum, followed by barley.

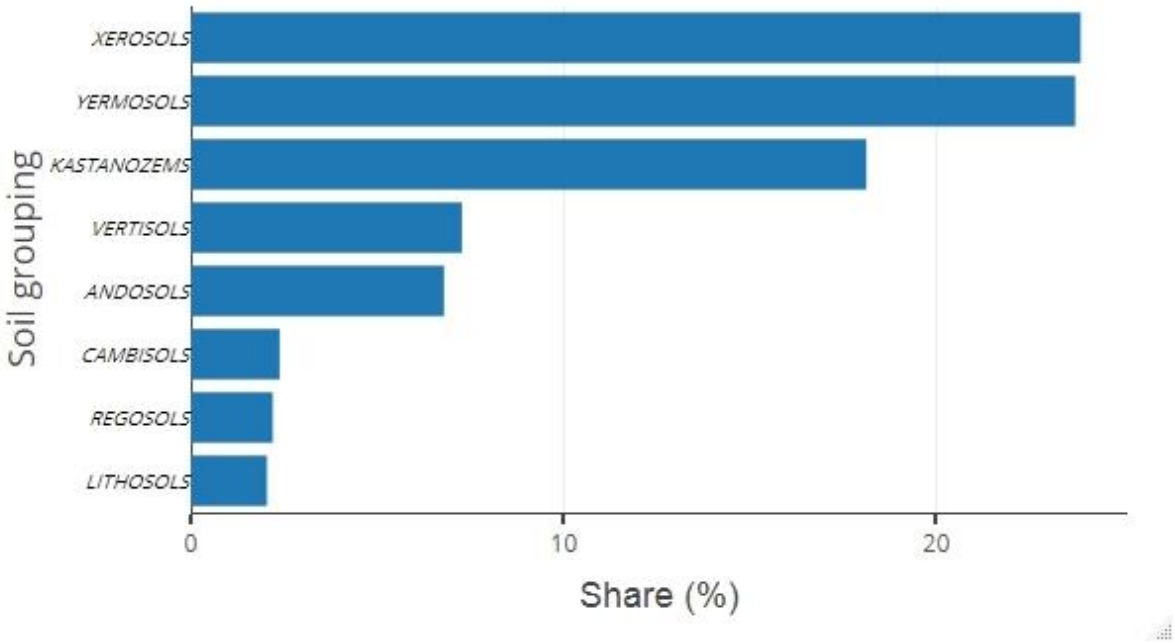

Figure 136. Share of major soil groupings in the Mexico region.

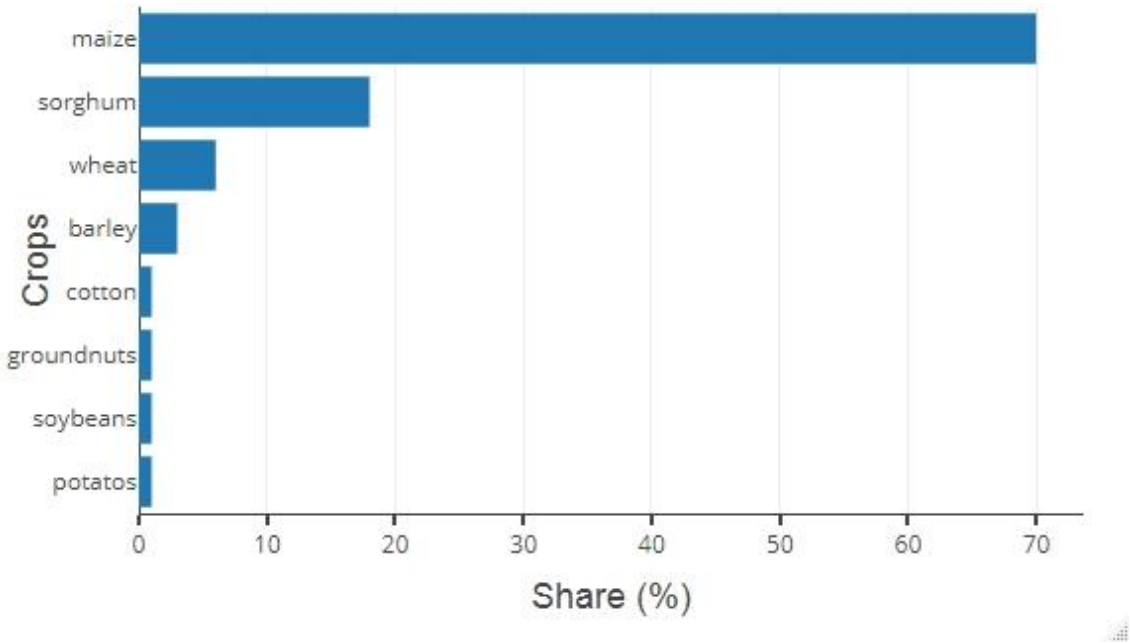

Figure 137. Share of major crops in the Mexico region.

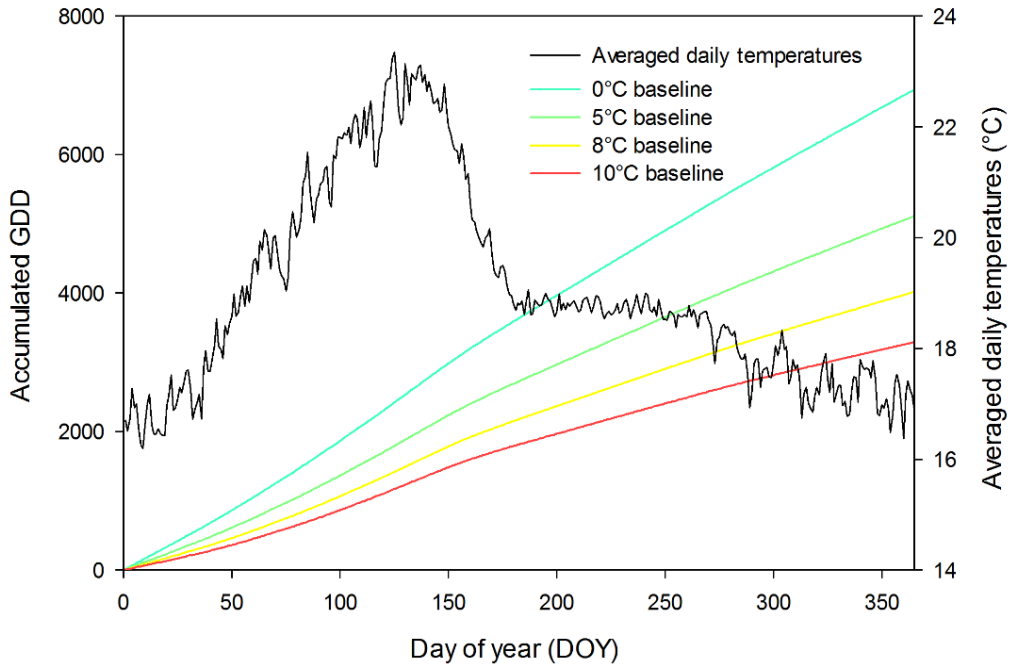

Figure 138. Average daily temperatures and resulting annual GDD accumulation calculated for four baselines in the Mexico region.

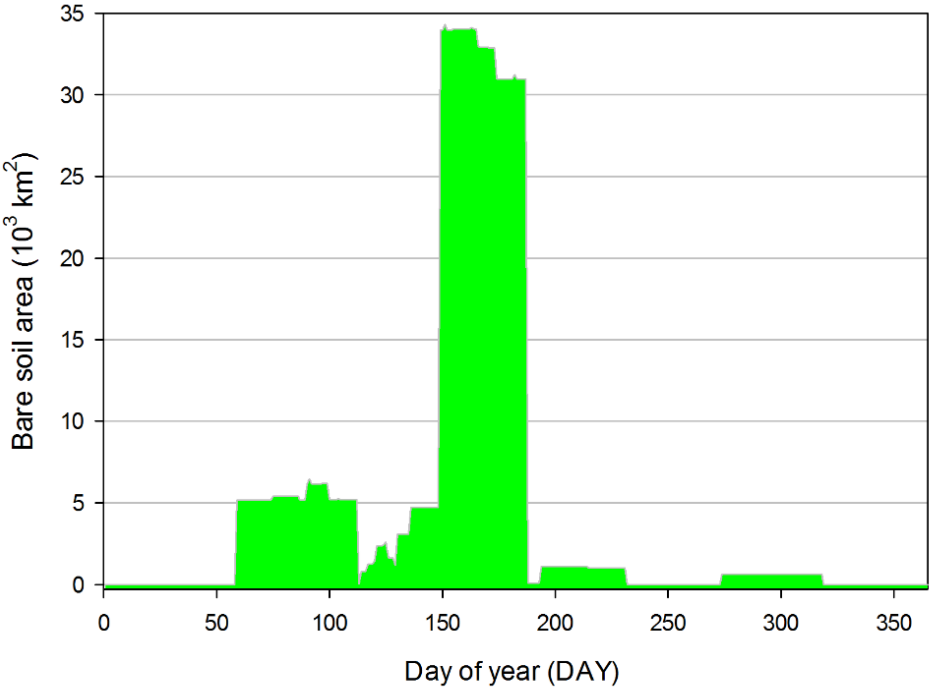

Figure 139. Annual variation of bare soil area in the Mexico region.

3.6.7. Central America

The NAce region is the southernmost region of the North America super region, located on a narrows isthmus connecting it with South America. The predominant climate in the region is humid and tropical, resulting in one of the most biodiverse ecosystems on the planet. Across the countries composing this region, the majority of primordial rain forests were converted to agriculture. The arable land was concentrated in the valleys, especially along the Pacific Coast, with more sparse arable land along the whole width of Honduras and some agricultural pockets in southern Panama (Figure 140).

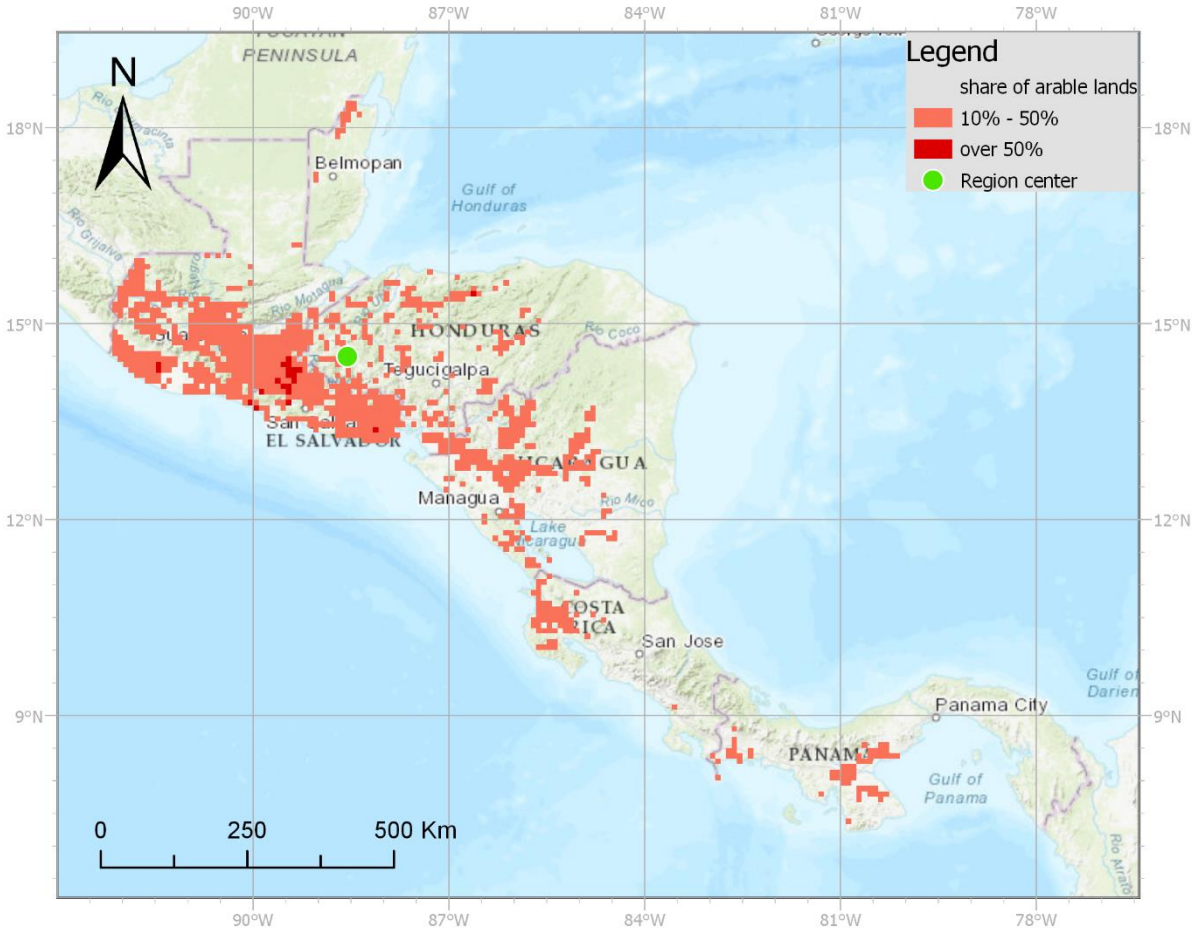

Figure 140. Distribution of arable land in the Central America region.

Almost half of the analyzed land belongs to the *Acrisols* soil grouping, characteristic of humid, tropical regions (Figure 141). Two soil groupings, *Nitosols* and *Cambisols,* taken together occupy a third of that land, followed by *Luvisols* that were found on almost 10% of it. The last noteworthy soil groupings are *Gleysols, Rendzinas* and *Andosols.* Between the analyzed major crops, the overwhelming majority of the land is dedicated to the cultivation of maize (Figure 142), with sorghum being the second most commonly planted crop; together

they constituted over 95% of the analyzed acreage. A little over 1% each was used for soybeans, groundnuts, and cassava. The annual accumulation of the GDD (Figure 143) was estimated based on mean daily temperatures obtained from a point situated at 14° north and 89° west, close to the border between Honduras and El Salvador, in the biggest concentration of arable land in the region. The annual variation of daily temperatures was low, with the highest just before the wet season reaching 25°C, and never dipping below 20°C. The annual course of bare soil shows a staggered shape, dictated by two dominating major crops (Figure 144). The first occurrence of bare soil was noted around the 121st DOY, after the planting of both maize and sorghum and reaching just over 6,500 km^2. After the 150th DOY, that area rose to almost 5,000 km^2 as a result of the planting of maize in northern parts of the region.

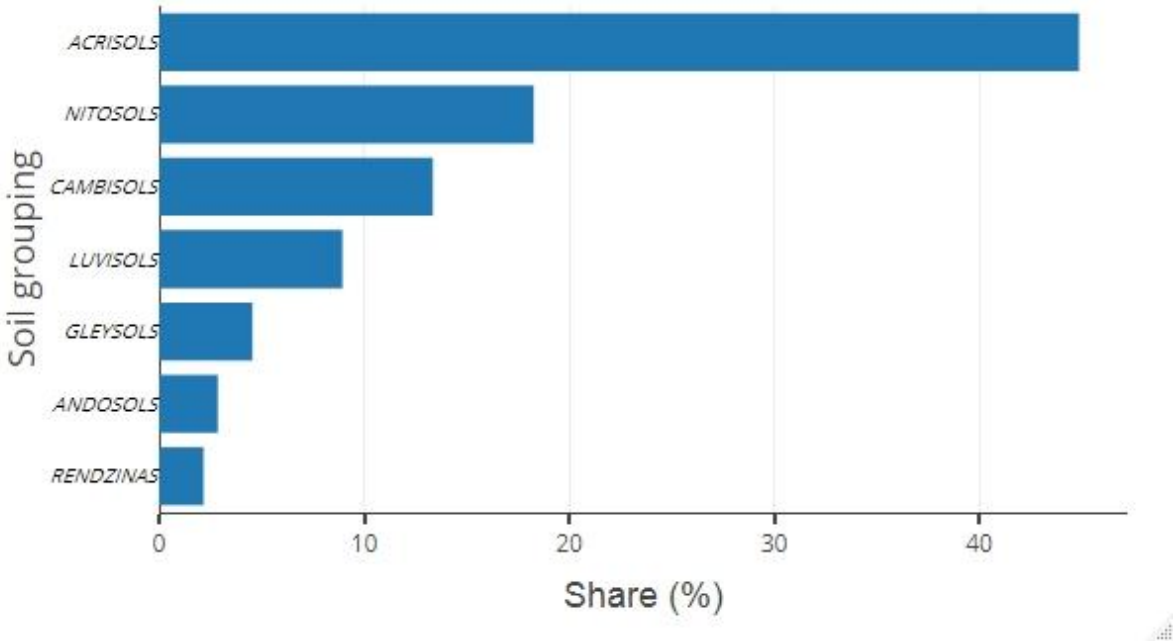

Figure 141. Share of major soil groupings in the Central America region.

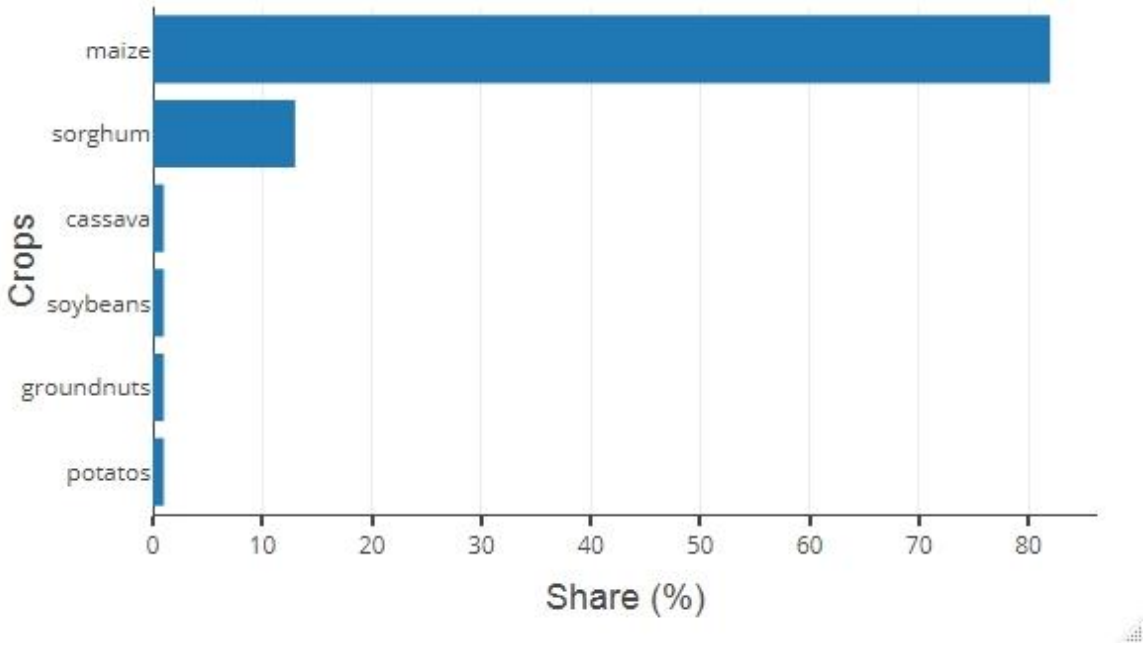

Figure 142. Share of major crops in the Central America region.

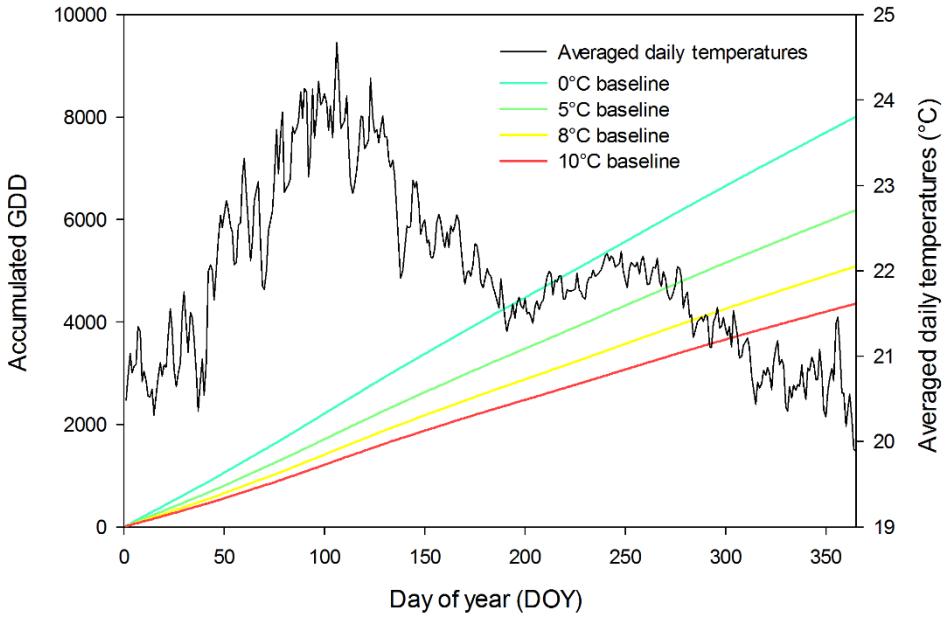

Figure 143. Average daily temperatures and resulting annual GDD accumulation calculated for four baselines in the Central America region.

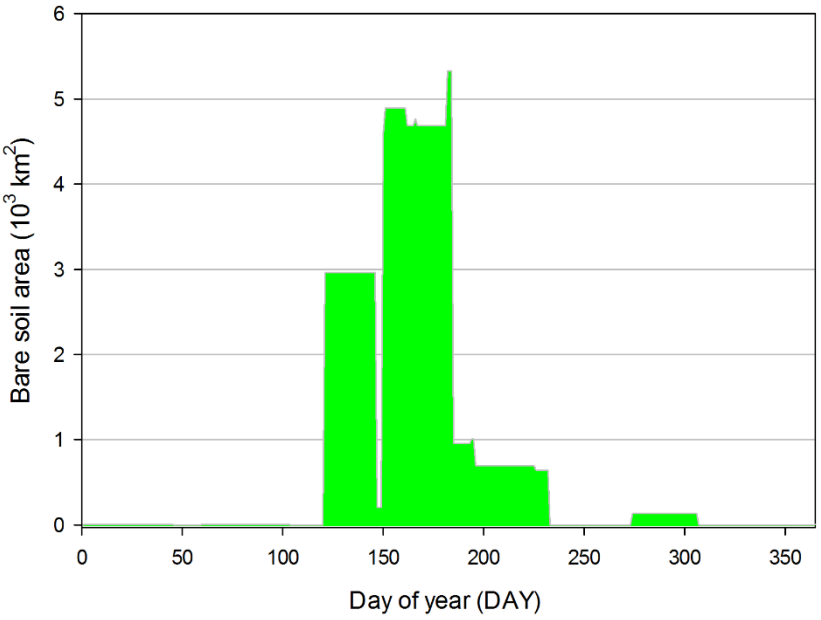

Figure 144. Annual variation of bare soil area in the Central America region.

3.6.8. Caribbean

The NAca region is comprised of over 700 islands situated in the Caribbean Sea and has the smallest land area of the North American regions. Due to the archipelagic nature of the region, agriculture is dispersed, concentrating on the largest islands, mainly Hispaniola and Cuba, whereas southern islands were found unsuitable for agriculture due to the arid climate. A significant portion of agricultural production occurring in the region was out of the scope of this work, seeing as there are large plantations of tobacco, coffee, sugarcane, bananas, and other cash crops. Of the analyzed land, the biggest concentration of arable land was located in the western parts of the island of Hispaniola, on Haitian territory, followed by arable land in Cuba. Arable land in the eastern parts of Hispaniola, on territories belonging to the Dominican Republic, was quite sparse (Figure 145).

Figure 145. Distribution of arable land in the Caribbean region.

The most widespread soil grouping was *Cambisols*, which was found on over a third of arable land (Figure 146). *Nitosols* occupied almost a quarter of the land, followed by *Luvisols* with a share of almost 15%. *Fluvisols* and *Acrisols* were each found on about 7% of analyzed land. Among the major crops studied, over half of the area was dedicated to the cultivation of maize (Figure 147). An area about two times smaller was used for cassava, and sorghum was the third most common crop, with a share of the area of over 15%. Groundnuts were cultivated on about 5% of arable land, and around half of that area was sown with potatoes. The average daily temperatures were obtained from the previously mentioned concentration of agriculture in the western parts of Hispaniola Island, located at 19° north and 73° west. The seasons are pronounced, but the overall annual amplitude is low, ranging between 24°C and

28°C, resulting in a smooth annual accumulation of GDD (Figure 148). Two distinct periods of bare soil were identified in the region, the first almost twice the size of the second (Figure 149). The planting of maize after the 90th DOY, followed by the planting of cassava about two weeks later started the first period. The peak, which was reached around the 105th DOY, amounted to almost 2,500 km^2, and was followed by the disappearance of bare soil around the 125th DOY. The second time a significant portion of arable land became bare occurred around three months later, owing once again to the planting of maize, reinforced this time by the planting of sorghum. The maximum area during that second period exceeded 1,000 km^2 lasting for around a week and a half.

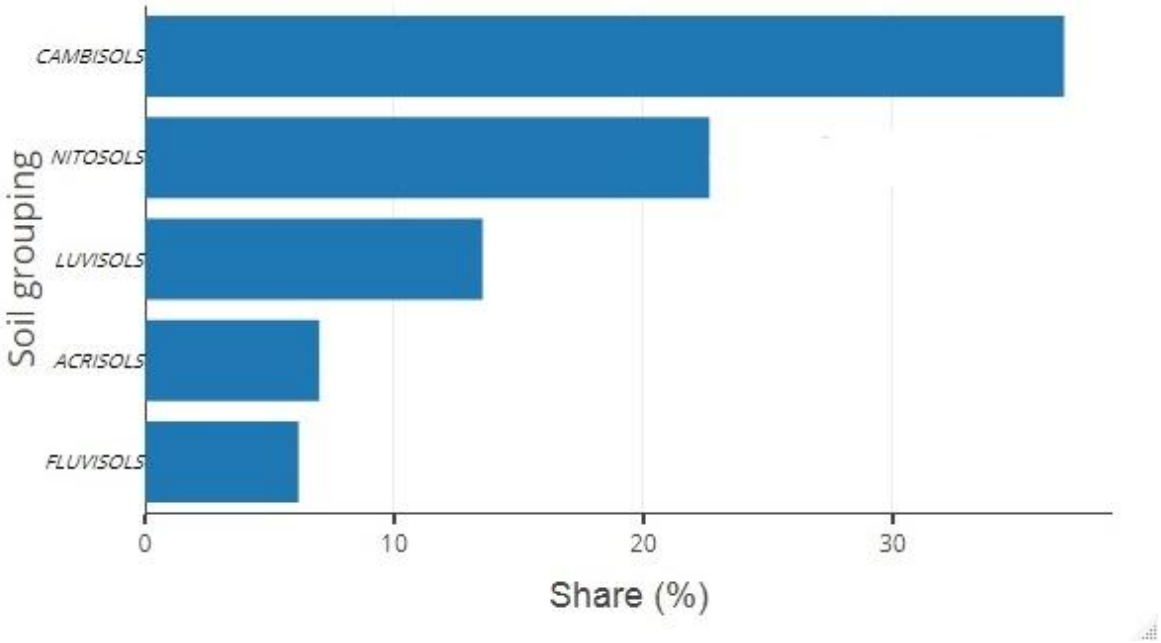

Figure 146. Share of major soil groupings in the Caribbean region.

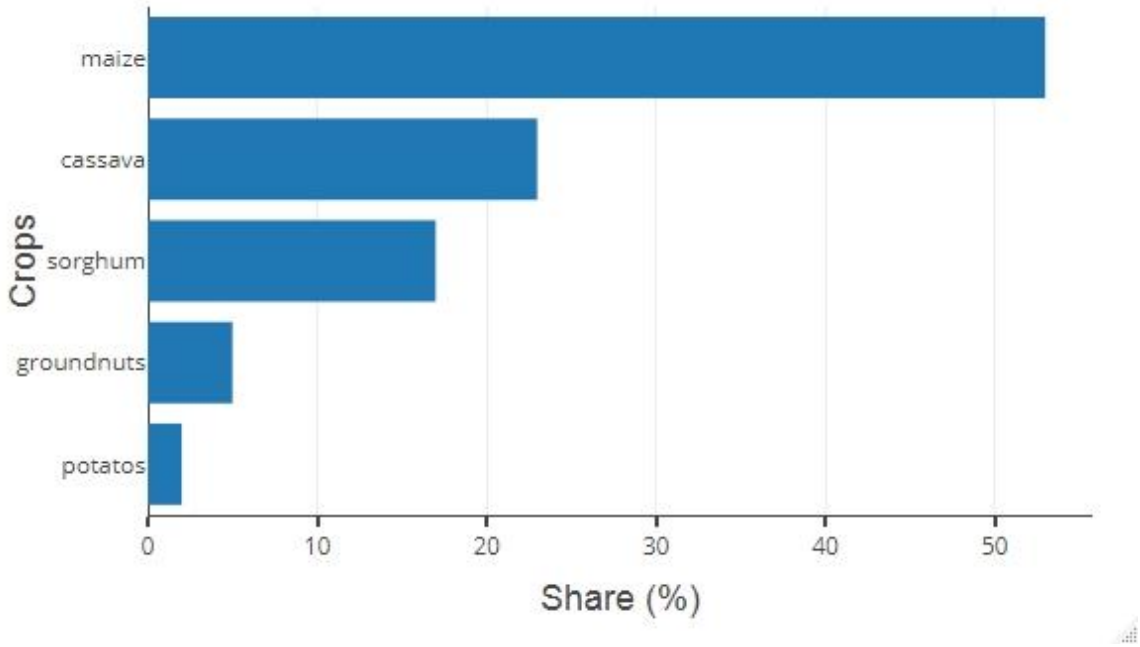

Figure 147. Share of major crops in the Caribbean region.

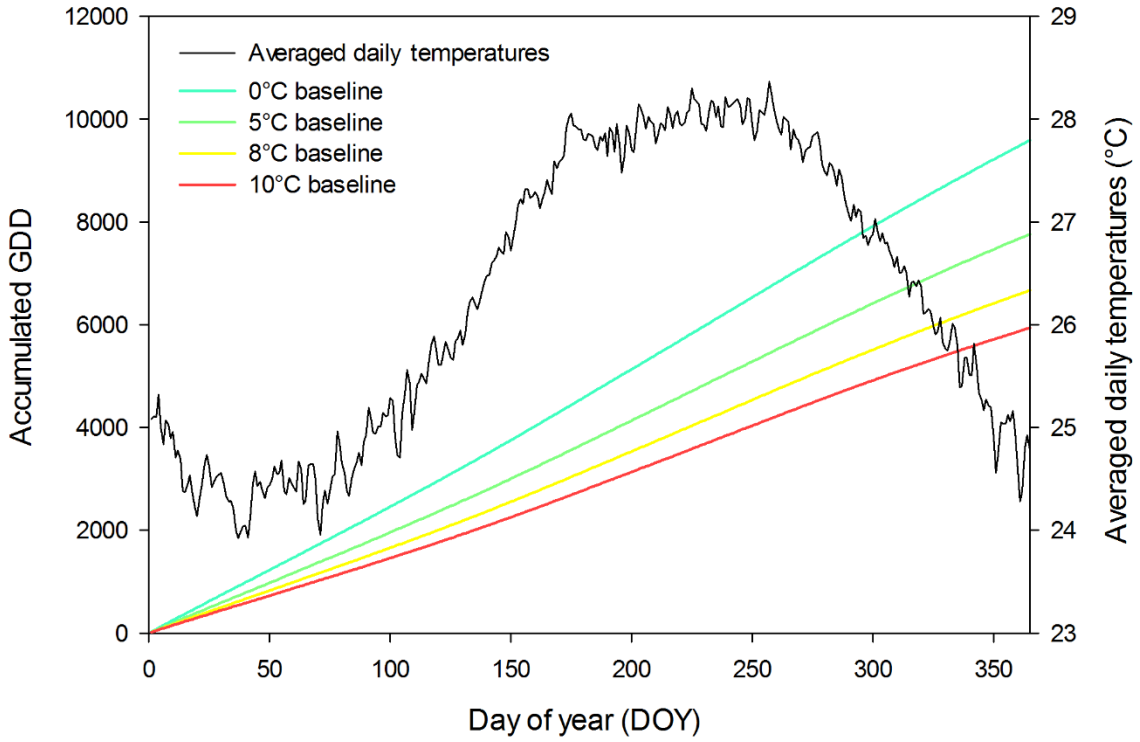

Figure 148. Average daily temperatures and resulting annual GDD accumulation calculated for four baselines in the Caribbean region.

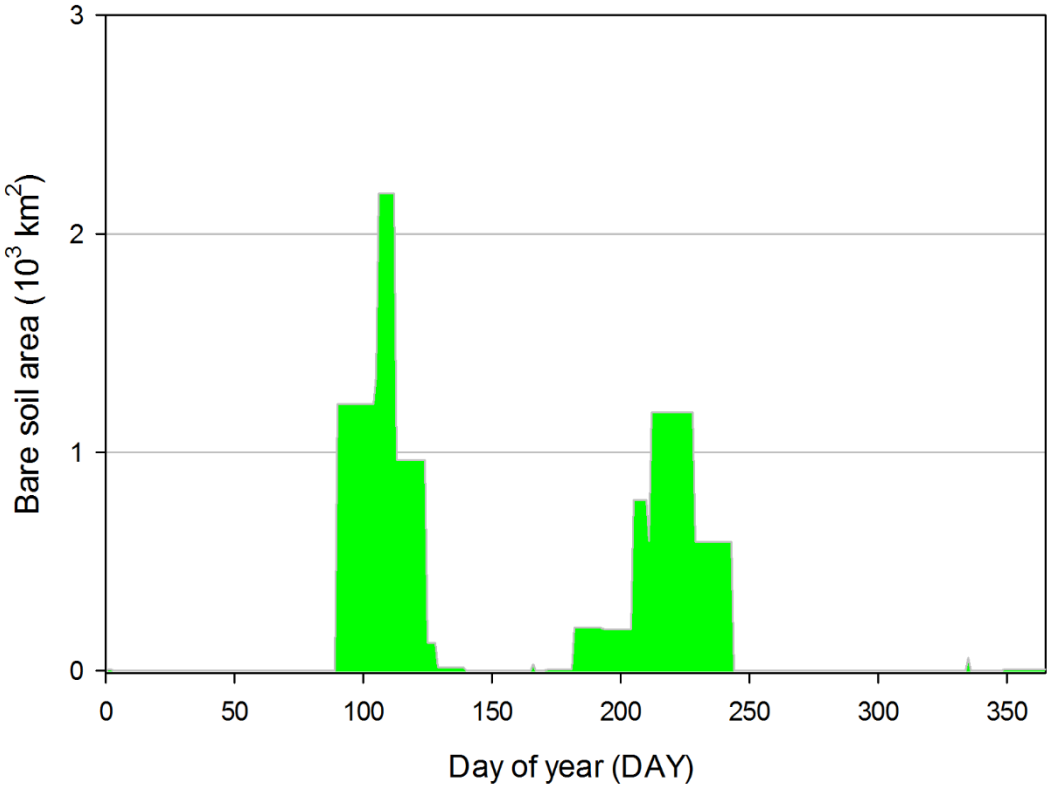

Figure 149. Annual variation of bare soil area in the Caribbean region.

3.7. South America

Located to the south of the North American super region, the majority of land belonging to South America lies in the southern hemisphere. The continent extends more than 7,500 km in a north–south direction, spanning numerous climate zones along the way. Those climates range from equatorial in the north to tundra in the south, with variations of temperate in between. Along the length of the western side of the continent run the Andes, east of which lies the Amazon rain forest, together with the largest river system in the world. In contrast to those humid places, the world's driest desert, the Atacama is also found in this continent. The human population is located predominantly along both western and eastern coasts, with the pattern of arable land following suit. Adoption of CA in South America is among the most rapid on the planet, with almost half of all the area under CA globally being in South America. The super region was divided into three regions (Figure 150):

- Brazil (SAbr)—encompasses around half of the continent's population and area;
- Andean States (SAas)—the region, anchored on the Andes, consists of the northern and western countries of South America;
- Southern Cone (SAsc)—located to the south of the previous two regions, this region has a tapering shape, hence its name.

South America is the only super region where soybeans are the most widely cultivated crop (Table 11). Almost a third of the arable land was dedicated to maize and half of that to wheat. Just those three crops together constitute almost 90% of the farmed area, with the remainder split between cassava, cotton, barley, and sorghum. Trace areas of potatoes and groundnuts were also noted. The annual variation of bare soil in this super region shows one main peak, followed by another, albeit a three to four times smaller one (Figure 151). The main peak exceeded 350,000 km^2 and the smaller one was about a fourth of the main one. Due to the fact that the majority of the arable land of South America is located in the southern hemisphere, the timing of those peaks shifted by half a year compared to northern regions, with the main one occurring between the 325th and the 350th DOY.

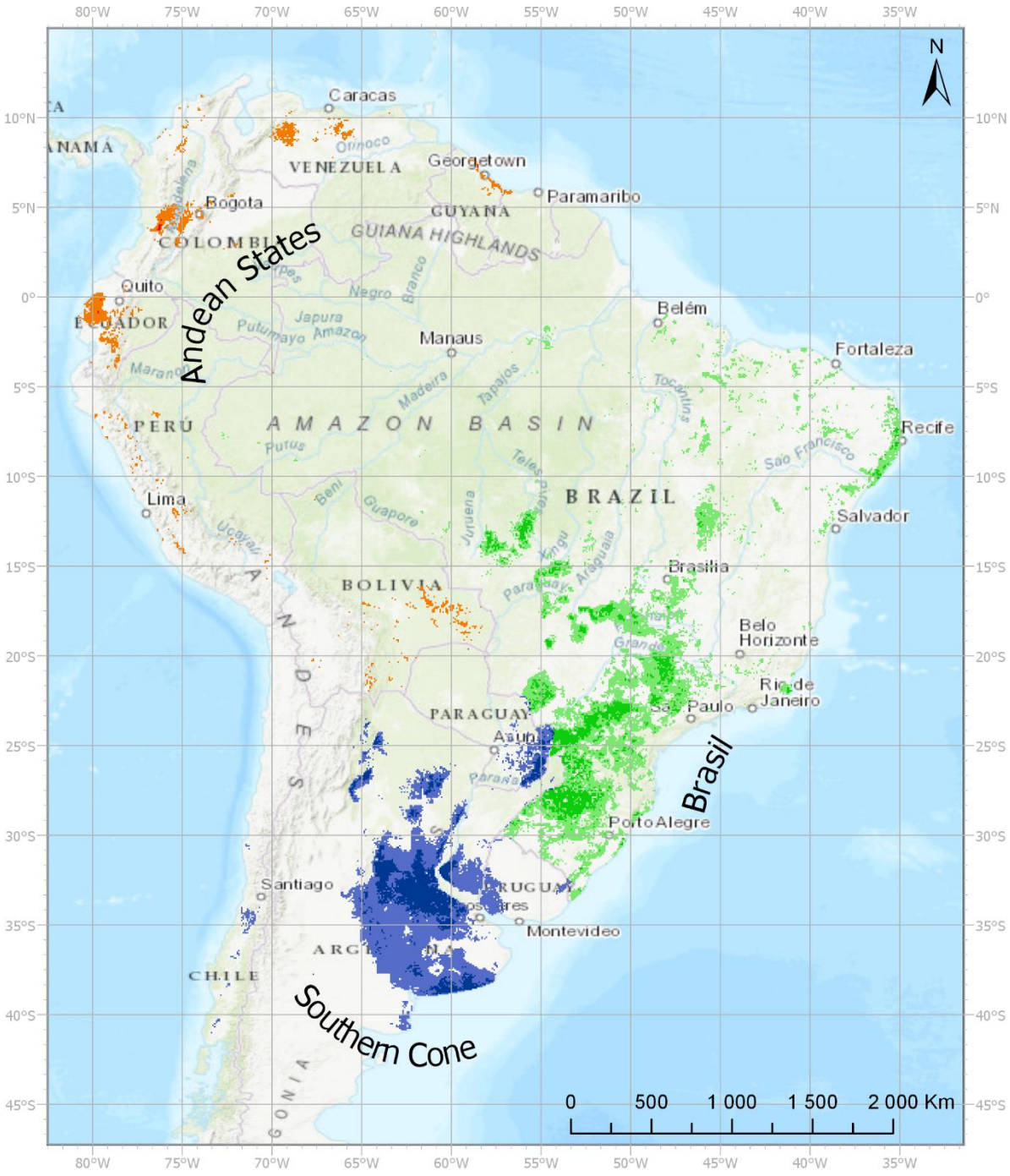

Figure 150. Arable land in the South America super region divided into regions.

Table 11. Area and share of arable land of major crops farmed in South America.

Major Crop	Area	
	(thousands km²)	(%)
Soybean	241.7	42.7
Maize	164.4	29
Wheat	85.1	15
Cassava	21.4	3.8
Cotton	15.9	2.8
Sorghum	14.6	2.6
Potato	9.1	1.6
Barley	7.7	1.4
Groundnut	4.3	0.8
Rye	0.7	0.1
Rapeseed	0.6	0.1
Sugar beet	0.5	0.1
Millet	0.3	0

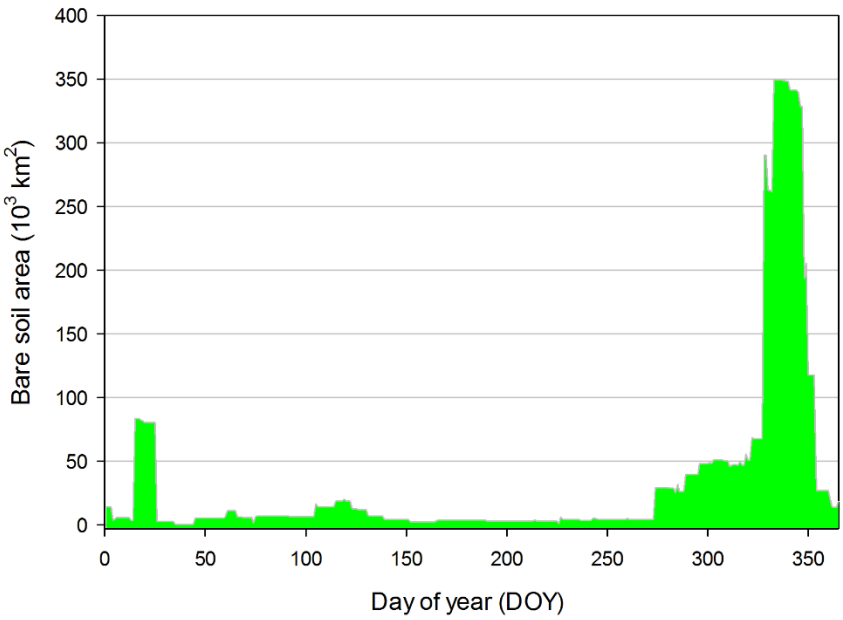

Figure 151. Annual variation of bare soil area in the South America super region.

3.7.1. Brazil

Brazil is by far the largest country of South America, both in its land area as well as in population. The main feature of the northern parts of the region is the Amazon rain forest together with its watershed. The majority of the arable land is located in southern parts of the country, south of the Tropic of Capricorn. Between the tropic and the equator, the arable land is more spread out, concentrated along the Rivers Paranaiba, Paraguay and San Francisco. A significant pocket of agriculture was also found in the province of Mato Grosso, not far from the border with Bolivia. The practice of CA was found in extensive areas of Brazil, with over half of the total cultivated area using that system (Figure 152).

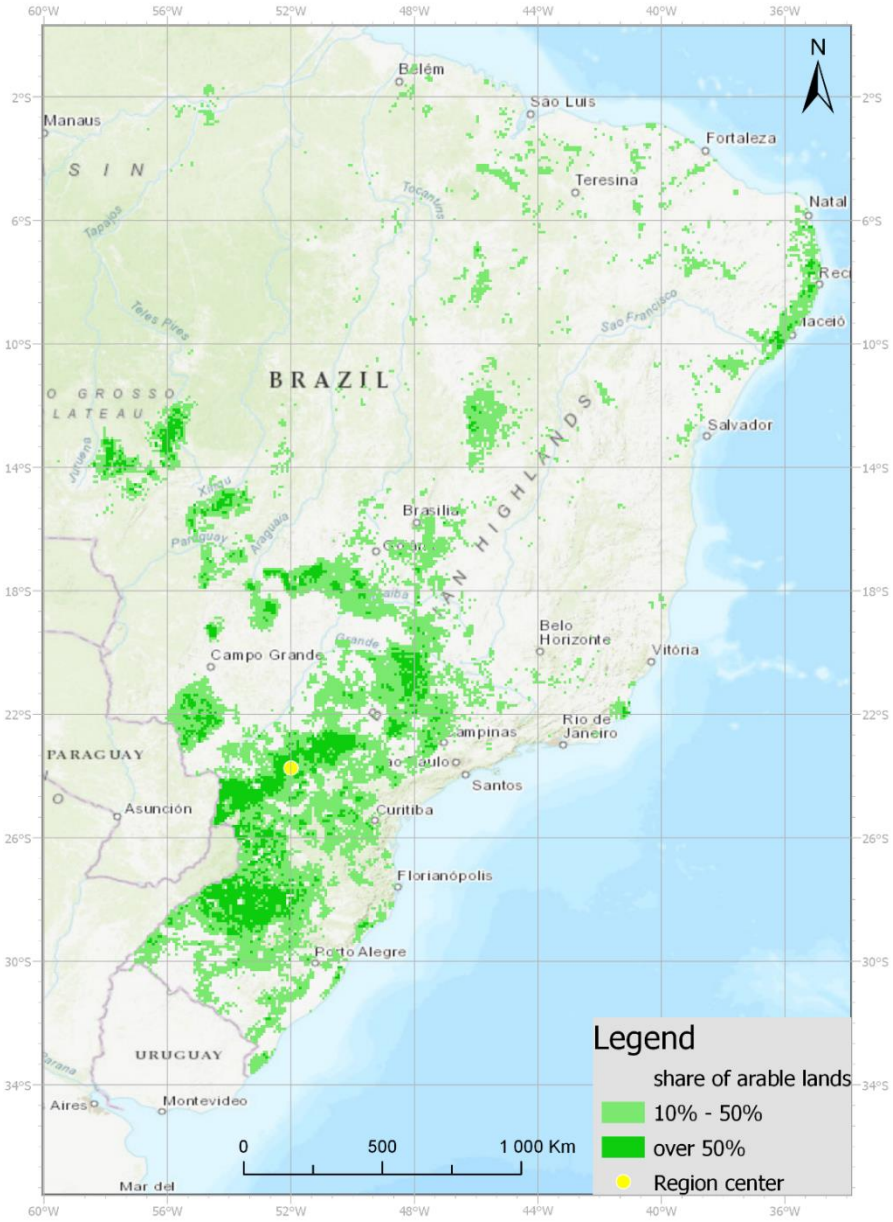

Figure 152. Annual variation of bare soil area in the Brazil region.

Almost half of the soils used in Brazilian agriculture belong to the *Ferrasols* grouping, with their characteristic red color (Figure 153). A fifth of this land sports *Luvisols* followed by a share of about 13% *Arenosols*. *Acrisols* occupied just below a tenth of arable land, and the last noteworthy soil grouping was *Lithosols*, with a share of almost 4%. The most important crop in Brazil was soybeans, which was found on almost half of the analyzed land (Figure 154). The area dedicated to the cultivation of maize was also extensive, having a share of almost 40%. Both cassava and wheat were each found on about 5% of arable land. The last notable crop cultivated in SAbr was cotton, farmed on about 3% of the land analyzed. The central point of the region, used for the extraction of mean daily temperatures was located at 23° south and 52° west, some 500 km west of São Paulo, in the southern agricultural pocket. The obtained temperatures showed annual variability and ranged between 15°C and 25°C, resulting in a smooth annual accumulation of GDD (Figure 155). Over 220,000 km^2 of bare soil was found during the maxima, which lasted for about three weeks, between the 328th and the 348th DOY (Figure 156). That period coincided with planting dates of maize and the majority of the soybeans. Three additional occurrences of bare soil were found throughout the year; however, they were over ten times smaller than the main one. The biggest of those three bare soil periods preceded the main one by a month and a half, caused by the earlier planting of maize.

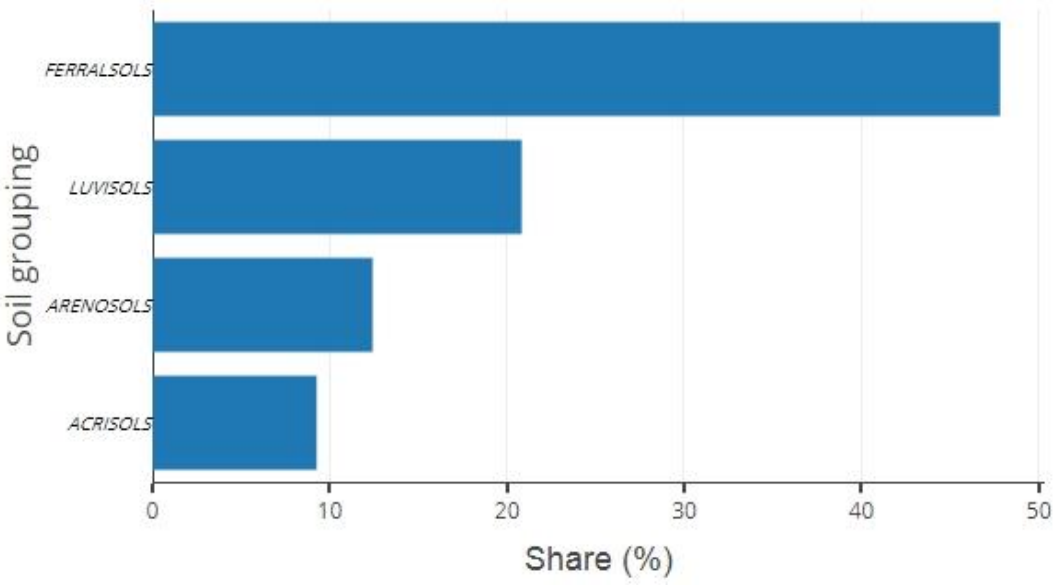

Figure 153. Share of major soil groupings in the Brazil region.

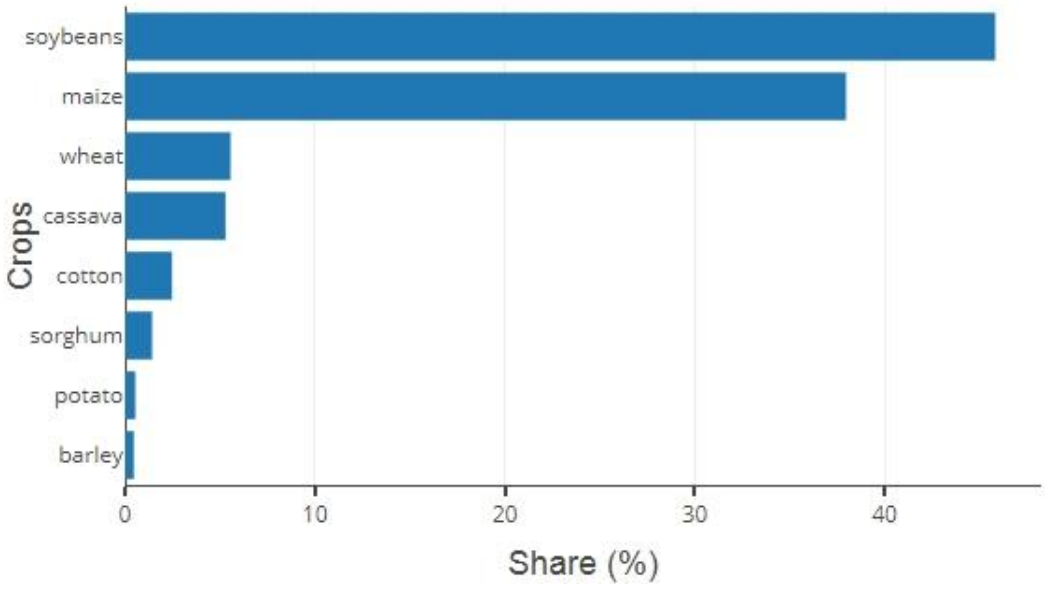

Figure 154. Share of major crops in the Brazil region.

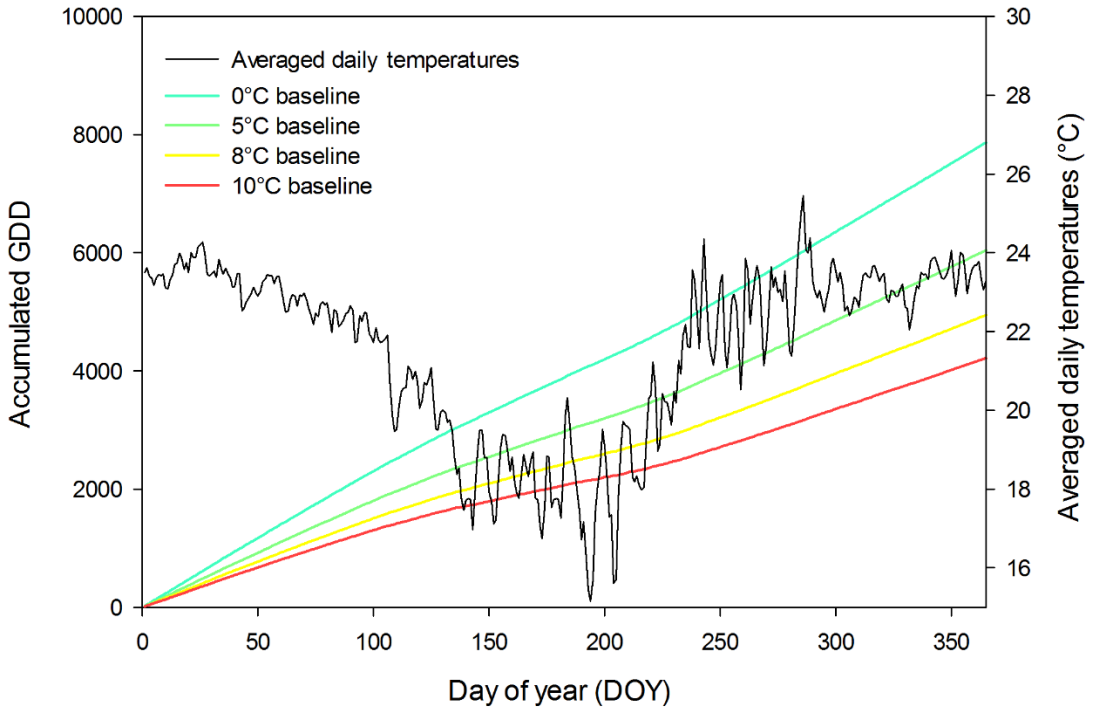

Figure 155. Average daily temperatures and resulting annual GDD accumulation calculated for four baselines in the Brazil region.

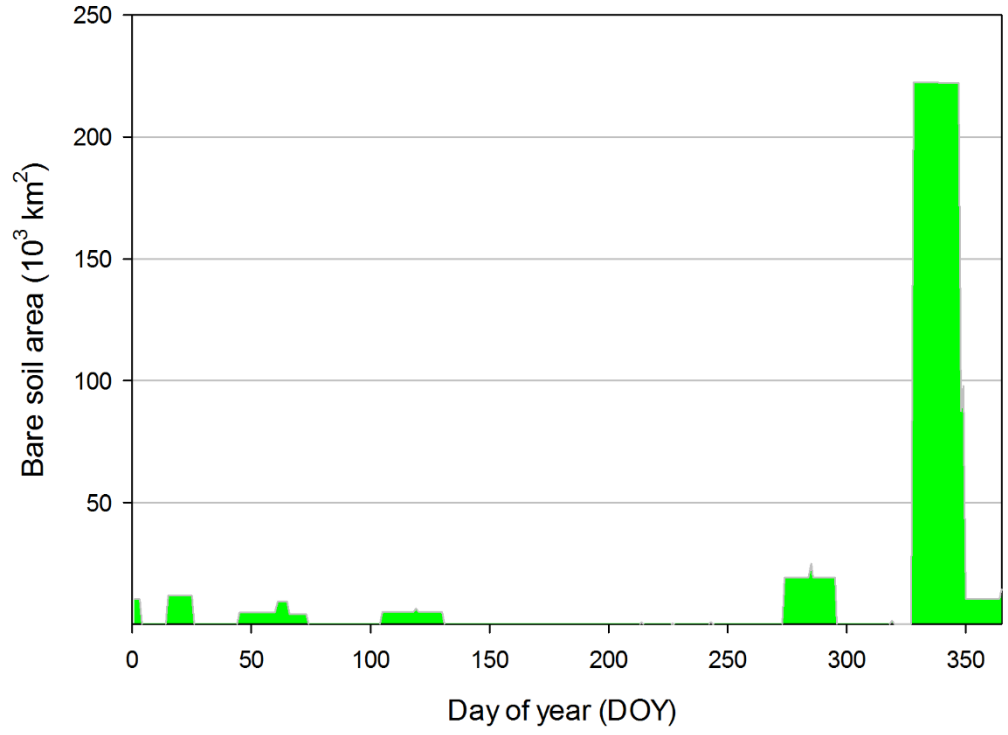

Figure 156. Annual variation of bare soil area in the Brazil region.

3.7.2. Andean states

The region spanning northern and northwestern parts of the continent, the SAas is defined by the Andean Mountains and northern extremities of the Amazon rain forest, both of which complicate agricultural activities. The region is bordered by the Atlantic Ocean in the north and by the Pacific Ocean in the west, those two being separated by the Isthmus of Panama. The overall amount of arable land within the region is relatively low, with less than 10% of the arable land of South America found in this region, despite its land area being similar to other regions. Most of the arable land is located in pockets around the coasts, most notably in Ecuador, northern parts of Venezuela, close to the River Magdalena in Colombia and in the Bolivian hinterlands (Figure 157). Compared to other regions in South America, the practice of CA was relatively uncommon.

Figure 157. Distribution of arable land in the Andean States region.

About a third of arable land belonged to the *Lithosols* grouping (Figure 158). *Luvisols* were found on almost 10% of arable land, and very similar areas were occupied by *Regosols, Andosols, Planosols, Cambisols* and *Nitosols*, each of those groupings with a share of about 7%. The most important cultivated crop in the region was maize, which was farmed on over 40% of the land analyzed (Figure 159). Another quarter of the arable land was split evenly between soybeans and potatoes. Areas used for cultivation of cassava, sorghum, and wheat were similar, each to be found on about 7% of the land, followed by about 5% for barley and cotton. The annual course of average daily temperatures obtained from a point located at 2° south and 77° west, showed almost no variation, ranging between 16°C and 18°C. The annual accumulation of GDD was therefore very smooth (Figure 160). Two main periods of bare soil can be distinguished in the region (Figure 161). During the biggest one, the area of bare soil reaches almost 20,000 km^2, the maximum of which happens around the 320th DOY. That whole period lasts for some three months, between the 274th and the 362nd DOY and starts with the planting of maize and potatoes, especially in western and southern parts of the region. The shorter bare soil period occurs before the main one and results from planting performed in northern and eastern parts of the region. During that period, the bare soil area reaches almost 14,000 km^2 around the 115th DOY.

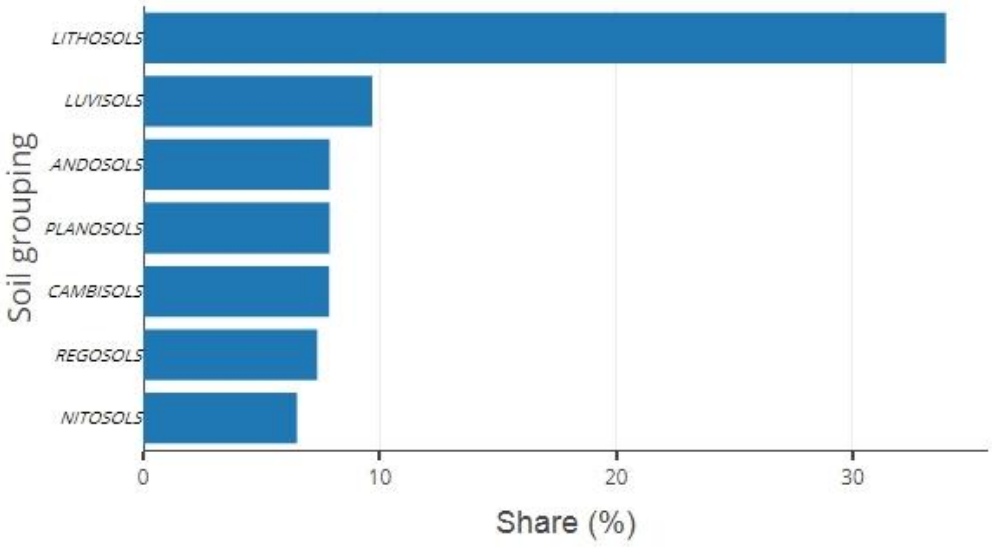

Figure 158. Share of major soil groupings in the Andean States region.

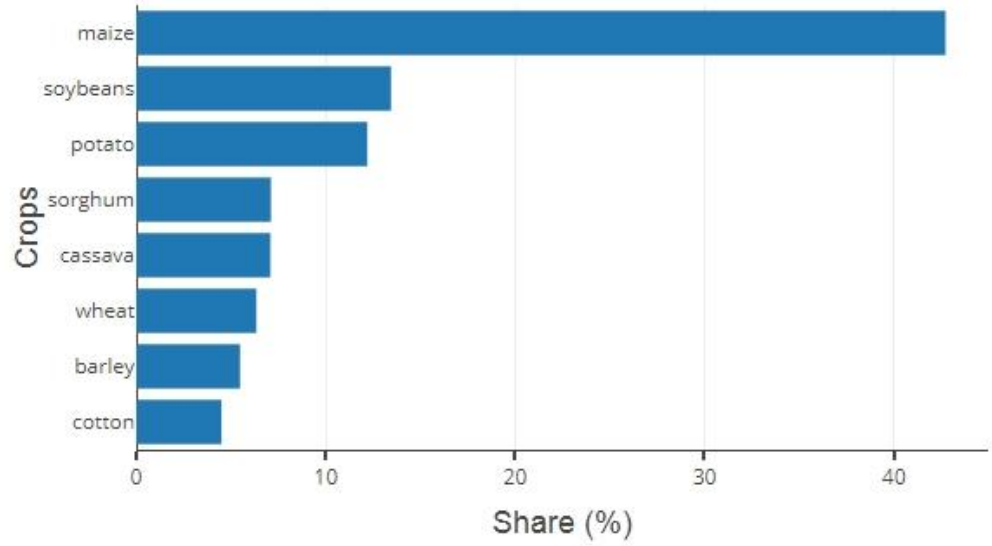

Figure 159. Share of major crops in the Andean States region.

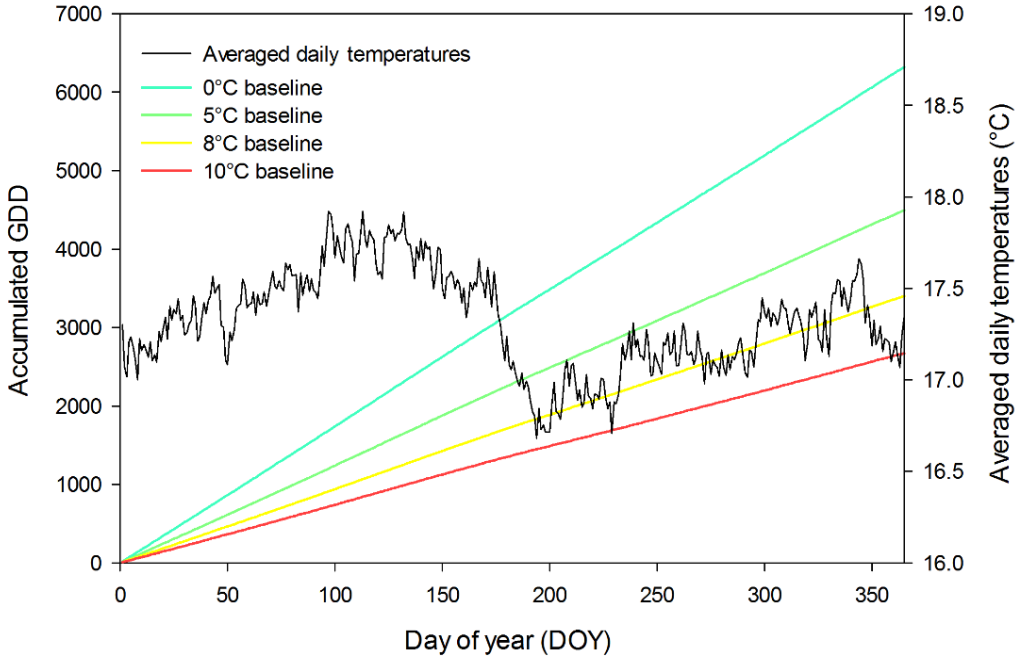

Figure 160. Average daily temperatures and resulting annual GDD accumulation calculated for four baselines in the Andean States region.

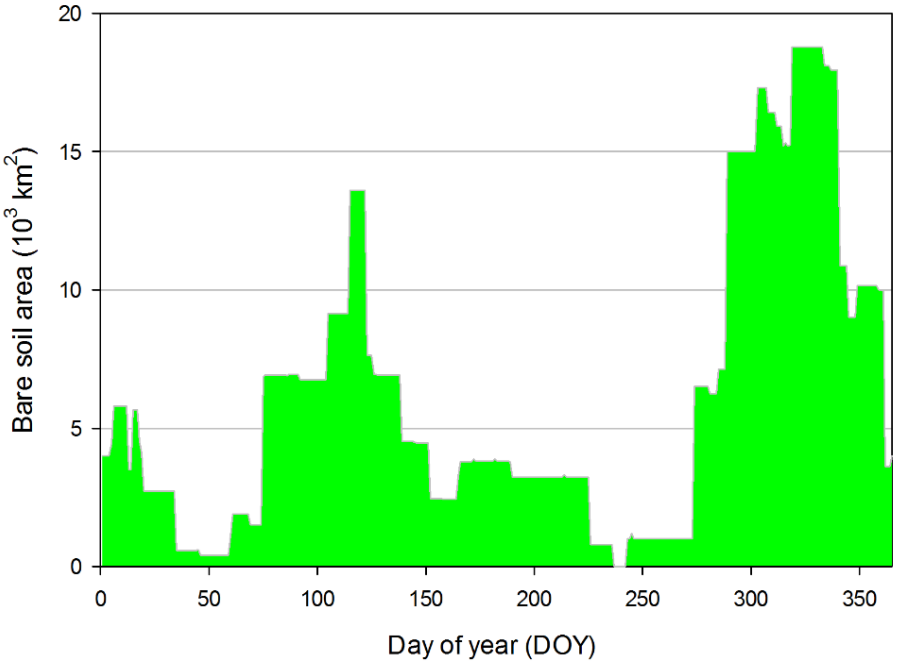

Figure 161. Annual variation of bare soil area in the Andean States region.

3.7.3. Southern Cone

Located to the south of the two other South American regions, SAsc has a shape narrowing in a southern direction. The whole region lies in the southern hemisphere and most of it south of the Tropic of Capricorn. Stretching over 4,000 km from northern to southern borders, the region encompasses various climate zones, between humid subtropical in the north to sub-Antarctic in the south. The main geographic features of the region include the Andean Mountains running parallel to the western coast and the Pampas on the eastern lowlands. The arable land in the region is concentrated in the aforementioned Pampas, around the Parana River while on the western side most arable land was located south of Santiago de Chile (Figure 162). As in another region in South America, CA is widespread in SAsc. In Argentina, the majority of soil is not tilled, likewise in Paraguay and Uruguay, while almost a third of arable land in Chile is not tilled.

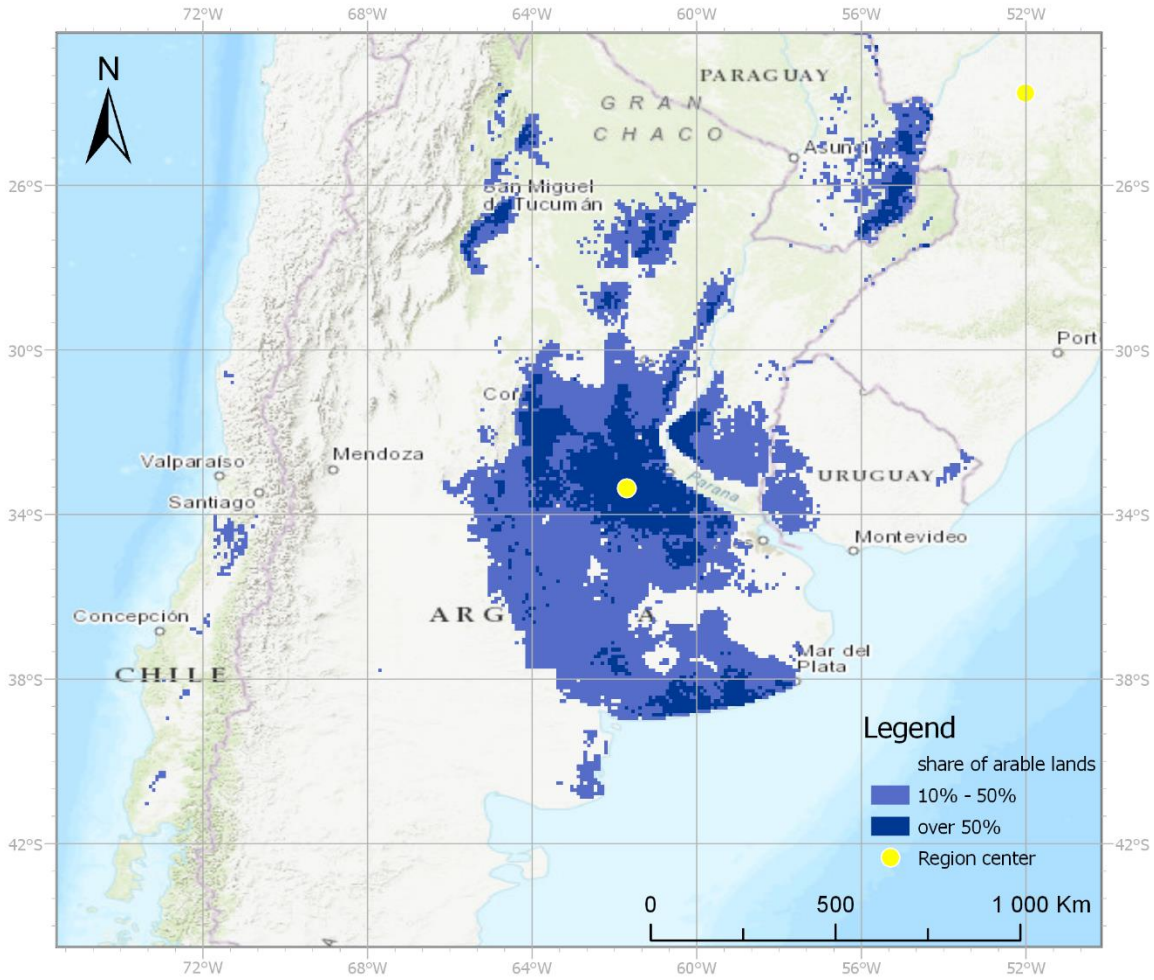

Figure 162. Distribution of arable land in the Southern Cone region.

The most widespread soil grouping among arable land in SAsc is *Phaozems*, which is found on almost half of the land (Figure 163). *Kastanozems* constituted a significant share of almost 15%, followed by a 10% share of *Fluvisols*. The last noteworthy soil groupings were *Solonetz* and *Xerosols*, each occupying around 5% of arable land. Three major crops dominate agricultural production in the region; those are soybeans, wheat and maize (Figure 164). Soybeans were cultivated on almost half of the analyzed land, a third of that land was dedicated to growing wheat, and maize was sown on about a half of the wheat's acreage. Other major crops were farmed on much smaller areas, like cotton and sorghum that were farmed on 3% each, and cassava, groundnuts and barley cultivated on about 1% each. The region's central point was located in the Pampas, at 33° south and 62° west, and the obtained mean daily temperatures showed seasonal variability, ranging between 10°C and 25°C. The annual accumulation of GDD was therefore constant, but more rapid in summer months (Figure 165). Two main peaks of the bare soil area were found in its annual variation (Figure 166). The main one reached almost 110,000 km^2 and lasted for about two weeks, starting after the 330th DOY. That peak was a culmination of the bare soil period that started before the 300th DOY and gradually increased in the area to reach the aforementioned peak, after which the area sharply declined and disappeared completely after the 360th DOY. The plants contributing the most to bare soil at that time were primarily soybeans and maize. The other period of bare soil was associated with the planting of wheat, which occurred around the 15th DOY. During that period, bare soil acreage exceeded 60,000 km^2 for a little over a week.

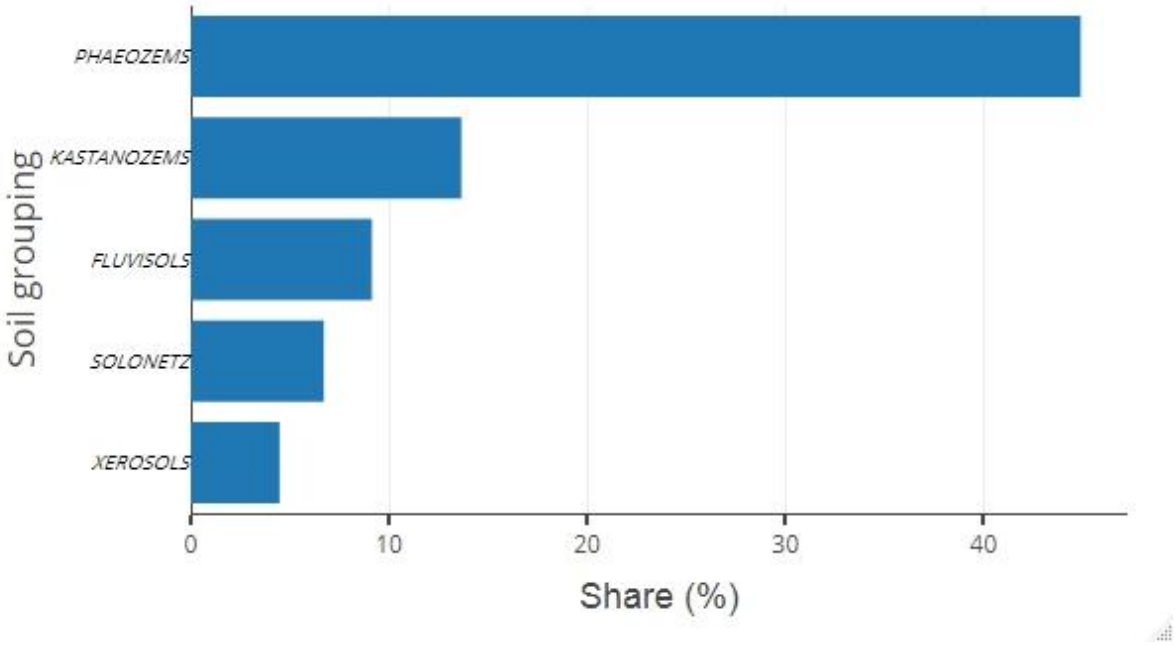

Figure 163. Share of major soil groupings in the Southern Cone region.

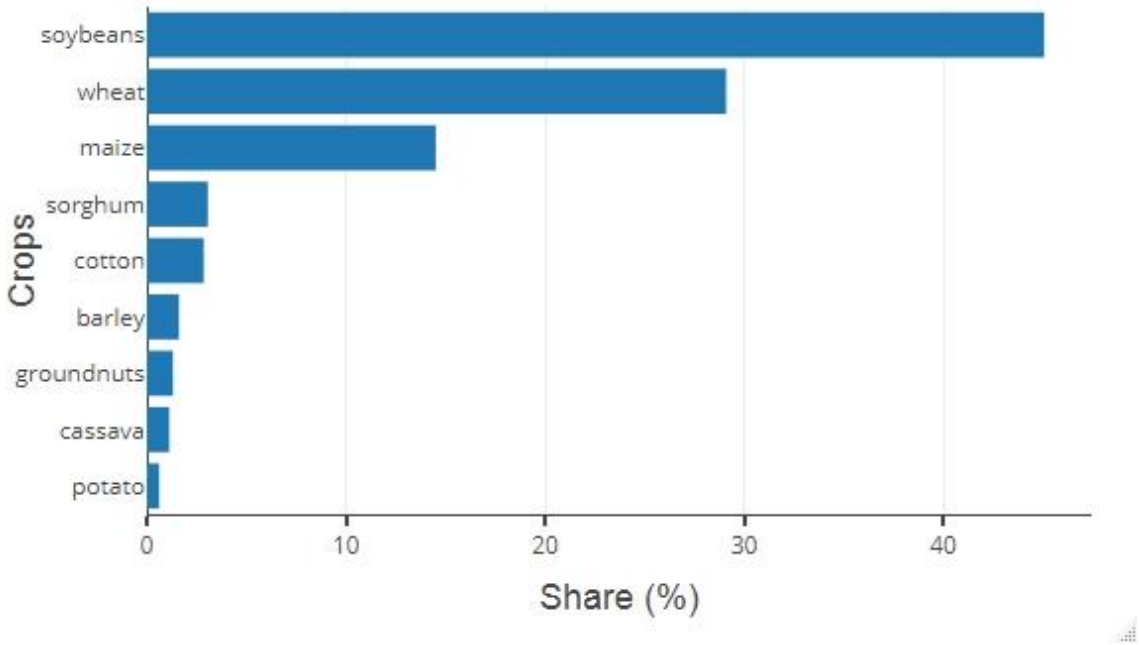

Figure 164. Share of major crops in the Southern Cone region.

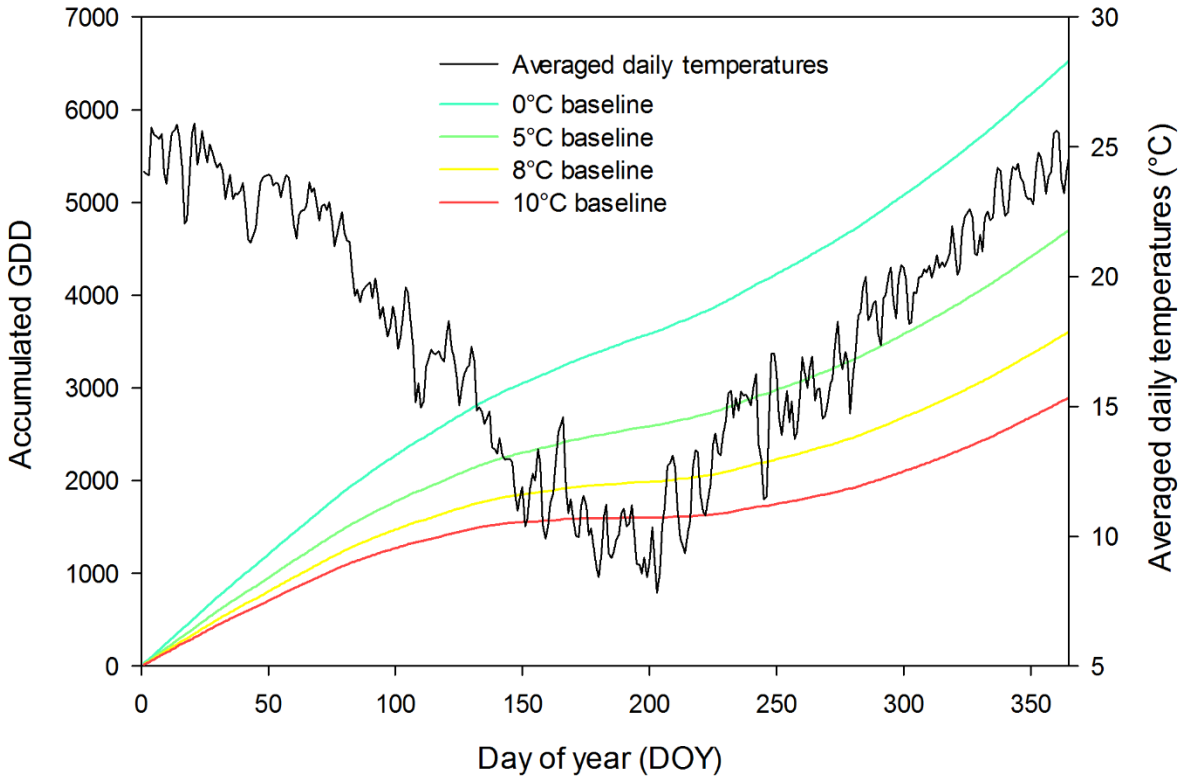

Figure 165. Average daily temperatures and resulting annual GDD accumulation calculated for four baselines in the Southern Cone region.

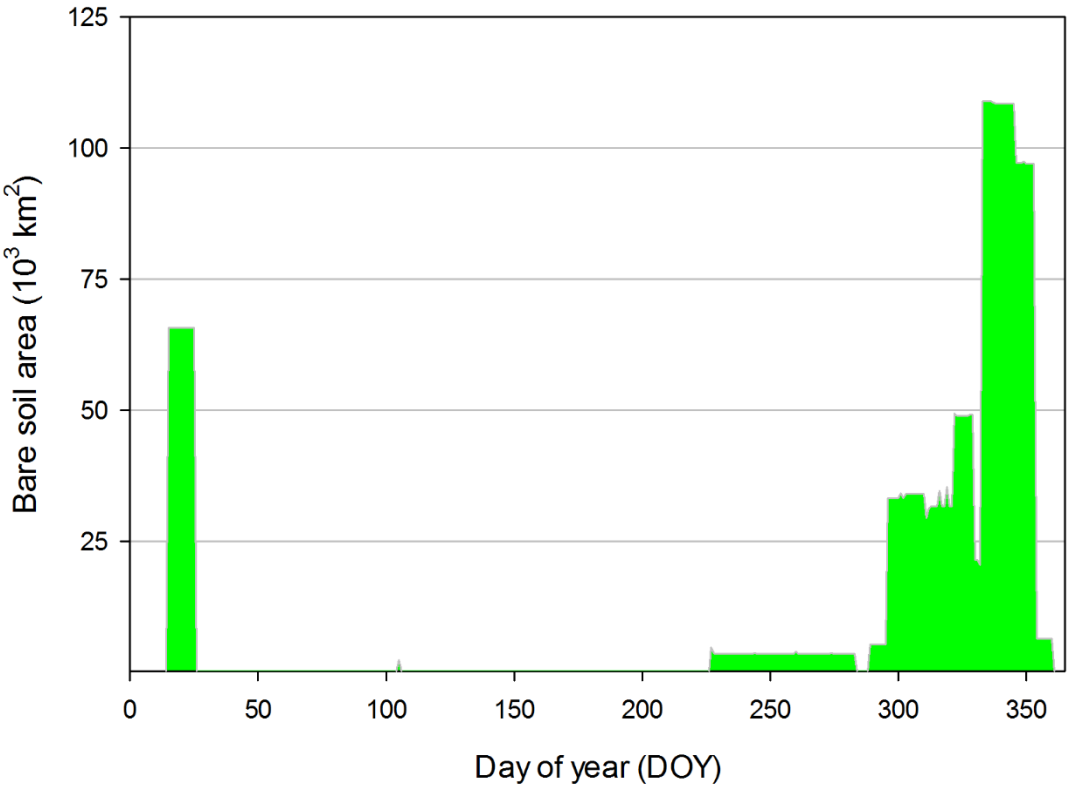

Figure 166. Annual variation of bare soil area in the Southern Cone region.

3.8. Oceania

As a region that is comprised of numerous islands and whose defining feature is an ocean, Oceania has by far the smallest land area of all super regions. The majority of that land area belongs to Australia, with only New Zealand included as well in the analysis. The climate in the northern part of Australia is very hot and dry; however, almost 50% of the country is used for the grazing of cattle. Just over 13% of agricultural land in Australia is arable due to the scarcity of fertile soils and a favorable climate. That arable land is located primarily in southeastern and southwestern parts of the continent, separated by a desert occupying central parts. In New Zealand, the arable land is located along the whole of the eastern coast of both islands. The super region was therefore subdivided into three regions (Figure 167):

- Eastern Australia (OCae)—encompassing the land to the east of the Great Desert; arable land forms a crescent along the southeastern parts of the continent, with its northern parts having much sparser agriculture than southern ones;
- Western Australia (OCaw)—similar to the eastern region, the arable land is situated in the continent's corner. The region is separated from the previous one by an immense desert;
- New Zealand (OCnz)—in both of the major islands of New Zealand, the arable land lies in a thin line predominantly on the eastern side.

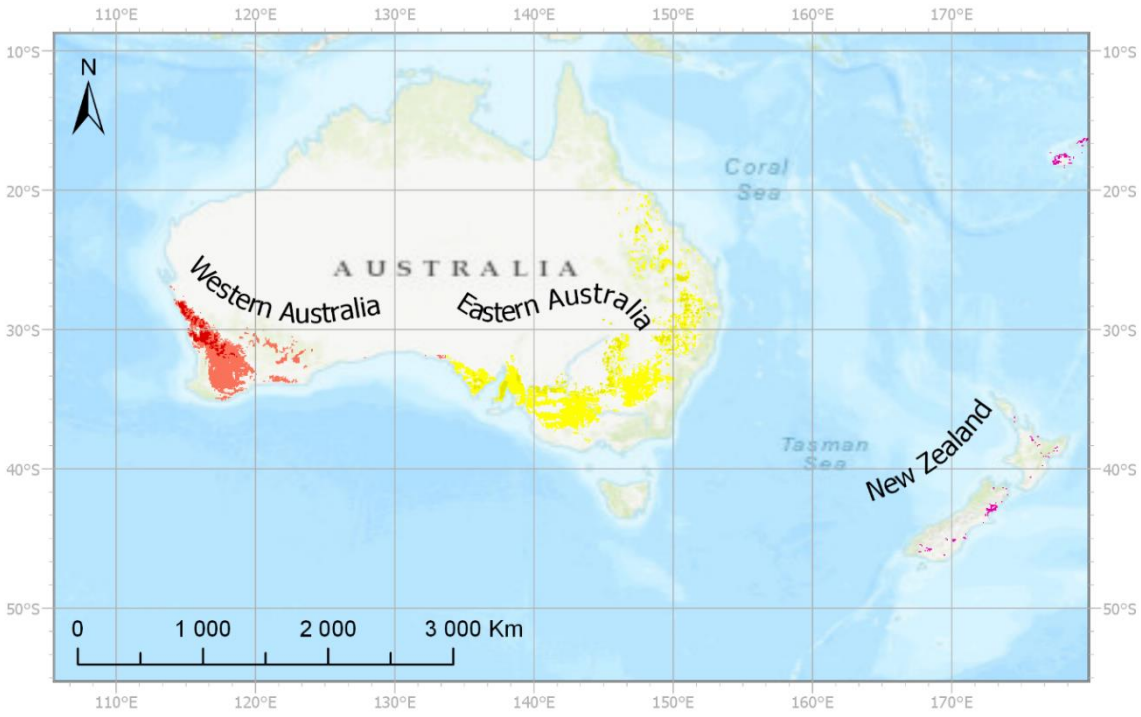

Figure 167. Arable land in the Oceania super region divided into regions.

Over three-quarters of the land analyzed was used for the cultivation of wheat, and together with barley, they exceeded 90% of the area (Table 12). Just over 5% of arable land was dedicated to growing rapeseed, and no other crop had a share over 1% in the whole of Oceania, resulting in a very homogenous region in terms of cultivated crops. Consequently, the annual variation of bare soil was dominated by the planting and growing periods of wheat (Figure 168). During the maximum period, which was found between the 150th and the 170th DOY, just over 25,000 km^2 of soil was exposed. An area of around 5,000 km^2 was bare for almost two months between the 320th and the 10th day of the following year.

Table 12. Area and share of arable land of major crops farmed in Oceania.

Major Crop	Area (thousands km^2)	(%)
Wheat	139.5	77.5
Barley	29.5	16.4
Rapeseed	10.3	5.7
Rye	0.3	0.2
Maize	0.2	0.1
Potato	0.2	0.1
Cassava	0.1	0.1

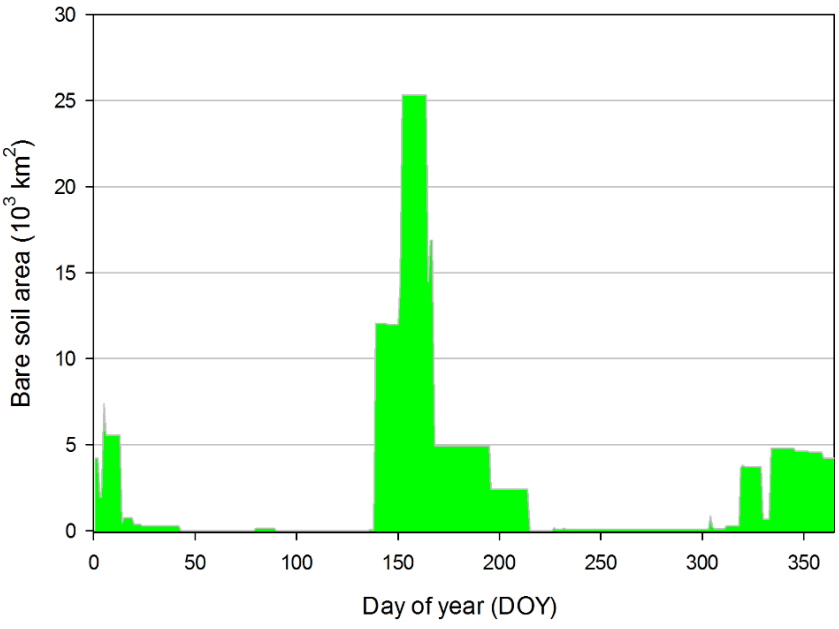

Figure 168. Annual variation of bare soil area in the Oceania super region.

3.8.1. Eastern Australia

Two-thirds of Australian arable land is located in this region, forming a continuous arc between the Eyre Peninsula to the west and the Great Dividing Range to the northeast, with the biggest concentration located in plains to the west of Canberra. The arid conditions of the desert found further inland limit the expansion of arable land in those directions, limiting those areas of agricultural activity to grazing. Its proximity to the Tropic of Capricorn, and resulting high temperatures and dry conditions, also hampers agricultural activity, with scarcely any arable land located north of the tropic (Figure 169).

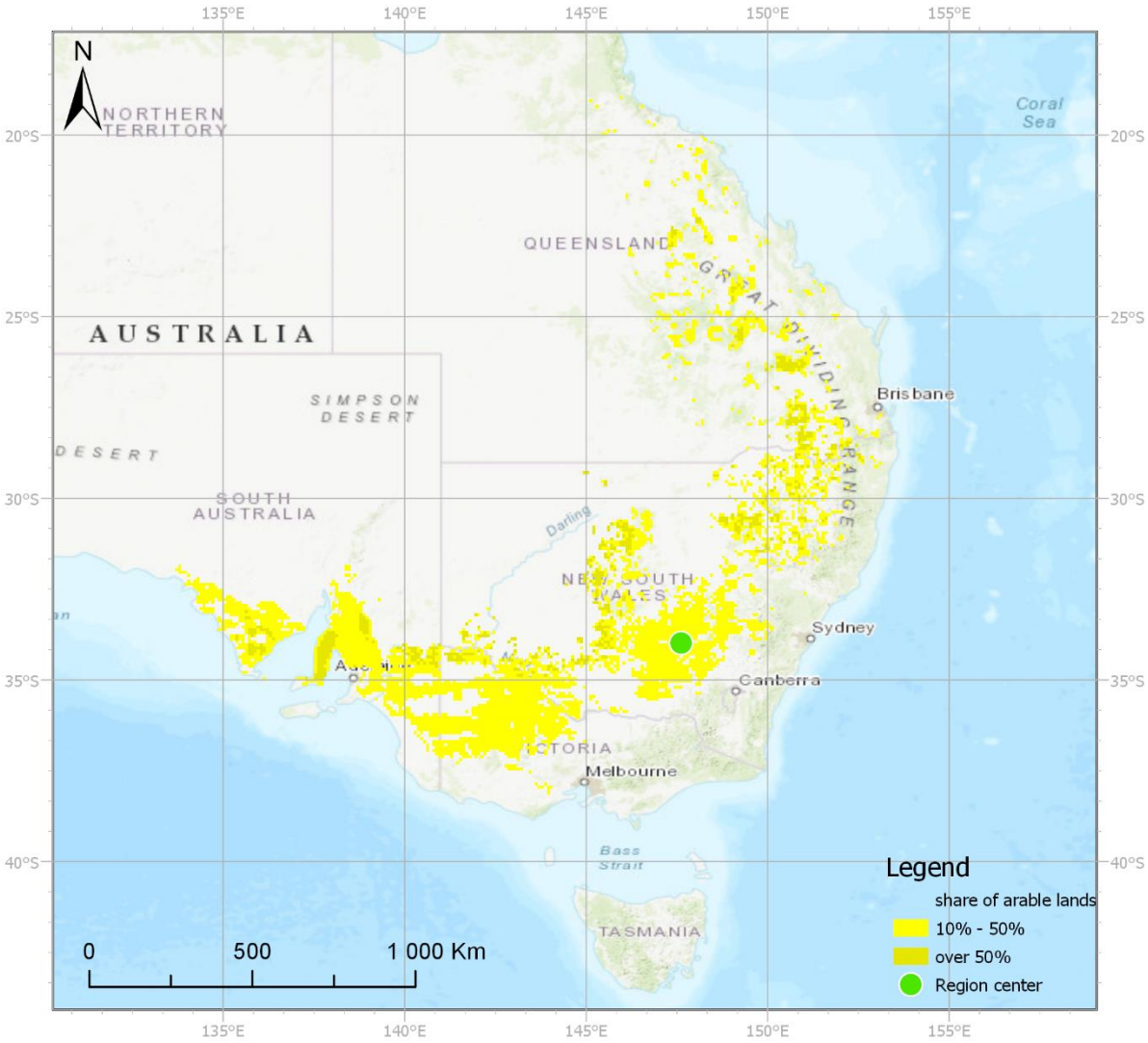

Figure 169. Distribution of arable land in the Eastern Australia region.

Over one-third of arable land is situated on *Luvisols*, making this soil grouping a dominating one in the region (Figure 170). About half of that area belongs to *Vertisols*, while *Xerosols, Planosols,* and *Solonetz* each have a share of between 10% and 12%. Among the

major crops analyzed, agriculture in Eastern Australia is dominated by the cultivation of wheat, with about two-thirds of arable land being dedicated to that crop (Figure 171). Barley represented a share of almost a fourth of arable land, while about 8% was dedicated to rapeseed. Sorghum was found to be the last notable major crop, having a share of over 5%. The mean daily temperatures were obtained from a point located at 34° south and 147° east, some 300 km to the west of Sydney. With the region situated in the southern hemisphere, the hottest period occurs between January and February, with average daily temperatures reaching 28°C and falling to around 8°C in June and July. With mean daily temperatures never dropping below zero, the accumulation of GDD occurred throughout the whole year (Figure 172). Two main peaks of bare soil area were observed in this region (Figure 173), the main one being over twice the size of the other one. The main peak occurred between the 140th and the 170th DOY, resulting from planting followed by the rapid development of wheat, after which the peak declined until the bare soil disappeared around the 215th DOY. It showed again, starting around 320th DOY, as a consequence of the planting of barley and shortly afterward of rapeseed; that period of bare soil lasted until around the 15th day of the following year. During the main peak, up to 15,000 km^2 lay bare, with almost 30,000 km^2 during the secondary peak.

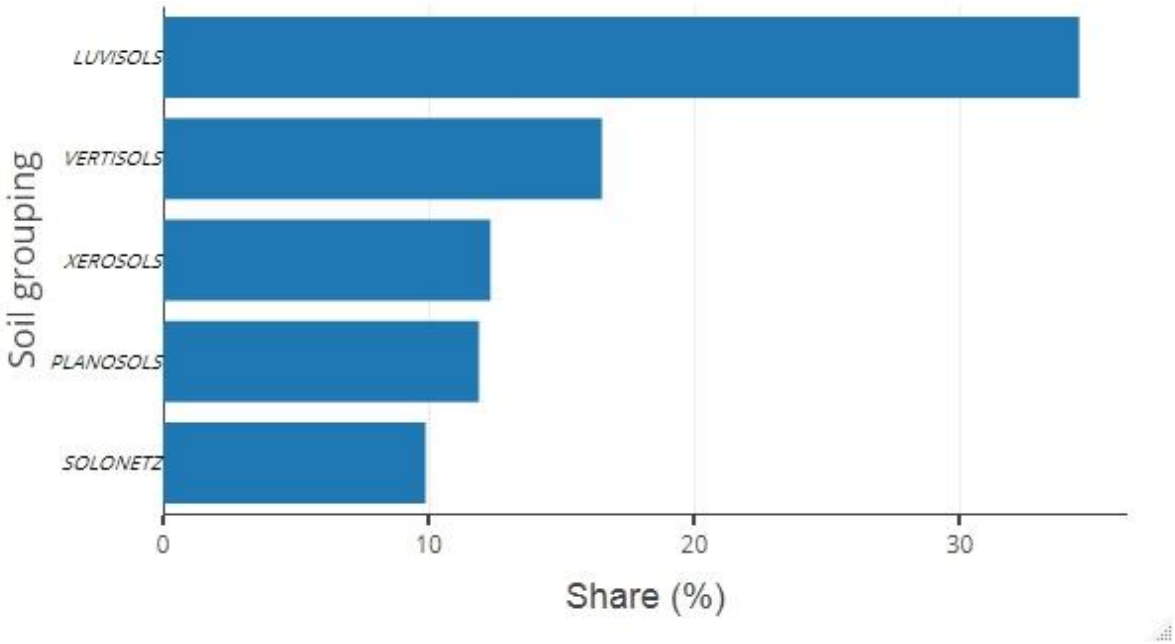

Figure 170. Share of major soil groupings in the Eastern Australia region.

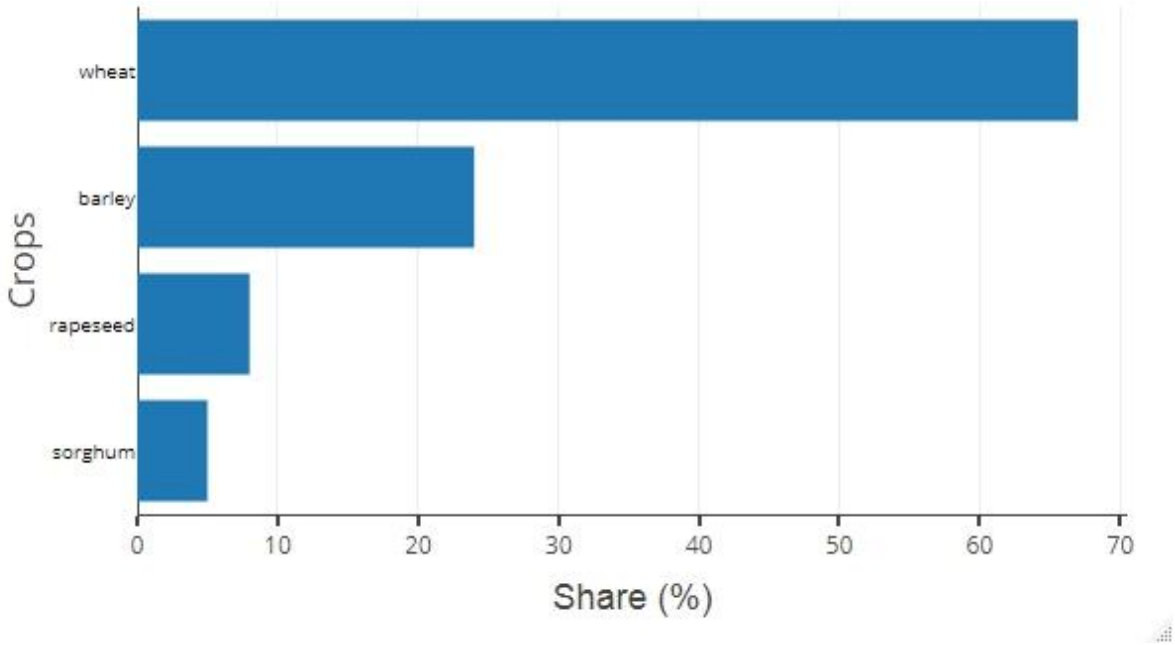

Figure 171. Share of major crops in the Eastern Australia region.

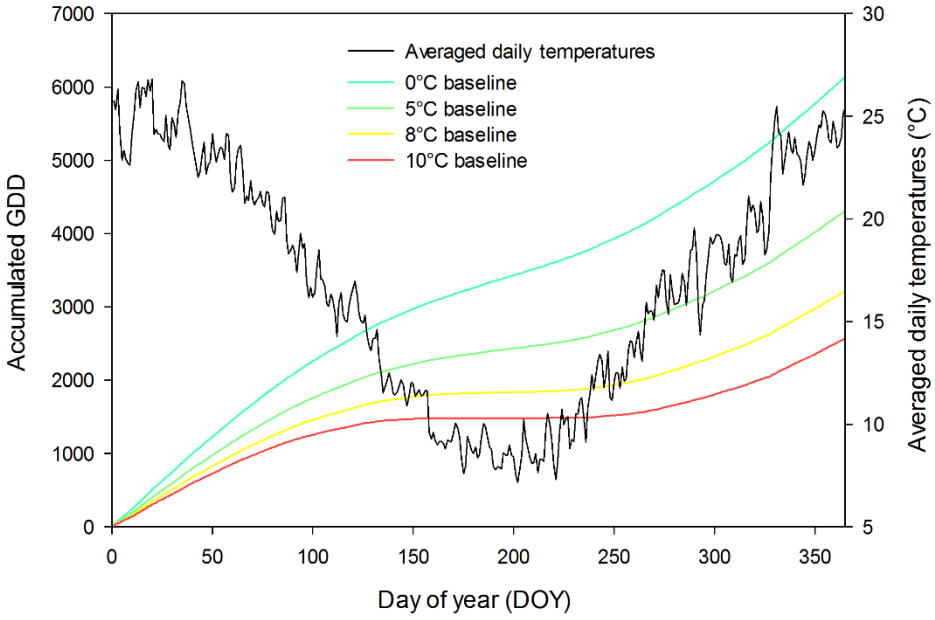

Figure 172. Average daily temperatures and resulting annual GDD accumulation calculated for four baselines in the Eastern Australia region.

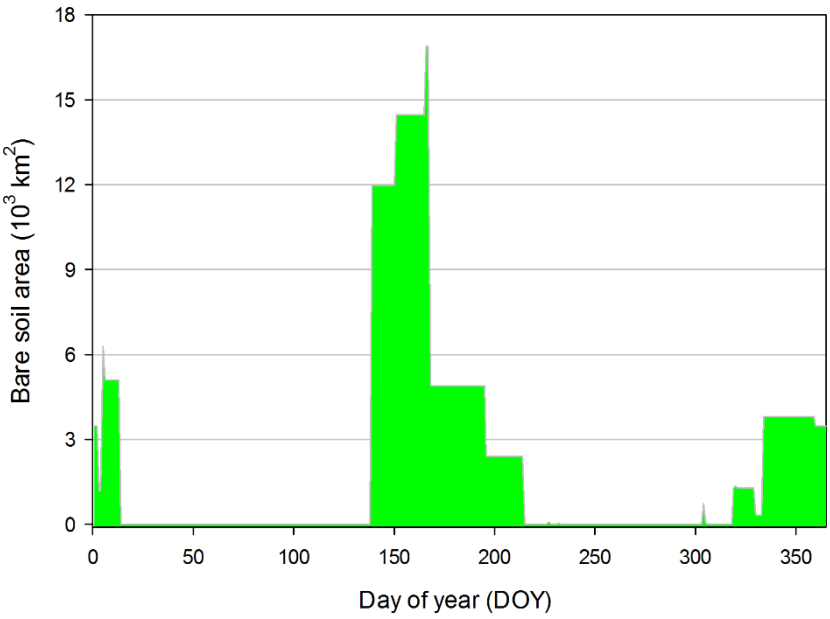

Figure 173. Annual variation of bare soil area in the Eastern Australia region.

3.8.2. Western Australia

In this region, the remaining third of Australia's arable land is located, separated from its eastern counterpart by the Outback deserts. Similar to the eastern region, the bulk of arable land is located in the southern part of the continent, where the climate can support the growing of crops. The largest concentration of arable land was found in the southwestern corner of the region, along the length of the Darling Scarp, around the Perth area. A portion of arable land can be found along the southern coast, centered around the city of Esperance, and more arable land is found further north, around Lake Cowan (Figure 174). Compared to the eastern region, the climate here is on average warmer and drier, which helps explain less extensive areas used for farming.

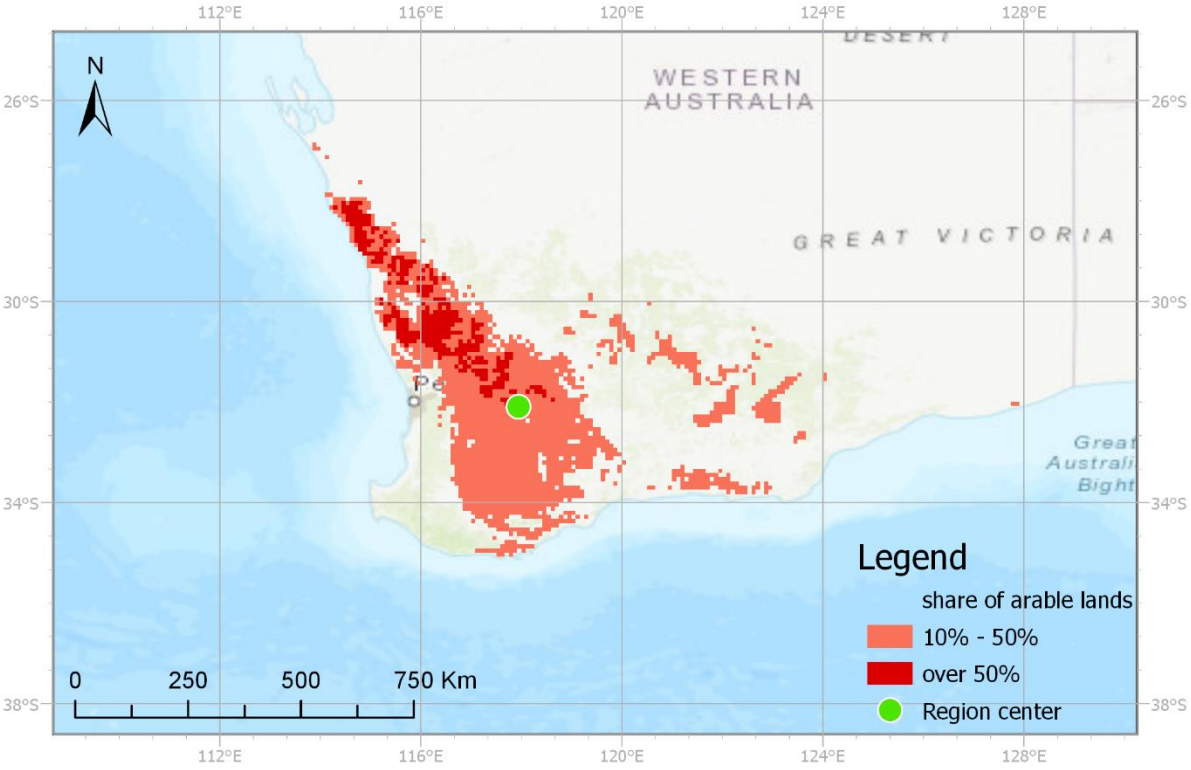

Figure 174. Distribution of arable land in the Western Australia region.

Western Australia is a unique region where *Planosols* are the dominant soil grouping, with almost half of all arable land situated on that grouping (Figure 175). *Solonetz* and *Yermosols* are a pair of soil groupings where each has a share of around 15% of arable land, followed by *Luvisols* and *Arenosols* that each occupy close to one-tenth of arable land. Agricultural production in Eastern Australia is dominated by the cultivation of wheat, with over three-quarters of arable land being used for the growing of that crop (Figure 176). Barley

represented a share of almost a fifth of arable land, while about 5% was dedicated to rapeseed. The maximal mean daily temperatures, obtained from a point located at 32° south and 118° east, were observed between January and February, reaching 26°C, similar to the eastern region. However, even during winter, those temperatures never fell below 15°C, noticeably warmer than in the eastern region. Such relatively stable daily temperatures throughout the year result in a very smooth accumulation of GDD (Figure 177). Arable land in Western Australia was found to be bare only briefly; the biggest area was exposed in the winter, following the planting of wheat around the 150th DOY and lasting for about two weeks (Figure 178). The rapid accumulation of GDD, even during winter months, results in the rapid development of crops and consequently to covering fields with vegetation. During that peak, the area of bare soil exceeded 11,000 km^2. The secondary peak was found between the 315th and the 330th DOY, reaching just short of 3,000 km^2, followed by a longer period of bare soil that lasted until around the 10th day of the following year.

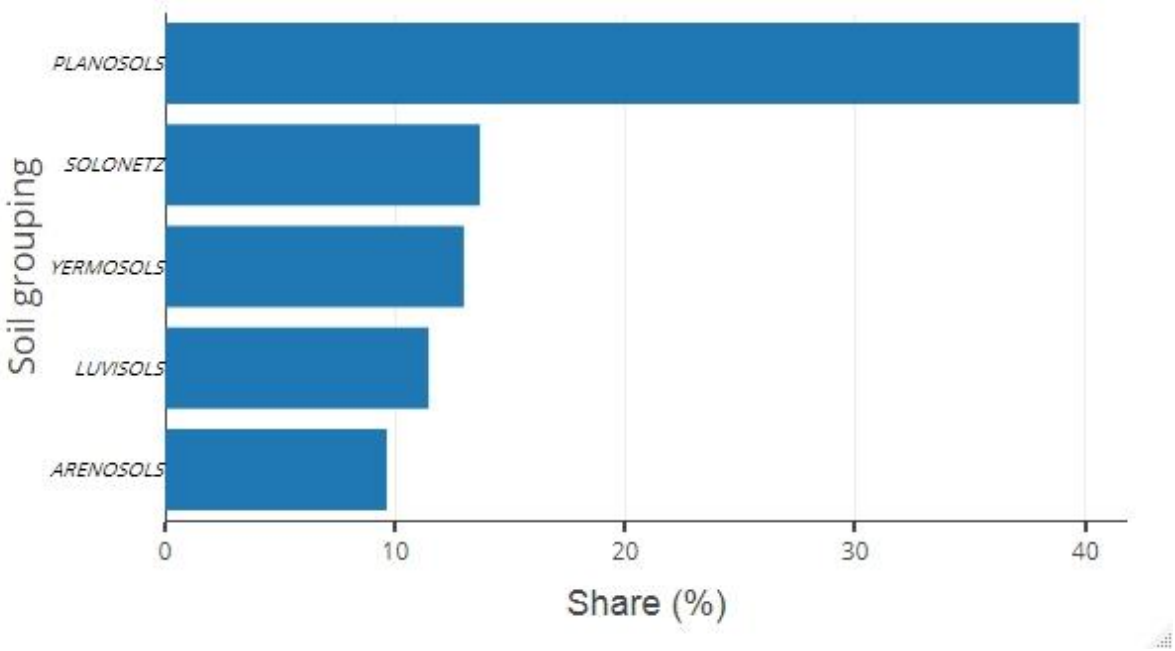

Figure 175. Share of major soil groupings in the Western Australia region.

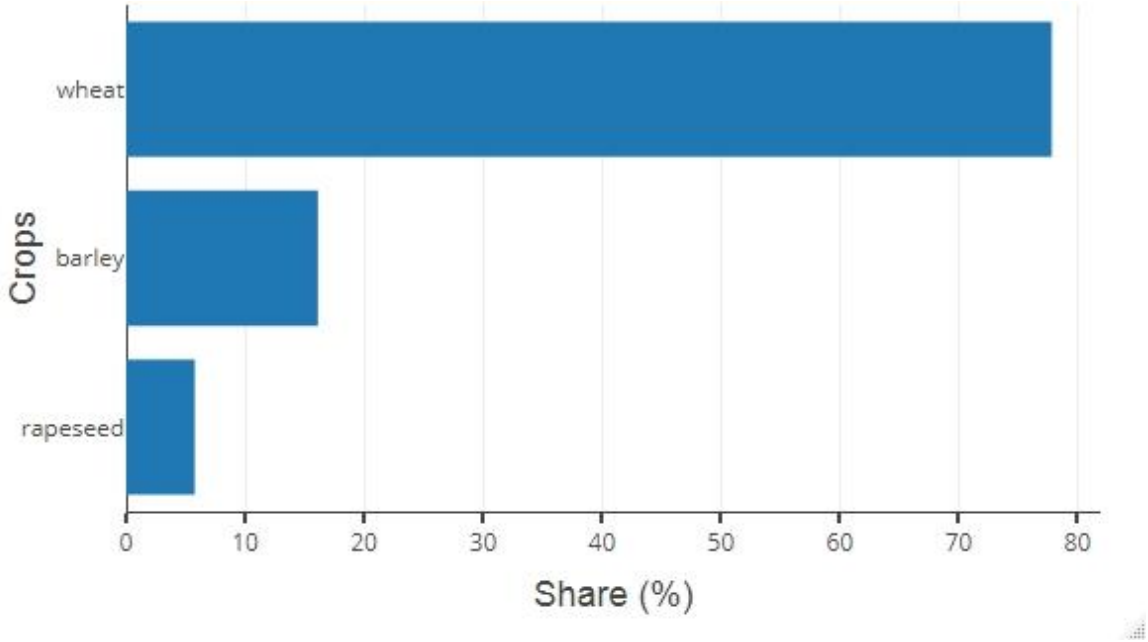

Figure 176. Share of major crops in the Western Australia region.

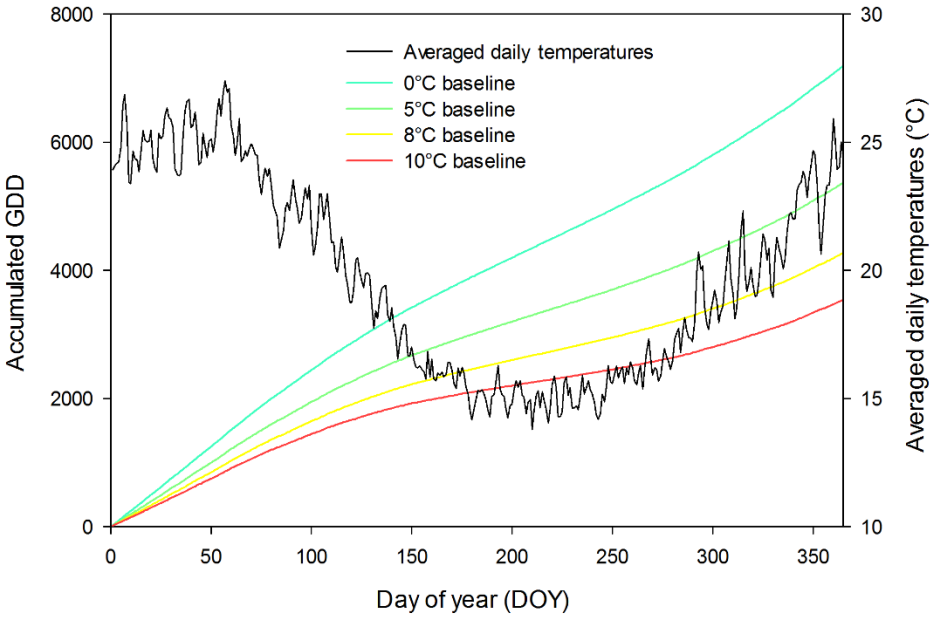

Figure 177. Average daily temperatures and resulting annual GDD accumulation calculated for four baselines in the Western Australia region.

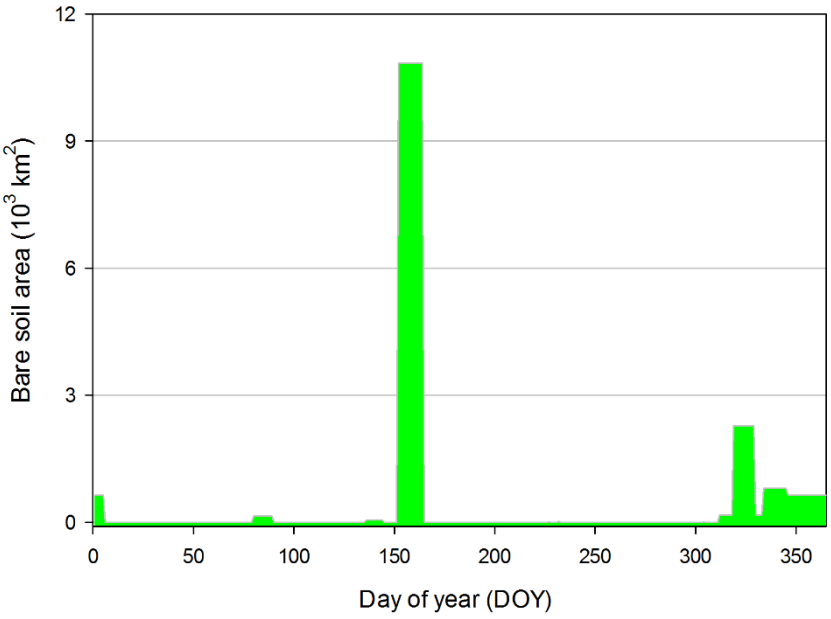

Figure 178. Annual variation of bare soil area in the Western Australia region.

3.8.3. New Zealand

New Zealand has the smallest land area of all the distinguished regions, and consequently, its area of arable land is also the lowest. Between the two main islands, most of the arable land is located on the southern one, while on the northern one only small pockets of agriculture were found spread out. On the southern island, agriculture was generally located around the eastern coast and the biggest pocket of arable land in the river valleys north of Christchurch. The western coasts of the country are mountainous and therefore limiting to large-scale agriculture (Figure 179).

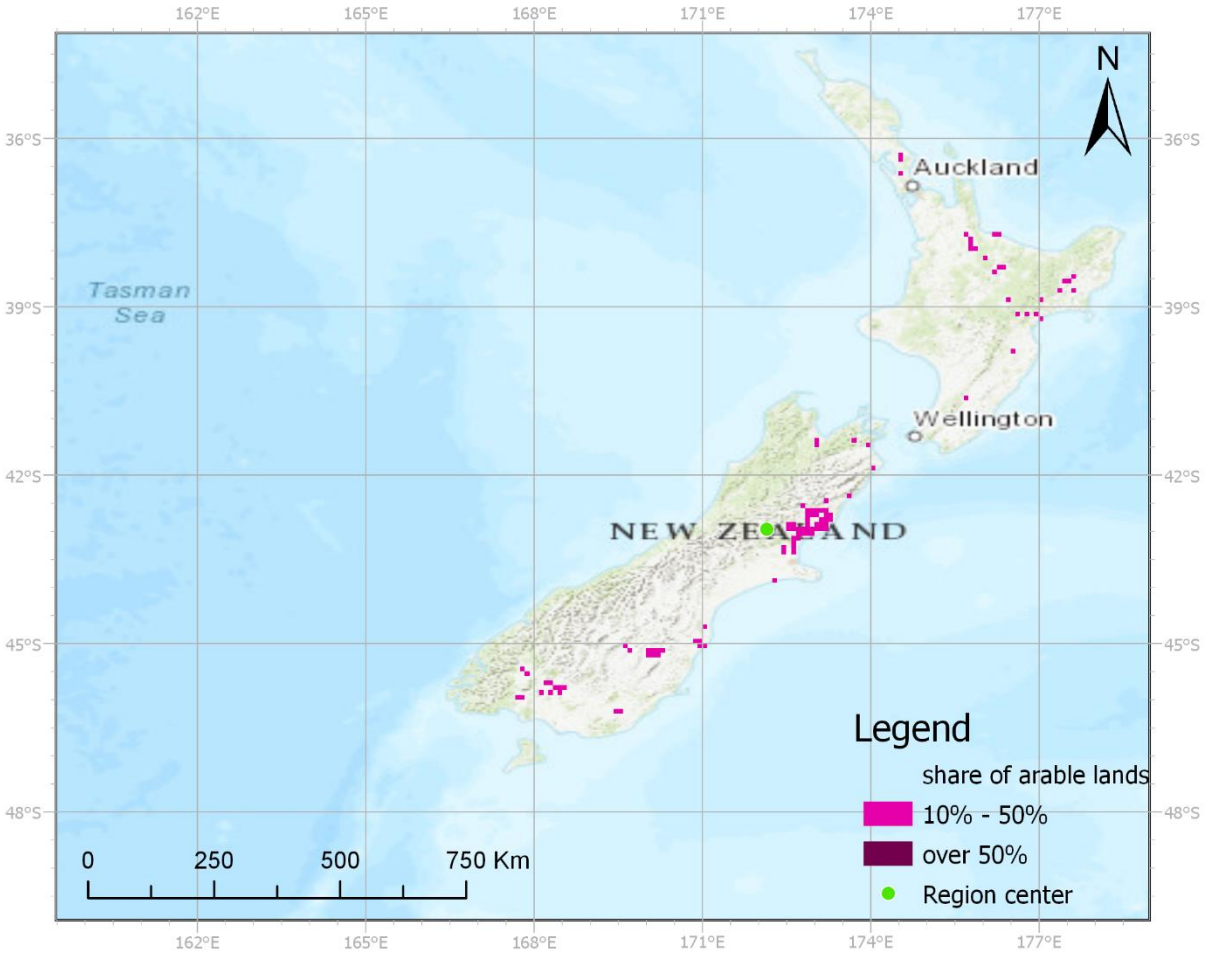

Figure 179. Distribution of arable land in New Zealand.

Despite a relatively low area of arable land, its composition of soil groupings is quite varied (Figure 180). Most expansive are *Cambisols*, which are found on almost half of the region's arable land. *Andosols* and *Acrisols* have a similar share of about 20% each. *Luvisols* close the list of major soil groupings with a share of a tenth of arable land. The two main agricultural products of New Zealand are cereals, barley and wheat, having a share of about

45% and 33%, respectively (Figure 181). Among the rest of the major crops analyzed, maize was farmed on over 10% of arable land, followed by about an 8% share of potatoes. The average daily temperatures were obtained from a point located at 43° south and 173° east, close to a pocket of arable land near Christchurch. The annual amplitude of those temperatures was low, as they ranged between 20°C in summer and 10°C in winter, never dropping below zero and facilitating plant cultivation. The annual accumulation of GDD (Figure 182) was therefore smooth; however, with a visible slowdown during winter. Planting of barley that occurred around the 5th DOY started a period of bare soil that lasted for around a month and a half, reaching over 800 km^2 at its maximum point (Figure 183). The planting of potatoes around the 230th DOY is responsible for starting another period of bare soil, which peaks between the 320th and the 345th DOY, amplified by the planting of maize and later of barley.

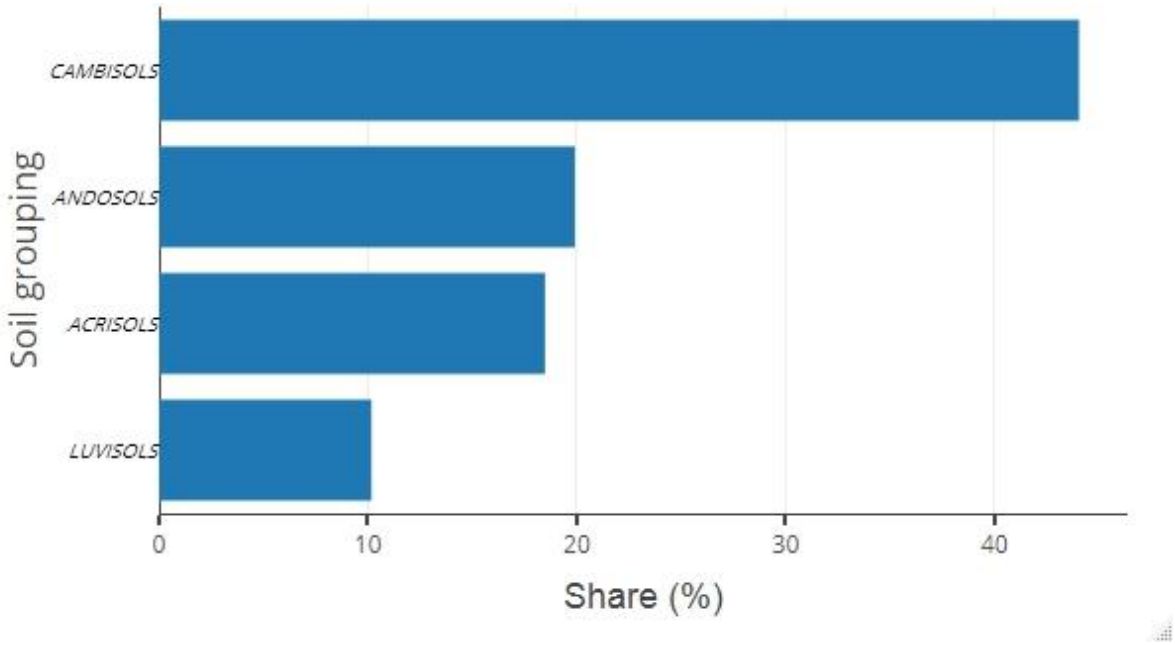

Figure 180. Share of major soil groupings in New Zealand.

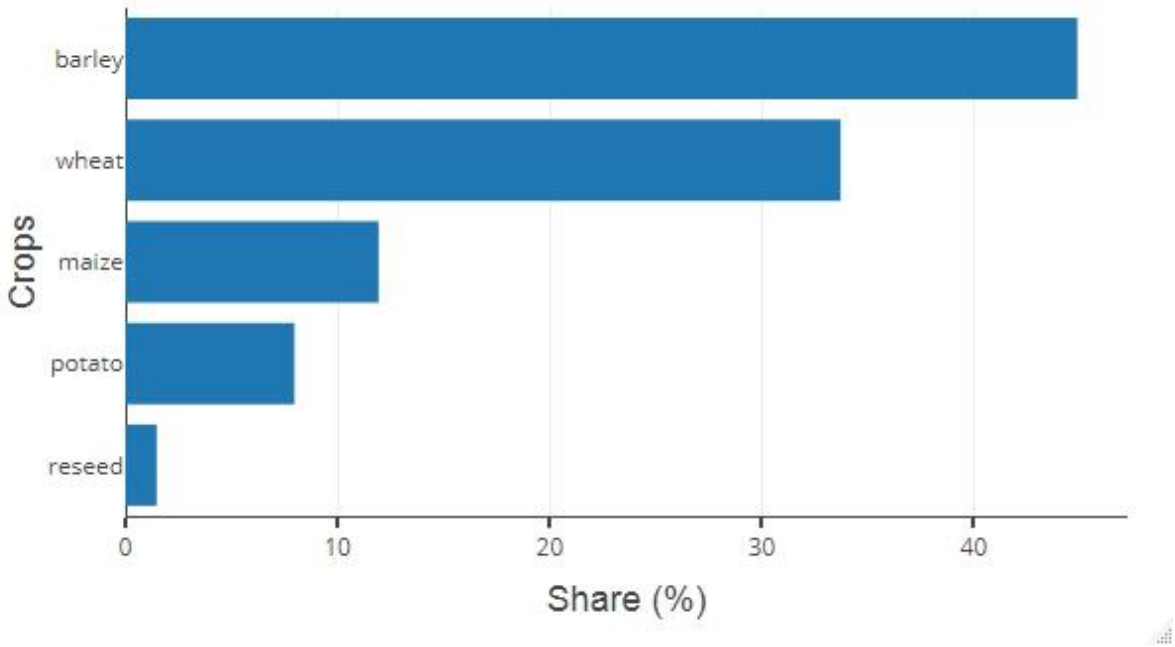

Figure 181. Share of major crops in New Zealand.

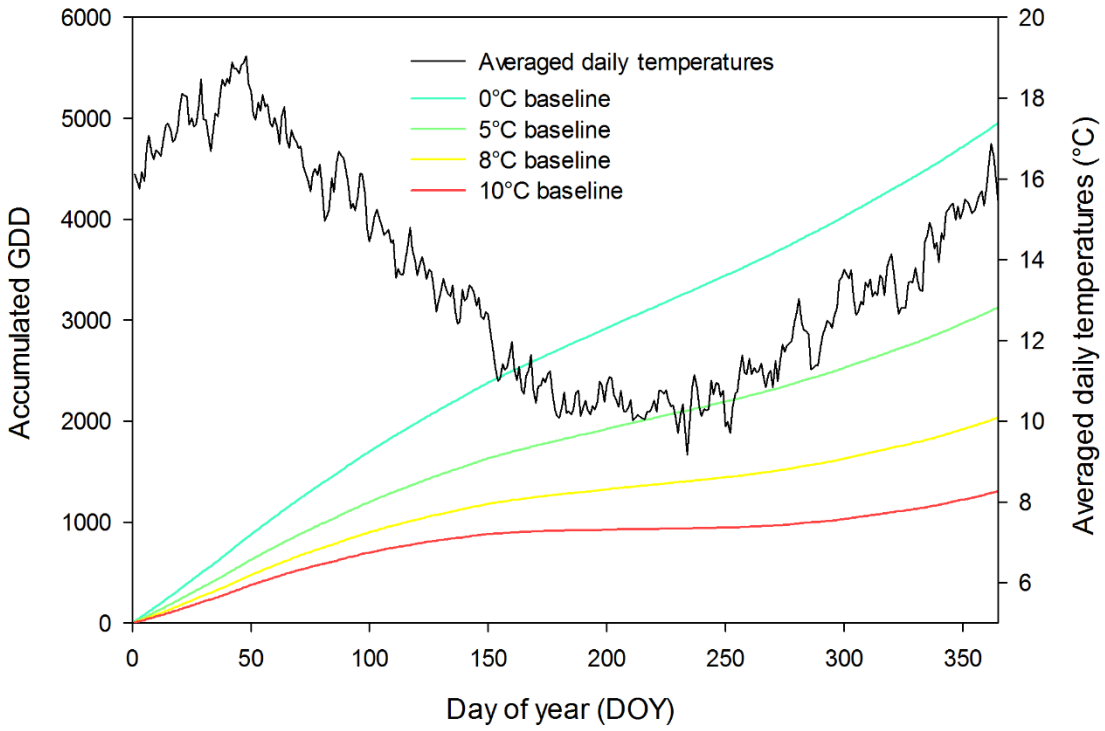

Figure 182. Average daily temperatures and resulting annual GDD accumulation calculated for four baselines in New Zealand.

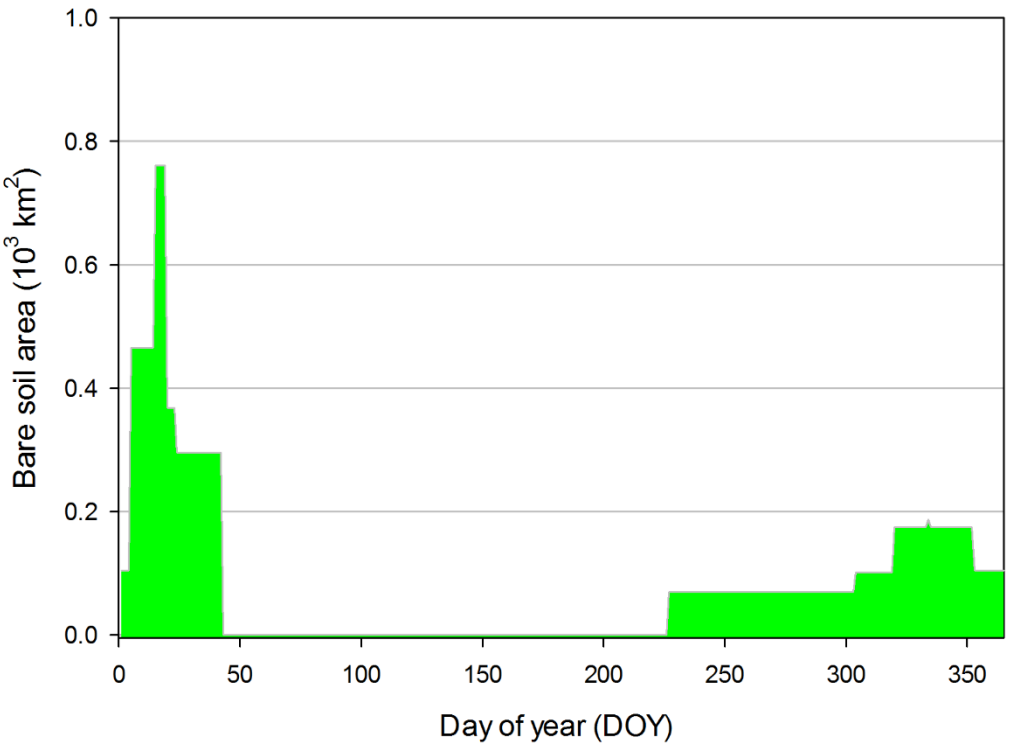

Figure 183. Annual variation of bare soil area in New Zealand.

4. Discussion

The main objective of this thesis was an estimation of the amount and major soil grouping of bare soil resulting from the planting of a choice of 13 major crops worldwide. This goal was achieved using publicly available data. By combining information from crop planting calendars and harvested areas of major crops, their growth, as predicted by GDD periods of bare soil, was estimated. To the best of the author's knowledge, no similar, independent estimations have been conducted, making validation of results difficult.

4.1. Choice of methods

The task of finding periods of bare soil could be achieved by various means, primarily through the classification of satellite imagery, the collection of information provided by the growers, or by statistical means. The remote sensing approach has been used in the author's previous works to establish the course of bare soil in Poland (Cierniewski, Krolewicz, *et al.*, 2015b) and Israel (Cierniewski, Ceglarek, Karnieli, *et al.*, 2018c). Images from Landsat 7 and 8 were used in those two previous works. The bare soil was identified using a function that compared the spectral response of consecutive spectral bands of those images. Each Landsat 7 and 8 scene has dimensions of approximately 170 km by 183 km, both having a spatial resolution of 30 m in spectral bands relevant for the task (the thermal band has a resolution of 100 m). With a revisit time of 16 days, a risk exists that images taken on a cloudy day could spoil the final results by occulting times when significant phenological changes take place. Using scenes from consecutive years increased the probability of catching a cloud-free scene. The methods have proved to be quite successful; however, the sheer number of Landsat scenes that would need to be analyzed to get global coverage to estimate the bare soil area would be tremendous. The number of unique Landsat scenes is somewhere in the ballpark of 16,000. Even limited to locations encompassing arable land, many thousands of unique scenes would remain. In order to get an annual variation of bare soil for those scenes, images from at least three consecutive years should be analyzed, bringing the number of images for each scene to over 60. It suffices to say that analyzing that many scenes would be well beyond the capacities of the author, so other methods had to be used.

Wide-coverage sensors could serve as an alternative to the aforementioned Landsat scenes, by increasing revisit time and compromising spatial resolution. The prime candidates of such sensors that offer publicly available data are vegetation sensors installed previously on SPOT and its successor on board the Proba-V satellite, or the MODIS sensor aboard the Terra and Aqua satellites. All of them offer revisit times of one or two days which greatly diminishes the risk of missing cloud-free periods. Vegetation sensors installed on either SPOT or Proba satellites offer four spectral bands with a spatial resolution of around 1 km and 1/3 km, respectively. MODIS, on the other hand, had as many as 36 spectral bands, with spatial resolution ranging between 250 m to 1 km between them. However, such spatial resolution, while appropriate in the research of global ecosystems, seems to be too coarse to be able to distinguish individual agricultural fields. In the case of the vegetation sensors, a low number of spectral bands would restrict potential spectral indices that could be used mostly for NDVI. Using MODIS images, that restriction does not apply, but the coarse resolution would still lead to many cases of pixel mixing. The estimation of the day when the soil stops being bare after planting would be difficult at that scale, while the number of images required to be analyzed would still be in the many thousands, and beyond the capability of the author to analyze.

The approach based on statistical data used in this work was used for the first time in a work concerned with the course of bare soil in Europe, divided into three regions (Cierniewski, Ceglarek, Kaźmierowski, *et al.*, 2018c). The obtained bare soil variation in the Polish region was comparable to the one previously estimated for the corresponding area of Poland using remote sensing methodology. In that sense, it gave some confidence regarding the methodology used in this work.

4.2. The utility of the results

The work described in this thesis was part of a project concerned with estimating the global annual variation of shortwave radiation reflected from dried bare soil in accordance with various assumptions concerning farming methods. The amount of shortwave radiation reflected from the surface is called albedo and is influenced by its properties, including its roughness and moisture content that are dynamic, as well as static ones like carbonate, iron, and soil organic matter contents. The results described in this thesis help achieve this objective twofold: firstly, by identifying periods of bare soil after the planting of major crops;

and secondly, by quantifying the acreage of major soil groups that are bare during those periods. As the project was concerned with shortwave radiation affected by agricultural practices, only periods of bare soil were of interest, and so, identifying them was the first step in the procedure. Among the factors that influence soil albedo, the influence of static factors can be indirectly obtained from their spectral reflectance. Knowledge of the composition of major soil groupings that constitute arable land for any region was used to obtain diffuse reflectance spectra for those soils found in any region, from publicly accessible databases. That spectral information was then used to estimate the base level of albedo for each soil grouping within a given region, which was afterward modified by values of dynamic properties that were assumed, based on previous studies. The results, showing the global annual variation of shortwave radiation from bare soil were described in an article by Cierniewski and Ceglarek (2018d).

4.3. Uncertainty of the results

The results obtained in this work are subject to the uncertainty that comes from various directions. The global aspect of the work was tackled by dividing the arable land into regions, which meant that any variance found inside such regions was lost. The work was performed using data that were easy to access, and which spanned a period of 30 years. The oldest sets are concerned with the geographic distribution of crops in the year 2000 as well as the distribution of arable land, also in the year 2000. The dataset describing global patterns in crop planting days used 30-year average climate data, in order to show planting dates for the year 2010. The average daily temperatures, used to calculate annual GDD accumulation, were obtained by averaging climate data from the year 1990 to 2000. The most recent dataset describes areas under conservation tillage for the year 2013. Except for climate data, which was arbitrarily selected concerning the period closest to the dataset of crop planting dates, all the datasets were the most recent ones in their respective subject. However, the assumption was that agriculture, especially concerning regions of such a big size as the selected regions, does not change rapidly.

The length of time that soil stayed bare after planting was estimated by calculating GDD accumulation, based on average daily temperatures from the 10-year period. That means that annual values of GDD don’t relate to any particular year, but rather show the dominating trend from multiple years. Those average temperatures were related to agricultural centers

of regions. As a consequence of analyses being conducted for regions, all areas of any crop that share planting dates had the same periods of bare soil within a given region, omitting inter-region variance.

As was previously mentioned in the methods section, soil area was considered to be bare if plants covered less than 15% of its surface. However, the GDD breakpoints for particular plant stages were taken from literature, and in most cases, the values were not precise but were a range of GDD values. Therefore, the exact moment when soil stops being bare cannot be estimated, it should be thought of as an approximation.

The work does not take into account all of the arable land in the world but is focused on 13 major crops, which together constitute the crops of about 70% of all arable land (Leff, Ramankutty and Foley, 2004). The omission of rice in the analysis may be surprising; however, rice is commonly cultivated on flooded fields which do not count as bare soil. Pulses as a group have a share of around 4% of arable area, split between many species, this split being the reason why they were not included, as not one of them would count as a major crop if taken alone.

Summarizing all of the sources of uncertainty, the periods of bare soil should be treated as rough estimations. The most useful part of the results are peaks that show periods throughout the year when maxima of bare soil appear, and which major soil groups are exposed at those times. Taking all of those factors into account, the estimates obtained in this work are on the cautious side, and in reality the area of bare soil for any day of the year is likely higher than the results presented above.

4.4. Future improvements

The research described in this thesis can be improved concerning a couple of points. Keeping in mind the sources of uncertainty listed in the previous paragraph, each of them could be a subject for improvement.

For starters, the global land was divided into 33 regions, which served as basic units for all of the subsequent calculations. With the assumption that temperatures and GDD accumulation were uniform inside any given region, any variability within was lost. The regions were delimited in such a way as to capture huge agricultural regions, but arable land is not clustered everywhere. The generalized bare soil courses obtained for each region are therefore approximations, where more localized variability is lost. In order to improve the

representation of spatial variability within regions, a change in the method of analyses of remote sensing imaginary seems like the best option. The reasoning behind the method selection is described in the previous paragraph. The other option would be to stick with the current method while delimiting a higher number of regions. That option is something worth considering in the future, as the number of regions was selected arbitrarily, based on divisions proposed by USDA in 1994 and modified by the author.

Another area of possible improvement is the number of individual crop types analyzed. In this work, 13 major crops with the exception of rice were analyzed, covering over two-thirds of all arable land. This, however, would be hard as there are not many works that map the global geographic distribution of crops besides the ones analyzed in this research. Apart from major crops that were already taken into account, most other individual crop species have a relatively low share of arable land, which would greatly multiply the number of analyses needed to be performed, if the required data were available in the first place.

The length of time soil stays bare after planting was estimated using the accumulation of the GDD after the day of planting. This is an approximation; firstly, because the day of planting depends on climate conditions and is not uniform between many farmers, even located in the same general area. This part of the uncertainty is propagated from the crop planting days calendar and should be acknowledged. The other part of this problem, besides the exact planting day, is the length of time before the crop develops enough to stop treating the soil as bare. The accumulation of GDD was estimated based on temperatures averaged over a ten-year period, from the central point of agriculture concentration within a region. This means that this accumulation was uniform for the whole region. In order to make that value more localized, a scheme where annual temperature variation and resulting GDD accumulation is calculated for each pixel would be necessary. This could result in forgoing the approach of working with the regions altogether, or more detailed bare soil variations within those regions. However, the complexity of this approach is the reason it was not attempted on a global scale.

The key aspect of this work was the assessment of soil groups that stay bare in order to estimate their albedo, and in consequence, the amount of radiation that could be reflected from that bare surface. The value of albedo can be modified by various factors, however many of them depend on the soil's parameters. In this work, the major soil groupings classified in accordance with the FAO–UNESCO system were used. That level of generalization of soil

groupings seems appropriate when analyzing radiative forcing on a global scale. In order to have more accurate predictions in the future, more detailed soil maps could be used; for example, regional maps classified in regional systems.

In order to have more complete annual variations of bare soil, periods when soil stayed exposed after harvesting should also be included. This, however, was not possible to estimate following the methods outlined in this project, as there is no equivalent to GDD that would predict for how long soil stays bare after harvest. The common practice in agriculture is to leave some of the crop to reside as soil cover after harvest, and this procedure can leave varying degrees of the soil surface covered. In order to include those periods in the work, remote sensing methods on a regional scale would need to be introduced.

The total amount of bare soil was reduced by the acreage that was cultivated using conservation agriculture (CA) methods, which tend to not leave the soil bare at any point in time. This was accounted for by reducing the area of bare soil by the share that such fields have in the total arable land in a given region. The acreage of CA in various regions was found in the literature. Those figures reported just a total area of CA within countries, without any detailed spatial information on where those fields were located. As a result, the reduction of bare soil area due to CA was uniformly proportional for all soil groupings present, as there was no real way to infer which parts of the region were under a CA regime. To the best of the author's knowledge, no global map of CA distribution exists yet, so an option to improve that situation would be to use satellite imagery.

5. Conclusions

The focus and the main goal of this thesis were to estimate the annual variation of bare soil area after planting around the globe, together with the proportion of soil groupings left uncovered by vegetation during those periods.

The estimated variation of global bare soil area shows considerable fluctuation throughout the year. In the northern hemisphere, the maxima of bare soil occur around the 140th day of the year (which sits in the middle of an extended period of bare soil, lasting between the 92nd and the 200th DOY (beginning of April until end of July)). During that period, the acreage of bare soil reaches up to 1.5 million km2, while on the 92nd and the 200th DOY it reached 900,000 km^2 and 700,000 km^2, respectively. Apart from that episode, the bare soil area also appears in late autumn and winter, starting around the 315th and lasting until the 20th day of the following year, ranging in that time between 100,000 and 200,000 km^2. In comparison, in the southern hemisphere, the maximal area of bare soil is almost four times smaller than in the northern one, reaching about 400,000 km^2 during a period lasting for about a month and starting around the 330th DOY (middle of November). Another span of bare soil was observed between the 15th and the 25th DOY (second half of January), and is just shy of 100,000 km^2.

Divided into super regions, it becomes apparent that Asia dwarfs other super regions in terms of arable land, which is reflected in its bare soil variation. Around the 140th DOY, almost 700,000 km^2 of soil is bare just in this super region, meaning it contributes short of half of the world's bare soil area at that time; that proportion is even higher around the 95th DOY when roughly 600,000 km^2 of soil lies bare in Asia alone. The maximum is followed by another peak two months later (around the 200th DOY), that reaches almost 400,000 km^2. In Europe, the first noticeable occurrences of bare soil show up starting around the 40th DOY (middle of February) and the acreage rises until around the 140th DOY (middle of May) when it reaches almost 500,000 km^2. After Europe achieves that maximum, the acreage of bare soil sharply declines, to rise again in the period between the 230th and the 290th DOY (middle of August to middle of October). The period when the maximum amount of bare soil occurs in North

America coincides with the maxima in Asia and Europe, occurring around the 140th DOY, like in the aforementioned super regions. That maximum sits close to the beginning of the bare soil period, lasting between the 115th and the 190th DOY (end of April until the beginning of July), during which the acreage first rapidly rises until the 140th DOY and then gradually falls, until it disappears around the 190th DOY. For the African super region, the timing when the maximum is observed is delayed by a month and a half in relation to the three previously described super regions, where it was observed about the 190th DOY. Due in part to the fact that arable land in Africa is located in both northern and southern hemispheres, more distinct periods of bare soil show up. Centered on the maxima is a period lasting between the 167th and the 230th DOY (middle of June to the middle of August), during which the acreage of soils without vegetation reaches almost 400,000 km^2. That period of maximum bare soil is preceded by a smaller one, occurring between the 95th and the 115th DOY (beginning to end of April) that attain over 120,000 km^2, and another stretch of bare soil commences on the 317th DOY, lasting until the 10th day of the following year (middle of November to middle of January), which is characterized by the smooth rise and fall of bare soil acreage, reaching almost 100,000 km^2. The arable land in South America lies predominantly in the southern hemisphere, which is reflected in a corresponding annual bare soil area variation. The maximum is noted around the 330th DOY (end of November) and reaches just shy of 500,000 km^2 and lasts for around two weeks. That maximum is preceded by a period of bare soil starting around the 274th DOY (beginning of October) when the acreage slowly rises to around 100,000 km^2 to then rapidly shoot up after the 330th DOY. After about 20 days, on the 350th DOY the bare soil area rapidly declines and falls to about 20,000 km^2. A shorter period, around two weeks long, of bare soil was also observed between the 14th and the 30th DOY (middle to end of January) which exceeded 100,000 km^2. In the case of the Oceania super region, the time when the maximum was observed was the 156th and the 165th DOY (first half of June) and it slightly exceeded 25,000 km^2. That maximum was observed during a period lasting from the 143rd to the 220th DOY (end of May to the beginning of August). The other significant period was observed lasting between the 322nd and the 15th day of the following year (middle of November to middle of January), oscillating around 5,000 km^2 and at times exceeding 7,000 km^2.

The most common soil groupings used in agriculture around the globe were found to be *Luvisols*, *Cambisols,* and *Lithosols* with a share of 16%, 10% and 10%, respectively, followed

by *Acrisols*, *Gleysols*, *Chernozems* and *Vertisols* that have a share of 9%, 8%, 6% and 6%, correspondingly. In Asia, the most common soil groupings within arable land are *Lithosols*, *Cambisols,* and *Gleysols* with their respective share of 20%, 14%, and 13%. Europe is the unique super region where the dominant arable soil grouping is *Chernozems* (33%) followed by *Cambisols* (15%) and *Luvisols* (14%). In the case of the North American super region, almost exactly a third of arable soil belongs to the *Kastanozems* grouping, followed by 23% of *Luvisols* and 13% of *Chernozems*. In turn, in Africa, half of the arable land is shared by *Luvisols* and *Arenosols* (30% and 21%, respectively) with the third most common grouping being *Vertisols,* having a share of 10%. *Ferrasols* is the most commonly farmed soil grouping in the South American super region, with their share of 29%, followed by *Phaozems* and *Luvisols* having their respective shares of 21% and 13%. In the last super region analyzed, Oceania, the dominating soil grouping was *Luvisols*, found to occupy 31% of arable land, *Planosols* coming second with a share of 24%, followed by *Solonetz* and *Vertisols*, each occupying 13%.

Further research should be focused on developing methods that would allow a more precise estimation of bare soil variation. Methods based on remote sensing of soils are desirable; however, they are inhibited by the global aspect of the study. In the context of analyzing shortwave radiation of bare soil, more detailed soil grouping could provide more accurate results.

References

Aggarwal, S. (2006) 'Principles of Remote Sensing', Satellite Remote Sensing and GIS Applications in Agricultural Meteorology, 151(3), p. 401. doi: 10.2307/633049.

Alexandratos, N. and Bruinsma, J. (2012) 'World AgricultWORLD AGRICULTURE TOWARDS 2030 / 2050 The 2012 Revision', ESA Working Paper, (12-03), p. 154. Available at: http://www.fao.org/docrep/016/ap106e/ap106e.pdf.

Arino, O., Ramos Perez, J. J., Kalogirou, V., Bontemps, S., Defourny, P. and Van Bogaert, E. (2012) 'Global Land Cover Map for 2009 (GlobCover 2009)', European Space Agency (ESA) & Universit catholique de Louvain (UCL). PANGAEA. doi: 10.1594/PANGAEA.787668.

Asfaw, E., Suryabhagavan, K. V. and Argaw, M. (2016) 'Soil salinity modeling and mapping using remote sensing and GIS: The case of Wonji sugar cane irrigation farm, Ethiopia', Journal of the Saudi Society of Agricultural Sciences. King Saud University, 17(3), pp. 250–258. doi: 10.1016/j.jssas.2016.05.003.

Baize, D., Arrouays, D., Jabiol, B. and Quantin, P. (1995) Référentiel pédologique 1995.

Bala, G., Caldeira, K., Wickett, M., Phillips, T. J., Lobell, D. B., Delire, C. and Mirin, A. (2007) 'Combined climate and carbon-cycle effects of large-scale deforestation', Proceedings of the National Academy of Sciences, 104(16), pp. 6550–6555. doi: 10.1073/pnas.0608998104.

Baumgardner, M. F., Silva, L. F., Biehl, L. L. and Stoner, E. R. (1986) 'Reflectance Properties of Soils', Advances in Agronomy, 38, pp. 1–44. doi: 10.1016/S0065-2113(08)60672-0.

Beddow, J. M., Pardey, P. G., Koo, J. and Wood, S. (2010) 'The changing landscape of global agriculture', The Shifting Patterns of Agricultural Production and Productivity Worldwide. T, pp. 8–38.

Betts, R. A. (2000) 'Offset of the potential carbon sink from boreal forestation by decreases in surface albedo', Nature, 408(6809), pp. 187–190. doi: 10.1038/35041545.

Bonan, G. B. (2008) 'Forests and Climate Change: Forcings, Feedbacks, and the Climate Benefits of Forests', Science, 320(June), pp. 1444–1449.

Brovkin, V., Ganopolski, A., Claussen, M., Kubatzki, C. and Petoukhov, V. (1999) 'Modelling climate response to historical land cover change', Global Ecology and Biogeography, 8(6), pp. 509–517. doi: 10.1046/j.1365-2699.1999.00169.x.

Brovkin, V., Claussen, M., Driesschaert, E., Fichefet, T., Kicklighter, D., Loutre, M. F., Matthews, H. D., Ramankutty, N., Schaeffer, M. and Sokolov, A. (2006) 'Biogeophysical effects of historical land cover changes simulated by six Earth system models of intermediate complexity', Climate Dynamics, 26(6), pp. 587–600. doi: 10.1007/s00382-005-0092-6.

Buringh, P. and Dudal, R. (1987) 'Agricultural land use in space and time', Land Transformation in Agriculture, pp. 9–43. Available at: http://www.cabdirect.org/abstracts/19881852142.html.

Busari, M. A., Kukal, S. S., Kaur, A., Bhatt, R. and Dulazi, A. A. (2015) 'Conservation tillage impacts on soil, crop and the environment', International Soil and Water Conservation Research. Elsevier, 3(2), pp. 119–129. doi: 10.1016/j.iswcr.2015.05.002.

Carvalho, G., Barros, A. C., Moutinho, P. and Nepstad, D. (2001) 'Sensitive development could protect Amazonia Did agriculture reduce How electricity could power the car of today', Nature, 409, p. 2001.

Cassidy, E. S., West, P. C., Gerber, J. S. and Foley, J. A. (2013) 'Redefining agricultural yields: From tonnes to people nourished per hectare', Environmental Research Letters, 8(3). doi: 10.1088/1748-9326/8/3/034015.

Cierniewski, J., Karnieli, A., Kazmierowski, C., Krolewicz, S., Piekarczyk, J., Lewinska, K., Goldberg, A., Wesolowski, R., Orzechowski, M., Kaźmierowski, C., Królewicz, S., Piekarczyk, J., Lewińska, K., Goldberg, A., Wesołowski, R., Orzechowski, M., Kazmierowski, C., Krolewicz, S., Piekarczyk, J., Lewinska, K., Goldberg, A., Wesolowski, R. and Orzechowski, M. (2015a) 'Effects of soil surface irregularities on the diurnal variation of soil broadband blue-sky albedo', IEEE Journal of Selected Topics in Applied Earth Observations and Remote Sensing, 8(2), pp. 493–502. doi: 10.1109/JSTARS.2014.2330691.

Cierniewski, J., Krolewicz, S., Kazmierowski, C., Ceglarek, J. and Kusz, P. (2015b) 'Shortwave radiation reflected from the territory of Poland throughout the year as an effect of smoothing soils previously plowed and harrowed', in 2015 IEEE International Geoscience and Remote Sensing Symposium (IGARSS). IEEE, pp. 4629–4632. doi: 10.1109/IGARSS.2015.7326860.

Cierniewski, J., Królewicz, S. and Kaźmierowski, C. (2017) 'Annual dynamics of shortwave radiation as consequence of smoothing of previously plowed and harrowed soils in Poland', Journal of Applied Meteorology and Climatology, 56(3), pp. 735–743. doi: 10.1175/JAMC-D-16-0126.1.

Cierniewski, J., Ceglarek, J., Karnieli, A., Ben-Dor, E., Królewicz, S. and Kaźmierowski, C. (2018a) 'Shortwave radiation affected by agricultural practices', Remote Sensing, 10(3). doi: 10.3390/rs10030419.

Cierniewski, J., Ceglarek, J. and Kazmierowski, C. (2018b) 'Annual dynamics of shortwave radiation reflected from bare soils in Europe', in Sobrino, J. A. (ed.) FIFTH RECENT ADVANCES IN QUANTITATIVE REMOTE SENSING Auditori. Valencia: Publicacions de la Universitat de Valencia.

Cierniewski, J., Ceglarek, J., Kaźmierowski, C. and Roujean, J. L. (2018c) 'Combined use of remote sensing and geostatistical data sets for estimating the dynamics of shortwave radiation of bare arable soils in Europe', International Journal of Remote Sensing. Taylor & Francis, 40(5–6), pp. 1–16. doi: 10.1080/01431161.2018.1474530.

Cierniewski, J. and Ceglarek, J. (2018d) 'Annual dynamics of shortwave radiation of bare arable lands on a global scale incorporating their roughness', Environmental Earth Sciences. Springer Berlin Heidelberg, 77(23). doi: 10.1007/s12665-018-7956-7.

Corsi, S., Friedrich, T., Kassam, A., Pisante, M. and Sà, J. de M. (2012) Soil Organic Carbon Accumulation and Greenhouse Gas Emission Reductions from Conservation Agriculture: A literature review. Rome: Food and Agriculture Organization of the United Nations (FAO).

Coulson, K. L. and Reynolds, D. W. (1971) 'The Spectral Reflectance of Natural Surfaces', Journal of Applied Meteorology, pp. 1285–1295. doi: 10.1175/1520-0450(1971)010<1285:tsrons>2.0.co;2.

CTIC (Conservation Tillage Information Center) (1993) 'Conservation tillage definitions and types of systems', Conserv Impact, 11(5), p. 6.

CTIC (Conservation Tillage Information Center) (2004) 'National crop residue management survey.', West Lafayette, IN:Conservation Technology Information Center.

Das, K. and Paul, P. K. (2015) 'Present status of soil moisture estimation by microwave remote sensing', Cogent Geoscience. Cogent, 1(1), pp. 1–21. doi: 10.1080/23312041.2015.1084669.

Davin, E. L., de Noblet-Ducoudré, N. and Friedlingstein, P. (2007) 'Impact of land cover change on surface climate: Relevance of the radiative forcing concept', Geophysical Research Letters, 34(13), p. n/a-n/a. doi: 10.1029/2007GL029678.

Davin, E. L. and Noblet-Ducoudre, N. (2010) 'Climatic impact of global-scale Deforestation: Radiative versus nonradiative processes', Journal of Climate, 23(1), pp. 97–112. doi: 10.1175/2009JCLI3102.1.

Defries, S., Foley, A. and Asner, P. (2004) 'Balancing human needs and ecosystem function Figure 1. Schematic representation of transitions in land use in a country or a region within a', Frontiers in Ecology and the Environment, 2(5), pp. 249–257.

Dematte, J. a. M., Huete, A. R., Ferreira Jr., L. G., Nanni, M. R., Alves, M. C. and Fiorio, P. R. (2009) 'Methodology for Bare Soil Detection and Discrimination by Landsat TM Image', The Open Remote Sensing Journal, 2(1), pp. 24–35. doi: 10.2174/1875413900902010024.

Derpsch, R., Friedrich, T., Kassam, A. and Hongwen, L. (2010) 'Current status of adoption of no-till farming in the world and some of its main benefits', International Journal of Agricultural and Biological Engineering, 3(1), pp. 1–25. doi: 10.3965/j.issn.1934-6344.2010.01.001-025.

Dewitte, O., Jones, A., Elbelrhiti, H., Horion, S. and Montanarella, L. (2012) 'Satellite remote sensing for soil mapping in Africa: An overview', Progress in Physical Geography, 36(4), pp. 514–538. doi: 10.1177/0309133312446981.

Diffenbaugh, N. S. and Sloan, L. C. (2002) 'Global climate sensitivity to land surface change: The Mid Holocene revisited', Geophysical Research Letters, 29(10), pp. 114-1-114–4. doi: 10.1029/2002gl014880.

Dobos, E. (2006) 'Albedo', Environmental Research. doi: 10.1081/E-ESS-120014334.

Du, C., Zhou, J., Wang, H., Chen, X., Zhu, A. and Zhang, J. (2009) 'Determination of soil properties using Fourier transform mid-infrared photoacoustic spectroscopy', Vibrational Spectroscopy, 49(1), pp. 32–37. doi: 10.1016/j.vibspec.2008.04.009.

Ellis, E. C., Goldewijk, K. K., Siebert, S., Lightman, D. and Ramankutty, N. (2010) 'Anthropogenic transformation of the biomes, 1700 to 2000', Global Ecology and Biogeography, 19(5), pp. 589–606. doi: 10.1111/j.1466-8238.2010.00540.x.

EMBRAPA (2006) Sistema brasileiro de classificação de solos, EMBRAPA. Centro Nacional de Pesquisa de Solos (Rio de Janeiro, RJ). doi: ISBN 978-85-7035-198-2.

FAO-UNESCO (1974) Soil maps of the world 1: 5,000,000 Volume I Legend, United Nations Educational, Scientific and Cultural Organization. Elsevier B.V. doi: 10.1016/j.geoderma.2013.05.003.

FAO-UNESCO (1988) Soil Map of the World. Revised legend. Rome: International Soil Reference and Information Centre.

FAO/UNESCO (2007) Digital soil map of the world, FAO-UN—Land and Water Division. Available at: http://www.fao.org/geone twork /srv/en/metad ata.show?id=14116 (Accessed: 20 June 2017).

FAO (2010) Crop Calendar. Available at: http://www.fao.org/agriculture/seed/cropcalendar (Accessed: 12 July 2018).

FAO (2018) FAOSTAT, Land Use. Available at: http://www.fao.org/faostat/en/#data/RL (Accessed: 4 March 2018).

FAO (2019) Soil classification, FAO SOILS PORTAL. Available at: http://www.fao.org/soils-portal/soil-survey/soil-classification/en/ (Accessed: 17 June 2018).

FAO (no date) Agriculture. Available at: http://www.fao.org/ag/agn/nutrition/Indicatorsfiles/Agriculture.pdf (Accessed: 5 March 2018).

Fenner, M. (1998) 'The phenology of growth and reproduction in plants', Perspectives in Plant Ecology, Evolution and Systematics, 1, pp. 78–91. doi: 10.1109/CRMICO.2002.1137327.

Fischer, G., Nachtergaele, F., Prieler, S., van Velthuizen, H. T., Verelst, L. and Wiberg, D. (2012) 'Global Agro-ecological Zones Assessment for Agriculture (GAEZ 2008)', FAO, Rome, Italy and IIASA, Laxenburg, Austria, pp. 1–50.

Foley, J. A., Defries, R., Asner, G., Barford, C., Bonan, G., Carpenter, S., Chapin III, F. S., Coe, M., Daily, G., Gibbs, H., H Helkowski, J., Holloway, T., Howard, E. A., Kucharik, C., Monfreda, C., Patz, J., Prentice, I., Ramankutty, N. and Snyder, P. K. (2005) 'Global consequences of land use', Science (New York, N.Y.), 309(5734), pp. 570–574.

Foley, J. A., Ramankutty, N., Brauman, K. A., Cassidy, E. S., Gerber, J. S., Johnston, M., Mueller, N. D., O'Connell, C., Ray, D. K., West, P. C., Balzer, C., Bennett, E. M., Carpenter, S. R., Hill, J., Monfreda, C., Polasky, S., Rockström, J., Sheehan, J., Siebert, S., Tilman, D., Zaks, D. P. M. and O'Connell, C. (2011) 'Solutions for a cultivated planet', Nature, 478(7369), pp. 337–42. doi: 10.1038/nature10452.

Fowler, C. and Mooney, P. (1990) Shattering: food, politics, and the loss of genetic diversity. Tuscon: University of Arizona Press.

Friedrich, T., Derpsch, R. and Kassam, A. (2012) 'Overview of the global spread of conservation agriculture', Field Actions Science Reports, 6(6), pp. 1–7. Available at: http://factsreports.revues.org/1941.

Frolking, S., Xiao, X., Zhuang, Y., Salas, W. and Li, C. (1999) 'Agricultural land-use in China: A comparison of area estimates from ground-based census and satellite-borne remote sensing', Global Ecology and Biogeography, 8(5), pp. 407–416. doi: 10.1046/j.1365-2699.1999.00157.x.

Gajri, P. R., Majumdar, S. P. and Sharma, P. K. (2009) 'Tillage.', in Fundamentals of soil science. 2nd edn. Pusa, New Delhi: Indian Society of Soil Science, pp. 162–179.

Gao, B. (1996) 'NDWI - A Normalized Difference Water Index for Remote Sensing of Vegetation Liquid Water From Space', Remote Sensing of Environment, 58, pp. 257–266.

Gibbard, S., Caldeira, K., Bala, G., Phillips, T. J. and Wickett, M. (2005) 'Climate effects of global land cover change', Geophysical Research Letters, 32(23), pp. 1–4. doi: 10.1029/2005GL024550.

Godfray, H. C. J., Beddington, J. R., Crute, I. R., Haddad, L., Lawrence, D., Muir, J. F., Pretty, J., Sherman, R. and Thomas, S. M. (2010) 'Food Security: The Challenge of Feeding 9 Billion People', 327(February 5967), pp. 812–818. doi: 10.1126/science.1185383.

Goldewijk, K. K. (2001) 'Estimating global land use change over the past 300 years: The HYDE database', Global Biogeochemical Cycles, 15(2), pp. 417–433. doi: 10.1029/1999GB001232.

Heistermann, M. (2006) 'Modelling the Global Dynamics of Rain-fed and Irrigated Croplands', Reports on Earth System Science, 37, p. 158.

Hillel, D. (1998) Environmental Soil Physics, Academic Press San Diego CA. doi: 10.2134/jeq1999.00472425002800060046x.

Huete, A. R. (1988) 'A Soil-Adjusted Vegetation Index (SAVI)', Remote Sensing of Environment, 25, pp. 295–309.

Hurtt, G. C., Rosentrater, L., Frolking, S. and Moore, B. (2001) 'Linking remote-sensing estimates of land cover and census statistics on land use to produce', Global Biogeochemical Cycles, 15(3), pp. 673–686. doi: 10.1029/2000GB001299.This.

Isbell, R. F. (2016) 'The Australian Soil Classification (2nd Edition)', p. 152.

Jiang, Z., Huete, A. R., Didan, K. and Miura, T. (2008) 'Development of a two-band enhanced vegetation index without a blue band', Remote Sensing of Environment, 112(10), pp. 3833–3845. doi: 10.1016/j.rse.2008.06.006.

Kassam, A., Derpsch, R. and Friedrich, T. (2014) 'Global achievements in soil and water conservation: The case of Conservation Agriculture', International Soil and Water Conservation Research. Elsevier Masson SAS, 2(1), pp. 5–13. doi: 10.1016/S2095-6339(15)30009-5.

Kondratyev, K. Y. (1969) Radiacjonnyje Charakteristiki Atmosfery i Zemnoy Powerchnosti. Leningrad, Russia: Gidrometeorologiczeskoye Izdatelstwo.

Kuzucu, K. A. and Balcik, F. B. (2017) 'Testing the Potential of Vegetation Iindices for Land Use/Cover Classification Using High Resolution Data', ISPRS Annals of the Photogrammetry, Remote Sensing and Spatial Information Sciences, 4(4W4), pp. 279–283. doi: 10.5194/isprs-annals-IV-4-W4-279-2017.

Lakshmi, V. (2013) 'Remote Sensing of Soil Moisture', ISRN Soil Science, 2013, pp. 1–33.

Lal, R. (2016) Encyclopedia of Soil Science. 3rd edn. Boca Raton, Florida: CRC Press.

Lee, C. (2011) 'Corn Growth Stages and Growing Degree Days : A Quick Reference Guide', Cooperative Extension Service, University of Kentucky, College of Agriculture, 202, p. 2.

Leff, B., Ramankutty, N. and Foley, J. a (2004) 'Geographic distribution of major crops across the world', Global Biogeochemical Cycles, 18(1), p. n/a--n/a. doi: 10.1029/2003GB002108.

Lev, S., Valentin, T., Irina, L. and Maria, G. (2001) 'Principles , structure and prospects of the new Russian soil classification system', pp. 29–34.

Li, S. and Chen, X. (2014) 'A new bare-soil index for rapid mapping developing areas using landsat 8 data', International Archives of the Photogrammetry, Remote Sensing and Spatial Information Sciences - ISPRS Archives, 40(4), pp. 139–144. doi: 10.5194/isprsarchives-XL-4-139-2014.

Littlejohns, J., Rehmann, L., Murdy, R., Oo, A. and Neill, S. (2018) 'Current state and future prospects for liquid biofuels in Canada', Biofuel Research Journal, 5(1), pp. 759–779. doi: 10.18331/brj2018.5.1.4.

Liu, H., Wang, B. and Fu, C. (2008) 'Relationships Between Surface Albedo, Soil Thermal Parameters and Soil Moisture in the Semi-arid Area of Tongyu, Northeastern China', Advances in Atmospheric Sciences, 25(5), pp. 757–764. doi: 10.1007/s00376-008-0757-2.1.Introduction.

Matthews, H. D., Weaver, A. J., Eby, M. and Meissner, K. J. (2003) 'Radiative forcing of climate by historical land cover change', Geophysical Research Letters, 30(2). doi: 10.1029/2002GL016098.

Matthews, H. D., Weaver, A. J., Meissner, K. J., Gillett, N. P. and Eby, M. (2004) 'Natural and anthropogenic climate change: Incorporating historical land cover change, vegetation dynamics and the global carbon cycle', Climate Dynamics, 22(5), pp. 461–479. doi: 10.1007/s00382-004-0392-2.

McMaster, G. S. and Wilhelm, W. W. (1997) 'Growing degree-days: One equation, two interpretations', Agricultural and Forest Meteorology, 87(4), pp. 291–300. doi: 10.1016/S0168-1923(97)00027-0.

Meiyappan, P. and Jain, A. K. (2012) 'Three distinct global estimates of historical land-cover change and land-use conversions for over 200 years', Frontiers of Earth Science, 6(2), pp. 122–139. doi: 10.1007/s11707-012-0314-2.

Melesse, A. M., Weng, Q., Thenkabail, P. S. and Senay, G. B. (2007) 'Remote Sensing Sensors and Applications in Environmental Resources Mapping and Modelling', 7, pp. 3209–3241. doi: 10.3390/s7123209.

Metternicht, G. I. and Zinck, J. A. (2003) 'Remote sensing of soil salinity: Potentials and constraints', Remote Sensing of Environment, 85(1), pp. 1–20. doi: 10.1016/S0034-4257(02)00188-8.

Midwest Plan Service (2000) 'Crop residue management with no-till, ridgetill, mulch-till and strip-till', in Conservation Tillage Systems and Management. 2nd edn. Ames, Iowa: Iowa State University Press, p. 270.

Mikhajlova, N. A. and Orlov, D. S. (1986) 'Opticheskie Svoystva Pochv i Pochvennych Komponentov', Russia: Nauka, p. 118.

Miller, P., Lanier, W. and Brandt, S. (2001) 'Using Growing Degree Days to Predict Plant Stages', Montana State University Extension Service, 9, p. MT00103 AG 7/2001.

Monfreda, C., Ramankutty, N. and Foley, J. A. (2008) 'Farming the planet: 2. Geographic distribution of crop areas, yields, physiological types, and net primary production in the year 2000', Global Biogeochemical Cycles, 22(1), pp. 1–19. doi: 10.1029/2007GB002947.

Monteith, J. L. and Szeicz, G. (1961) 'The radiation balance of bare soil and vegetation', Quarterly Journal of the Royal Meteorological Society, 87(372), pp. 159–170. doi: 10.1002/qj.49708737205.

Mulder, V. L., de Bruin, S., Schaepman, M. E. and Mayr, T. R. (2011) 'The use of remote sensing in soil and terrain mapping - A review', Geoderma. Elsevier B.V., 162(1–2), pp. 1–19. doi: 10.1016/j.geoderma.2010.12.018.

NCAR (2018) National Center for Atmospheric Research. Available at: https://ncar.ucar.edu/ (Accessed: 6 September 2017).

Obade, V. and Lal, R. (2013) 'Assessing land cover and soil quality by remote sensing and geographical information systems (GIS)', Catena. Elsevier B.V., 104, pp. 77–92. doi: 10.1016/j.catena.2012.10.014.

Oguntunde, P. G., Ajayi, A. E. and Giesen, N. van de (2006) 'Tillage and surface moisture effects on bare-soil albedo of a tropical loamy sand', Soil and Tillage Research, 85(1–2), pp. 107–114. doi: 10.1016/j.still.2004.12.009.

Oke, T. R. (1987) Boundary layer climates. Routledge.

Ortiz, B., Tapley, M. and Santen, E. van (2012) 'Planting date and variety selection effects on wheat yield', Alabama Cooperative Extension system, p. 4. Available at: https://store.aces.edu/ItemDetail.aspx?ProductID=17545&SeriesCode=&CategoryID=&Keyword=1442.

Oxford English Dictonary (2013) Oxford English Dictonary. Available at: https://en.oxforddictionaries.com/definition/arable (Accessed: 3 February 2018).

Perry, D. A. (1994) Forest ecosystems. Baltimore, Maryland: Johns Hopkins University Press. Available at: https://jhupbooks.press.jhu.edu/title/forest-ecosystems.

Phillips, R. D., Blinn, C. E., Watson, L. T. and Wynne, R. H. (2009) 'An adaptive noise-filtering algorithm for AVIRIS data with implications for classification accuracy', IEEE Transactions on Geoscience and Remote Sensing, 47(9), pp. 3168–3179. doi: 10.1109/TGRS.2009.2020156.

Pinty, B., Verstraete, M. M. and Dickinson, R. E. (1989) 'A physical model for predicting bidirectional reflectances over bare soil', Remote Sensing of Environment, 27(3), pp. 273–288. doi: 10.1016/0034-4257(89)90088-6.

Polskie Towarzystwo Gleboznawcze (2011) Soil Science Annual. Warszawa: Wydawnictwo „Wieś Jutra".

Portmann, F. T., Siebert, S., Bauer, C. and Döll, P. (2008) 'Global dataset of monthly growing areas of 26 irrigated crops', Frankfurt Hydrology Paper, 6, p. 400.

Portmann, F. T., Siebert, S. and Döll, P. (2010) 'MIRCA2000-Global monthly irrigated and rainfed crop areas around the year 2000: A new high-resolution data set for agricultural and hydrological modeling', Global Biogeochemical Cycles, 24(1), pp. 1–24. doi: 10.1029/2008gb003435.

Ramankutty, N. and Foley, J. A. (1998) 'Characterizing Patterns of Global Land Use: An Analysis of Global Croplands Data, Global Biogeochem. Cycles, 12(4), 667-685. ', Global Geochemical Cycles, 12(4), pp. 667–685.

Ramankutty, N. and A. Foley (1999) 'Estimating historical changes in global land cover : Croplands historical have converted areas', Global Biogeochemical Cycles, 13(4), pp. 997–1027. doi: 10.1029/1999GB900046.

Ramankutty, N. (2000) The Role of Croplands in the Terrestrial Biosphere: Past, Present, and Future. University of Wisconsin, Madison, USA.

Ramankutty, N., A. Foley, J., Norman, J. and Mcsweeney, K. (2002) The Global Distribution of Cultivable Lands: Current Patterns and Sensitivity to Possible Climate Change, geb. doi: 10.1046/j.1466-822x.2002.00294.x.

Ramankutty, N., Evan, A. T., Monfreda, C. and Foley, J. A. (2008) 'Farming the planet: 1. Geographic distribution of global agricultural lands in the year 2000', Global Biogeochemical Cycles, 22(1), pp. 1–19. doi: 10.1029/2007GB002952.

von Randow, C., Manzi, A. O., Kruijt, B., de Oliveira, P. J., Zanchi, F. B., Silva, R. L., Hodnett, M. G., Gash, J. H. C., Elbers, J. A., Waterloo, M. J., Cardoso, F. L. and Kabat, P. (2004) 'Comparative measurements and seasonal variations in energy and carbon exchange over forest and pasture in South West Amazonia', Theoretical and Applied Climatology, 78(1–3), pp. 5–26. doi: 10.1007/s00704-004-0041-z.

Regmi, A., Takeshima, H. and Unnevehr, L. J. (2009) 'Convergence in Global Food Demand and Delivery', Ssrn, (56). doi: 10.2139/ssrn.1354244.

Richter, R. and Schläpfer, D. (2002) 'Geo-atmospheric processing of airborne imaging spectrometry data. Part 2: Atmospheric/topographic correction', International Journal of Remote Sensing, 23(13), pp. 2631–2649. doi: 10.1080/01431160110115834.

Roberts, D. A., Roth, K. L. and Perroy, R. L. (2011) 'Hyperspectral Vegetation Indices', in Thenkabail, P. S., Lyon, J. G., and Huete, A. R. (eds) Hyperspectral Remote Sensing of Vegetation. 1st edn. Boca Raton, Florida: CRC Press, p. 1478. doi: 10.1201/b11222-20.

Roerink, G. J., Danes, M. H. G. I., Prieto, O. G., De Wit, A. J. W. and Van Vliet, A. J. H. (2011) 'Deriving plant phenology from remote sensing', in 2011 6th International Workshop on the Analysis of Multi-Temporal Remote Sensing Images, Multi-Temp 2011 - Proceedings, pp. 261–264. doi: 10.1109/Multi-Temp.2011.6005098.

Rouse, W., Haas, H. and Deering, W. (1973) 'Monitoring Vegetation Systems in the Great Plains With Erts .', in Proceedings, 3rd Earth Resource Technology Satellite (ERTS) Symposium, pp. 309–317.

Sacks, W. J., Deryng, D., Foley, J. A. and Ramankutty, N. (2010) 'Crop planting dates: An analysis of global patterns', Global Ecology and Biogeography, 19(5), pp. 607–620. doi: 10.1111/j.1466-8238.2010.00551.x.

SCSA (Soil Conservation Society of America) (1987) Glossary of soil science terms. Ankeny: Soil Science Conservation Society of America.

Senker, P. (2011) Foresight: the future of food and farming, final project report, Prometheus. doi: 10.1080/08109028.2011.628564.

Shi, X. H., Yang, X. M., Drury, C. F., Reynolds, W. D., McLaughlin, N. B. and Zhang, X. P. (2012) 'Impact of ridge tillage on soil organic carbon and selected physical properties of a clay loam in southwestern Ontario', Soil and Tillage Research. Elsevier B.V., 120, pp. 1–7. doi: 10.1016/j.still.2012.01.003.

Skole, D. L., Chomentowski, W. H., Salas, W. A. and Nobre, A. D. (2006) 'Physical and Human Dimensions of Deforestation in Amazonia', BioScience, 44(5), pp. 314–322. doi: 10.2307/1312381.

Soil Survey Staff (1975) 'Soil Taxonomy', p. 754.

Soil Survey Staff (1998) 'Key to Soil Taxonomy', p. 326 p.

Stagnari, F., Ramazzotti, S. and Pisante, M. (2009) 'Conservation Agriculture: A Different Approach for Crop Production Through Sustainable Soil and Water Management: A Review', in Lichtfouse E. (eds) Organic Farming, Pest Control and Remediation of Soil Pollutants. Sustainable Agriculture Reviews. 1st edn. Dordrecht: Springer. doi: 10.5860/choice.47-5011.

Tekwa, I. and Shehu, H. (2011) 'Soil nutrient status and productivity potentials of lithosols in Mubi Area, Northeastern Nigeria', Agriculture and Biology Journal of North America, 2(6), pp. 887–896. doi: 10.5251/abjna.2011.2.6.887.896.

Thatcher, A., Waterson, P., Todd, A. and Moray, N. (2018) 'State of Science: ergonomics and global issues', Ergonomics. Taylor & Francis, 61(2), pp. 197–213. doi: 10.1080/00140139.2017.1398845.

The Royal Society (2008) 'Sustainable biofuels: prospects and challenges', The Royal Society:Sustainable biofuels: prospects and challenges., (January), pp. 1–79. doi: ISBN 978 0 85403 662 2.

The World Bank (2018) The World Bank, Arable Land (% of land area). Available at: https://data.worldbank.org/indicator/ag.lnd.arbl.zs (Accessed: 2 February 2018).

Thenkabail, P. S. and Lyon, J. G. (2011) Hyperspectral Remote Sensing of Vegetation. 1st Editio. Boca Raton: Taylor & Francis. doi: 10.3390/rs70809610.

Thomsen, L. M., Baartman, J. E. M., Barneveld, R. J., Starkloff, T. and Stolte, J. (2015) 'Soil surface roughness: comparing old and new measuring methods and application in a soil erosion model', Soil, 1(1), pp. 399–410. doi: 10.5194/soil-1-399-2015.

Tilman, D., Balzer, C., Hill, J. and Befort, B. L. (2011) 'Global food demand and the sustainable intensification of agriculture', Proceedings of the National Academy of Sciences, 108(50), pp. 20260–20264. doi: 10.1073/pnas.1116437108.

Tinti, A., Tugnoli, V., Bonora, S. and Francioso, O. (2015) 'Recent applications of vibrational mid-infrared (IR) spectroscopy for studying soil components: A review', Journal of Central European Agriculture. Journal of Central European Agriculture, 16(1), pp. 1–22. doi: 10.5513/JCEA01/16.1.1535.

Toulmin, C. (2012) 'The Futures of Agriculture The Future of Food and Farming', (42), pp. 1–4.

Trostle, R. (2008) 'Global Agricultural Supply and Demand: Factors Contributing to the Recent Increase in Food Commodity Prices', Economic Reasearch Service, WRS-0801, pp. 1–30.

Turner, B. L., Lambin, E. F. and Reenberg, A. (2007) 'The emergence of land change science for global environmental change and sustainability', 104(52), pp. 20666–20671.

Twine, T. E., Kucharik, C. J. and Foley, J. A. (2004) 'Effects of Land Cover Change on the Energy and Water Balance of the Mississippi River Basin', Journal of Hydrometeorology, 5(4), pp. 640–655. doi: 10.1175/1525-7541(2004)005<0640:eolcco>2.0.co;2.

United Nations, Department of Economic and Social Affairs, P. D. (2017) World Population Prospects: The 2017 Revision, Key Findings and Advance Tables.

United States Department of Agriculture (USDA) (2006) 'USDA Agricultural Baseline Projections to 2015', USDA Agricultural Baseline Projections, p. 113. Available at: http://www.ers.usda.gov/publications/oce061/.

United States Department of Agriculture / Joint Agricultural Weather Facility (USDA/JAWF) (1994) Major World Crop Areas and Climatic Profiles, Agricultural Handbook. Washington, DC: United States Department of Agriculture.

Valin, H., Sands, R. D., van der Mensbrugghe, D., Nelson, G. C., Ahammad, H., Blanc, E., Bodirsky, B., Fujimori, S., Hasegawa, T., Havlik, P., Heyhoe, E., Kyle, P., Mason-D'Croz, D., Paltsev, S., Rolinski, S., Tabeau, A., van Meijl, H., von Lampe, M. and Willenbockel, D. (2014) 'The future of food demand: Understanding differences in global economic models', Agricultural Economics (United Kingdom), 45(1), pp. 51–67. doi: 10.1111/agec.12089.

Vermote, E., Justice, C., Claverie, M. and Franch, B. (2016) 'Preliminary analysis of the performance of the Landsat 8/OLI land surface reflectance product', Remote Sensing of Environment. Elsevier B.V., 185, pp. 46–56. doi: 10.1016/j.rse.2016.04.008.

Wood-Sichra, U., Joglekar, A. B. and You, L. (2016) Spatial Production Allocation Model (SPAM) 2005: Technical Documentation, HarvestChoice Working Paper. Washington, DC.

Worthington, C. and Hutchinson, C. (2005) 'ACCUMULATED GROWING DEGREE DAYS AS A MODEL TO DETERMINE KEY DEVELOPMENTAL STAGES AND EVALUATE YIELD AND QUALITY OF potat', Proc. Fla. State Hort. Soc, 1, pp. 98–101. Available at: http://fshs.org/proceedings-o/2005-vol-118/118/098-101.pdf.

Wulf, H., Mulder, T., Schaepman, M. E., Keller, A. and Jorg, P. C. (2015) 'Remote Sensing of Soils', Zurich Open Repository and Archive, pp. 1–71. doi: 10.1007/978-3-662-53740-4.

Xue, J. and Su, B. (2017) 'Significant Remote Sensing Vegetation Indices: A Review of Developments and Applications', Journal of Sensors, 2017, pp. 1–17. doi: 10.1155/2017/1353691.

You, X., Meng, J., Zhang, M. and Dong, T. (2013) 'Remote sensing based detection of crop phenology for agricultural zones in China using a new threshold method', Remote Sensing, 5(7), pp. 3190–3211. doi: 10.3390/rs5073190.

You, L., Wood-Sichra, U., Bacou, M. and Koo, J. (2014) Crop Production: SPAM. Available at: http://harvestchoice.org/node/9716.

Zhang, X., Friedl, M. A. and Schaaf, C. B. (2006) 'Global vegetation phenology from Moderate Resolution Imaging Spectroradiometer (MODIS): Evaluation of global patterns and comparison with in situ measurements', Journal of Geophysical Research: Biogeosciences, 111(4), pp. 1–14. doi: 10.1029/2006JG000217.